PHD

Targeted delivery of methotrexate to melanoma using melanocortin analogues

Whelan, Laura Jane

Award date:
1995

Awarding institution:
University of Bath

TARGETED DELIVERY OF METHOTREXATE TO MELANOMA USING MELANOCORTIN ANALOGUES

Submitted by Laura Jane Whelan
for the degree of Ph.D.
of the University of Bath

1995

ProQuest LLC
789 East Eisenhower Parkway
P.O. Box 1346
Ann Arbor, MI 48106-1346

ABSTRACT

The work presented in this thesis has focussed on the potential for site specific drug delivery to the MSH receptors located on the surface of melanoma cells. Methotrexate (MTX) was the drug chosen for this model due to its relatively small size (FW:454.5), the wealth of information already available on MTX and the facility with which it could be chemically manipulated for our purposes.

The potent analogue of the naturally occurring alpha-melanocyte stimulating hormone (α-MSH) i.e. [Nle^4,D-Phe^7]α-MSH was chemically conjugated to MTX forming N$^\alpha$MTX-[Nle^4,D-Phe^7]α-MSH, the study of which comprises the bulk of this work.

Although the majority of experiments were performed on the B16 murine melanoma cell line, additional cell lines used included: the MeWo human melanoma cell line, SVK14 keratinocytes and a transformed 293 human embryonic kidney (HEK) cell line, expressing the melanocortin MC3 receptor.

With reference to drug delivery to melanoma, the binding and internalisation following interaction with the MC1 receptor was examined. The results of the continual and Pulse-Chase labelling suggested that receptor mediated endocytosis of ^{125}I-N$^\alpha$MTX- [Nle^4,D-Phe^7]α-MSH did occur. Acid washing steps were taken to determine what proportion of radioactivity associated with the cell was intracellular and hence receptor-specific. Continuous accumulation of ligand by B16 cells in the presence of NH_4Cl led to the conclusion that under normal conditions, degradation of ^{125}I-N$^\alpha$MTX-[Nle^4,D-Phe^7]α-MSH occurred in the lysosomes.

The interaction of N$^{\alpha}$MTX-[Nle^4,D-Phe^7]α-MSH with the MC3 receptor was assessed by competition assays in the presence of ^{125}I- [Nle^4,D-Phe^7]α-MSH. It was established that binding to the MC3 receptor does occur but with lower affinity as compared to the affinity for the MC1 receptor.

Growth inhibition was studied using the MTT tetrazolium dye cytotoxicity assay in the presence of MTX and N$^{\alpha}$MTX-[Nle^4,D-Phe^7]α-MSH for all of the cell lines described above, so that comparisons of the $E.C._{50}$ values generated could give valid conclusions as to the efficacy of the latter over the former.

Finally the intracellular mass of MTX required to effect growth inhibition of B16 cells was determined. This was achieved by the combination of the trypan blue assay with the MTT assay and the ^{3}H-MTX uptake assay which led to the conclusion that 5.44×10^5 molecules of MTX are necessary to produce 50% growth inhibition.

Due to the fact that N$^{\alpha}$MTX-[Nle^4,D-Phe^7]α-MSH did not bind selectively to MC1 receptors and that N$^{\alpha}$MTX-[Nle^4,D-Phe^7]α-MSH required a much higher (greater than 3 orders of magnitude) extracellular concentration than MTX before it exerted the same effects on the cells it has been concluded that this conjugate was not as successful as a site specific agent against melanoma as was hoped. The low toxicity of the conjugate was assumed to be explained by the low capacity of the receptor-mediated internalisation pathway. It was not feasible to deliver sufficient MTX by this mechanism, though in the future it may be possible to achieve melanoma-specific cytotoxicity if a more toxic agent is used.

Acknowledgements

I would like to thank all my supervisors for their support and encouragement, Dr. Stephen Moss, Professor D. J. G. Davies and especially Dr. Colin Pouton for his constructive criticism and constant optimism in the face of my eternal pessimism. I would also like to thank Dr. George Olivier for synthesising the peptide and the peptide conjugate employed in this study. Special thanks to Ulrike without whose friendship, advice and tolerance this thesis would have been infinitely more difficult to write. My thanks also extend to my father and my sister, Jill for financial and emotional support and many friends including: Emma Cane, Daniel Carey, Dethard Lampe, Neil Merrett, Máiread O' Donnell, Andy Richards, Dunevia Thomas, Anne Walsh and Toby Young who all played vital roles in maintaining my sanity!

Finally I would like to thank the Royal Pharmaceutical Society of Great Britain for their financial support and the collaboration of members of the SERC/ DTI funded LINK programme in "Selective Drug Delivery and Targeting" and the University of Bath for providing research facilities.

This thesis is dedicated to Eithné Marie-Céline Whelan.

Abbreviations

AML	Acute Myeloid Leukaemia
α-MSH	alpha - Melanocyte Stimulating Hormone
BSA	Bovine Serum Albumin
CPZ	Chlorpromazine
DAMPA	4-amino-4-deoxy-N^{10}-methylpteroic acid
DIPCDI	Diisopropylcarbodiimide
DMF	N,N-Dimethylformamide
DMSO	Dimethylsulphoxide
DNA	Desoxyribonucleic Acid
$E.C._{50}$	Effective Concentration of inhibitor at which 50% of cells were inhibited relative to control cells.
EDT	Ethane-1,2-dithiol
EDTA	Ethylenediaminetetraacetic Acid
Fmoc	Fluorenylmethoxycarbonyl
FA	Folinic acid
FAB-MS	Fast Atom Bombardment-Mass Spectrometry
FCS	Foetal Calf Serum
^{3}H-MTX	Tritiated Methotrexate
HCl	Hydrochloric acid
HEK	Human Embryonic Kidney
HEPES	N-(2-hydroxyethyl)piperazine-N-2'-ethane sulphonic acid
HOBT	1-Hydroxybenzotriazole
HPLC	High Performance Liquid Chromatography

$I.D._{50}$	Inhibition dose at which 50% of cells were inhibited relative to control cells.
MALDI-TOF-MS	Matrix Assisted Laser Desorption Ionisation - Time Of Flight - Mass Spectroscopy
MC Receptor	Melanocortin Receptor
MeCN	Acetonitrile
MIF	MSH Inhibiting Factors
MRF	MSH Releasing Factors
MTS	(3-(4,5-Dimethylthiazol-2-yl)-5-(3-carboxymethoxyphenyl)-2-(4-sulphophenyl)-2H-tetrazolium, inner salt.
MTT	(3-[4,5-Dimethylthiazol-2-yl]-2,5-diphenyltetrazolium bromide); Thiazolyl Blue
MTT formazan	(1-[4,5-Dimethylthiazol-2-yl]-3,5-diphenylformazan
MTX	Methotrexate
MTX-NLDP	N^{α}MTX-[Nle^4,D-Phe^7]α-MSH
NaOH	Sodium Hydroxide
NEAA	Non-Essential Amino Acids
NH_4Cl	Ammonium Chloride
NLDP	[Nle^4,D-Phe^7]α-MSH
PBS	Phosphate Buffered Saline
P.D.	*pars distalis*
P.I.	*pars intermedia*
PMS	Phenazine Methosulphate
POMC	Pro-opiomelanocortin
PUVA	Psoralen Ultra Violet Class A
PVP	Polyvinyl pyrrolidone

RNA	Ribonucleic Acid
RPMI	Roswell Park Memorial Institute
S.D.	Standard Deviation
SFM	Serum Free Medium
TFA	Trifluoracetic Acid
UV	Ultra Violet
XTT	(Sodium 3'-(1-phenylaminocarbonyl-3,4-tetrazolium)bis(4-methoxy-6-nitrobenzenesulphonate) hydrate

Amino Acids

Ala	alanine
Arg	arginine
Asn	asparagine
Asp	aspartic acid
Cys	cysteine
Gln	glutamine
Glu	glutamic acid
Gly	glycine
His	histidine
Leu	leucine
Lys	lysine
Met	methionine
Nle	norleucine
Phe	phenylalanine
Pro	proline
Ser	serine
Trp	tryptophan
Tyr	tyrosine
Val	valine

TABLE OF CONTENTS

Chapter 1.

Introduction

The ultimate aim of any medicinal product is to eradicate the symptoms of illness and hence cure the patient. Although no drug can be said to be 100% risk-free, in many instances the side-effects are judged to be negligible in comparison to the beneficial effects. In cancer chemotherapy however, many of the commonly used agents e.g. vincristine, daunorubicin and methotrexate etc., have side-effects of a more serious nature and in these cases it is important to assess whether the benefit : risk ratio is high enough to justify their use. To combat these side-effects new approaches have been employed under the general heading of drug delivery systems. There are many ways in which a drug may be delivered to a diseased area, in order to produce "selective toxicity" i.e. " the injury of one kind of living matter without harming another kind with which the first is in intimate contact " (Albert, 1973). This is a departure from the older theories founded upon the belief that by killing cells all over the body, the diseased or damaged cells would also be killed. This approach has lost a lot of support and momentum due to its haphazard nature which caused undesirable effects throughout the body.

This project is focused on melanoma cancer and its treatment by use of site specific methotrexate (MTX). Site specific drug delivery has progressed a long way from the initial conception of antibodies and "magic bullets" by Paul Ehrlich in 1906 (Basu, 1990). The theory of site specific drug delivery in this instance relates to the affinity of the melanocortin receptor sites on the surface of the cell for the hormone alpha-melanocyte stimulating hormone (α-MSH). An analogue of the naturally occurring hormone, [Nle^4,D-Phe^7]α-

MSH, has been used in preference to other analogues due to its stability towards oxidation and degradation and its facility of iodination at the tyrosine residue (position 2) without subsequent loss of biological activity of the molecule (Sawyer *et al.*, 1980). [Nle^4,D-Phe^7]α-MSH is more active than α-MSH and showed prolonged effects in some of the assays as well as a higher binding affinity, (Tatro *et al.*, 1990).

Once bound to the receptor site, the [Nle^4,D-Phe^7]α-MSH is internalised and then broken down intracellularly in the lysosomes. The aim of attaching MTX to the hormone analogue is that this will, in theory, guide MTX to the cell surface of cells expressing MSH receptors e.g. melanoma cells, melanocytes etc., in preference to the more general pathway followed by the free drug. In the normal way MTX uptake is mediated via the folic acid pathway as MTX competes for the same receptor site as folate analogues. Due to the uptake of MTX by all cell types many unwanted adverse effects are encountered. By using the N$^{\alpha}$MTX-[Nle^4,D-Phe^7]α-MSH conjugate it is hoped that an alternative and more discriminating pathway would be utilised and consequently (1) fewer drug molecules should be needed for targeting and (2) fewer side effects should be encountered leading to an overall improvement in the chemotherapy of the patient.

1.1. Methods of Drug Delivery.

The mode of transport utilised in order to achieve effective drug concentration at the pertinent site of action varies in complexity depending on the ease or difficulty with which the target cells are located. Local delivery to the nasal mucosa e.g. nose drops, delivery to the rectum e.g. suppositories, delivery to

the lungs e.g. inhalation treatment for asthma, are all commonly used because the sites of action are relatively easy to target and so the agents can be delivered directly.

However, site specific drug delivery is the optimum choice for cancer chemotherapy. Cytotoxic drugs exert lethal effects not only on the cancerous cells but also on healthy tissues and cells especially where the cells have a rapid turnover rate e.g. bone marrow. This is achieved by means of attaching specific groups e.g. antibodies and hormones, to other non-specific groups e.g.: drug moieties, specifically in this case the targeting of methotrexate to the melanocortin receptors on the surface of cells by attaching it to the hormone analogue [Nle^4,D-Phe^7] α-MSH.

1.2. Melanocyte Stimulating Hormone (MSH).

α-MSH is a 13 amino acid posttransational product of the pro-opiomelanocortin (POMC) gene. The amino acid sequence of α-MSH and [Nle^4,D-Phe^7]α-MSH are given in Figure 1.1. α-MSH, adrenocorticotropic hormone (ACTH), β-MSH and γ-MSH are structurally related pituitary peptide hormones and all share a core heptapeptide amino acid sequence: **Met-Glu/Gly-His-Phe-Arg-Trp-Gly/Asp** and are commonly referred to as the melanocortins or the melanotropic peptides. Figure 1.2. shows the sequence of events in their production (Mains *et al.,* 1977, Mains and Eipper, 1979, Crine *et al.,* 1979). The melanotropic peptides and especially α-MSH have been the subject of an extensive review by Eberle, (1988). Therefore only the information pertinent to this study is mentioned here and no detailed discussion on β-MSH, γ-MSH or ACTH is included.

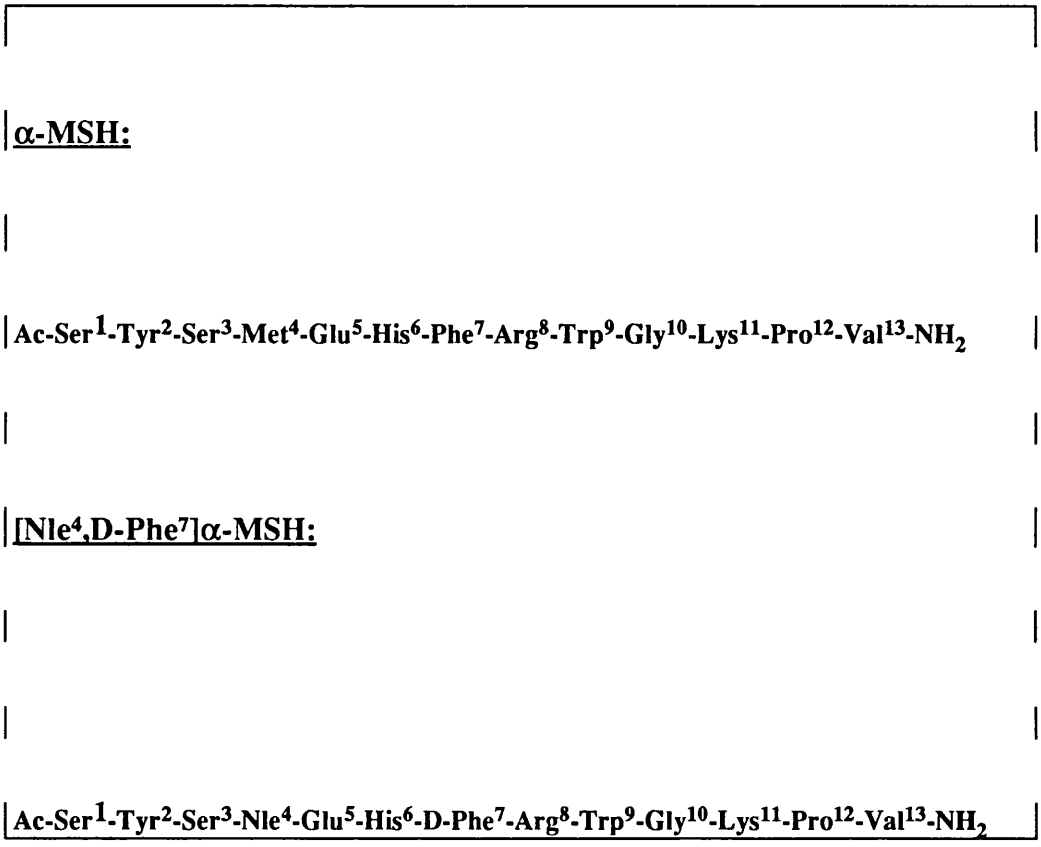

Figure 1.1. This figure shows the amino acid sequences of the hormone, α-MSH and an analogue of this hormone, [Nle^4,D-Phe^7]α-MSH.

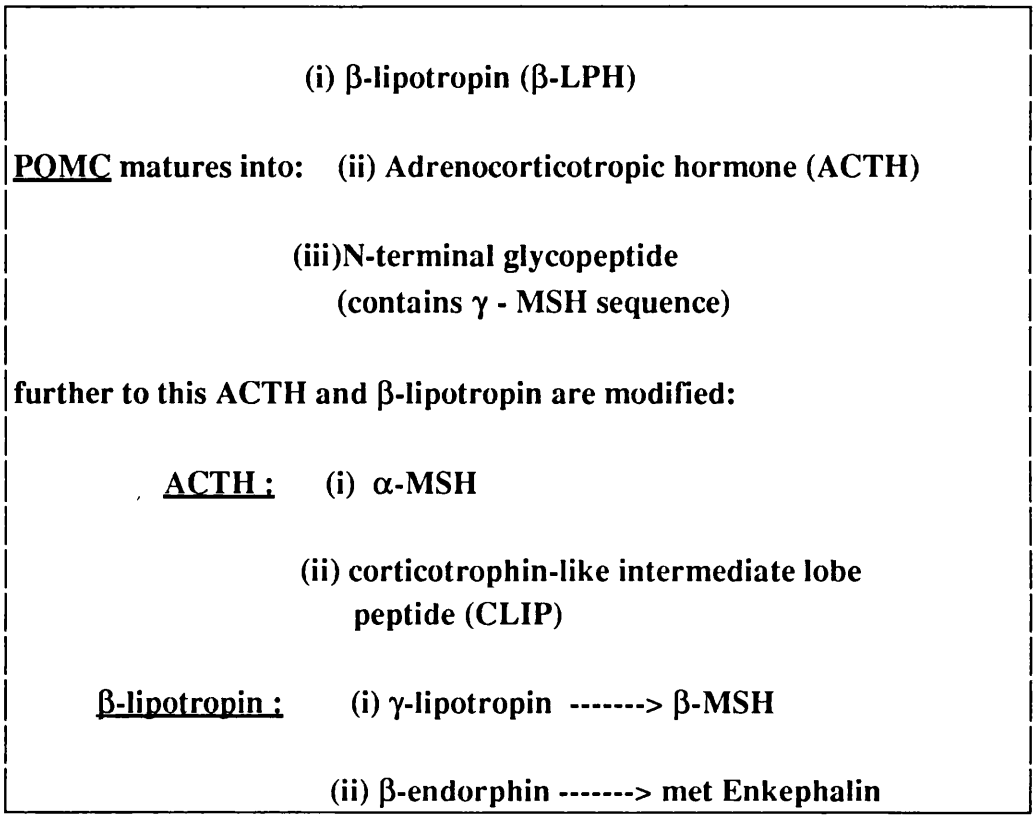

Figure 1.2. Sequence of events following excision of POMC gene and resulting in the formation of the melanotropins.

1.2.1. Biosynthesis of MSH.

In the mammal, MSH is synthesised mainly in the *pars intermedia* (P.I.) of the pituitary gland also in the brain and the *pars distalis* (P.D.). However there is also some evidence of peripheral tissue synthesis such as in the skin, testes and other organs expressing the POMC precursor e.g. placenta and gut. In the P.I. the production of MSH occurs in type 1 cells which are rich in mitochondria and also contain rough endoplasmic reticulum (RER), Golgi apparatus and an abundance of secretory vesicles. The P.I. is poorly vascularised and is innervated by three types of nerve fibre in the mammal (i) aminergic (mainly dopaminergic) (ii) cholinergic and (iii) peptidergic.

The biosynthesis and secretion of MSH from the P.I. is under humoral control of the hypothalamic factors both excitatory and inhibitory. The inhibitory hypothalamic effects are mediated via MSH release inhibiting factors (MIF) e.g. dopamine, GABA, serotonin, enkephalin and somatostatin and excitatory effects via MSH releasing factors (MRF) e.g. (nor)adrenaline and vasopressin. Other regulatory effects on MSH secretion have been suggested to be mediated via direct negative or positive feedback loops. Stress provokes a 3-10 fold increase in circulating ACTH, α-MSH and other POMC peptides, it is thought to act by upsetting the normal balance of stimulatory and inhibitory factors. (See Eberle (1988), Chapter 10).

1.2.1.1. [Nle^4,D-Phe^7] α-MSH.

This is a structural analogue of the naturally occurring hormone which is differentiated by substitution of the Nle^4 and DPhe^7 in the amino acid sequence of α-MSH. It mimics the actions of α-MSH but is 26 times more potent than the native hormone (Tatro *et al.,* 1990) and was used extensively in this work as part of the drug targeting conjugate to target MTX to melanoma cells. Figure 1.1. shows the amino acid sequence of [Nle^4,D-Phe^7] α-MSH.

1.2.2. Functions of MSH.

α-MSH affects pigment cells of amphibians through its effects on melanophores. Pigment cells comprise of melanophores, erythrophores, xanthophores, leuophores and iridophores, (Fujii and Oshima, 1986). Melanophores may be subdivided into dermal and epidermal melanophores both of which possess specific organelles, melanosomes in which brown / black melanin is synthesised and stored. Melanin formation involves production of two types of melanin, eumelanin and phaeomelanin which are

derived from the same precursor tyrosine. The main functions of α-MSH on pigment cells include pigment dispersion, melanogenesis, (Hadley *et al.*, 1987, Levine *et al.*, 1987) differentiation (dendrite formation), proliferation and growth inhibition. Due to this α-MSH is of importance for physiological colour change. The alteration of configuration i.e. with the DPhe^7 significantly affects α-MSH by increasing its potency, (Tatro *et al.*, 1990, Sahm, 1994).

α-MSH induces a marked increase in tyrosinase activity and tumour melanogenesis of B16 melanoma cells whilst retarding the proliferation of growth of these murine melanoma cells (Lee *et al.*, 1972); however, Hadley *et al.*, (1987) found that proliferation of Cloudman S91 monolayer cultures were not inhibited by prolonged exposure to either α-MSH or [Nle^4,D-Phe^7] α-MSH, a finding which was supported by this study.

1.2.3. Melanocortin Receptors.

The existence of multiple melanocortin receptors has been suggested by many, (Tatro, 1990, DeWied and Jolles, 1982, Cannon *et al.*, 1986) and five have been identified to date, (Mountjoy *et al.*, 1992, Chhajlani and Wikberg, 1992, Gantz *et al.*, 1993a, Gantz *et al.*, 1993b and Chhajlani *et al.*, 1993). The melanocortin receptors are guanine nucleotide-binding protein (G-protein)-coupled cell surface receptors through which the POMC-derived peptides e.g.: α-MSH, β-MSH, γ-MSH and ACTH mediate their actions, (Gantz *et al.*, 1993(a)). They are the smallest G-protein coupled receptors known, containing between 297 and 363 amino acids (Mountjoy *et al.*, 1992). Melanocortin receptors are located at many sites throughout the body e.g. melanocytes, adrenal cortex, brain, gut and placenta and a number of functions are associated with each receptor although the functions of the MC4

and the MC5 receptors have still to be fully elucidated, (Gantz *et al.*, 1993(b), Chhajlani *et al.*, 1993).

1.2.3.1. MC1 Receptors:

Mountjoy *et al.*, (1992) identified the murine and human MSH receptor now known as the MC1 receptor simultaneously to Chhajlani and Wikberg's identification of the human MSH receptor (1992).

Mountjoy *et al.*, (1992) stably transfected 293 human embryonic kidney (HEK) cells with the gene encoding the melanoma MSH receptor. The cells were then incubated with α-MSH, [Nle^4,D-Phe^7]α-MSH and ACTH which resulted in a two to threefold elevation in cAMP relative to the 293 cells containing the vector alone. The receptor was specific for peptides with melanotropic activity, responding to [Nle^4,D-Phe^7]α-MSH stimulation more than α-MSH and least of all to ACTH.

Chhajlani and Wikberg (1992) described the insertion of the cloned human MSH cDNA receptor protein into a vector and transient expression in COS-7 cells. This cloned receptor specifically bound an ^{125}I- labelled MSH analogue namely: ^{125}I- [Nle^4,D-Phe^7]α-MSH. The bound ligand could be displaced by the following melanotropic peptides in decreasing order of potency: [Nle^4,D-Phe^7]α-MSH > α-MSH = β-MSH > ACTH > γ-MSH, however it could not be displaced by the non-melanotropic peptide : β-endorphin, findings which all agree with Mountjoy *et al.*, (1992).

Functions of the MC1 receptors:

Northern Blot analysis of the murine and human MSH receptors showed the specific localisation in melanocytes. Chhajlani *et al.*, (1993) have suggested that since the MC1 receptors are only expressed in melanocytes this is the receptor most likely to mediate melanin synthesis and involvement with the growth and pigment production via the melanotropic peptides.

1.2.3.2. MC2 Receptors.

The human MC2 receptor (ACTH receptor) was cloned by Mountjoy *et al.* (1992) using the same technique as described for the cloning of the MC1 (MSH) receptor. Northern blot analysis showed that the cloned receptor was expressed specifically in the adrenal cortex. It was found primarily across the zona fasiculata i.e. the site of glucocorticoid production and also in the cortical half of the zona glomerulosa which is the site of aldosterone production. The function of the MC2 receptor, due to its localisation and also its high binding affinity to ACTH is related to adrenal cortical function, (Mountjoy *et al.*, 1992).

1.2.3.3. MC3 Receptors.

The MC3 receptor was characterised by Gantz *et al.*, (1993a). A major difference in the pharmacological characteristics between the MC1 and the MC3 receptor lies in their respective responses to β-MSH and γ-MSH. Because the MC3 receptor appears to recognise ACTH and α-MSH, β-MSH and γ-MSH equally well, Gantz *et al.*, (1993a) reasoned that the core heptapeptide might be the specific site of the melanocortins that is recognised by the receptor a theory supported by others, Mountjoy *et al.*, (1992) and Chhajlani and Wikberg, (1992). Northern blot analysis performed by Gantz *et al.*, (1993a) showed expression of the MC3 receptors in the brain, placenta and gut tissue but not in melanoma cells or in the adrenal gland. *In situ* studies showed that they are also expressed in the cortex, thalamus, hippocampus and the hypothalamus.

Gantz *et al.*, (1993a) have suggested that the MC3 receptor may partake in mediating some of the putative actions of the melanotropins in higher cortical functions e.g. behaviour. They have also postulated on the possible roles of

the MC3 receptor in the switch in sensitivity of the foetal adrenal gland from α-MSH to ACTH prior to parturition which was observed by Silman *et al.*, (1976) and also the rise in α-MSH levels in maternal circulation in the latter stages of pregnancy reported by Clark *et al.*, (1978).

1.2.3.4. MC4 Receptors.

Gantz *et al.*, (1993b) reported the cloning, expression and gene localisation of a fourth human melanocortin receptor (MC4). This receptor is expressed primarily in the brain and its expression is notably absent from the adrenal cortex (MC2), melanocytes (MC1) and placenta (MC3). It is structurally most similar to the MC3 receptor with which it shares 58% and 76% overall amino acid identity and similarity, respectively (Gantz *et al.*, 1993b).

The functions of this receptor have still to be elucidated although due to its expression in the brain, it is thought to be involved in the central nervous system (CNS) functions and memory.

1.2.3.5. MC5 Receptors.

MC5 receptors described as MC2 receptors by Chhajlani *et al.*, (1993) who first reported their existence, however if the nomenclature of Mountjoy *et al.*, (1992) and Gantz *et al.*, (1993a and 1993b) is followed then they are more correctly called the MC5 receptors. This receptor is expressed in brain tissue but not in melanoma cells. Although the functions of this receptor have not been discovered, it is thought that due to their expression in the brain the MC5 receptors are more likely to mediate the more diverse actions of MSH (Chhajlani *et al.*, 1993). These actions include effects on memory and temperature control (Clark *et al.*, 1985) and modulation of immune inflammatory responses (Cannon *et al.*, 1986).

1.2.4. Uptake of MSH.

The uptake of α-MSH into the cells where it exerts its effects is not easy to characterise due to the difficulty of radiolabelling the hormone and hence tracing the movements of the hormone and its subsequent binding to, and internalisation by, the cell. Therefore the analogue [Nle^4,D-Phe^7] α-MSH is used for the internalisation assay techniques and the assumption is that α-MSH undergoes the same type of process. The experiments of internalisation are described in detail in Chapter 2 and entail the radiolabelling of [Nle^4,D-Phe^7] α-MSH with ^{125}I (Adams, 1993). These studies have led to the conclusion that the uptake of [Nle^4, D-Phe^7] α-MSH in to a cell is brought about by receptor-mediated endocytosis (Goldstein *et al.*, 1979).

1.2.4.1. Endocytosis and Transcytosis:

Knowledge of endocytosis and transcytosis is essential for the development of drug delivery systems when macromolecules, e.g. dextran, albumin, antibodies and hormones, are used as drug or drug carriers. (Poznansky and Juliano, 1984).

Endocytosis is a general term that refers to the process by which cells ingest extracellular materials by trapping them within inward foldings of the plasma membrane that pinch off from the surface to form intracellular vesicles (coated vesicles), (Goldstein *et al.*, 1979). Roth and Porter (1964) first described coated pits and coated vesicles in the mosquito oocyte. They postulated that the uptake of adsorbed proteins from the extracellular fluid (ECF) during yolk formation, was mediated via these structures. Subsequent investigations found that coated pits and vesicles mediate protein uptake in specialised cells of higher animals, (Friend and Farquhar, 1967).

Macromolecules inside these vesicles can be processed through various intracellular organelles and, in some cases, recycled back to the plasma membrane. In polarised cells e.g. epithelial cells and hepatocytes, internalised macromolecules can be transported to the opposite side of the plasma membrane, a process known as transcytosis, (Shen *et al.*, 1992).

Biological pathways have both a passive and active nature and include:

(i) Fluid phase pinocytosis: This is a continuous and non-specific process and the means by which extracellular fluid (ECF) is internalised. Shen *et al.*, (1992) describe this as a passive and non-saturable process.

(ii) Phagocytosis; which is a process of internalisation of large particles and it only occurs in specialised cell types e.g. macrophages and granulocytes, (Shen *et al.*, 1992)

(iii) Endocytosis (receptor mediated and non-receptor mediated):

1.2.4.2. Receptor Mediated Endocytosis.

The subject of receptor-mediated endocytosis has been studied extensively, (Goldstein *et al.*, 1979, Tomlinson, 1987, Basu, 1990 and Shen *et al.*, 1992). 10% plasma membrane-associated proteins (receptors) can have special affinity for a variety of molecules including peptides and proteins, known as ligands, (Shen *et al.*, 1992). It is the means by which the melanotropic peptides enter cells, a coupled process by which the peptides are first bound to specific receptors (MC1-MC5) and then rapidly internalised by the cell. Following binding to the receptor on the cell surface, the ligand-receptor complex is internalised via (a) clathrin-dependent or (b) clathrin-independent endocytotic process.

Clathrin-dependent pathway:

Subsequent to the accumulation of ligand-receptor complex in the clathrin-coated regions, these coated pits invaginate from the plasma membrane and form coated vesicles by pinching inward from the membrane. Once the coated vesicles are formed, the clathrin coats are lost resulting in the formation of smooth membrane vesicles, known as endosomes, (Shen *et al.*, 1992). Examples of ligands entering cells this way include: low-density lipoprotein (LDL), transferrin (Tf) and insulin.

Clathrin-independent pathway:

This pathway refers to the formation of vesicles from the invagination of non-clathrin-coated plasma membrane. In contrast to the clathrin-dependent pathway this process occurs in receptors with a low population and a slow rate of internalisation and the exact mechanism of internalisation is still largely unknown, (Shen *et al.*, 1992). Ligands such as IgG-ferritin, cholera toxins and ricin enter cells in this way.

1.2.4.3. Receptor-Ligand Internalisation.

In some cases internalisation may not be required for the physiological function of the ligands because the binding alone may be sufficient to initiate the actions associated with the ligand e.g. binding of α-MSH to MSH receptors results in increased levels of cAMP, prior to internalisation, (Mountjoy *et al.*, 1992, Chhajlani and Wikberg, 1992). The intracellular sorting and processing of ligands is controlled by compartments which occur in the following sequence: early endosomes, late endosomes, prelysosomes and lysosomes.

Endosomes and lysosomes are known to be the major acidic compartments of the cell ranging from pH 6.0-4.5, respectively. If ligands are dissociated from

their receptors in these acidic compartments, they are further transported and degraded in lysosomes and their receptors can be recycled e.g. LDL (Basu, 1990).

Ligands that remain associated with the receptor will either (i) recycle with their receptor e.g. transferrin or (ii) the ligand-receptor complex will go to the lysosome where both will be degraded e.g. epidermal growth factor. The final option is for the receptor to be degraded in the lysosome while the ligand is transported across the cell e.g. immunoglobulin A, (Shen and Ryser, 1979, Basu, 1990).

Figure 1.3. shows the different processes of endocytosis.

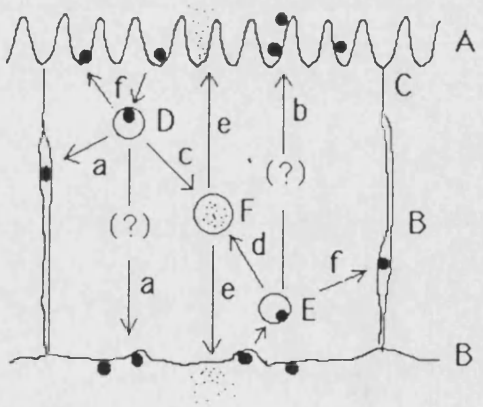

Figure 1.3. A simplified scheme of endocytosis and transcytosis in epithelial cells. Ligands can bind to either the apical (A) or the basolateral (B) membrane. These two membranes are separated by the tight junction (C). After internalization, membrane-bound ligands will be located in the apical (D) or the basolateral (E) endosome. Endosome-entrapped ligands can be further processed via the following pathways: (1) apical-to-basal (a) or basal-to-apical (b) transcytotic pathway which involves still unknown compartments (?). (2) endosome-to-lysosome pathways (c and d), followed by the degradation in lysosomes (F) and releasing of degraded products via exocytotic pathways (e); and (3) recycling pathways (f) which may or may not involve the Golgi apparatus. **(Adapted from Shen *et al.*, 1992)**

1.2.5. Clinical significance of α-MSH.

α-MSH is produced by and is active in the CNS of animals where it has effects on memory, adaptation, nerve generation, fever control and also during the foetal development. It has been postulated (Eberle, 1988) that there are five areas where α-MSH-related compounds could ultimately be used as pharmaceuticals with clinical relevance namely; treatment of pigment disorders, diagnosis and therapy of melanoma, treatment of certain types of dementia. It is also associated with the enhancement of nerve-regeneration and protection from nerve-damage and in the control of fever and inflammation.

1.2.5.1. Treatment of pigment disorders:

Hadley and co-workers (1987) and Levine *et al.,* (1987) have proposed the use of [Nle^4,D-Phe^7] α-MSH in the correction of acquired integumental hypopigmentary disorders and also as an artificial suntan agent. However the results of *in vitro* work are not necessarily representative of the *in vivo* situation and a major drawback of this therapy is the possibility of inducing melanoma in the patient.

1.2.5.2. α-MSH in the diagnosis and therapy of melanoma:

It has been suggested (MacKie, 1983) that as melanoma tumours are dependent upon the endocrine system, α-MSH and other POMC-related peptides may be involved in the aetiology of the disease. α-MSH may be exploited by determination of its plasma levels, as increased plasma levels would indicate a more progressed disease state, and also the detection of α-MSH receptors on the biopsies of tumours.

The first line of treatment for melanoma is surgical, however where this is not possible either due to the advanced state of the disease or inaccessibility of the site, radiotherapy is a possibility. It is known (Cobb, 1956, Seiji and Itakura,

1966) that melanotic melanoma is more radiation-resistant than any other tumour, probably due to the protective effect of melanin brought about by the stable free radical nature of melanin. Pretreatment with chlorpromazine (CPZ) increases the sensitivity of melanoma by binding and thus inactivating, melanin. Mishima (1973) proposed the combination of CPZ and boron neutron capture therapy.

1.2.5.3. α-MSH in the treatment of dementia:

Due to the actions of α-MSH peptides as potent neuropeptides they have been investigated with regard to their ability to improve memory of the elderly as they were previously successful in stimulating both behaviour and memory of experimental animals. One of the α-MSH/ACTH analogues: Met(O_2)-Glu-His-Phe-*D*-Lys-Phe-NH-$(CH_2)_8$-NH_2 has been shown to be very active at stimulating the cholinergic system (Geiger *et al.*, 1986) and therefore may be useful as a potential anti-dementia drug.

1.2.6. Cytotoxic MSH complexes.

The subject of hormone-drug conjugates has been the subject of an extensive review by Varga, (1985).

The direction of a toxin specifically into tumour tissues would have obvious advantages in terms of selectivity of drug action.

Previously there have been six types of conjugations in combination with MSH derivatives (i) daunomycin, (ii) N-nitrosocarbamates, (iii) diphtheria toxin, (iv) cytotoxic T cells and (v) melphalan, and (vi) ^{111}In. In this project a seventh combination has been synthesised and tested, namely the use of methotrexate (MTX) conjugated to the analogue of α-MSH, [Nle^4,D-Phe^7] α-MSH.

1.2.6.1. *Daunomycin:*

The conjugate of β-MSH with daunomycin exhibits a threefold increase in potency towards Cloudman S91 cells relative to free daunomycin, (Varga *et al.*, 1977). The specificity of its action is demonstrated by the lack of toxicity towards 3T3 fibroblast cells. The data are based solely on *in vitro* studies and *in vivo* data may or may not support these findings.

1.2.6.2. N-Nitrosocarbamoyl-α-MSH compounds:

By coupling the C-terminal fragments of α-MSH to 2-chloroethylnitroso-carbamoyl, products with distinct *in vivo* inhibitory action on melanoma xenografts are yielded, (Jeney *et al.*, 1986). Concentrations of 50-100mg/kg are necessary for significant growth inhibition in mice.

1.2.6.3. Diphtheria toxin-α-MSH fusion protein:

Murphy *et al.*, (1986) constructed a chimeric diphtheria toxin α-MSH gene in which the toxin receptor binding domain is replaced by the α-MSH gene sequence thus guiding the toxin specifically to melanoma cells. *In vitro* cytotoxicity experiments on human NEL-M1 cells proved the conjugate was selectively toxic to these cells whereas control cells were unaffected. *In vivo* studies have yet to confirm the usefulness of this conjugate however a possible mode of resistance in humans may be due to the immunisation programme of humans in some countries, e.g. United Kingdom, which in turn may make it intolerable. Other toxins that have been suggested instead include ricin and abrin.

1.2.6.4. α-MSH/ Antibody conjugates directed to cytotoxic T cells:

This method was first introduced by Liu *et al.*, (1988) and is based on the findings that MAbs to the invariant component of the T cell receptor (TCR) induce cytolytic activity of these cells. The conjugation of [Nle^4,D-Phe^7] α-

MSH to these antibodies seems to promote lysis of melanoma cells, B16 and 6B7 and human M1313 melanoma cells (Liu *et al.*, 1988)

1.2.6.5. Melphalan:

Morandini *et al.*, (1994) proposed the introduction of melphalan into α-MSH fragments, two C-terminal fragments (Pep3 and Pep4) and two central fragments (Pep1 and Pep2). This led to an examination of their selectivity as well as cytotoxicity against melanoma, carcinoma and fibroblast cells. The final analysis was that a clear, selective cytotoxic effect on melanoma cells could be observed with Pep1 and Pep 2. The cytotoxic effect on melanoma cells is likely to be mediated via α-MSH receptors, since there was an inhibition of cytotoxic effects in melanoma cells in the presence of an α-MSH agonist.

1.2.6.6. ^{111}In:

Apart from the obvious advantages of selectively targeting therapeutic agents to melanoma, a significant improvement in patient mortality rates could be effected by tackling the imaging of metastases. Once localised, these could then be surgically removed rather than waiting for symptoms to arise at a point where surgery is no longer an option. Bard *et al.*, (1986) have successfully managed to target ^{111}In to Cloudman S91 melanoma cells both *in vitro* and *in vivo* by use of α-melanocyte-stimulating hormone (α-MSH). The coupling of α-MSH diethylenetriaminepenta-acetic acid (DTPA) followed by labelling with ^{111}In gave rise to MSH-DTPA-^{111}In. This was then incubated for 3 hours with Cloudman S91 cells where the presence of 60nM α-MSH inhibited the binding of MSH-DTPA-^{111}In and hence showed the latter's specific affinity for MSH receptors. DBA/2 mice were used for in vivo work, intraperitoneal injection of MSH-DTPA-^{111}In and a control polyalanine derivative PA-DTPA-^{111}In were both tested. Tissue distribution showed that

radioactivity delivered as MSH-DTPA-^{111}In was selectively retained by tumour tissue.

Further studies by Bard *et al.*, (1990), employed two molecules of MSH with DTPA forming: *bis*-MSH-DTPA which was then radiolabelled with ^{111}In. Although this was equally effective *in vitro* to their previous conjugate, there were enhanced tissue specificity effects in DBA/2 mice bearing the same tumour.

1.2.7. Biotransformation and Inactivation of MSH.

Once the melanotropins are released from their cells of origin they may undergo biotransformations which modify their innate biological properties. This process may occur via the cleavage of single amino acid residues. α-MSH breakdown *in vitro* is approximately exponential with a mean half life of 39 minutes for a sample at 37°C and 54 minutes at 4°C in RPMI-FCS media and in human plasma the half life is 25 minutes at 37°C and 125 minutes at 0°C, (Eberle, 1988). Blood clearance of α-MSH is more important in skeletal muscle and skin than in the liver and kidneys as shown by occlusion experiments.

The advantages of [Nle^4,D-Phe^7]α-MSH over the native hormone lie in its resistance to inactivation by frog and rat serum enzymes, (Castrucci *et al.*, 1984). The D-Phe^7 portion of the [Nle^4,D-Phe^7]α-MSH adds stability against biotransformation and degradation where the α-MSH is susceptible at the Phe^7-Arg^8 bond as a primary source of cleavage. Once cleavage has occurred the fragments are attacked by exopeptidases and degraded to free amino acids, (Tatro *et al.*, 1990).

1.3. Cytotoxic Drug Classification.

In general the groups of cytotoxic drugs are characterised by their mechanism of action on the target cells and fall into the following five groups:

1.3.1. Alkylating agents:

The alkylating agents act by arresting cell division by alkylating and cross-linking guanine bases in DNA e.g. nitrogen mustards., cyclophosphamide and chlorambucil. Cyclophosphamide is a biologically inactive nitrogen mustard analogue which requires oxidation to express its alkylating activity. It is used over a wide range of clinical activities e.g. lymphomas, sarcomas of soft tissue and bone and carcinomas of the breast, lung, ovary, cervix and colon, (Carter, 1975).

1.3.2. Nitrosoureas: (Chloroethylnitrosoureas)

These agents act principally through alkylation of DNA although carbamoylation of proteins by isocyanates generated from the decomposition of nitrosoureas, may also contribute to their antitumour activity or toxicity, (Schein *et al.*, 1978, Gallant *et al.*, 1993).

Clinical activity has been demonstrated in brain tumours, lymphomas, melanoma and gastrointestinal cancers, (Schein *et al.*, 1978).

1.3.3. Antimetabolites:

The antimetabolites impair the synthesis of purine and pyrimidine bases by preventing the incorporation of the bases into nucleic acids e.g. methotrexate, mercaptopurine and azathioprine. Generally the pharmacokinetics of these agents resemble the natural substances with which they compete or replace and hence inhibit cell metabolism and growth, (Balis *et al.*, 1983).

Methotrexate (MTX) is a folate analogue which binds more tightly to dihydrofolate reductase (DHFR) than does folate. The conversion of dihydrofolate to tetrahydrofolate is thereby inhibited and the pool of reduced folates required for the synthesis of thymidylate and purines is depleted, (Shen and Azarnoff, 1978).

Therapeutic indications for MTX include, choriocarcinoma, non-Hodgkin's lymphomas, osteosarcoma, metastatic meningeal neoplasms, some brain tumours, the histiocytoses and carcinomas of the breast, head and neck, lung, ovary, cervix and bladder, (Bertino, 1975).

Cytarabine (Cytosine Arabinoside) is another antimetabolite which, after intracellular conversion, functions as an antagonist of the physiological substrate deoxycytidine triphosphate and also competitively inhibits DNA polymerase. Cytarabine triphosphate is also incorporated to a limited extent into both RNA and DNA, (Chu, 1971).

It is used primarily for the treatment of leukaemia and lymphoma and is one of the most active agents against acute non-lymphocytic leukaemia, (Gale, 1979).

5-Fluorouracil (5-FU) kills cells by inhibition of thymidylate synthetase thus depleting the cell of thymidine nucleotides and thereby inhibiting DNA synthesis and impairing RNA metabolism and function, (Balis *et al.*, 1983).

5-Fluorouracil is active against gastrointestinal, breast, pancreatic, ovarian and head and neck carcinomas, (Myers *et al.*, 1976).

1.3.4. Antibiotics:

Antibiotics bind to DNA and prevent replication e.g. daunorubicin and actinomycin D. Doxorubicin (adriamycin) and daunorubicin (daunomycin) are glycosidic antibiotics found in different species of the fungus

Streptomyces. Structurally they consist of a planar tetracycle ring linked by a glycosidic bond to the amino sugar, daunosamine, (Young *et al.*, 1981). Both drugs act primarily by intercalation with DNA, although other binding or free radical reactions may explain some of the toxicity and antitumour effects. Doxorubicin is clinically active against a wide range of malignancies e.g. acute leukaemias, non-Hodgkin's lymphomas, Hodgkin's disease and many carcinomas. Daunorubicin is mainly used for acute leukaemias, (Young *et al.*, 1981).

1.2.5. Vinca Alkaloids:

Alkaloids arrest metaphase of the cell cycle and hence prevent cell proliferation e.g. vinblastine and vincristine. The vinca alkaloids are naturally occurring, dimeric indole derivatives initially isolated from the periwinkle plant, (Balis *et al.*, 1983). Although the antitumour effect of the vinca alkaloids has been largely attributed to their ability to arrest mitosis by dissolution of microtubular mitotic spindles, they also inhibit a variety of biosynthetic pathways which possibly contributes to their cytotoxicity, (Creasey, 1978).

Vinblastine is used mainly in the treatment of Hodgkin's disease and testicular cancer. Vincristine has a much broader spectrum of action against acute lymphocytic leukaemia, the lymphomas, breast cancer and a number of paediatric solid tumours. Vindesine has shown activity against solid tumours e.g. colorectal cancer, lung cancer and breast cancer, (Balis *et al.*, 1983).

1.4. Methotrexate.

Methotrexate is an antimetabolite which exerts cytotoxic actions in the S phase of the cell cycle, maximal effects are exhibited in the logarithmic growth phase when the cells are rapidly proliferating. The effect of MTX on the cloning efficiency of cells was clearly related to the growth rate of the culture from which the cells were taken for testing. MTX kills cells at 6.7 times the rate and produced a 20 fold greater inhibition of deoxyuridine incorporation into DNA from logarithmic as opposed to plateau phase cells, (Hryniuk *et al.*, 1969).

MTX was first synthesised in 1949 by Seeger *et al.*, and first clinically used in 1953 in the treatment of childhood acute lymphoblastic leukaemia (ALL). It has a number of unique features which are responsible for its popularity in research and treatment. MTX is active in a wide scale of different malignant diseases for example: childhood acute lymphoblastic leukaemia (ALL), (van der Kleijn, 1984), osteogenic sarcoma (Embleton *et al.*, 1981), non-Hodgkin's lymphomas, osteosarcoma (Balis *et al.*, 1983), human small cell lung cancer (Curt *et al.*, 1985), treatment of psioriasis (Chabner, 1982) an effect which is synergistically enhanced by oral psoralen photochemotherapy (PUVA) (Morison *et al.*, 1982) and rheumatoid arthritis (Furst and Kremer., 1988).

It has the largest dose range of application (3-33,600 mg/m^2) (Borsi and Moe, 1987) and many different routes of administration (i.v., i.m., p.o., i.thecal. and i.ventricular).

It is the only antineoplastic agent which has an antidote (folinic acid) in clinical use, (Bernard *et al.*, 1991).

The determination of MTX concentration in serum is a clinical routine and its level in other biological fluids (CSF, urine) is easily measured.

1.4.1. Structure.

Methotrexate (MTX) is classified as an antimetabolite and is the 4-NH_2 N-10 methyl analogue of folic acid. MTX consists of three major parts similar to the physiological folate co-factors, (Seeger *et al.*, 1949):

(i) a multi-ring pteridine group, (ii) para-aminobenzoic acid and (iii) terminal glutamic acid residue. Figure 1.4. shows the structures of MTX and folic acid.

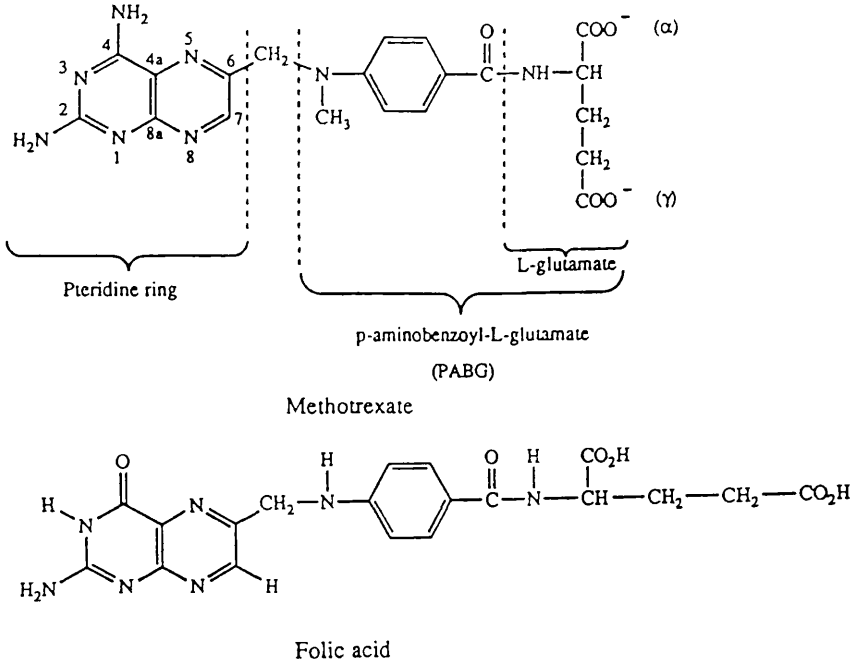

Figure 1.4. This shows the structures of methotrexate and folic acid.

1.4.2. Uptake of MTX.

MTX is a relatively large (FW:454.5), polar, lipid-insoluble molecule and transport into the cells occurs via one of two mechanisms, (Warren *et al.*,1978).

The first and most common pathway of entry is an active process i.e. it requires energy and it is carrier mediated and is saturable, (Goldman *et al.*,

1968, Huennekens and Henderson, 1975). MTX in addition to leucovorin, competes for uptake into the cell. *In vitro* evidence (Kamen *et al.*, 1988) suggests that the internalisation could be mediated via a surface membrane receptor (folate binding protein which has the properties of a membrane receptor) that recycles.

The internalisation process involves several steps, folate binding to the membrane receptor, the ligand-receptor complex then moves into the cell and once inside the cell the ligand is released from the receptor in an acidic intracellular compartment and moves into the cytoplasm after which the unoccupied receptor returns to the cell surface. This membrane folate binder has a high affinity for 5-methyltetrahydrofolic acid (utilised by cells for the biosynthesis of methionine, serine, deoxythymidylic acid and purines) but at least a 10 fold higher affinity for folic acid and a 5-10 fold lower affinity for MTX (Kamen and Capdevila, 1986).

The second process is not as well documented and is thought to involve a diffusion of molecules of MTX (Warren *et al.*, 1978, Hill *et al.*, 1979). This process occurs in the presence of very high concentrations of MTX (> 20mM). Although it is less efficient due to its passive nature, the advantage of this route of entry is that it enables the uptake of MTX into cells where this would otherwise be impossible due to the saturation of uptake pathway caused by the high extracellular concentrations of MTX.

1.4.3. Mechanism of Action of MTX.

Once inside the cell, MTX binds to DHFR and thus inactivates this enzyme. This is significant because DHFR is a vital enzyme in the reduction of dihydrofolic acid (FH_2) to tetrahydrofolate (FH_4) and thus maintains the intracellular levels of the latter. The result of inhibition of DHFR is a

diminished level of FH_4 which in turn causes depletion of thymidylate and purine synthesis which require N^{5-10} methylene FH_4 and N^{10} formyl FH_4 respectively, (Chabner and Young, 1973). Concentrations of 10^{-7}M MTX or greater will be sufficient to block both of these reactions and the consequence of inhibition of either reaction results in cessation of DNA synthesis. In order to ensure that MTX works most effectively to halt the reduction of FH_2, it is imperative that an excess of MTX is present to combat the competition for substrate that will inevitably ensue as the intracellular level of FH_2 rises. Levels of MTX in excess of DHFR must also be present to ensure inhibition of enzyme activity (Bertino, 1975, Jolivet *et al.*, 1983).

1.4.4. Metabolism of MTX.

Methotrexate is metabolised to (i) polyglutamates, (ii) 7-hydroxy-methotrexate (7-OH-MTX) and (iii) 4-amino-4-deoxy-N^{10}-methylpteroic acid (DAMPA).

Intracellularly MTX is comprehensively catabolised to polyglutamate derivatives (Jolivet *et al.*, 1983) and the consequences of this are as follows:

1. MTX polyglutamates accumulate to a higher equilibrium state with extracellular drug than does the parent compound.
2. MTX polyglutamates have either an equal if not higher affinity for DHFR than free MTX and they appear to dissociate less readily which implies a lower threshold of inhibition.
3. The intracellular retention time of polyglutamates increases with chain length, however, it is independent of the extracellular concentration of MTX.
4. The cytotoxicity of MTX can be augmented by the chemical addition of glutamyl residues which in turn extend the inhibitory enzymatic effects to include not only DHFR but also thymidylate synthetase (Szeto *et al.*, 1979)

and aminoimidazolecarboxamide ribonucleotide transformylase (Baggott, 1983).

The biotransformation from MTX to 7-OH-MTX may be mediated via hepatic parenchymal cells. 7-OH-MTX effects MTX by competing with MTX for uptake however it has one hundred fold less activity than MTX to inhibit DHFR. Due to its high level of insolubility in aqueous solution it has been implicated as a possible mediator of potentially fatal renal failure in high dose MTX (HD-MTX) therapy. The advantage of 7-OH-MTX is that the polyglutamyl derivatives formed are retained longer intracellularly than 7-OH-MTX and bind tightly to DHFR (Lankelma *et al.*, 1978, Bremnes *et al.*, 1989, Fahrig *et al.*, 1989).

DAMPA exhibits two hundred fold less activity than MTX in inhibiting DHFR and its biological importance is thought to be minimal (Jolivet *et al.*, 1983).

1.4.5. Elimination of MTX.

The elimination of MTX is biphasic, bile is the major excretory route for MTX (50%) and 7-OH-MTX (3.6%) (Bremnes *et al.*, 1989).

Plasma disappearance of MTX occurs in 3 phases:

1. Initial elimination due to distribution of MTX into tissues and also into bile and urine.
2. Drug elimination via biliary and renal excretion (postulated enterohepatic cycling of the drug).
3. Intracellular confinement of MTX as polyglutamates and strong binding to target enzymes.

Elimination of 7-OH-MTX favours elimination in the bile due to the fact that it is less water soluble and more lipophilic than MTX (Fahrig *et al.*, 1989).

1.4.6. Methotrexate Resistance.

MTX resistance can occur in many ways including a reduction in affinity of DHFR for MTX, increased levels of DHFR due to gene amplification of DHFR synthesis, decreased membrane transport of MTX, decreased formation of MTX polyglutamates and varying rates of thymidylate synthesis.

1.4.6.1. Reduced affinity of DHFR for MTX:

This mechanism of resistance may occur naturally or may be brought about by the chemical modification of DHFR by mutation of eight amino acids at positions pertinent to the hydrogen bonding or hydrophobic interactions with MTX (Thillet *et al.*, 1988).

1.4.6.2. Increased levels of DHFR due to gene amplification:

Gene amplification may occur *in situ* (Juraskova, 1988) and this mechanism of resistance is investigated by Assaraf and Schimke, (1987) using fluoresceinated MTX and flow cytometry to identify MTX transport deficiency. In terms of its toxicity towards oxygenated or hypoxic tumour cells, MTX shows no preferential toxicity (Teicher *et al.*, 1981). However rodent cell lines can develop resistance to MTX during hypoxic stress i.e. O_2 concentration <10 ppm for 24 hours prior to reoxygenation, (Sanna and Rofstad, 1994) and the mechanism of drug resistance is thought to be mediated via the amplification of the DHFR gene (Rice *et al.*, 1987) although this was not confirmed by other studies (Wilson *et al.*, 1989, Sakata *et al.*, 1991, Kalra *et al.*, 1993).

1.4.6.3. Decreased membrane transport of MTX:

This may occur in cases where the active uptake system has been affected and there is a reduction in the affinity of the carrier for MTX, (Zager *et al.*, 1973, Hill *et al.*, 1979, Underhill and Flintoff, 1989). The transport kinetics of MTX satisfy the criteria of the carrier model and maintains, at least in part, the same transport mechanism as folic and folinic acid. The elucidation of these transport characteristics may help to clarify the nature of transport defects which have been noted in several lines of malignant cells, (Goldman *et al.*, 1968)

1.4.6.4. Decreased formation of MTX polyglutamates:

Although it is clear that polyglutamation allows enhanced accumulation of free MTX and extends drug action in addition to promoting inhibition of more enzymes, the evidence that decreased polyglutamation accounts for resistance is still preliminary (Jolivet *et al.*, 1983). This mechanism of resistance is not well characterised biochemically but was reported for a human breast cancer cell line (Cowan and Jolivet, 1983).

1.4.6.5. Altered rates of thymidylate synthesis:

The lower the rate of thymidylate synthesis the less susceptible a cell line will be to MTX because the rate of synthesis is an important determining factor of MTX cytotoxicity, (Moran *et al.*, 1979, Haber *et al.*, 1993).

1.4.7. Degradation of MTX.

In the pH region of 7 there seems to be a first order rate constant and the minimum degradation rate was observed at pH 6.6-8.2 . Hansen *et al.*, (1983) obtained a pH rate profile from first order kinetic plots and demonstrated a

maximum stability of MTX in aqueous solution at pH 7. In the pH range of 7-7.5 the rate of degradation was 0.04 $days^{-1}$ but at pH >6.5, N^{10}-methyl-folic acid was the only degradation product formed (Hansen *et al.*, 1983).

1.4.8. "Rescue" of cells after MTX administration:

There are many ways in which cells may be "rescued" after administration of MTX:

(i) Delivery of the drug to the cell may be decreased by hydrolysis of the extracellular drug (carboxypeptidase G1) or by physical means (charcoal absorption), (ii) increase in cellular dihydrofolate concentration (sufficient to displace MTX), (iii) administration of hypoxanthine and thymidine, (Moran *et al.*, 1979), (iv) indirect rescue could be mediated via the use of protein synthesis inhibitors e.g. asparaginase. Normal cells can increase their production of protein but tumour cells cannot, and therefore experience the synergistic effects of the sequential combination. The most well known method of rescue however is, (v) folinic acid (citrovorum factor). Schoenback *et al.*, (1950) first reported on the reversal of MTX and aminopterin toxicity by folinic acid. The exact mechanism of action is unclear although it may be mediated by one of the following mechanisms (a) competitive inhibition of entry of MTX in to the cell (b) decreased polyglutamation of MTX arising from competition at the level of folylpolyglutamate synthase and / or (c) provision of reduced folate cofactors thereby preventing the blockage of tetrahydrofolate synthesis within the cells. The administration of folinic acid has also been studied to gain the most effective regimen for patients on high dose MTX therapy or with compromised renal function. Although many differences have been observed between the *in vitro* and *in vivo* treatment

regimens, these were minimised as much as possible by Bernard *et al.*, (1991) who examined the effects of folinic acid (FA) on MTX.

An inverse relationship was noted between the degree of MTX cytotoxicity reversal and duration of time interval between MTX and FA administration. Between 18 and 24 hours after MTX administration, FA could still effectively act to decrease the cytotoxic effects however at time intervals greater than this, FA was not able to do so. By decreasing the time interval, MTX cytotoxicity was partially or even totally reversed by FA. This was however dependent on the cell line tested and the ratio of FA:MTX, (Bernard *et al.*, 1991).

1.4.9. Side effects of MTX.

The side effects of MTX relate to the fact that MTX inhibits the growth of all rapidly dividing tissue. The side effects most notably associated with MTX therapy include: leukopenia, thrombocytopenia and reticulocytopenia, (Condit, 1971). All replicating forms in the bone marrow are affected and although recovery follows in the next few days, this may adversely affect patients who have a folate deficiency or impaired marrow function.

The toxicity of MTX may also be enhanced by impaired renal function and the presence of compromised kidney function is a major indication for the use of citrovorum factor rescue (Bleyer, 1981, Bertino, 1975), although fever has also been reported with high dose MTX therapy even in the presence of citrovorum factor (Gottlieb *et al.*, 1970).

Moderate doses of MTX may result in mucositis but the degree of this is due to both the dose and duration of drug administration (Jolivet *et al.*, 1983).

High dose (HD) MTX therapy has definite antitumour activity in various types of leukaemia e.g. osteosarcoma, non-Hodgkin's lymphoma, in

adenocarcinoma of the head and neck and in small cell lung cancer, (Frei *et al.*, 1980). HD MTX therapy i.e. 1-30 g/m^2, duration of infusion (range 6-42 hours), and frequency of administration (range weekly to every 3 to 4 weeks) in the presence of leucovorin rescue, is usually well tolerated although toxicity varies with the pretreatment characteristics of the patient and dosage regimen used (Hryniuk and Bertino, 1969).

For each target tissue there is a critical minimum extracellular level (concentration threshold) and a critical minimum duration of exposure (time threshold), both of which must be exceeded for toxicity to occur. The severity of toxicity is directly proportional to the duration of MTX exposure beyond the time threshold and relatively less dependent on the magnitude of MTX elevation above the extracellular concentration threshold, (Balis *et al.*, 1983). Nausea, anorexia, vomiting and occasionally diarrhoea may also follow MTX administration especially if high doses are given (1-5 mg/kg), (Bertino, 1975). Toxic doses may lead to gastrointestinal ulceration and bleeding. The occurrence of skin rashes is common in 10-20% of patients and varies in severity from a pruritic type rash to vasculitis and widespread herpetiform skin eruption, (Bertino, 1975). Hair loss may occur in 5-10% of patients especially older patients. The two types of liver damage associated with the administration of large doses and long duration of MTX are: (i) a reversible transient toxicity and (ii) hepatic fibrosis, respectively, (Bertino, 1975, Jolivet *et al.*, 1983). Left upper quadrant pain, postulated by Hryniuk and Bertino (1969) to be due to splenic capsule inflammation has been reported in leukaemic patients treated with large doses of MTX. Unexpected side effects may be due to the binding of MTX to melanosomes (Wilczok *et al.*, 1990). Finally MTX is known to be a potent abortifacient especially in the first trimester. It has also been reported to impair spermatogenesis, although this

returned to normal after therapy, (Jolivet *et al.*, 1983) and may be mutagenic (Bertino, 1975).

1.4.10. Augmentation of MTX cytotoxicity:

Goldman *et al.*, (1968) discovered that sodium azide and iodoacetate prevented efflux of MTX from cells and therefore enhanced its toxicity. Vincristine increases the intracellular levels of MTX (Zager *et al.*, 1973) and is used in combination therapy. While depletion of thymidine and hypoxanthine, in tissue culture, from the medium prevents tumour cells from salvaging them and hence contributes to toxicity (Haber *et al.*, 1993).

1.5. Targeting of MTX:

Methotrexate exhibits many limitations in terms of (i) toxicity, (ii) resistance, (iii) metabolism, (iv) limited access to sites in the body, (v) short half life and (vi) large volume of distribution.

To overcome these problems a structural analogue of MTX e.g. trimetrexate, has been used either to overcome MTX resistance (Romanini *et al.*, 1989) and also in combination with 5,10-dideazatetrahydrofolate (DDATHF) and 10-propargyl-5,8-dideazafolate (PDDF) to exert synergistic effects (Gaumont *et al.*, 1992). The other solution to circumvent some of the intrinsic problems associated with the use of MTX involves structural variations on the basically efficacious molecule for example the chemical conjugation to: antibodies, high molecular weight dextrans, bovine serum albumin and hormones which has formed the basis for reviews by Sezaki and Hashida (1984) and Sinko *et al.*, (1987).

1.5.1. Antibody linkage to MTX:

Many different studies have been performed on the effects of conjugating, directly or indirectly, MTX to antibodies raised against a particular target antigen expressed by the cells in question, (Ghose and Blair, 1978, Garnett *et al.*, 1983, Kawashima *et al.*, 1994, Endo *et al.*, 1987, Endo *et al.*, 1988, Hudecz *et al.*, 1993).

MTX has been seen as a suitable candidate for conjugation with antitumour antibodies because the time dependent nature of its cytotoxic activity may be compatible with the slow kinetics at the tumour site of the i.v. administered antibodies (Halpern *et al.*, 1983).

1.5.1.1. Direct linkage of MTX to monoclonal antibodies:

In the direct conjugation of MTX to monoclonal antibodies of a mouse mammary tumour (MM46), Endo *et al.*, (1988) found that the active ester reacts not only with the amino groups but also with carboxyl groups to give conjugates with varying bond stability. These differences in bond stability have lead to subsequent differences in the uptake systems for the conjugates.

The amide bond-linked MTX is taken up by the cells via endocytic internalisation whereas the more unstable bond (ester-linked) tends to release the MTX extracellularly and hence this MTX enters via the active uptake pathway. The latter mechanism contributes to the non-specific cytotoxicity of the IgG-MTX conjugates. Treatment with hydroxylamine decreases the cytotoxicity of aMM46-MTX conjugate by one sixth of the untreated conjugate, due to its effect of the extracellularly released MTX. It would be expected that free MTX reaches the cytosol more efficiently than conjugated MTX whose entry depends on many factors including: (i) efficiency of antigen-mediated endocytosis, (ii) lysosomal digestion of IgG-MTX and (iii)

the permeability of the lysosomal membrane to digested IgG-MTX molecules. Those results suggest that an oligopeptide spacer between the antibody and MTX would enhance the activity of the conjugates.

1.5.1.2. Indirect linkage of MTX to monoclonal antibodies:

Due to the fact that there are only a small number of functional groups available per antibody molecule which may be successfully used for chemical coupling, without significant loss of antibody-binding activity, carrier molecules have become very popular, (Garnett *et al.*, 1983). Indirect conjugation of drug to antibody i.e. by use of a carrier may help to overcome the limitations in number of drug molecules capable of direct attachment to the antibody. Human serum albumin (HSA), is commonly used as a carrier as it is relatively stable in aqueous media and has a large number of amino groups in addition to a single thiol group which makes it a good choice (the latter characteristic is important as it allows only single antibody binding), (Sezaki and Hashida, 1984).

Work has been done by Garnett *et al.*, (1983) using the carrier-linked MTX (MTX-HSA) chemically coupled to a monoclonal antibody raised against human osteogenic sarcoma cell line, 791T. Although this drug-carrier-antibody conjugate resulted in some specificity against antibody reactive cell lines and also toxicity which was equipotent to free MTX, it was still necessary to investigate whether: (i) the *in vitro* results were representative of an *in vivo* situation and (ii) the uptake and subsequent mechanism of action of the conjugate was similar or dissimilar to that of the free MTX.

To mimic the *in vivo* situation, both $(MTX_{32}\text{-}HSA)_{1\text{-}3}$-791T/36 and MTX were incubated with 791T cells for 15 minutes before removal of unbound material and subsequent assessment of cytotoxicity. This brief exposure was

devised to represent the action in the vascular system, and the results showed a higher degree of cytotoxicity of the $(MTX_{32}\text{-}HSA)_{1\text{-}3}$-791T/36 over the free MTX. By competition binding of the $(MTX_{32}\text{-}HSA)_{1\text{-}3}$-791T/36, in the presence of free antibody, with antibody sensitive and antibody-insensitive cells, it was shown that the cytotoxic actions of the conjugate were reduced in the former but not in the latter. This demonstrated that antibody binding was crucial for selective cytotoxicity.

Further studies on $(MTX_{32}\text{-}HSA)_{1\text{-}3}$-791T/36, (Garnett *et al.*, 1985) were performed to examine the mechanism of action of $(MTX_{32}\text{-}HSA)_{1\text{-}3}$-791T/36 in comparison to that of free MTX. Results showed that folinic acid exerted inhibitory effects on the cytotoxic actions of the $(MTX_{32}\text{-}HSA)_{1\text{-}3}$-791T/36 which was greater than the inhibitory effects on MTX but nonetheless may imply a similar route of entry to MTX. The assumption is that this occurs by the cleavage of MTX from HSA in the lysosomes which, once released extracellularly may enter the cell *via* the folic acid pathway followed by MTX. Another hypothesis based on the effects of the lysomotropic agents, NH_4Cl, in inhibiting the $(MTX_{32}\text{-}HSA)_{1\text{-}3}$-791T/36 proposes that the conjugate may be endocytosed and further to this, found in an acidic intracellular compartment.

The degradation products of tritosomal digestion of this $(MTX_{32}\text{-}HSA)_{1\text{-}3}$-791T/36 have also been the source of extensive studies by Fitzpatrick, (1994). Four derivatives were found by HPLC analysis and were identified as tritosomes, MTX-Lys (α-ε), MTX-Lys(ε-α) and free MTX. The total release of MTX in any form corresponded to 5.6% of the input conjugated MTX and only 9.9% of this released material was underivatised MTX. This result was surprising in that such a low level of drug release could be associated with a conjugate that is more cytotoxic than MTX alone, against the target cell line.

The conclusion of this study was that in addition to a carrier molecule, it would be advantageous to also include a spacer, so the final conjugate is: drug-spacer-carrier-antibody. This spacer would ensure that upon digestion by lysosomal enzymes, free MTX is efficiently released.

Results of Whiteley *et al.*, (1981) suggest that carrier bound drugs do have altered properties from those exhibited by the free entity, however they do not necessarily lead to enhanced drug action in a particular host. MTX-BSA is retained for longer period *in vivo* but *in vitro* results suggest lower uptake of the carrier bound drug. Covalent binding and subsequent injection of MTX to BSA, MSA, bovine IgG, chymotrypsinogen and various molecular weight dextrans result in higher and more prolonged serum concentrations in addition to decreased rate of excretion of MTX compared to free drug. It is thought that the response to carrier bound MTX may be caused by altered pharmacokinetics but also indicates that carriers play more than a passive role. MTX and MTX-BSA are taken up via different transmembrane transport mechanisms (Chu *et al.*, 1981) *in vitro* the entry of carrier-bound entities is thought to be via pinocytosis (DeDuve *et al.*, 1974) and this may be one way to overcome resistance in affected cell lines. This is also true of poly-L-lysine conjugated to MTX which was taken up into Chinese Hamster cells resistant to free MTX, due to transport deficiency, (Shen and Ryser, 1979).

1.5.1.3. Bispecific monoclonal antibody:

A more advanced conjugation involves a bispecific monoclonal antibody against both MTX and a human tumour associated antigen (Pimm *et al.*, 1990). This double pronged attack on the tumour specifically enhanced the *in vitro* cytotoxicity of MTX-HSA for gp72 positive tumour cells. The ratio of

MTX:HSA was also of the order 40:1 which was an improvement on the direct linkage to the antibody.

1.5.2. Disadvantages of drug-antibody targeting.

Monoclonal antibody-mediated targeting is the most versatile and general modality of drug delivery at present according to Basu (1990). However cytotoxic moieties conjugated to such antibodies should be delivered specifically to the selected cell type. Although MAb can direct immunoconjugates with a high degree of selectivity to target cells there are still limitations due to:

(i) the number of cell surface antigens

(ii) the number of drug molecules attachable to the antibody

(iii) poor efficiency of internalisation of conjugates, leading to:

(iv) reduced accumulation of pharmacologically effective intracellular concentrations of the drug

(v) cross reactivity with non-target cells.

(vi) potential immunogenicity *in vivo*

Differences which exist between the *in vitro* and *in vivo* results of monoclonal antibody (MAb) data may be due to the fact that tissue culture cells are in exponential growth and any cell line that differentially expresses a measured antigen during this growth phase would demonstrate altered Mab binding. Another possible source of discrepancy between the in vitro and *in vivo* data may arise as a result of the altered stability of radiolabels *in vivo*, ^{111}In versus ^{125}I, (Halpern *et al.*, 1983). Hudecz *et al.*, (1993) concluded that MTX immunoconjugates produced less impressive responses *in vitro* and *in vivo* than similar conjugates of doxorubicin, daunomycin or mitomycin C, due to influences of the carrier on the biodistribution of MTX-branched polypeptide

conjugates (Hudecz *et al.*, 1992). The covalent attachment of MTX to branched polypeptides results in reduction of *in vitro* cytotoxicity and this is attributed not to the relative size of the carrier nor the amino acid sequence but to the identity of the terminal amino acid. However the incorporation of glutamic acid in to the side chain did significantly prolong the blood clearance of MTX-branched polypeptides, (Hudecz *et al.*, 1993).

1.6. Aims and Objectives.

The main obstacle to be overcome in the treatment of cancer is the fact that cancerous cells exhibit few or no differences from normal tissues to provide a basis for selective toxicity and as a result side effects frustrate effective therapy. The aim of this study is to minimise the arbitrary side effects associated with the drug of choice i.e. methotrexate (MTX) by conjugating it to an analogue of the naturally occurring hormone α-MSH, namely, [Nle^4,D-Phe^7]α-MSH. Therefore the disadvantages associated with the folic acid uptake pathway of MTX leading to a general distribution of MTX throughout the body, may be surmounted by use of receptor-mediated drug delivery i.e. using the natural uptake pathway of the hormone. In theory the [Nle^4,D-Phe^7] α-MSH will localise the MTX to a melanoma cell specific receptor, and once bound, the receptor-ligand complex will be internalised. Although MTX is not usually associated with the treatment of melanoma cancer, it is the model drug used in this study due to its small size, (FW: 454), relative to [Nle^4,D-Phe^7]α-MSH (FW:1648) which minimises any size / conformational difficulties at the receptor site, and ease of chemical attachment of the analogue [Nle^4,D-Phe^7]α -MSH, forming N$^{\alpha}$MTX-[Nle^4,D-Phe^7]α-MSH.

To effectively employ this method of drug delivery a detailed knowledge of (i) the nature of the ligand, (ii) relative distribution of the receptor on various cell types and (iii) the intracellular pathway followed by the receptor-ligand complexes is necessary. To this end, many binding and internalisation studies were undertaken to elucidate the pathways taken by [Nle^4,D-Phe^7]α-MSH and N$^\alpha$MTX-[Nle^4,D-Phe^7]α-MSH.

Most importantly the growth inhibitory effects of MTX and N$^\alpha$MTX-[Nle^4,D-Phe^7]α-MSH in a variety of cells lines were examined to see whether the N$^\alpha$MTX-[Nle^4,D-Phe^7]α-MSH had an improved level of efficiency. The effects of [Nle^4,D-Phe^7]α-MSH, and lysosomal degrading agents; (monensin and chloroquine) were also examined.

A number of cell lines were employed; B16 murine melanoma cells gave rise to much of the experimental work and results. It is a cell line that has been used extensively in our laboratories and hence many of its characteristics have already been the subject of other studies, (Richards, 1992, Erskine-Grout, 1993, Adams, 1993, Sahm, 1994). MeWo human melanoma cells were also used as a comparative melanoma cell line although it was known that human melanoma cells do not possess nearly as many MSH receptors on their cell surface. SVK14 keratinocytes were employed specifically because they possess few, if any, MSH receptors on their surface and hence would be a valid control in the study of any site specific actions attributed to N$^\alpha$MTX-[Nle^4,D-Phe^7]α-MSH. 293 cells transformed with the gene encoding the MC3 receptor were used to test if the actions of N$^\alpha$MTX-[Nle^4,D-Phe^7]α-MSH were associated specifically with the MC1 receptor i.e. B16 and MeWo cells or if the effects were also equally prominent in cells expressing the MC3 receptors. This would have serious repercussions on the usefulness of N$^\alpha$MTX-[Nle^4,D-Phe^7]α-MSH since MC3 receptors are located in the gut,

placenta but also in the brain and CNS side-effects would be counterproductive to the aim of this study. 293 cells transformed with the pcDNA neo vector alone, were used to elucidate whether the process of transfection in any way enhanced the cells susceptibility to N^{α}MTX-[Nle^{4},D-Phe^{7}]α-MSH and hence were used as another control.

CHAPTER 2.

MATERIALS AND METHODS.

2.1.Cell Lines:

Although the majority of the work presented utilises the B16 murine melanoma cell line, other work was performed on human-derived cell lines listed below.

All cells were propagated in RPMI-1640 medium with the exception of the 293 cell lines which had a 1ml supplement of fungizone (250μg/ml) to the medium.

CELL LINE	OBTAINED FROM:	GROWN IN:
B16	L.Kelland. I.C.R. Sutton	RPMI-FCS
293 (vector only)	R.Cone.Vollum Inst. Oregon.	RPMI-FCS
293(vector with encoded gene for MC3 receptor)	R.Cone. Vollum Inst. Oregon.	RPMI-FCS (fungizone)
MeWo	L.Seymour. University of Keele.	RPMI-FCS
SVK14	J.Taylor. I.C.R.F.	RPMI-FCS

2.2. Solutions:

Water:

The water employed in the preparation of media and solutions was freshly double glass distilled by a bi-distillation Fistreem Still (Fisons Ltd.) fitted with a Fistreem predioniser (Fisons Ltd.).

Balanced Salt Solution:

Phosphate buffered saline (PBS) (without calcium and magnesium) was obtained from Oxoid Ltd. in tablet form. Ten tablets were dissolved in 1L of freshly double distilled water and then distributed in to 100ml bottles which were then sterilised and stored at 4°C.

Ethylenediaminetetraacetic Acid (EDTA):

A 0.02% w/v EDTA solution was prepared by dissolution in sterile PBS. Once dissolved the solution was passed through a 0.2μm diameter filter (Sartorius Ltd.) and 20ml aliquots were pipetted into sterile universals (Sterilin Ltd.). These were then kept frozen at -20°C until required.

Base Solutions:

Sodium bicarbonate (7.5% w/v) and sodium hydroxide (2M), both from BDH Chemicals were prepared with double distilled water, sterilised and stored at room temperature.

Trypan Blue:

Trypan blue stain was obtained from Sigma Ltd. and was stored as a 0.1% solution (in PBS) at room temperature.

2.3. Growth Media and Constituents:

RPMI 1640 (Flow Laboratories) was obtained as 10x liquid concentrate containing phenol red indicator but deficient in L-glutamine and sodium bicarbonate.

Supplements to the medium included L-glutamine (200mM), an antibiotic solution (pen/strep) of penicillin (5000IU/ml) and streptomycin (5000μg/ml), fungizone, (amphotericin B 250μg/ml) and non-essential amino acids (NEAA) which were all obtained from Gibco Laboratories.

Storage:

Growth medium and NEAA were refrigerated at 4°C, while L-glutamine and pen/strep were frozen at -20°C.

Foetal Calf Serum (FCS):

FCS from Flow Laboratories was batch-tested for the support of cell growth and was supplemented at 10%v/v to normal growth medium. Batch No: 10835 was used for all experiments. Serum arrived in 500ml glass bottles and was stored at -20°C prior to usage.

All cell growth media were aseptically prepared from sterile components according to the following formulae. Media were then stored at 4°C and what remained unused after two weeks was discarded.

	RPMI-FCS
10X RPMI-1640 medium	**50ml**
Water	**421.5ml**
L-glutamine (200mM)	**5ml**
pen/strep (5000IU/ml)	**5ml**
NEAA	**5ml**
$NaHCO_3$ (7.5% w/v)	**13.5ml**
FCS	**55.6ml**

All media required the addition of a small volume (approx. 1ml) of sterile 1M NaOH (BDH Chemicals) in order to achieve a final pH of 7.2-7.4.

Autoclave-labile solutions were sterilised in small volumes by membrane filtration using sterile 0.2μm filters from Sartorius Filters. All other solutions were sterilised in an autoclave (British Sterilizer Co. Ltd., Swingclave Type SFT-LAB) at 121°C for 15 minutes.

2.4. EQUIPMENT:

All cells were stored in 2ml ampoules and shelved in the vapour phase of a Union Carbide LR-40 liquid nitrogen store at approximately -148°C.

Sterile tissue culture flasks (25, 75, 175cm^2) were purchased from Falcon Laboratories. Tissue culture tubes (100 x 16mm) were obtained from Sterilin Ltd. Polypropylene 2ml ampoules with screw caps, used for the storage of cells at -148°C were obtained from Corning Laboratories.

All sterile operations involving the cells were performed in a vertical recirculating laminar flow cabinet (MDH Ltd.). Protocols which did not require sterility were performed at the laboratory bench.

An inverted biological microscope WILD M40 (Wild Heerbrugg Ltd.) was used for the observation of growing cell cultures and the haemocytometer counting of cells.

The cultures were incubated in a LEEC PF2 anhydric incubator (Laboratory and Engineering Company) with forced air circulation and adjusted thermostatic controls which gave a constant temperature of 37°C. The consistency of temperature was checked regularly with a digital thermometer which had a thermocouple probe (Jenway Ltd.).

2.4.1. Preparation of Glassware:

Glassware was soaked in a 2% solution of RBS25 (Fisons Ltd.) at approximately 40°C for 30 minutes. After three rinsings in single distilled water it was left to stand in double distilled water for no longer than one hour. The glassware was then air-dried and sterilised by dry heat at 160°C (Gallenkamp Sterilising Oven) for a minimum of one hour.

Non-glass items; e.g. pipette tips, were treated in a similar manner but after drying they were autoclave sterilised (Drayton Castle Laboratory Steriliser) at 121°C for 15 minutes.

2.5. Subculture of cell lines:

Although the time taken for different cell lines to reach confluency varied, the cells were all subcultured once this confluent state was deemed to have been attained. This was defined as when the entire lower surface of the culture flask was covered by cells and also further growth was restricted by contact inhibition and the depletion of available nutrients in the media (this was optically observed by the colour change of media to yellow).

Initially the culture was examined visually in order to confirm the healthy appearance of the cells and the absence of any free-floating cellular debris or other signs of contamination.

At the laminar flow cabinet, the old medium was decanted off and the cells were washed twice with 5ml aliquots of PBS. The flask was gently agitated in order to ensure the cell monolayer was completely rinsed during each wash. 2ml of 0.025% EDTA was then introduced to the flask and it was placed in the incubator for 10 minutes.

Upon removal the flask was shaken to encourage dislodgement of the cells before the addition of 5ml of fresh media.

Using a sterile, plugged Pasteur pipette, the cell suspension was aspirated and transferred to a sterile test tube so that cell density could be determined prior to the inoculation of a new passage of cells. A constant seeding density of 1×10^6 cells per $175cm^2$ flask was used in the presence of 45ml of fresh media. The cells were gassed for 25 seconds with a mixture of 5% CO_2 / 95% air and incubated at 37°C.

2.6. Freezing of cells and cell storage:

In order to ensure adequate stocks of cells, cells were routinely frozen. Once they had reached confluence, the cells were detached (as previously described) and the suspension placed in a centrifuge (Jouan B3-11 Bench centrifuge) at 1000 x g for 10 minutes.

The supernatant was then decanted leaving the cell pellet, which was then resuspended in filter sterilised RPMI-FCS which contained 10% DMSO (cryoprotectant). Replicate volumes of 1.5ml were pipetted in to polypropylene ampoules (J.Bibby Sciences) and then placed in to a liquid nitrogen store. Here the cells cooled to below -70°C in the vapour of the liquid nitrogen at a rate of 1°C per minute. Once the cells were uniformly frozen, they were transferred to a liquid nitrogen freezer (Union Carbide LR-40) for long term storage.

2.7. Recovery of cells from storage:

Once removed from the nitrogen store, an ampoule was placed in pre-warmed (37°C) water in an incubator and allowed to thaw rapidly for 2-3 minutes. The contents of the ampoule were then aseptically transferred to a sterile tube containing 9ml of fresh medium. This was then centrifuged at 1000 x g for 10 minutes, after which the supernatant was removed and the cells resuspended in 3ml of growth medium. Finally the contents were poured into a new 175cm^2 flask containing 45ml of growth medium and gassed and incubated in the normal manner.

2.8. Counting of Cells:

1. Cells were detached and 0.4ml of the cell suspension was transferred to a sterile test tube.
2. 0.1ml of 0.1% Trypan blue dye solution was added and mixed thoroughly.
3. Using a Pasteur pipette, a small amount of the mixture was loaded onto a grid haemocytometer and the number of viable cells in the four corners and the central square were counted.

   Trypan blue dye is excluded from cells which have an intact cell membrane i.e. are viable.
4. The number of cells per ml was calculated using the following equation:

$$\text{viable cells per ml} = \frac{(\text{total cells in all 5 chambers}) \times 10^4}{4}$$

2.9. PEPTIDE SYNTHESIS :

2.9.1. Synthesis of [Nle^4, DPhe^7]α–MSH:

The synthesis of this peptide and the peptide derivative of methotrexate (MTX) was carried out by Dr. G.W.J. Olivier, however the main points of the methods used will be described.

Peptides were prepared by solid-phase using Fmoc strategy (Atherton and Sheppard, 1989). The carboxamide forms of the peptides were prepared using the AM-linker on Pepsin K resin. All the amino acid reagents were employed as their pentafluorophenyl esters with the exceptions of serine, where the 3,4-dihydro-4-oxobenzotriazin-3-yl ester was used, and Fmoc-D-Phe-OH, which was treated with DIC and HOBT to form its HOBT ester *in situ.*

Side chain protecting groups were as follows: Arginine; methoxytrimethylbenzenesulphonyl (Mtr), Glutamic Acid; *t*-butoxy (OBut), Histidine; *t*-butoxycarbonyl (Boc), Lysine; (Boc), Serine; *t*-butyl (But), Tyrosine; (But). In each case a four fold molar excess of reagents was used.

Deprotection and cleavage was effected by the use of 2% EDT, 2% anisole and 1% water in TFA for 12 hours, at room temperature.

Peptide purification took place using semi-preparative HPLC with a gradient elution of 0.1% TFA in water and 0.1% TFA in acetonitrile water (70:30) at a flow rate of 3ml per minute.

The eluent was monitored by UV spectrophotometry at 217nm. Fractions were collected at 30 second intervals and checked by analytical scale HPLC. Peptide fractions containing the peptide were then pooled and freeze-dried.

Confirmation of peptide purity was undertaken by co-chromatographic techniques with purchased [Nle^4,D-Phe^7]α-MSH (Sigma Chemical Co.), FAB-MS and MALDI-TOF MS: α-MSH M+H calculated;1664.8, found 1664; [Nle^4,D-Phe^7]α-MSH, M+H calculated 1646.8, found 1647.

Stock concentration of peptide (1mg/ml) was made up in sterile 0.1mM HCl and was stored at 4°C prior to usage.

2.9.2. Synthesis of N^{α}-MTX-[Nle^4, DPhe^7] α-MSH:

To prepare N$^{\alpha}$MTX-[Nle^4,D-Phe^7]α-MSH, Fmoc-[Nle^4,D-Phe^7]-α-MSH on resin was deprotected, at the N terminus, using 20% piperidine in DMF. A mixture of MTX and diisopropylcarbodiimide (DIPCDI) in DMF were added to form the N$^{\alpha}$MTX-[Nle^4,D-Phe^7]α-MSH product. FAB-MS was used for confirmation of the identity. It is noteworthy that N$^{\alpha}$MTX-[Nle^4,D-Phe^7]α-MSH was expected to be a mixture of two products coupled to the α or γ carboxyl groups of the glutamate residue of MTX. Also racemisation at this glutamate residue occurred making the product a mixture of 4 compounds. HPLC suggested similar amounts of the 4 species.

2.10. Radio iodination of [Nle^4,D-Phe^7]-α-MSH:

[Nle^4,D-Phe^7]-α-MSH was iodinated at the tyrosine residue (position 2) using Chloramine T methods described by Eberle (1988). The preliminary purification was performed using a disposable extraction column. This product was further purified using reversed phase HPLC to allow separation of the monoiodinated and the di-iodinated compounds.

Solutions:

Solutions 1 to 4 were prepared as stock solutions and stored at 4°C, whereas solutions 5 to 8 were prepared on the day of the experiment.

1. 0.25M Na_2HPO_4
2. 0.25M NaH_2PO_4
3. 1% TFA (Aldrich)
4. 50, 60, 80% methanol with 1% TFA.

5. 0.25M phosphate buffer (pH 7.4) From (1) and (2)

6. 0.25% BSA in 0.05M phosphate buffer (pH 7.4)

7. 1% Polypep (Sigma) in 0.05M phosphate buffer (pH 7.4)

8. 0.1% Chloramine T (BDH Chemicals Ltd.) in H_2O (dissolved immediately prior to use).

Preconditioning of the Column:

A C18 reverse phase 'Bond Elut' column packed with Spherisorb ODS was prepared and conditioned in the following way;

3 x 1ml 1% TFA

3 x 1ml 80% methanol / 1% TFA

1 x 1ml 1% Polypep (solution 7)

3 x 1ml 80% methanol / 1% TFA

3 x 1ml 1% TFA

Iodination Procedure:

1.5µl of stock [Nle^4,D-Phe^7]-α-MSH (1mg/ml) was placed in an eppendorf to which 20µl of phosphate buffer was added. In the fume cupboard, 10µl of ^{125}INa (equivalent to 1.5mCi) was added to the peptide and finally 10µl of 0.1% Chloramine T initiated the reaction which was allowed to proceed for 30 seconds, and then halted by the addition of 0.6ml of BSA.

The reaction mixture was then transferred to the column, which was then washed in the following way (in order to remove any free Na^{125}I):

2 x 1ml 0.25M phosphate buffer.

4 x 1ml 50% methanol / 1% TFA.

2 x 1ml 60% methanol / 1% TFA.

The last 6ml of washings were kept and loaded on to an analytical grade HPLC for purification.

Purification:

Once the methanolic fractions had been loaded, the chromatography was achieved using an exponential gradient as follows; the eluate was monitored at 217nm.

TIME(mins)	SOLVENT A (%)	SOLVENT B (%)	GRADIENT
0	95	5	Linear
5	95	5	Linear
50	40	60	Exponential
55	40	60	Exponential
60	95	5	Linear

where, A= 0.1% TFA / H_2O

B= 70% Acetonitrile, 0.1% TFA / H_2O

1ml fractions were collected every minute from 25 to 40 minutes after injection. Free [Nle^4,D-Phe^7]α-MSH was eluted first, followed by monoiodinated and finally di-iodinated peptide (see figure 2.1.). The radioactivity of the fractions was assessed by reading them on a gammacounter (LKB 1277 Gammamaster) and those fractions associated with the peak of the monoiodinated peptide were pooled and the activity of the final mixture counted.

The radiolabelled peptide was then stored in solution at -20°C for no longer than 3 weeks.

Calculation of Radiotracer Concentration:

Assumption:

Ratio of ^{125}I : [Nle^4,D-Phe^7]-α-MSH, 1 : 1.

1 matom $^{125}I = 1 \times 10^{-3}$ moles [^{125}I-Tyr^2]-[Nle^4,D-Phe^7]-α-MSH

Specific Activity of carrier free Na $^{125}I = 80.5 \times 10^{12}$ Bq / matom

1 mole [^{125}I-Tyr^2]-[Nle^4,D-Phe^7]-α-MSH $= 80 \times 10^{12} \times 10^3$ Bq

Since:

1 Bq = 1 disintegration per second

1 Bq = 60 disintegrations per minute

the efficiency of the gammacounter was 70%

Therefore:

$$1 \text{ mole}[^{125}\text{I-Tyr}^2]\text{-[Nle}^4\text{,D-Phe}^7\text{]-}\alpha\text{-MSH} = 80.5 \times 10^{12} \times 10^3 \times 60 \times \frac{70}{100} \text{ cpm}$$

$$= 3.38 \times 10^{18} \text{ cpm.}$$

No. of cpm equivalent to:

0.5ml of 1M ^{125}I-[Nle^4,D-Phe^7]-α-MSH $= 1.69 \times 10^{15}$ cpm.

Therefore :

$$\frac{\text{no. of cpm in a given sample}}{1.69 \times 10^{15}\text{cpm}} = \text{no. of moles of } ^{125}\text{I-[Nle}^4\text{,D-Phe}^7\text{]}\alpha\text{-MSH}$$

2.11.Radioiodination and purification of N$^{\alpha}$MTX-[Nle^{4},D-Phe^{7}]α-MSH:

The procedure was performed according to the protocol of Richards (1992) and was identical to that previously described for [Nle^{4},D-Phe^{7}]-α-MSH with the following exceptions;

(i) The volume of peptide solution employed was 5µl. (Stock solution 1mg/ml).

(ii) Reaction time with Chloramine T was 5 minutes.

(iii) Subsequent to the completion of the reaction the column was washed as indicated below;

2 x 1ml 0.25M phosphate buffer.

2 x 1ml 40% methanol / 1% TFA.

2 x 1ml 50% methanol / 1% TFA.

2 x 1ml 60% methanol / 1% TFA.

Only the residue from the 60% methanolic washes were retained and purified (approx. 2ml).

(iv) UV detection of the unconjugated peptide took place at 217nm, however this was altered to 310nm for the conjugated peptide due to the presence of the MTX chromophore. (See figure 2.2.)

2.12. Degradation of N$^{\alpha}$MTX-[Nle^{4},D-Phe^{7}]α-MSH:

3.05 x 10^{5} B16 cells were seeded per 25cm^{2} tissue culture flasks. 10ml of RPMI-FCS containing 5 x 10^{5}M N$^{\alpha}$MTX-[Nle^{4},D-Phe^{7}]α-MSH was added. The cells were gassed and placed in an incubator at 37°C. At various time intervals (24, 48 and 72 hours) a flask was removed and the medium decanted. The medium was then centrifuged and analysed by HPLC at 217 and 300nm using a linear gradient. A control flask which contained no N$^{\alpha}$MTX-[Nle^{4},D-

Phe^7]α-MSH was treated in a similar manner. The table below shows the gradient of the two solvents A and B used for the HPLC analysis and the time intervals.

TIME (MIN.)	% A	% B
0	95	5
5	95	5
80	20	80
85	20	80
90	95	5

where: A = 0.1% TFA / H_2O

B = 70% MeCN / 0.1% TFA / H_2O

2.13. RADIOLIGAND BINDING AND INTERNALISATION:

Materials:

Serum Free Medium (SFM):

This was prepared by the addition of 50ml RPMI-1640 to 13.5ml of $NaHCO_3$ and purified water to 500ml.

HEPES: (*N*-(2-hydroxyethyl) piperazine-N'-2-ethane sulphonic acid)

(10x concentration):

6g HEPES was added to 100ml SFM and buffered to pH 7.2-7.4 using 1M NaOH.

Aliquots of 5ml were stored at -20°C.

Bovine Serum Albumin (BSA)(10x concentration):

2g of BSA was added to 100ml of SFM. Aliquots of 5ml were stored at -20°C.

Binding Buffer:

This was prepared by the addition of 25mM HEPES and 0.2% BSA to serum free medium using the quantities indicated below:

5ml of HEPES, 5ml of BSA and SFM to 50ml.

Citric Acid Buffer:

A 0.1M Citric acid monohydrate buffer was employed consisting of 10.51g of citric acid, 2.72g of NaCl and 11.72ml of 1M NaOH which was then made up to a volume of 500ml with double distilled deionised water. This buffer had a pH of 2.5 which was sufficient for the removal of externally bound ligand from the surface of the cells (Adams, 1993). It was stored at 4°C and prepared monthly.

20mM NH_4Cl:

0.5345g of NH_4Cl was made up to 500ml with SFM. This solution was prepared every four weeks and stored at 4°C.

2.13.1. Time Course Experiment:

This experiment was performed to ascertain the time necessary for a particular cell line to attain saturation binding with a specific ligand.

Protocol:

1. Cells were seeded at a density of 5 x 10^5 cells per well in 24 well plates, gassed and incubated in the normal way.
2. On removal from the incubator they were washed twice with SFM and allowed to cool to 4°C.
3. 0.5ml of binding buffer containing a fixed concentration (0.1nM) of ^{125}I-[Nle^4,D-Phe^7]-α-MSH was added to the cells. Eight of the sixteen replicate wells also received an excess quantity (10^{-6}M) of non-iodinated ligand in order to assess the non-specific binding.

4. The cells were then re incubated on ice at 4°C.
5. At various time intervals (30, 60, 120, 240, 480 and 1440 min.) the cells were removed and the residual peptide was removed by two rinsings with SFM.
6. The cells were then lysed and removed by the addition of 0.5ml NaOH (1M) and the radioactivity associated with the cells determined by reading on the gammacounter.

2.13.2. Binding Isotherm:

Using a method adapted from Siegrist *et al.* (1988), the binding assays were carried out in accordance with those described by Erskine-Grout (1993).

Protocol:

1. Cells were seeded at a density of 5 x 10^5 cells per well in 24 well plates, gassed and incubated overnight in the normal manner.
2. On removal from the incubator they were washed twice with SFM and allowed to cool to 4°C.
3. 0.5ml of binding buffer containing varying concentrations of ^{125}I-[Nle^4,D-Phe^7]-αMSH was added to the cells. Eight of the sixteen replicate wells also received an excess quantity (1 x 10^{-7}M)of non radiolabelled ligand in order to assess the non-specific binding.
5. The cells were then reincubated at 4°C, on ice for 8 hours, after which the residual peptide was removed by two washings of ice-cold SFM.
6. After this the cells were lysed and removed by the addition of 0.5ml of 1M NaOH. The radioactivity was then read on the gammacounter and the estimation of receptor number and the association constant was calculated using MINSQ non linear least square regression suitable for ligand binding analysis.

2.13.3. Competitive Binding Assay:

Competition binding was observed using the same protocol as described for the binding isotherms, however the binding buffer contained a fixed amount of the radiolabelled peptide (usually 1 x 10^{-10}M) and varying concentrations of the peptide to be tested in the range of 10^{-6} -10^{-12} M.

2.13.3.1. Equation used for Competition Binding Assay:

The equation below was used in order to ascertain the dissociation constants for the unlabelled conjugate versus the tracer;

$$\text{cpm (test conc.)} = \frac{(\text{cpm max.} - \text{cpm min.})[A]}{[A] + (K_dA)([B] / K_dB)} + \text{cpm min.}$$

where:

cpm test = cpm bound at appropriate conc. of inhibitor
cpm max = maximum bound cpm
cpm min = minimum bound cpm (non-specific)

receptor specific cpm = cpm max- cpm min
[A] = concentration of radio tracer
[B] = concentration of unlabelled competitor
(KdA) = dissociation constant of radio tracer
(KdB) = dissociation constant of radiolabelled competitor

The above equation was derived from the following considerations:

The relative % maximum binding of the tracer [A] is given by:

$$\text{Fraction of maximum binding} = \frac{(\text{cpm test} - \text{cpm min})}{(\text{cpm max} - \text{cpm min})}$$

Non-linear regression analysis was used to estimate parameters from the data using the equation above.

$$\text{Fraction of maximum binding} = \frac{[A]}{[A] + (K_dA)[B] / K_dB}$$

2.13.4. Internalisation of N$^{\alpha}$MTX-[Nle^4,D-Phe^7]α-MSH by B16 cells:

(in the presence of 20mM NH_4Cl)

1. 5 x 10^5 cells per well were seeded in 24 well plates, gassed and incubated overnight in RPMI-FCS at 37°C.
2. On removal from the incubator the plates were washed twice with SFM and then re incubated for 15 minutes at 37°C in SFM containing 20mM NH_4Cl.
3. Plates were then inverted to remove the SFM and 1 x 10^{-10}M ^{125}I-N$^{\alpha}$MTX-[Nle^4,D-Phe^7]α-MSH in 0.5ml binding buffer (with NH_4Cl) was added to the cells. Eight of the sixteen replicate wells also had an excess (1 x 10^{-7}M) of non-iodinated material in order to assess the non-specific binding.
4. The cells were again incubated at 37°C and removed at the following time intervals; 15, 30, 60, 90,120, 180 and 240 minutes.
5. At the end of the required time the binding buffer was discarded and half of the wells were subjected to an acid wash at 4°C for 5 minutes, after which all the plates were washed twice with ice cold SFM.
6. The cells were then lysed by the addition of 0.5ml 1M NaOH and the contents of each well assayed for activity on the gammacounter.

2.13.5. Pulse Chase Internalisation of N$^{\alpha}$MTX-[Nle^4,D-Phe^7]α-MSH :

1. Cells (5 x 10^5 per well) were seeded in 24 well plates, gassed and incubated overnight at 37°C.
2. The following day the plates were washed twice with SFM, and then 0.5ml binding buffer containing 1 x 10^{-10}M N$^{\alpha}$MTX-[^{125}I Tyr^2,Nle^4,D-Phe^7]α-MSH was placed on the cells which were then incubated at 4°C for 2 hours.
3. The radioactivity was then washed off with SFM and the plates were incubated at 37°C for various time points; 15, 30, 60, 90, 150 and 240 minutes.
4. After each time period half of the wells were treated with an acid wash at 4°C for 5 minutes and then all the cells were washed twice with SFM.
5. The cells were then digested with 0.5ml of 1M NaOH and the radioactivity present in each well read on the gammacounter.

2.13.6. Pulse Chase Internalisation of N$^{\alpha}$MTX-[Nle^4,D-Phe^7]α-MSH in the presence of NH_4Cl:

The protocol was exactly the same as for the previous internalisation however the cells were treated with SFM containing NH_4Cl (20mM) for 15 minutes at 37°C prior to the addition of the radiolabelled peptide. Subsequent washings were all done with SFM that contained NH_4Cl.

2.14. Growth Inhibitory Effects of MTX and N^{α}MTX-[Nle^4,D-Phe^7]α-MSH as assessed by the MTT Assay:

Methotrexate (MTX): [(+) Amethopterin] (4-amino-10-methylfolic acid)

FW: 454.4 $C_{20}H_{22}N_8O_5$

Initially this was obtained in powder form from Sigma Chemical Co. and dissolved in a mixture of PBS: NaOH (0.1M) 90:10 however as the NaOH interfered with the cells, for the assays described, the MTX was purchased from Lederle Laboratories as a single sterile vial containing 50mg Na_2MTX / 2ml (pH 8.5). Routinely made to 1.1 x 10^{-2}M with sterile RPMI-FCS (from which further dilutions could be made).

MTX

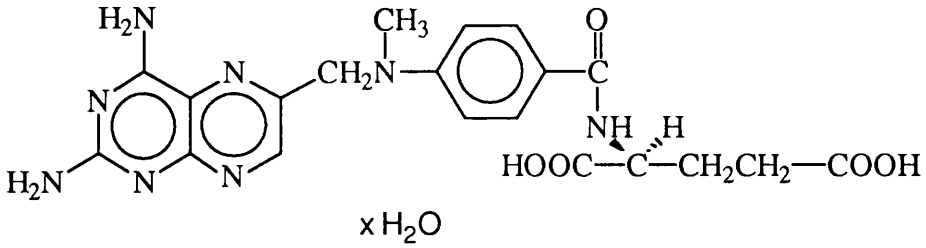

(3-[4,5-dimethylthiazol-2-yl]-2,5 diphenyltetrazolium bromide); Thiazolyl Blue (MTT):

FW: 414.3 $C_{18}H_{16}N_5SBr$

This was obtained as 1g powder (Sigma Chemical Co.) and was dissolved in PBS and then sterile filtered to achieve a stock concentration of 10mg/ml.

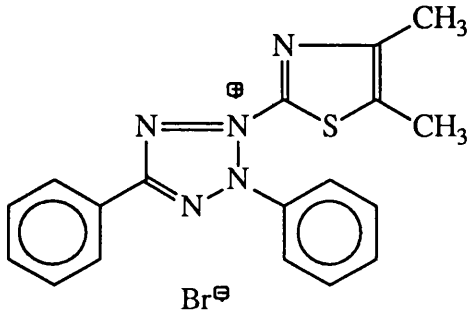

MTT

(1-[4,5-dimethylthiazol-2-yl]-3,5-diphenylformazan (MTT Formazan):

FW: 335.4 $C_{18}H_{17}N_5S$

Obtained 1g powder from Sigma Chemical Co. and made up in dimethylsulphoxide for control experiments.

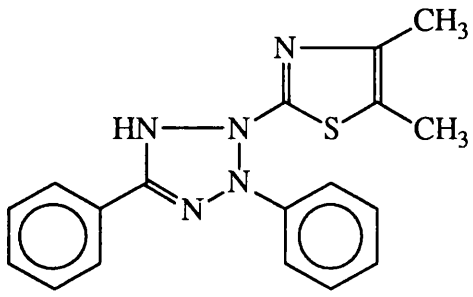

MTT Formazan

Dimethylsulphoxide (DMSO):(Spectrophotometric grade)

This was purchased in 1 litre volumes from Aldrich Chemicals.

After preliminary experiments to ascertain the optimum conditions for the assay, the following protocol was routinely observed:

Protocol:

1. Serial dilutions of MTX or N^{α}MTX-[Nle^4,D-Phe^7] were prepared using RPMI-FCS as a diluent, from 1.1 x 10^{-2}M down to 1.1 x 10^{-13}M.
2. Cells were then seeded in 96 microwell plates at a density of 4 x 10^3 cells per well.
3. 200µl of the MTX or N^{α}MTX-[Nle^4,D-Phe^7] solution was added to each well with 8 replicates per concentration gradient.
4. The cells were then gassed and incubated at 37°C for a period of time which allowed three doublings of the cells under investigation.
5. Control cells were treated in a similar manner but the growth inhibitory agent was omitted.

After 72 hours: (MTT Assay)

6. On removal from the incubator, each plate was inverted in order to dispose of the medium. Each well was then washed (carefully to avoid detachment) twice with SFM.
7. 20µl of a 10mg/ml solution of MTT was then added to each well and supplemented with 180µl of RPMI-FCS, before being incubated at 37°C for a further 3 hours.
8. After 3 hours, the MTT was removed by inversion of the plate and 200µl DMSO was pipetted into each well. The plates were then agitated on an orbital mixer (A500 Jencons Scientific Ltd.) for 5 minutes to ensure complete solubilisation of the Formazan blue crystals.

9. Finally the plate was read on an Titertek plate reader at a test wavelength of 540nm and a reference wavelength of 690nm. Results were then analysed using a standard Excel (Microsoft) speadsheet.

2.15.1. Determination of the intracellular mass of methotrexate necessary to effect cell kill using tritiated methotrexate:

[3',5',7-^{3}H] Methotrexate, Sodium salt. ^{3}H-MTX

This was obtained as the freeze-dried solid from Amersham Life Sciences. It had a specific activity of 470GBq/mmol (12.7 Ci/mmol) and was stored at -20°C.

1. Once the cells had been seeded at 4 x 10^3 per well, serial dilutions of the ^{3}H-MTX were added to the cells and the plate was then incubated for 72 hours.
2. Once removed from the incubator the unbound ^{3}H-MTX was removed by washing the cells 5 times with SFM. This was done carefully to avoid detachment.
3. The cells were then taken up in a 1M solution of NaOH, to which an equal volume of 1M HCl was added in the scintillation vial. Finally 2ml "Optiphase" scintillation fluid was placed into the vial.
4. The individual vials (which each represent one well) were then read twice on the β-emitter scintillation counter. The first reading was done immediately after detachment and the final reading was performed 72 hours later. The latter was used for all the subsequent calculations.
5. The "dpm" readings obtained were then related to the specific activity of the ^{3}H-MTX in order to assess the number of molecules of MTX which were taken up by the cell.

6. Two more 96 well plates were seeded with B16 cells at 4 x 10^3cells per well. These were incubated at 37°C in the presence of varying concentrations of MTX (1.1 x 10^{-2}M down to 1.1 x 10^{-13}M) as per protocol 2.14.

After 72 hours:

7. The MTT assay was performed on one of the plates and this gave an estimate of the $E.C._{50}$ value.
8. The cells in the second plate were counted as per protocol 2.8. and this gave another estimate for the $E.C._{50}$ value.
9. Therefore, two estimates of the intracellular mass may be determined per experiment i.e. from the $E.C._{50}$ values generated from the MTT and Trypan Blue viability assays.

Sample Calculation:

An $E.C._{50}$ value of 5 x 10^{-8}M MTX estimated from the MTT assay,
which corresponds to a level of: "x" moles ^{3}H-MTX/well
and corresponds to: "y" cells/well
which implies: "x/y" moles /cell

Therefore:

x/y multiplied by Avogadros no.= "z" no. of molecules MTX/ cell

Conclusion:

The cells require "z" no. of molecules MTX in order to reduce the viability of the cells to 50% relative to control cells.

i.e. an extracellular concentration of 5 x 10^{-8}M ensures that "z" no. of molecules of MTX reaches the intracellular regions and effects growth inhibition.

2.15.2 Quench Curve of ^{3}H-MTX:

1. Using ten scintillation vials, 10µl of a known amount of ^{3}H-MTX was placed in each along with 2ml of "Optiphase" scintillation fluid.
2. Each vial, with the exception of the first one, was then "quenched" with varying amounts of chloroform, 50,100,200,400,600,800,1000,1500 and finally 2000µl.
3. The vials were then put on the Rackbeta scintillation counter and the standard curve was plotted. The points obtained were then programmed into the machine for future use. See figure 2.3.

Calculations:

In the tritiated methotrexate obtained there are 9.25 MBq of activity.

500µl of PBS was added.

Therefore:

9.25×10^6 Bq in 500µl

1Bq = 1 decay per second

9.25×10^6 dps in 500µl

5.55×10^8 dpm in 500µl

1.11×10^6 dpm per µl

Hence if there is a 1:1000 dilution ,

10µl = 11,100 dpm (approx.).

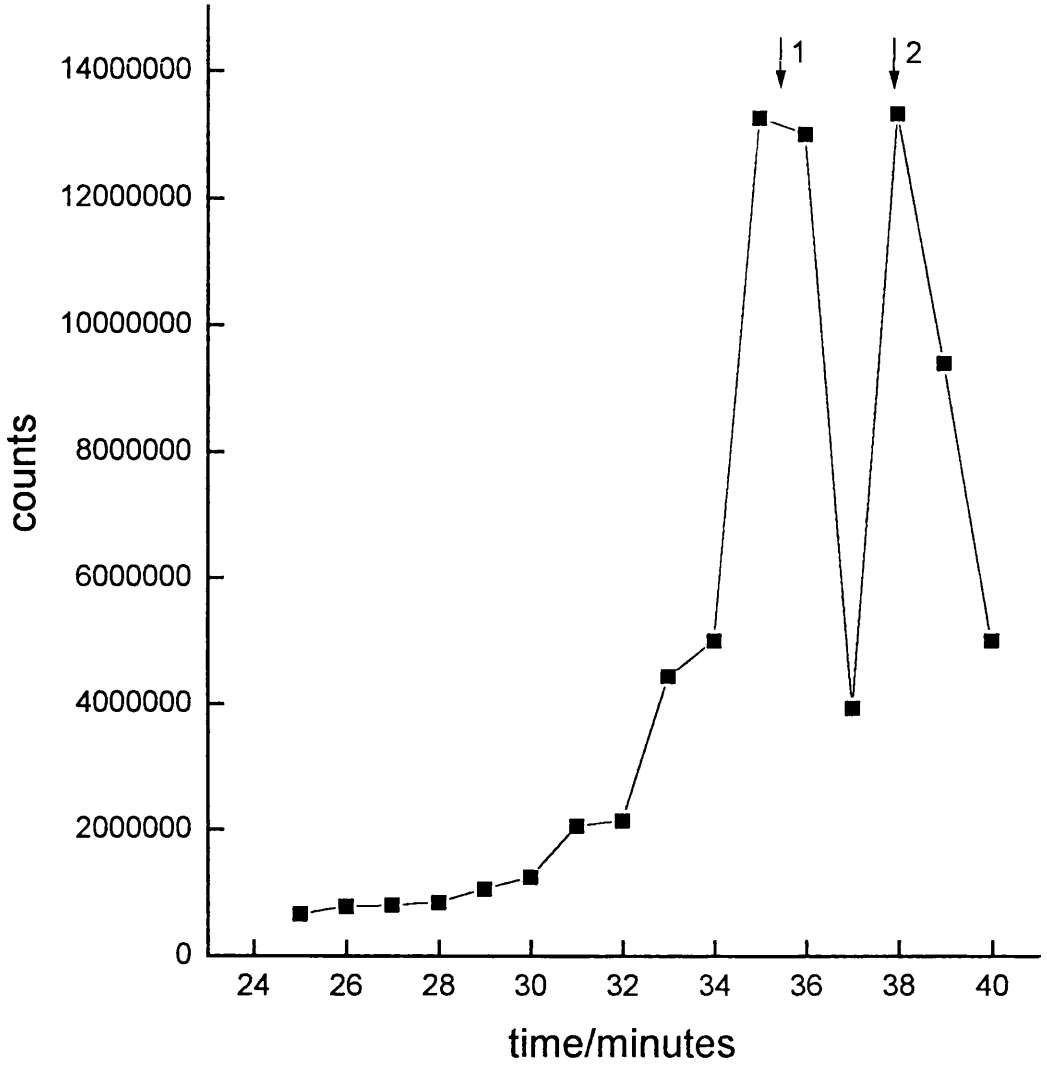

Figure 2.1. This figure shows the radioactive counts obtained from the reaction products of the iodination of [Nle^4,D-Phe^7]α-MSH as measured by UV adsorption at 217nm. Peaks 1 and 2 are thought to represent the mono-iodinated and di-iodinated peptide respectively.

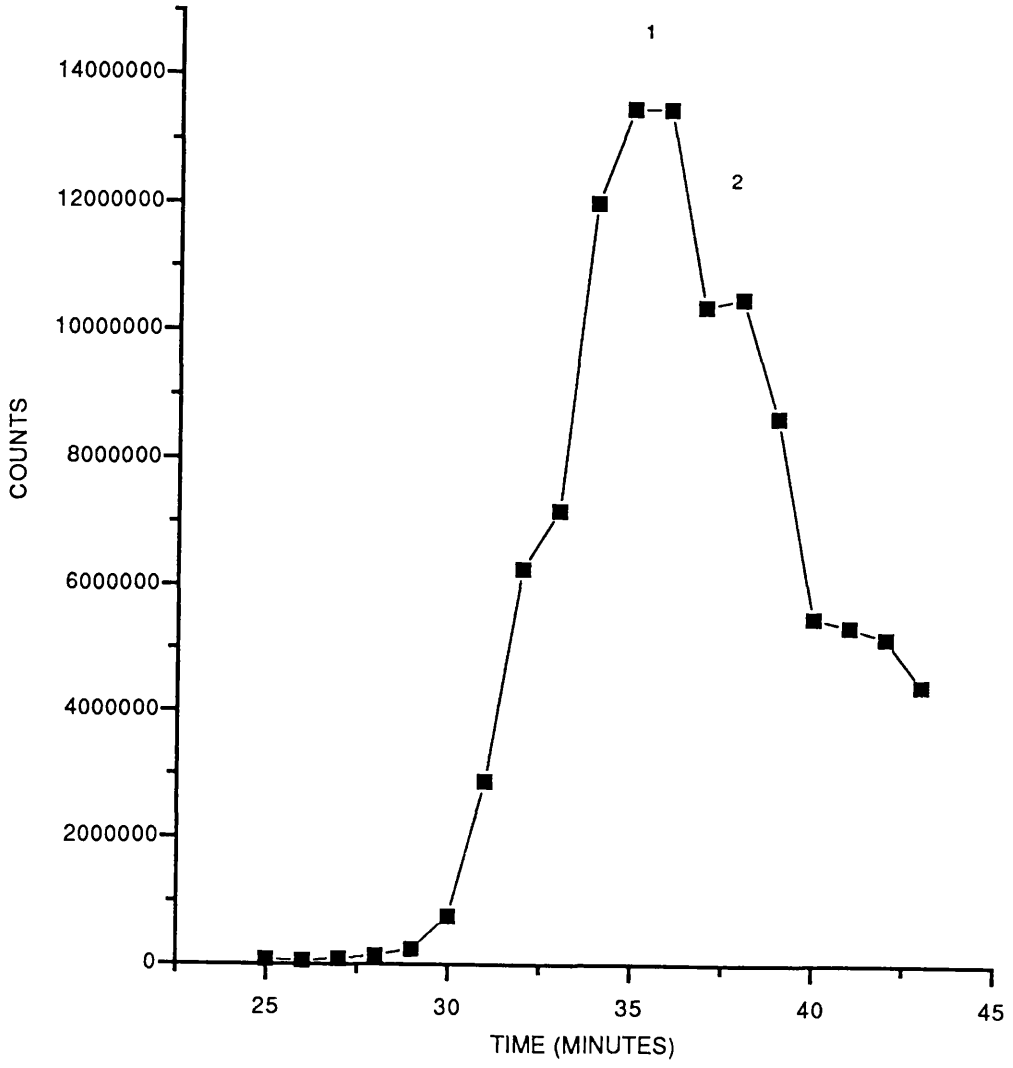

Figure 2.2. This figure shows the radioactive counts of products from the iodination of N$^{\alpha}$MTX-[Nle^{4},D-Phe^{7}]α-MSH. Peak 1 is thought to represent the mono-iodinated conjugate and peak 2 the di-iodinated conjugate.

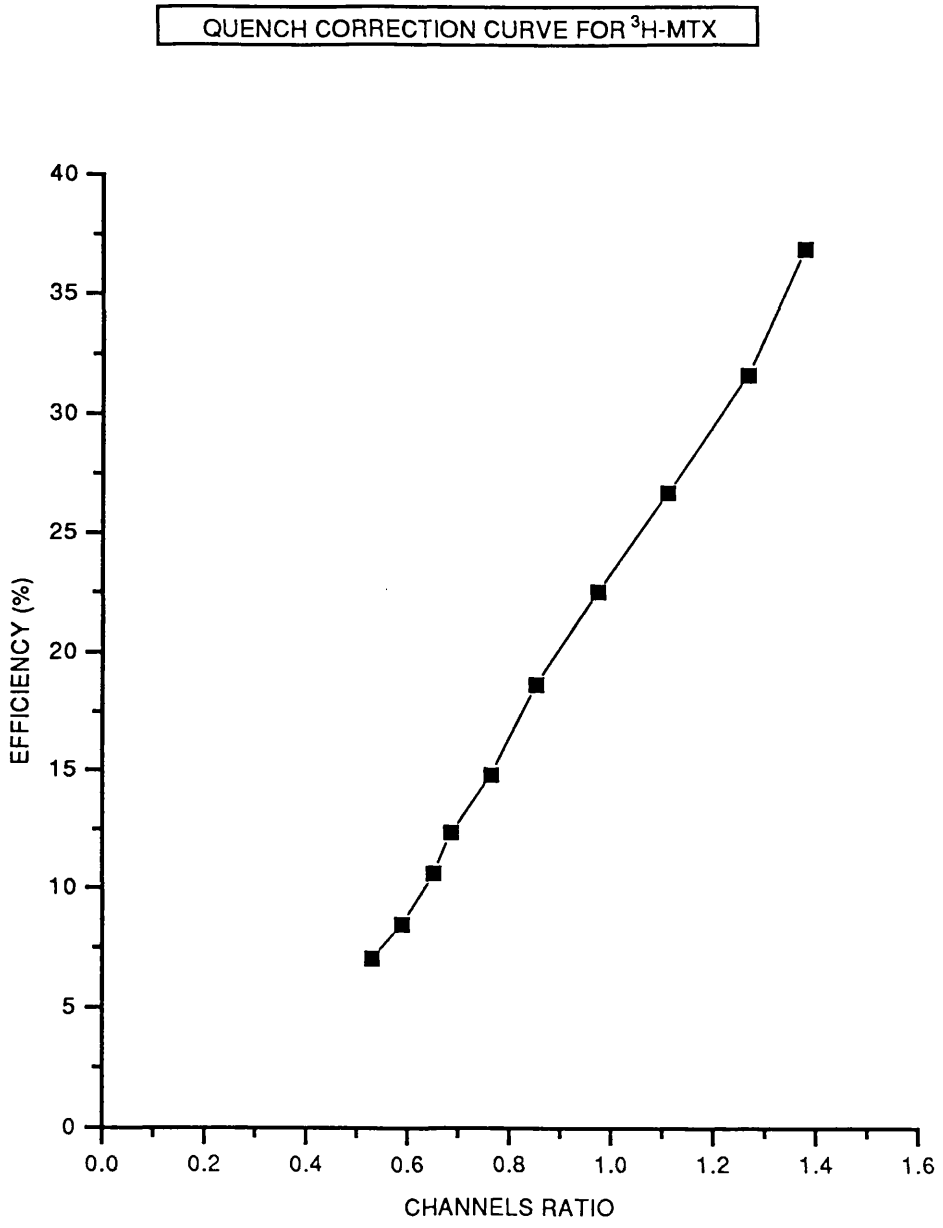

Figure 2.3. This figure represents the quench correction curve for ^{3}H-MTX which links the efficiency (E) to the channels ratio (R). *As per protocol described 2.15.2.*

CHAPTER 3:

The MTT Assay: Development of an optimised assay of cell viability based on the original Mosmann method.

3.1. INTRODUCTION:

A routine assay of viability or toxicity was required to be established. There are several viability or cytotoxicity assays available. For this study the MTT assay was chosen as it was judged to be the most useful assay procedure to employ for a number of reasons (see Sections 3.4. and 3.5.). The MTT test is a simple colorimetric assay based on the ability of living cells to reduce a tetrazolium based compound (MTT) to an insoluble blue formazan product, (Mosmann, 1983, Arnould *et al.*, 1990). Listed below are some of the other common assays together with their respective advantages and disadvantages:

3.2. Short term assays: Viability

Dye Exclusion:

Viable cells are impermeable to nigrosin, Trypan blue and hence by uptake of the dye, the cells are assumed to have a damaged membrane. This allows viability to be assessed by microscopy.

However, dye exclusion tends to overestimate viability e.g. 90% of cells thawed from liquid nitrogen may exclude Trypan blue but only 60% prove to be capable of attachment 24 hours later.

Dye Uptake:

Viable cells take up diacetyl fluorescein and hydrolyse it to fluorescein to which the cell membrane of live cells is impermeable. Live cells fluoresce green, dead cells do not. Non-viable cells may be stained with ethidium bromide or

propidium bromide and will fluoresce red. Viability is expressed as the percentage of cells fluorescing green. This technique is labour intensive and not suitable for routine quantitative screening.

3.3. Long term assays:

Plating Efficiency:

Frequently cells subjected to toxic influences e.g. antineoplastic drugs, will only show an effect several hours or days later.

Plating efficiency, as measured by the number of cells proliferating after a certain drug stress, is the best measure of survival and proliferative capacity, provided that the cells plate with a high enough efficiency so that the colonies can be considered representative. Unfortunately many animal cells have poor plating efficiencies particularly freshly isolated normal cells. This test is also time consuming to set up and analyse, particularly where a large number of samples are involved and the duration of each experiment may be anything from two to four weeks.

Microtitration Assays:

These are an alternative to the plating efficiencies as they can assay cells at higher densities:

(i) Chromium Release: $[^{51}Cr]^{3+}$

Reduced $^{51}Cr^{2+}$ is taken up by the cells and oxidised to $^{51}Cr^{3+}$ to which the membrane of viable cells is impermeable. Dead cells release the $^{51}Cr^{3+}$ into the medium. A reduction in viability is detected by gammacounting aliquots of media from cultures previously labelled with $Na_2{}^{51}CrO_4$ for released ^{51}Cr.The test works well for experiments lasting a few hours but over longer periods, spontaneous release of ^{51}Cr may be a problem.

(ii) Methionine:[^{35}S]

Active protein synthesis requires uptake of methionine. Thus total ^{35}S uptake over a fixed time period is a reflection of the number of viable cells present in a culture.

(iii) Thymidine:[^{3}H]

Labelling with thymidine ^{3}H examines the rate of DNA synthesis of the cell population.

(iv) Uridine:[^{3}H]

Labelling with uridine examines the rate of RNA synthesis of the cell population.

(v) Semiautomated microculture method:

This was devised by Finlay *et al.* (1984) using methylene blue stain, the cells are grown, treated with the drug under investigation and then stained cells are air-dried and solubilised. Absorbance of the stained cells is determined using a spectrophotometer and the optical density is directly related to cell viability.

(vi) Tetrazolium dye (MTT) metabolic assay:

This method employs the use of MTT: (3-[4,5-Dimethylthiazol-2-yl]-2,5-diphenyltetrazolium bromide, Thiazoyl blue), which is a tetrazolium dye. The reaction which takes place is the reduction of the tetrazolium salt to a blue coloured product (MTT Formazan) by the mitochondrial enzyme succinate dehydrogenase. This reaction can only take place in the presence of active mitochondria i.e. in the presence of viable cells.

3.4. The MTT Assay:

Even though it was originally developed to measure living cell numbers in lymphocytes by Mosmann (1983), the MTT assay has been modified and subsequently used in many systems e.g. primary cultured hepatocytes (Oka *et*

al., 1992), macrophages, (Jiao *et al.*, 1992) leukaemic cells, from cell lines and patients with acute myeloid leukaemia (AML), (van de Loosdrecht *et al.*, 1994) and lung cancer cell lines, (Carmichael *et al.*, 1988).

The MTT assay has also been one of the subjects of comparative *in vitro* cytotoxicity tests in conjuction with neutral red (NR) assay, uridine incorporation and protein measurements, (Husoy *et al.*, 1993). The areas of comparison were performance and sensitivity of these toxicity assays and also the intraassay agreement. The MTT assay exhibited no problems with regard to reproducibility of results although a general recommendation for more comparative studies to be undertaken with this assay was given by the authors. The cytotoxicities of drugs such as melphalan and daunorubicin were measured in a P388D1 mouse macrophage cell line and B16 mouse melanoma cell line using the MTT and tritiated thymidine uptake assays, (Arnould *et al.*, 1990). The results indicated that while both assays were found to be similar in terms of sensitivity and reproducibility, both for adherent and floating cell lines, the MTT assay had the advantages of low cost and time saving and also avoided the problems related to the manipulation and counting of radioactivity. Carmichael *et al.* (1987a and 1987b) compared the efficacy of the MTT assay with a clonogenic assay and a dye exclusion assay in their assessments of chemosensitivity and radiosensitivity of certain cell lines. In both cases the MTT assay yielded reproducible results and due to its ability to be semiautomated it was thought to be of great value in screening large numbers of potential chemosensitising and radiosensitising agents. It is also useful in drug screening with panels of human tumour cells lines examined by Alley *et al.* (1988) and was found to supersede the prototype tetrazolium salt, triphenyl tetrazolium chloride due to the latter's shortcomings *vis a vis* , slow reaction rate, lack of tissue localisation and susceptibility to reoxidation. The MTT assay is used

today in the United States National Cancer Institute's anticancer drug screening program (Alley *et al.*, 1988).

In addition to its use in comparative assays, the MTT assay has been used as an adjunct to other assay procedures e.g. digital cell image analysis (Etievant *et al.*, 1991). In this instance the MTT assay assessed the effects, on cell proliferation, of a range of drugs e.g. navelbine and adriamycin whereas the digital cell image analysis assessed the effects of the same drugs on cell kinetics. Thus both the proliferation and the kinetics of the cell line could be investigated simultaneously.

3.5. Rationale for selection of the MTT assay:

The MTT assay was selected for the current project due to the relative ease of the protocol which ensured that:

(a) A sufficient number of replicates could be performed.

(b) The time taken for the assay and also to process the results was relatively short.

(c) There were no radiolabelled substances involved.

(d) It yielded efficient and accurate results which were easily understood as they could be directly related to cell viability.

(e) MTT is relatively inexpensive to purchase.

(f) The MTT assay can be used for all cell types.

3.6. Disadvantages of the MTT Assay:

The disadvantages of the MTT assay relate mainly to the fact that the MTT formazan product is insoluble and therefore must be solubilised by the addition of an organic solvent. In recently described tetrazolium assays e.g. the MTS assay, (3-(4,5-dimethylthiazol-2-yl)-5-(3-carboxymethoxyphenyl)-2-(4-sulpho-

phenyl)-2H tetrazolium, inner salt) described by Buttke *et al.*, (1993) and Cory *et al.*, (1991) or the XTT assay, (sodium 3'-[1-[(phenylamino)-carbonyl]-3,4-tetrazolium]-bis(4-methoxy-6-nitro)benzene-sulphonic acid hydrate, (Scudiero *et al.*, 1988, Roehm *et al.*, 1991), the need for a solvent is obviated by the production of a water soluble product.

Neither of these assays are without their own complications, however. The MTS assay needs the incorporation of an electron-coupling agent such as phenazine methosulphate (PMS) as an intermediate electron acceptor in the conversion of MTS to its formazan product, (due to the fact that MTS is anionic at physiological pH). MTS is suitable if more than one assay is to be performed at the same time i.e. it can be used in combination with the ^{3}[H]TdR assay.

The main advantage of this assay seems to be that in the presence of PMS the absorbance values are higher i.e. it can be used for cells where there is a minimal detection range. For work with the melanoma cells this was not a requirement as the values obtained were always high enough to be detected and analysed.

With the XTT assay, many problems arise (Roehm *et al.*, 1991) (i) there is a slow rate of colour formation, it takes 4 hours at least and will still be reacting after 8 hours, (ii) not all cell lines can be used with XTT, (iii) even those cells that can metabolise XTT can only do so in an efficient manner when an electron coupling agent e.g. PMS (Scudiero *et al.*, 1988) or menadione, (Garn *et al.*, 1994) is added, (iv) the product yielded is orange-yellow which absorbs maximally at 450nm, this implies that yellow metabolites and reagents can potentially interfere with the spectrophotometric assay and (v) the XTT reagent must be prepared daily unlike MTT or MTS. For our purposes the MTT assay gave results that were reproducibly consistent and even though the solubilisation step entailed the use of the potentially hazardous

dimethylsulphoxide (DMSO), this solvent solubilised the product completely with speed and ease. DMSO is not favoured by others (Scudiero *et al.*, 1988) due to the safety hazard of personnel exposure to large quantities of the solvent and also the deleterious effects of DMSO on laboratory equipment.

The only other disadvantage of the MTT assay and it is one that it shares with all other microtitration techniques, is that it is impossible to distinguish between differential responses between cells within a population and the degree of response in each cell. This implies that a 50% inhibition of cells could mean that 50% of the cells respond or that each cell is inhibited by 50%. Hence the MTT assay is not able to distinguish between the cytostatic or cytocidal effects of the agent. This may seem like a big drawback but, in the light of comparative studies (Arnould *et al.*, 1990; Carmichael *et al.*, 1987a,b) where the MTT assay is tested along with more established techniques e.g. clonogenic assays and dye uptake, the $I.D._{50}$ values derived show a strong correlation between the methods, thus confirming the value of this assay for routine *in vitro* cytotoxicity assays.

3.7. Linearity of the assay:

In order to establish the range within which the assay was linear insofar as it complied with the Beer-Lambert law, experiments were undertaken, the results of which are shown in Figure 3.1. The experiment involved the measurement of the absorbance of varying concentrations of MTT formazan (Sigma M2003) in DMSO at 540 and 690nm. Figure 3.2. shows the readings obtained for varying concentrations of MTT formazan (Sigma M2003) in DMSO using a spectrophotometer at 540nm and Figure 3.3. is an expansion of Figure 3.2. in which the extent of linearity is shown.

According to the Beer Lambert law,

$$\log \left(\frac{I_0}{I} \right) = \varepsilon c l$$

or,

$$\varepsilon = \frac{A}{cl}.$$

where:

I_0 = Intensity of the incident light
(or the light intensity passing through a reference cell)

I = Light transmitted through the sample solution

A = Absorbance of the solution

c = Concentration of the solute in mol / dm^3

l = Path length of the sample in cm

ε = molar absorptivity
(correctly expressed in units of 10^{-2} m^2 / mol)

Figure 3.1. shows that the Beer Lambert Law holds up to an absorbance of 1.0 and is close to linear up to an absorbance of 2.0AU.

Figures 3.2. and its expansion in 3.3, clearly show that above an absorbance of 2.0AU, the graph reaches a plateau and the Beer-Lambert relationship does not hold.

Another test for linearity was carried out using cells (B16 murine melanoma) which were seeded at a variety of densities in the microwells. MTT was then added and the cells were supplemented with growth medium in the normal way. After a 3 hour incubation the assay was conducted in the usual manner to produce the results shown in Figure 3.4. Seeding densities within the range 1.8 x 10^2 cells per well and 5 x 10^4 cells per well were used, (eight replicates were performed in each case). A significant absorbance was obtained at a level of 1.5 x 10^4 cells which persisted up to a value of 0.94AU which corresponded to 5 x 10^4 cells per well.

3.8. Spectra of MTT and MTT Formazan:

In order to demonstrate whether MTT interfered with the assay of MTT formazan at the test wavelength, an equimolar (5 x 10^{-5}M) concentration of MTT and MTT formazan were assayed using a spectrophotometer. The results are shown in the table below and also in Figure 3.5. At 540nm MTT did not interfere with the assay of MTT formazan as MTT does not absorb at that wavelength. These data also show that the reference wavelength used (690nm) was appropriate as it does not interfere with the test, unlike the reference wavelength that was used by Sladowski *et al.* (1993), 630nm, at which point there was still too much absorption due to the formazan product. The reference wavelength (690nm) was used to correct for any precipitation of serum protein which may have occurred.

Table 3.5. Spectrophotometric absorbance readings obtained at various wavelengths for an equimolar concentration (5 x 10^{-5}M) MTT and MTT Formazan.

λ (nm)	MTT (AU)	MTT formazan (AU)
492nm	0.037	0.862
510nm	0.036	0.887
540nm	0.032	0.729
570nm	0.029	0.626
620nm	0.020	0.312
630nm	0.017	0.211
690nm	0.008	0.022

3.9. Optimal Incubation Time:

Mosmann (1983) found that the optimal incubation time was 4 hours, however this was questioned by Denizot and Lang (1986) who found that "in view of the relatively small increase in sensitivity obtained between 3 and 4 hours, we chose 3 hours". Hansen *et al.*, (1989) reduced incubation time again as they noted that after 1-2 hours the final optical density had been produced. In this study it was found that a 3 hour incubation period was adequate.

3.10. Solvents for MTT formazan:

The Mosmann method used acid-isopropanol (0.4N HCl in isopropanol) as the solvent for MTT Formazan but isopropanol is known to precipitate serum proteins (Sandberg, 1977) and this solvent also causes a phenomenon known as "colour fading" where the MTT Formazan exhibited a very blunted absorbance at 570nm and an increase in absorbance at 300 and 420nm. This colour fading was explained by an irreversible shift in absorbance maximum which seemed to be a direct result of medium acidification.

Denizot and Lang, (1986) opted for the use of propanol or ethanol as having eliminated the serum protein from the assay, the formazan could then be dissolved in pure organic solvent. This elimination process involves extra washing steps and makes the procedure more time consuming and less accurate as there is a risk of losing cells and formazan (Hansen *et al.*, 1989). Twentyman and Luscombe (1987) tried a number of solvents and found that mineral oil and acid isopropanol were slow to dissolve the formazan crystals and that solubilisation was still incomplete after 5 minutes agitation on a plate shaker but that DMSO "dissolved the formazan crystals extremely rapidly without excessive agitation". DMSO has been used in many assay protocols cf: Carmichael *et al.*, (1987a, 1987b), Stratford and Stephens (1989), Jabbar *et al.*,

(1989) and Alley *et al.*, (1988), the latter of whom undertook an assessment of other formazan solvent systems including DMF, hexane and propylene glycol, but elected to use DMSO on the grounds of the improved chemical stability of culture generated MTT formazan in DMSO. The other advantage of DMSO is that it rapidly solubilises serum protein and this accounts for the improved extraction and detection of MTT formazan generated within cultured cell systems. In all the work presented here DMSO was used. Spectrophotometric grade was used in order to stabilise absorbance readings and also reduce background absorbance.

3.11. Control experiments with 96-microwell plates:

Control experiments were performed to validate the method and are shown in Figure 3.6. Wells containing 4 x 10^4 cells were exposed to MTT and showed the characteristic absorption profile of the formazan derivative (Col 1-3, n=24). Data points are means and S.D. of absorbance values obtained using a range of filters available on the microplate reader. Maximum absorbance occurred at 530nm. By 690nm the absorbance due to MTT formazan was low and this wavelength could be used to subtract the baseline absorbance of approximately 0.1 from that which was due to the formazan derivative. Other data represented on the plot show the absorbance of other control experiments. The plastic plate itself had an absorbance in the region of 0.04AU (Col 11-12., n=16). The solvent, DMSO, added to the blank absorbance by approximately 0.03. (Col.10, n=8). The presence of 4 x 10^4 cells in the well in the absence of any MTT gave the plot shown by the filled circles (Col 4-6., n=24). The presence of medium alone in the absence of cells is shown by Col. 7-9 (n=24).

3.11.1. Optimal Seeding Density and Growth Period:

The growth of B16 cells was assessed over a 72 hour period. Seeding densities of 2.60×10^3, 4.03×10^3, 5.38×10^3, 1.07×10^4 and 2.15×10^4 cells per well were used and the cells were then counted with a haemocytometer.

Table 3.8.(a). This table shows B16 cells seeded at given densities (Column 1) and allowed to proliferate for 72 hours before being manually counted with a haemocytometer. Columns 2 and 3 represent the number of cells per well present after 72 hours, in two replicate experiments. Each value is the mean of 4 wells.

Column 1 Seeding Density	Column 2 (cells/well)	Column 3 (cells/well)
2.69×10^3	2.19×10^4	3.81×10^4
4.03×10^3	4.31×10^4	2.81×10^4
5.38×10^3	2.83×10^4	4.72×10^4
1.07×10^4	6.94×10^4	9.44×10^4
2.15×10^4	3.5×10^4	1.03×10^5

The optimum seeding density is one which allowed exponential growth over 72 hours and at the time of the assay, otherwise if the control cells were allowed to plateau then no deductions could be made in any subsequent growth inhibitory assays, as to whether the rest of the cells were affected by the antineoplastic agent or whether this could be attributed to the natural decline of the cell population.

Table 3.8.(a) shows that the first three densities seem to be proliferating well, however the last two have reached confluence and have proceeded to decline. On visual inspection it was clear that these cells were in decline even though this

is not reflected in the table above. Thus, the optimal seeding density lies between 2.69 x 10^3 and 1.07 x 10^4 cells per well. An experiment was then undertaken to check whether the final cell counts could be related to the linear portion of the MTT formazan graphs (Figures 3.1., 3.2. and 3.3.). 4 x 10^3, 8 x 10^3 and 1.2 x 10^4 cells per well were seeded for 3, 5 and 7 days and the results of this study are shown below:

Table 3.8.(b): This shows the results of a 3, 5 and 7 day incubation period with seeding densities of 4 x 10^3, 8 x 10^3 and 1.2 x 10^4 B16 cells per well. The values are given as net absorbance (540-690nm). Each value is the mean of 4 wells.

Net Absorbance (540-690nm)

SeedingDensity	3Day(AU)	5Day(AU)	7Day(AU)
4x 10^3 cells/well	0.868	1.073	0.909
8 x 10^3	0.755	0.954	0.882
1.2 x 10^4	0.802	0.866	0.922

4 x 10^3 cells per well was chosen as the lower limit for seeding B16 cells as experiments in which 1 x 10^3 cells per well and 2.5 x 10^3 cells per well were used, failed to proliferate. On the basis of the results above, it was decided that, for future work, a seeding density of 4 x 10^3 cells per well would be used and also an incubation time of 72 hours.

72 hours was chosen because B16 cells undergo 3 doublings within this time and hence will reach a level of approximately 3.2 x 10^4 cell/well, which has the advantages of (i) being within the limits of the capacity of the well and (ii) eliciting absorbance values that are still within the linear range, (iii) enabling more rapid results as more experiments may be set up within a given time period and (iv) ensuring that the medium has not been depleted of nutrients,

(during a 7 day incubation the cells would need refeeding and this would have introduced an unnecessary risk of contamination).

Another important point is that as with all cells, B16 cells go through phases in their life cycle, from the initial lag phase, where the cells are becoming accustomed to the new environment (medium, temperature, atmosphere), through the logarithmic or growth phase when the cells multiply up to a level of confluence which then plateaus off to signify the commencement of the declining phase due to the depletion of nutrients, space etc., when the cells begin to die. Ideally the absorbance values should be located in the region of the logarithmic phase of growth, (positive slope) i.e. a value of approximately 1.0AU for the control cells so that (i) it is within the linear range and (ii) the $E.C._{50}$ can be defined as the concentration of inhibitor corresponding to 0.5AU. This will be a real indication of the number of viable cells at the time of assay. In contrast if a value of 1.0AU was found for the control cells but it was on the negative slope (decline phase) then this could not be associated with a respective $E.C._{50}$ because the cells at this point would be subject to influences other than the cytostatic agent e.g. nutrient depletion, space confinement leading to contact inhibition, hence no clear conclusions could be drawn about the efficacy of the agent.

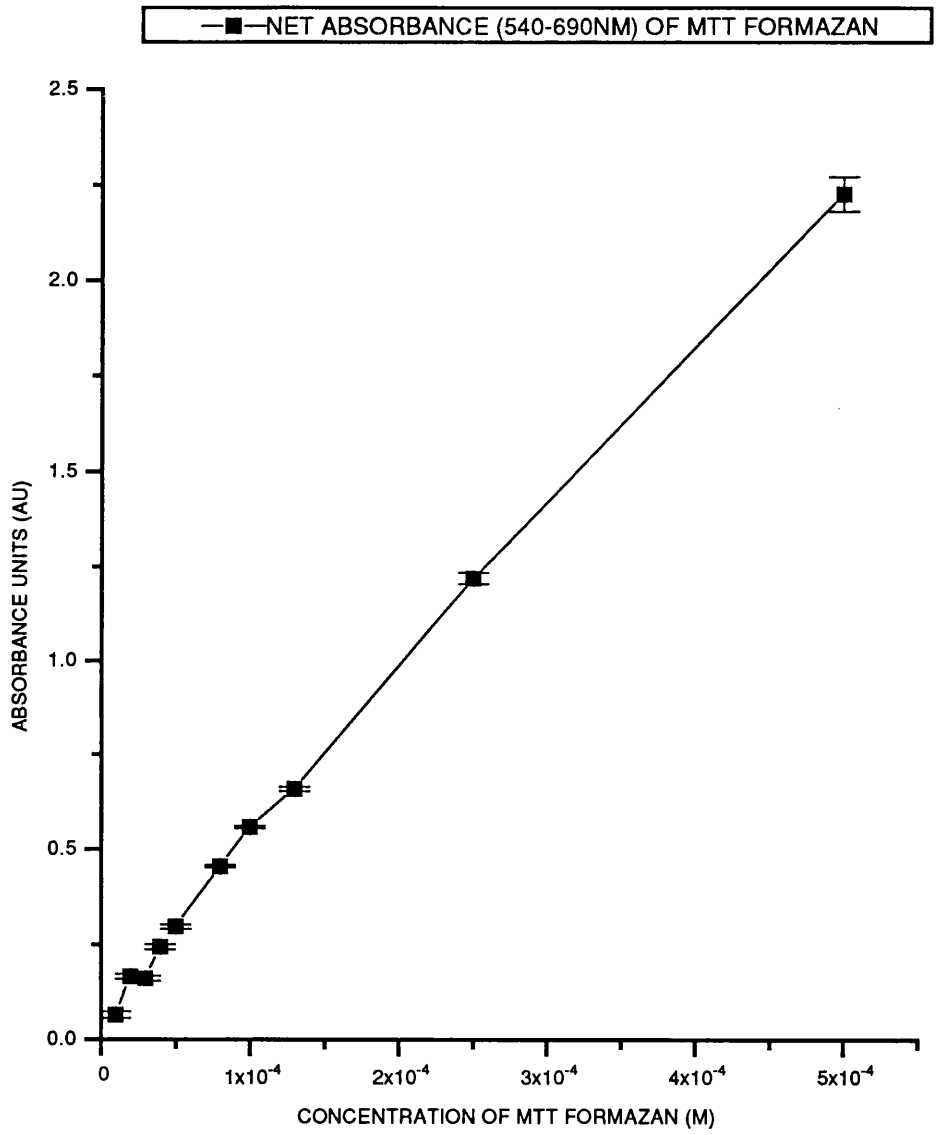

Figure 3.1. Net absorbance readings (540-690nm) obtained for increasing concentrations of MTT formazan in DMSO using a Titertek platereader at a test wavelength of 540nm and a reference wavelength of 690nm.

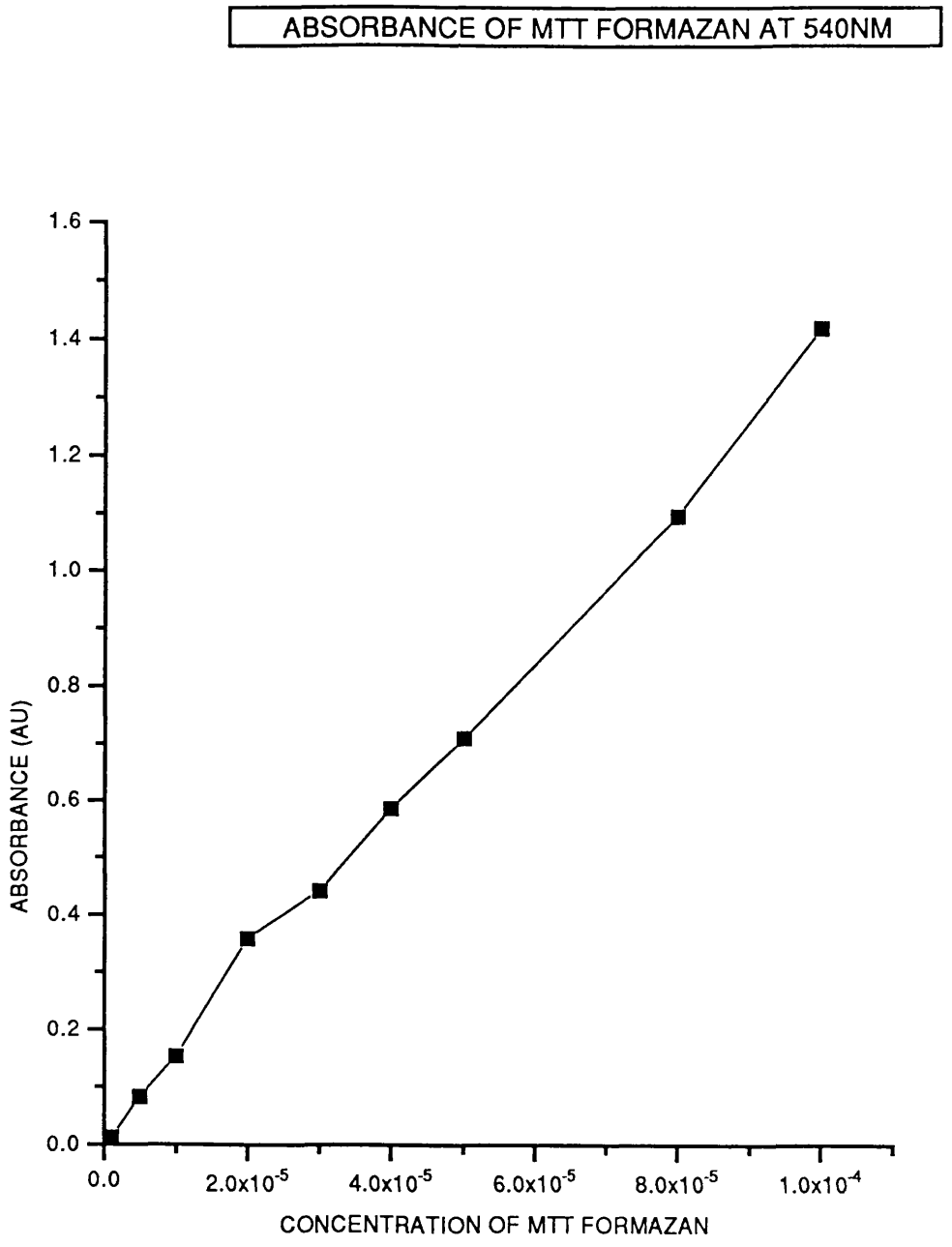

Figure 3.2. Absorbance readings (540nm) obtained for increasing concentrations of MTT formazan in DMSO as measured by a spectrophotometer.

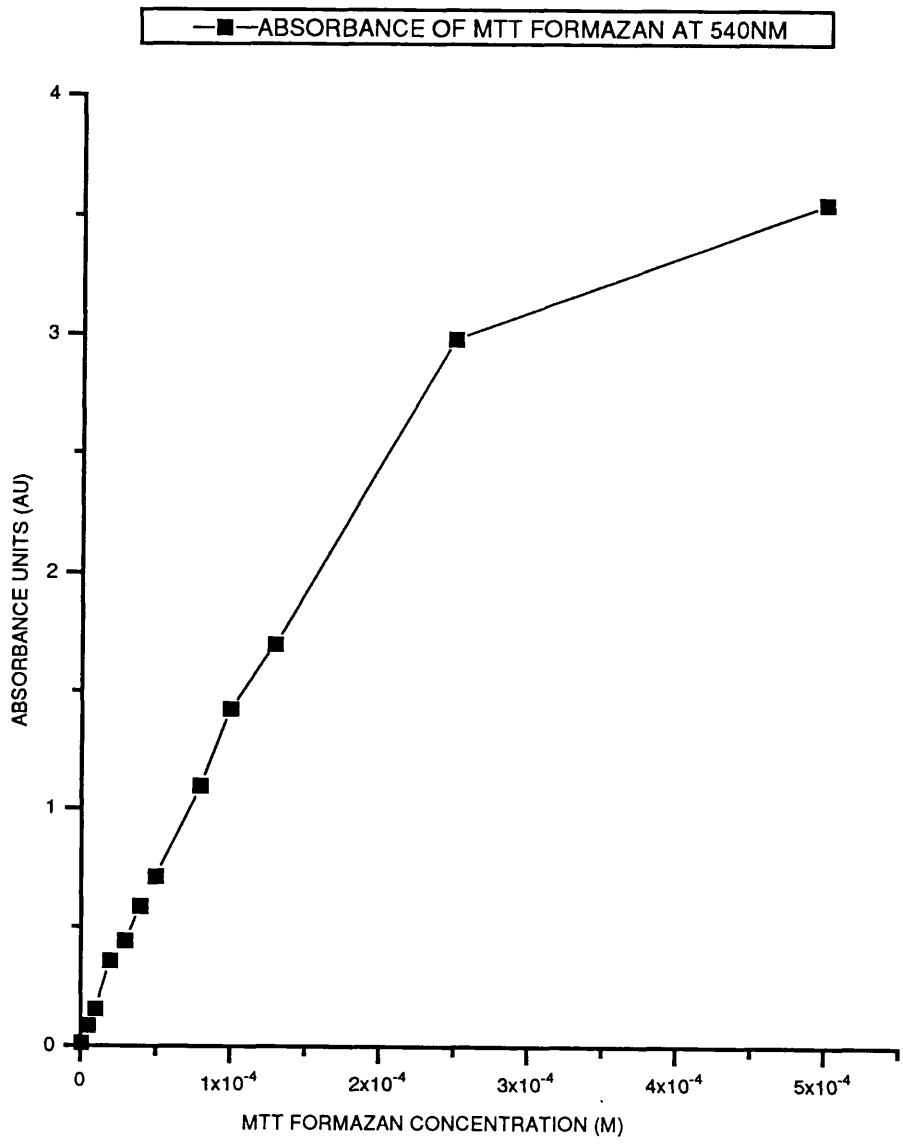

Figure 3.3. Absorbance readings (540nm) obtained for increasing concentrations of MTT formazan in DMSO as measured by a spectrophotometer. Concentrations up to 5 x 10^{-4}M are used in order to show the limits of linearity.

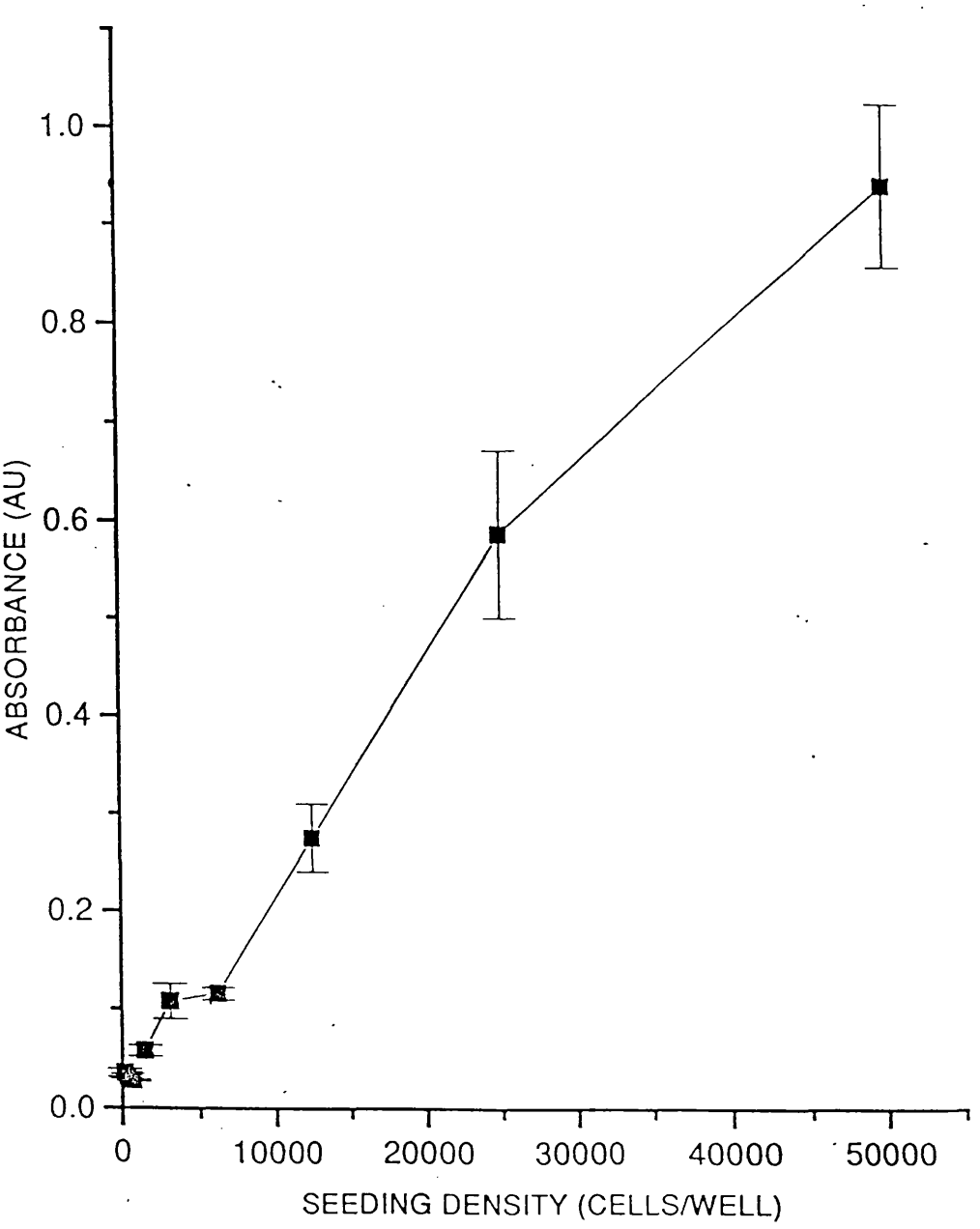

Figure 3.4. Net absorbance (540-690nm) due to MTT formazan after 3 hours at 37°C versus seeding density of B16 cells. A test wavelength of 540nm and a reference wavelength of 690nm are used.

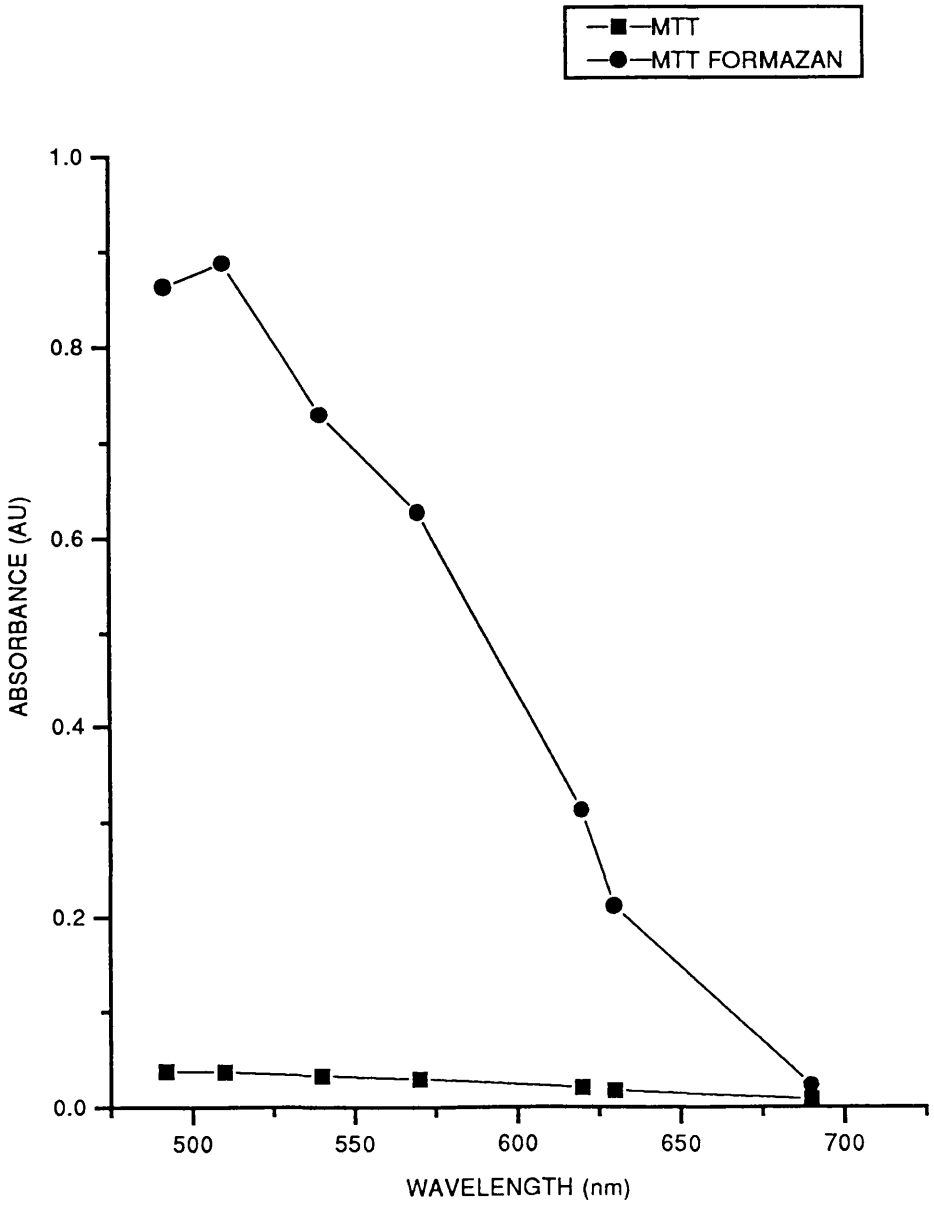

Figure 3.5. Absorbance readings obtained for 5 x 10^{-5}M of MTT and MTT formazan at various wavelengths from 400nm to 750nm.

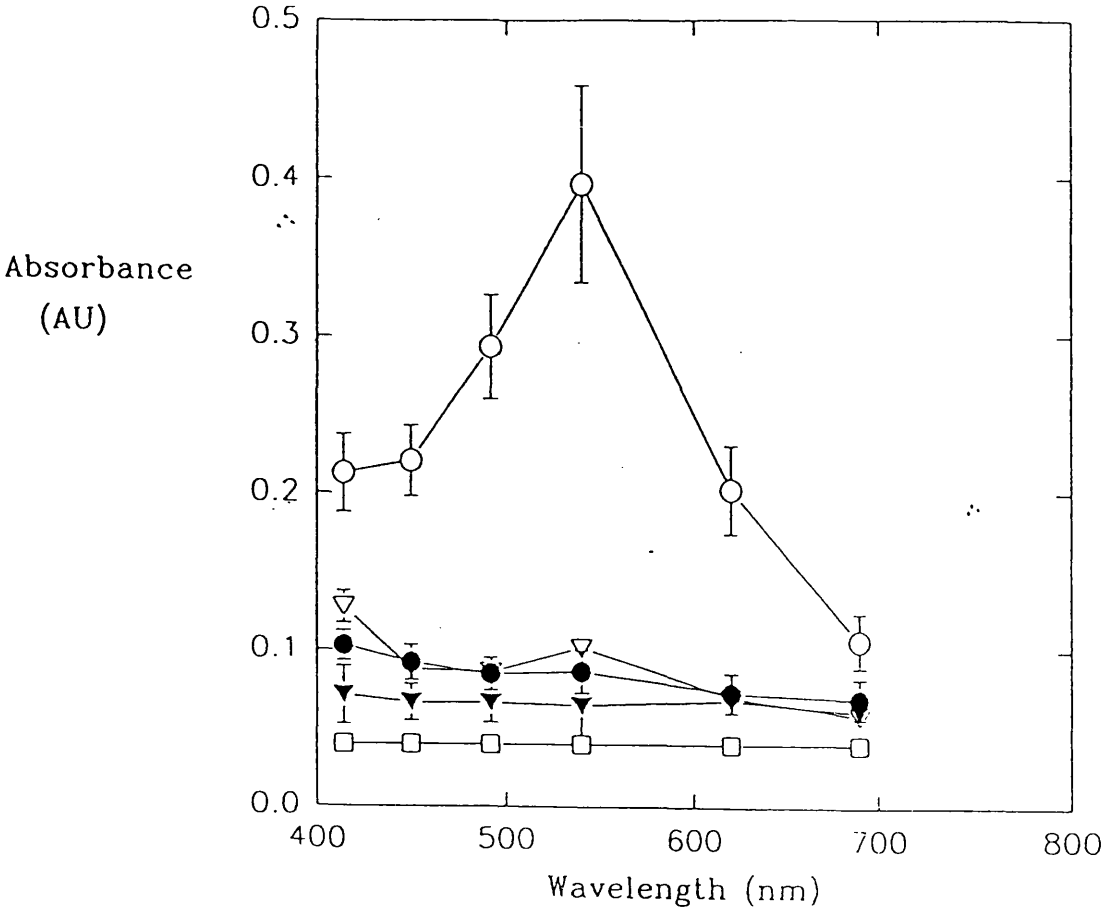

Figure 3.6. This figure shows control experiments which were performed to validate the MTT assay. A 96 microwell plate was used for the experiment and the columns were used as follows:

○ Col.1-3	**4 x 10^4 cells per well, with medium and MTT, followed after 3 hours by DMSO.**
● Col.4-6	**4 x 10^4 cells per well with medium without MTT or DMSO.**
▽ Col.7-9	**No cells, but medium and MTT, followed after 3 hours by DMSO.**
▼ Col.10	**DMSO alone.**
□ Col.11-12	**Empty plastic microwell plate.**

CHAPTER 4.

Assessment of cytotoxicity of methotrexate (MTX) using the MTT assay.

4.1. INTRODUCTION:

The overall aim of this project was to deliver the antineoplastic agent, MTX, to a specific receptor on the surface of melanoma cells and to therefore minimise non-specific side-effects. It was hoped to achieve this goal by the attachment of MTX to the hormone analogue [Nle^4,D-Phe^7]α-MSH as this would direct the MTX to the melanocortin receptors on the cell surface. Before assessing the specific improvements, if any, that N$^{\alpha}$MTX-[Nle^4,D-Phe^7]α-MSH yielded, it was first necessary to elucidate the effects of the free MTX on melanoma and non-melanoma cell lines.

Methotrexate is an antimetabolite which acts most effectively during the S-phase of the cell cycle and can be potentially cytotoxic when this coincides with the logarithmic growth phase. As the concentration of extracellular MTX increased in the microwell the viability of the cells decreased. The MTT assay exploited the relationship between extracellular concentration of MTX and cell viability because only cells with active mitochondria can reduce the MTT (yellow) to its MTT Formazan (blue/purple) product. This test yielded results which could be (i) observed visually i.e. the depth of the purple colour reflected the level of viability of the cells and (ii) quantitatively assessed by the Titertek platereader where the net absorbance values could be related to the viability of the cells.

4.2. Methods:

4.2.1. MTX-MTT assay:

Concentrations of MTX ranging from 10^{-2} to 10^{-12}M were employed in order to find where the $E.C._{50}$ value lay. Once this was determined, the range was narrowed to get a more accurate estimate.

All the cells were seeded at a density of 4 x 10^3 cells/well in 96 microwell plates. The cells were exposed to MTX in medium, over an incubation period equivalent to three doubling times of the cell line under investigation. The MTT assay was then performed. Control cells were treated in exactly the same way but the MTX was omitted.

4.3. Results :

The $E.C._{50}$ value was defined as the concentration of MTX that reduced the net absorbance (540-690nm) of the cells to 50% of that exhibited by the control cells.

B16 murine melanoma cells:

As can be seen from the table 4.1 and Figures 4.1. and 4.2., the $E.C._{50}$ value lay between 2 x 10^{-9}M and 4 x 10^{-8}M MTX (approx.) which gave an average value of 1.67 x 10^{-8}M. Therefore not all of the B16 cells were as susceptible to MTX as others even though the protocol observed was identical in all cases. This level of variation was common for B16 cells throughout all of the work presented. Further experiments (see Chapter 6) confirmed this by yielding values in the same range.

4.3.1. B16 murine melanoma cells:

MTX-MTT assay:

Table 4.1. This table represents the mean net absorbance values calculated by subtracting the reference aborbance readings at 690nm from the test absorbance readings at 540nm. The columns labelled 39, 42, 43, 44, and 47 represent the results of five separate experiments. Each value is the mean of 8 replicates with the exception of the control cells which involved 16 replicates. Column 1 contains the concentrations of MTX used. The $E.C._{50}$ and standard deviation values were generated using the MINSQ non-linear regression program (weighting =2).

NET MEAN ABSORBANCE (AU)

MTX (M)	(39)	(42)	(43)	(44)	(47)
Control	1.142	2.240	1.923	1.776	2.108
1.1×10^{-11}	------	2.188	2.103	1.412	------
1.1×10^{-10}	------	2.433	2.113	1.927	------
2.2×10^{-10}	------	------	1.708	1.584	1.985
5.5×10^{-10}	------	------	2.119	1.800	2.060
1.1×10^{-9}	0.653	1.192	2.069	1.505	------
2.2×10^{-9}	------	------	1.847	1.610	1.598
5.5×10^{-9}	------	------	2.228	2.003	1.940
1.1×10^{-8}	0.385	0.433	1.909	1.425	-------
2.2×10^{-8}	------	------	1.463	1.488	0.870
5.5×10^{-8}	------	------	0.946	0.839	0.527
1.1×10^{-7}	0.240	0.261	0.582	0.423	0.171
2.2×10^{-7}	------	------	0.336	0.408	0.290
5.5×10^{-7}	------	------	0.174	0.273	0.158
1.1×10^{-6}	0.175	0.182	0.214	0.152	0.180
1.1×10^{-5}	0.120	0.128	0.165	0.117	0.174
1.1×10^{-4}	0.139	0.115	0.200	0.120	0.188
1.1×10^{-3}	0.171	0.118	0.132	------	------
1.1×10^{-2}	0.144	0.085	0.105	------	------
$E.C._{50}$(M)	5.3×10^{-9}	2.0×10^{-9}	3.0×10^{-8}	$4.0\ 10^{-8}$	6.3×10^{-9}
S.D.(+/-)	3.1×10^{-9}	1.0×10^{-9}	5.9×10^{-9}	7.4×10^{-9}	3.1×10^{-9}

4.3.2. MeWo human melanoma cell line:

MTX-MTT Assay:

Growth experiments were undertaken to optimise the conditions of the assay and it was found that a 6 day incubation period allowed the cells to double three times (doubling time of MeWo = 48 hours (Figure 4.3.(a)). This incubation time was also suitable because it avoided the refeeding of the cells. The cells were seeded at a density of 4 x 10^3 cells/well which, as can be seen from Figure 4.3.(b), after 3 doubling reaches a level of 3.2 x 10^4 cells/well which yields absorbance readings in the region of 1.0 AU.

Table 4.2 shows the results of three replicate experiments with the MeWo cell line and the $E.C._{50}$ values obtained. From the results shown in table 4.2 and Figures 4.4. and 4.5. it was clear that the MeWo cells were inhibited by MTX. As the concentration of MTX increased from 10^{-13} to 10^{-2}M so the absorbance values and hence viability of the MeWo cells decreased. The $E.C._{50}$ values ranged from 4 x 10^{-9} to 9 x 10^{-11} M MTX (approx.) and lead to a mean $E.C._{50}$ value for MeWo cells of 1.31 x 10^{-9} M MTX. This value was an order of magnitude lower than the value for B16 cells and implied that the MeWo cells were more sensitive to the effects of the antimetabolite.

Table 4.2. This shows the results of three replicate experiments (71,73 and 76) in which the MeWo cells were incubated for 6 days at 37°C with various concentrations of MTX (shown in Column 1). The results are presented as net mean absorbance readings (540-690nm). Each point is the mean of eight replicates with the exception of control values which are the mean of sixteen replicates. The $E.C._{50}$ and standard deviation values were generated using the MINSQ non-linear regression program (weighting=1).

NET MEAN ABSORBANCE (AU)

MTX (M)	71	73	76
Control	2.141	2.476	1.097
1.1×10^{-13}	------	2.486	------
1.1×10^{-12}	1.632	2.014	1.235
1.1×10^{-11}	1.607	1.916	1.309
1.1×10^{-10}	1.384	0.952	0.611
1.1×10^{-9}	1.167	0.582	0.538
1.1×10^{-8}	0.642	0.254	0.349
1.1×10^{-7}	0.277	0.104	0.248
1.1×10^{-6}	0.350	0.111	0.164
1.1×10^{-5}	0.297	0.108	0.149
1.1×10^{-4}	0.233	0.119	------
1.1×10^{-3}	0.270	0.104	------
1.1×10^{-2}	0.233	0.058	------
$E.C._{50}$(M)	3.7×10^{-9}	1.0×10^{-10}	9.4×10^{-11}
S.D.(+/-)	1.0×10^{-9}	4.0×10^{-11}	7.0×10^{-11}

4.3.3.SVK14 cells:

SVK14 cells were keratinocytes and therefore possessed few if any MSH receptors. It would be expected that due to this MTX alone would act quite efficiently at killing the cells via the folic acid pathway, which was present, however the N^{α}MTX-[Nle^4,D-Phe^7]α-MSH conjugate would not be expected to produce such a dramatic effect on the viability of the cells because of the restricted entry pathway.(See chapter 5).

The results shown in table 4.3 and Figure 4.6 represented the effects of MTX on these keratinocytes. It was quite clear from experiment no. 88, that an extracellular concentration of 1.1 x 10^{-11}M MTX or greater was effective at killing the cells. In experiment no. 94, the concentrations of MTX were more dilute i.e., down to 1.1×10^{-13} M but this was still too concentrated for the cells. Hence, it can be deduced that an extracellular concentration of 10^{-13} M or greater was effective at inhibiting the growth of SVK14 keratinocytes.

Table 4.3. This shows the results of two replicate experiments (88,94) performed with SVK14 keratinocytes. The net mean absorbance is calculated by subtracting the reference readings (690nm) from the test readings(540nm). Each point is the mean of eight replicates. Control values are the mean of sixteen replicates. Concentrations of MTX(M) are given in column 1. It was not possible to estimate accurate values for the $E.C._{50}$ values using the MINSQ non-linear regression programme.

	NET MEAN ABSORBANCE (AU)	
MTX (M)	**88**	**94**
Control	**0.960**	**1.121**
1.1×10^{-13}	**-------**	**0.073**
1.1×10^{-12}	**-------**	**0.030**
1.1×10^{-11}	**0.027**	**0.037**
1.1×10^{-10}	**0.025**	**0.028**
1.1×10^{-9}	**0.025**	**0.037**
1.1×10^{-8}	**0.027**	**0.027**
1.1×10^{-7}	**0.034**	**0.032**
1.1×10^{-6}	**0.032**	**0.031**
1.1×10^{-5}	**0.033**	**0.025**
1.1×10^{-4}	**0.031**	**0.028**
1.1×10^{-3}	**0.037**	**-------**
1.1×10^{-2}	**0.033**	**-------**
$E.C._{50}$	**$< 10^{-11}$M**	**$< 10^{-13}$M**

4.3.4. Transformed 293 cell lines:

Native 293 cells are derived from human embryonic kidney (HEK) cells and do not contain the MC3 receptor. These cells are transfected with a vector (pcDNA neo) which contained the gene encoding for the MC3 receptor. Subsequently selection was used to obtain a clone with stable expression of the MC3 receptor. Control 293 cells were also transduced with pcDNA neo and these were used on a comparative basis to see whether the process of transfection of the vector altered the cells response to either MTX or N$^{\alpha}$MTX-[Nle^{4},D-Phe^{7}]α-MSH. In table 4.4. and Figure 4.7 the results of two experiments using transformed 293 cells with and without MC3 receptors are shown labelled as 146 and 147 respectively.

Table 4.4. This shows the net mean absorbance values (540-690nm) for 293 cells transfected with the vector holding the encoded gene for MC3 receptors (146) and 293 cells which possessed the vector but no encoded gene (147) obtained after incubation with a range of concentrations of MTX (column 1). Each point is the mean of eight replicates.The E.C.$_{50}$ and standard deviation values were generated using the MINSQ non-linear regression program (weighting=1).

	NET MEAN ABSORBANCE	
MTX (M)	**146**	**147**
Control	**0.815**	**0.970**
1.1 x 10^{-13}	**0.696**	**0.598**
1.1 x 10^{-12}	**0.664**	**0.253**
1.1 x 10^{-11}	**0.496**	**0.291**
1.1 x 10^{-10}	**0.264**	**0.204**
1.1 x 10^{-9}	**0.406**	**0.186**
1.1 x 10^{-8}	**0.152**	**0.133**
1.1 x 10^{-7}	**0.101**	**0.120**
1.1 x 10^{-6}	**0.156**	**0.116**
1.1 x 10^{-5}	**-------**	**0.093**
1.1 x 10^{-4}	**0.112**	**0.130**
E.C.$_{50}$(M)	**3.0 x 10^{-11}**	**2.8 x 10^{-13}**
S.D.(+/-)	**2.8 x 10^{-11}**	**3.0 x 10^{-13}**

The results presented in table 4.4. and Figure 4.7., suggested that the transformed 293 cells without the MC3 receptors were more sensitive to the effects of MTX than the 293 cells with the MC3 receptors i.e. less MTX was necessary in order to effectively inhibit the growth of these cells. This result was not established by replication during this study, and though non-linear regression appeared to give good estimates of $E.C._{50}$ values, visual inspection suggests the errors involved were considerable, so that it was not clear how significant was the difference between the two experiments.

4.4. Summary.

The cell lines examined exhibited an increasing order of sensitivity to MTX as follows:

B16 < MeWo < transformed 293 cell line (with MC3 receptor) < transformed 293 cell line (without MC3 receptor) < SVK14 keratinocytes.

MTX was assumed to be taken up via the folic acid transport pathway present in all cells. The cumulative results of five separate experiments using the B16 cell line are shown in Table 4.1. It can be seen from the range over which the $E.C._{50}$ values lay, that these data were reproducible. The standard deviation values also indicated an acceptable level of intraexperimental differences. After Experiments "39" and "42" were performed, more concentrations were included to give a fuller profile of the inhibitory effects of MTX on these murine melanoma cells. MeWo human melanoma cells were more (tenfold) sensitive to the effects of MTX as shown by the differences in their respective average $E.C._{50}$ values. It was also noticed while performing the experiments that as the passage of the MeWo cell line increased from "71" (passage I_{21}) to "76" (passage I_{26}) there was an increased sensitivity to the effects of MTX.

This was the only cell line where such a phenomenon was noticed by the operator and whether this sensitivity to MTX would have continued over further passages needs to be determined in future work. As with the B16 cells the standard deviation showed that intraexperimental differences were not high. Some of the control values for the absorbance for both the B16 and the MeWo cell lines were greater than 2.0AU and hence outside the limits of linearity. The MINSQ non-linear regression programme was used with a weighting=1 which took account of this potential source of error. SVK14 keratinocytes displayed the greatest degree of sensitivity. Unfortunately only two experiments were performed and an accurate value for the $E.C._{50}$ was not obtained. It was still clear however that these cells only needed an extracellular concentration of 10^{-13}M or greater MTX to effect cell death. Preliminary experiments were performed using transformed 293 cells with and without MC3 receptors. The results of which are shown in Table 4.4., the 293 cells with MC3 receptors, although more sensitive to MTX than either B16 or MeWo cell lines were more resistant than the 293 cells without MC3 receptors or SVK14 keratinocytes. SVK14 keratinocytes and both of the transformed 293 cell lines are used as control cell lines and their results will gain more relevance when judged with those of Chapter 5.

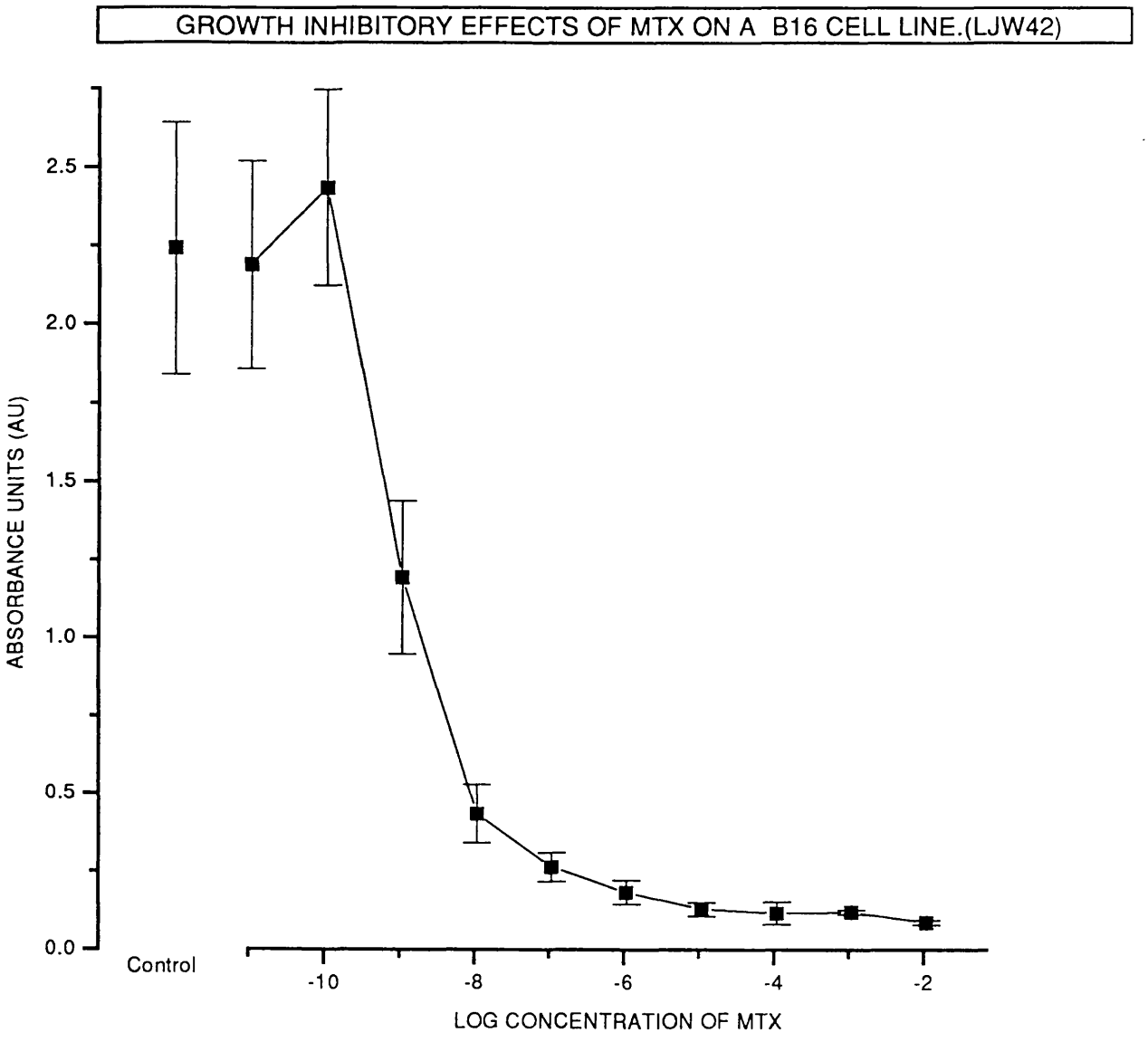

Figure 4.1. Net absorbance readings (540-690nm) obtained with B16 cells incubated with MTX. Each point is the mean of 8 replicates. Control values are the mean of 16 replicates. Standard deviation is shown by error bars.

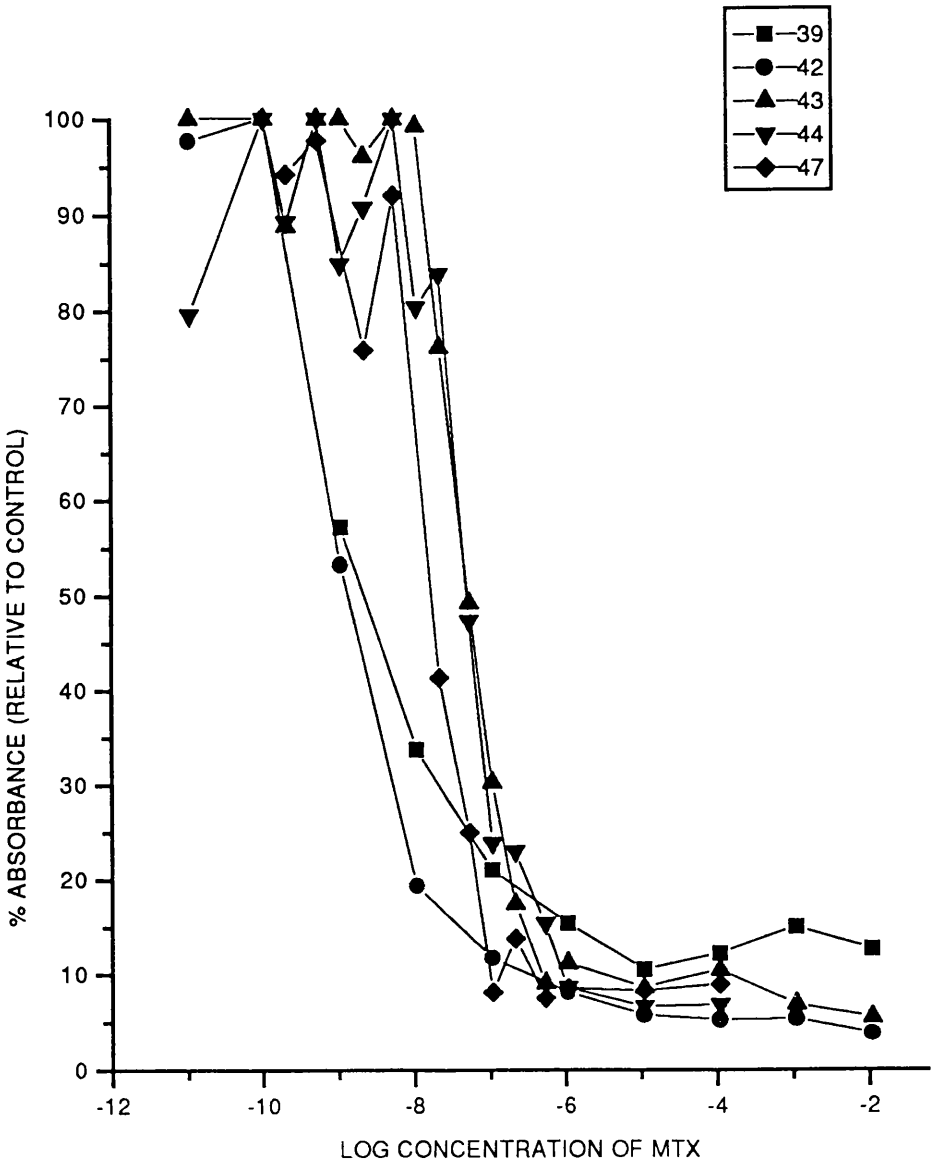

Figure 4.2. Relative values obtained for absorbance of B16 cells exposed to MTX. The results of 4 replicate experiments are shown. Each point is the mean of 8 wells. Error bars have been omitted for clarity.

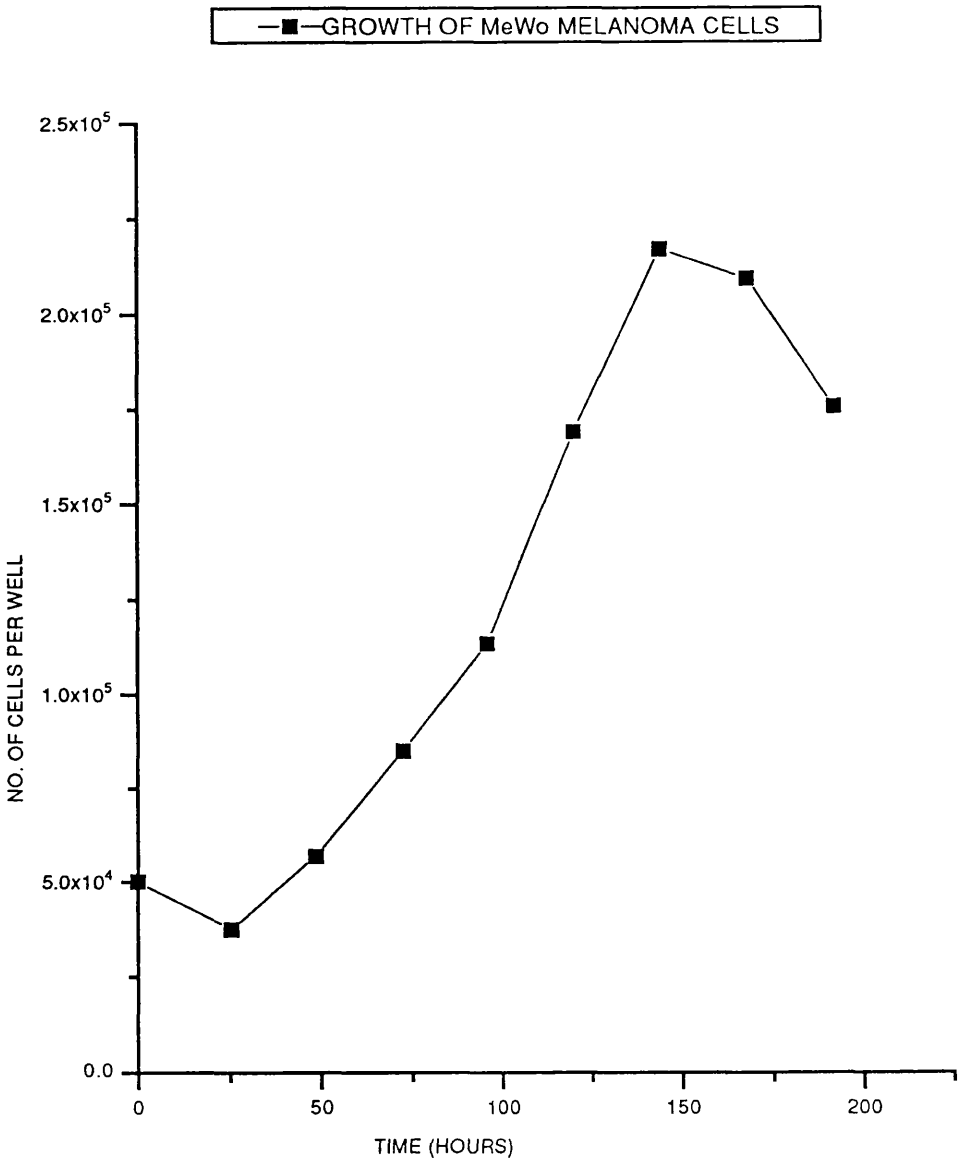

Figure 4.3.(a). Growth curve obtained for MeWo cells seeded at 5 x 10^4cells per well in RPMI-FCS. Cells were incubated at 37°C and counted using the Trypan Blue dye exclusion assay. Error bars have been omitted for clarity.

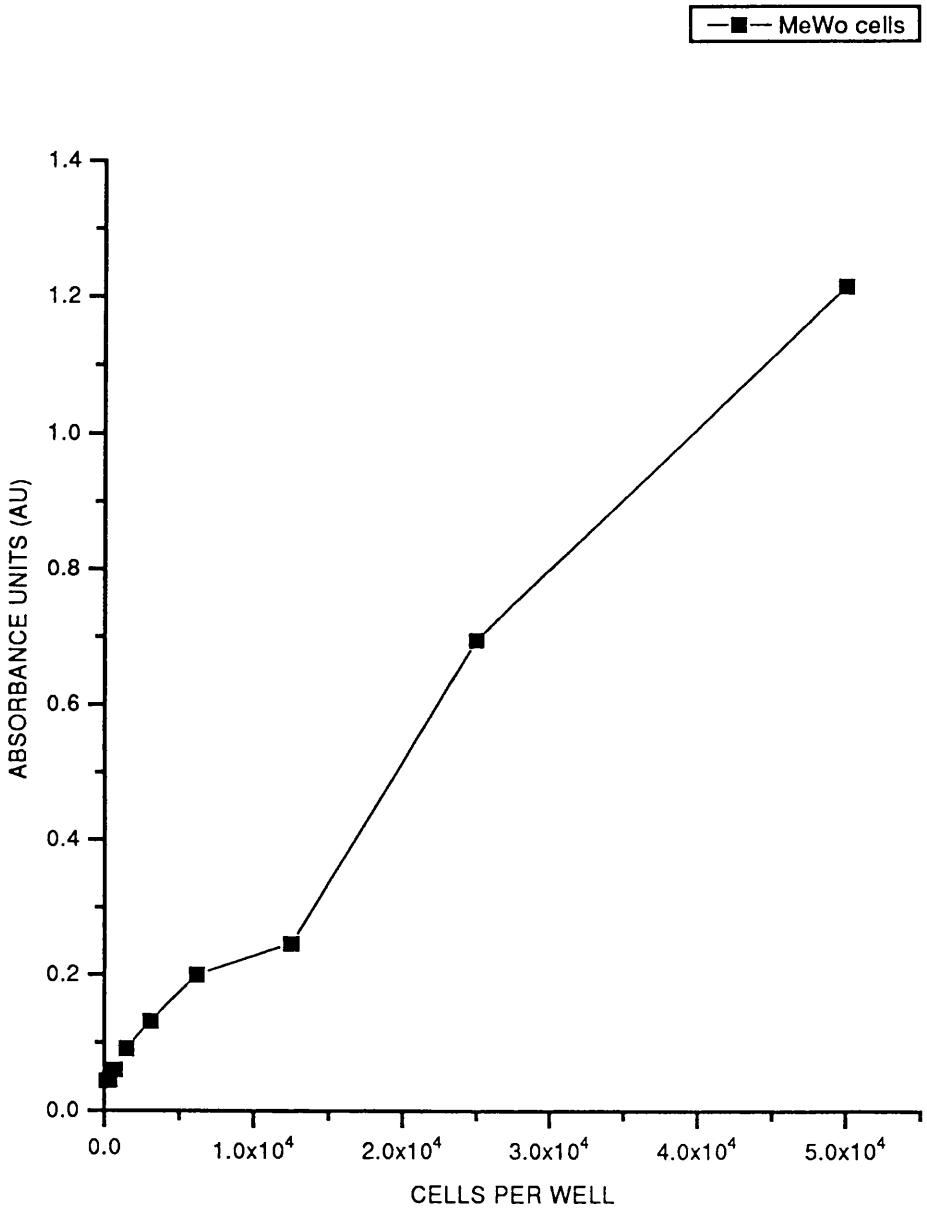

Figure 4.3.(b). Net absorbance readings (540-690nm) obtained for MeWo cells versus the number of cells seeded per well. Each point is the mean of 8 wells. Error bars have been omitted for clarity.

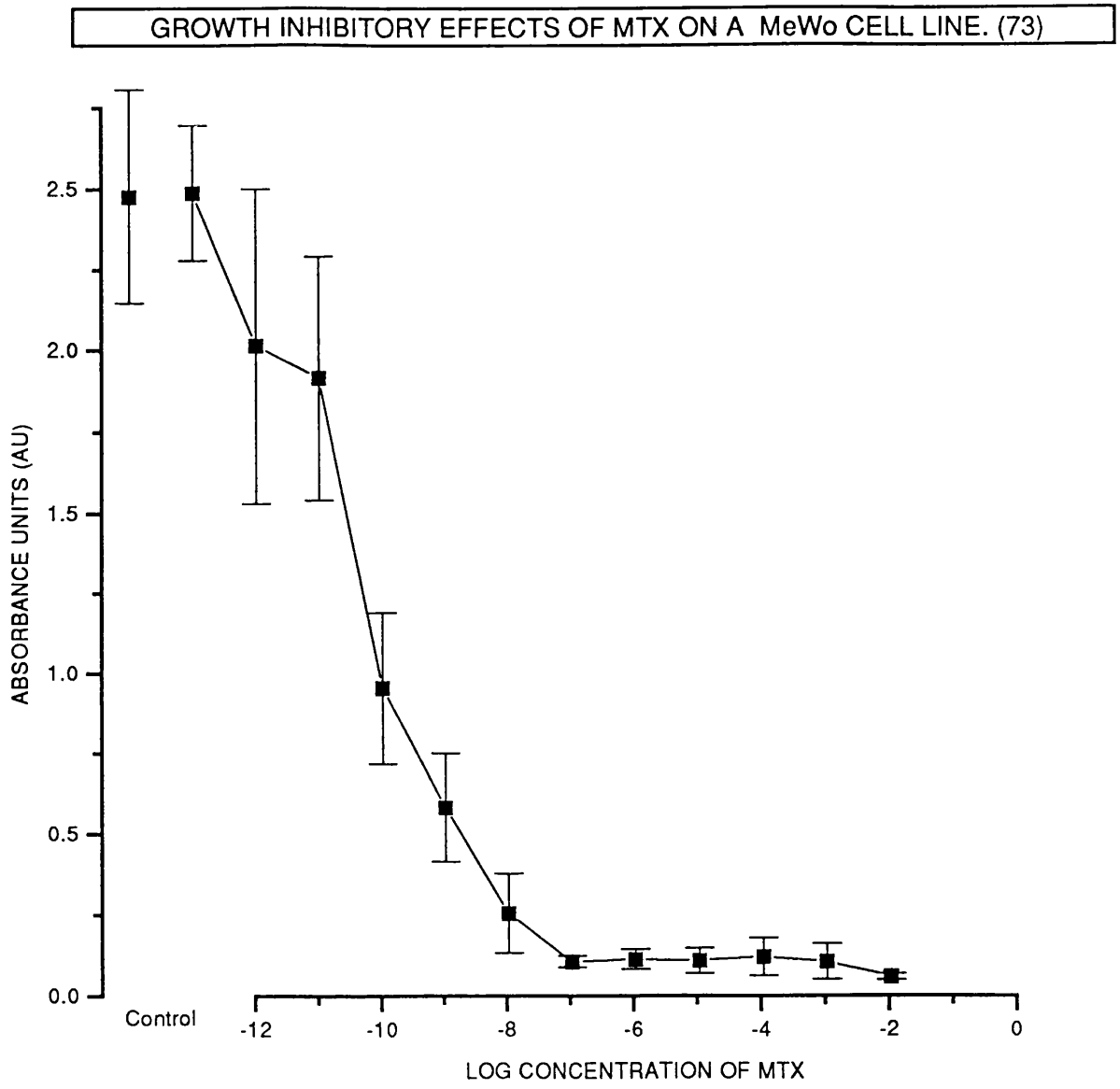

Figure 4.4. Net absorbance readings (540-690nm) obtained for MeWo cells exposed to MTX. Each point is the mean of 8 wells. Control values are the mean of 16 wells. Standard deviation is shown by error bars.

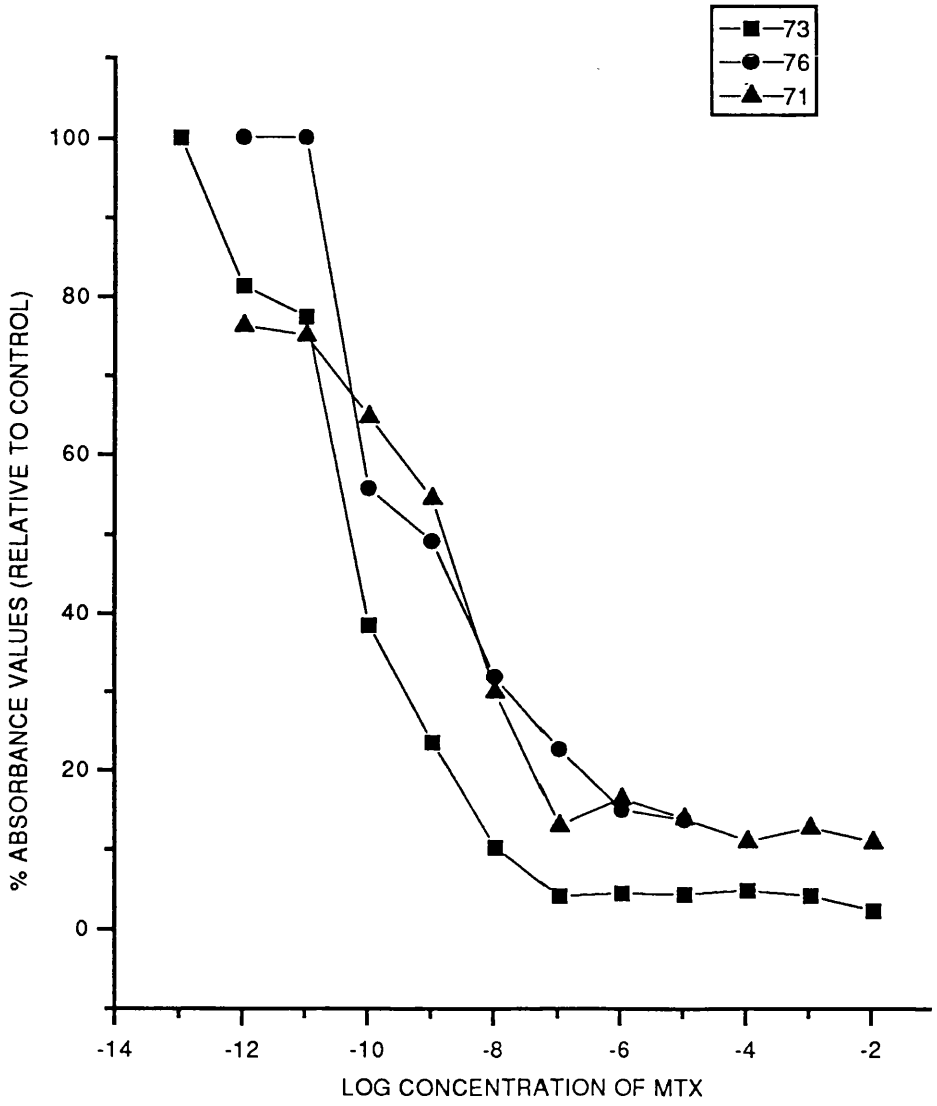

Figure 4.5. Relative values obtained for the absorbance of MeWo cells exposed to MTX. Results of 3 replicate experiments are shown. Each point is the mean of 8 wells. Error bars have been omitted for clarity.

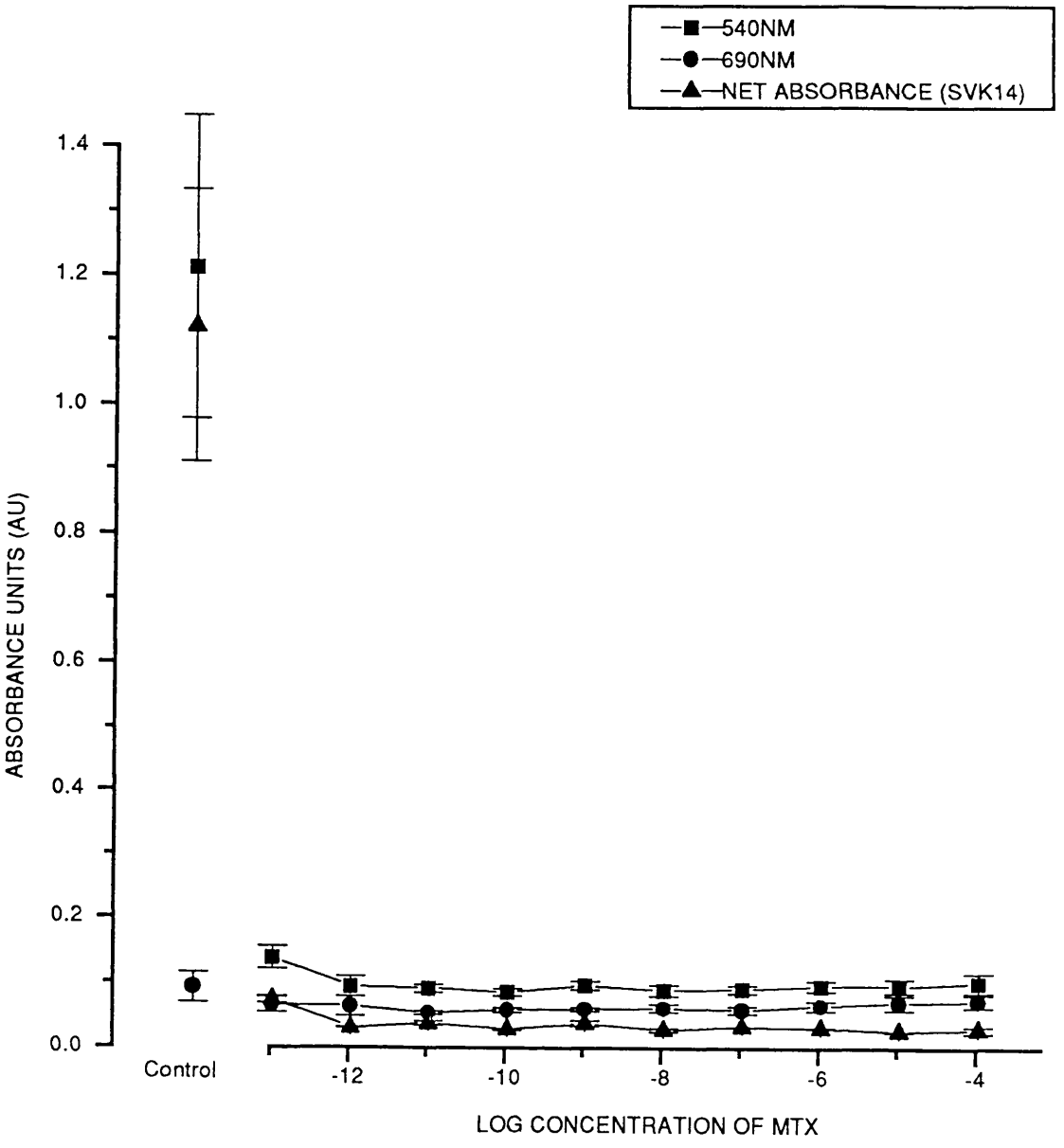

Figure 4.6. Absorbance readings obtained at test (540nm) , reference (690nm) and net absorbance (540-690nm) readings for SVK14 keratinocytes exposed to MTX.Each point is the mean of 8 wells. Standard deviation is shown by error bars.

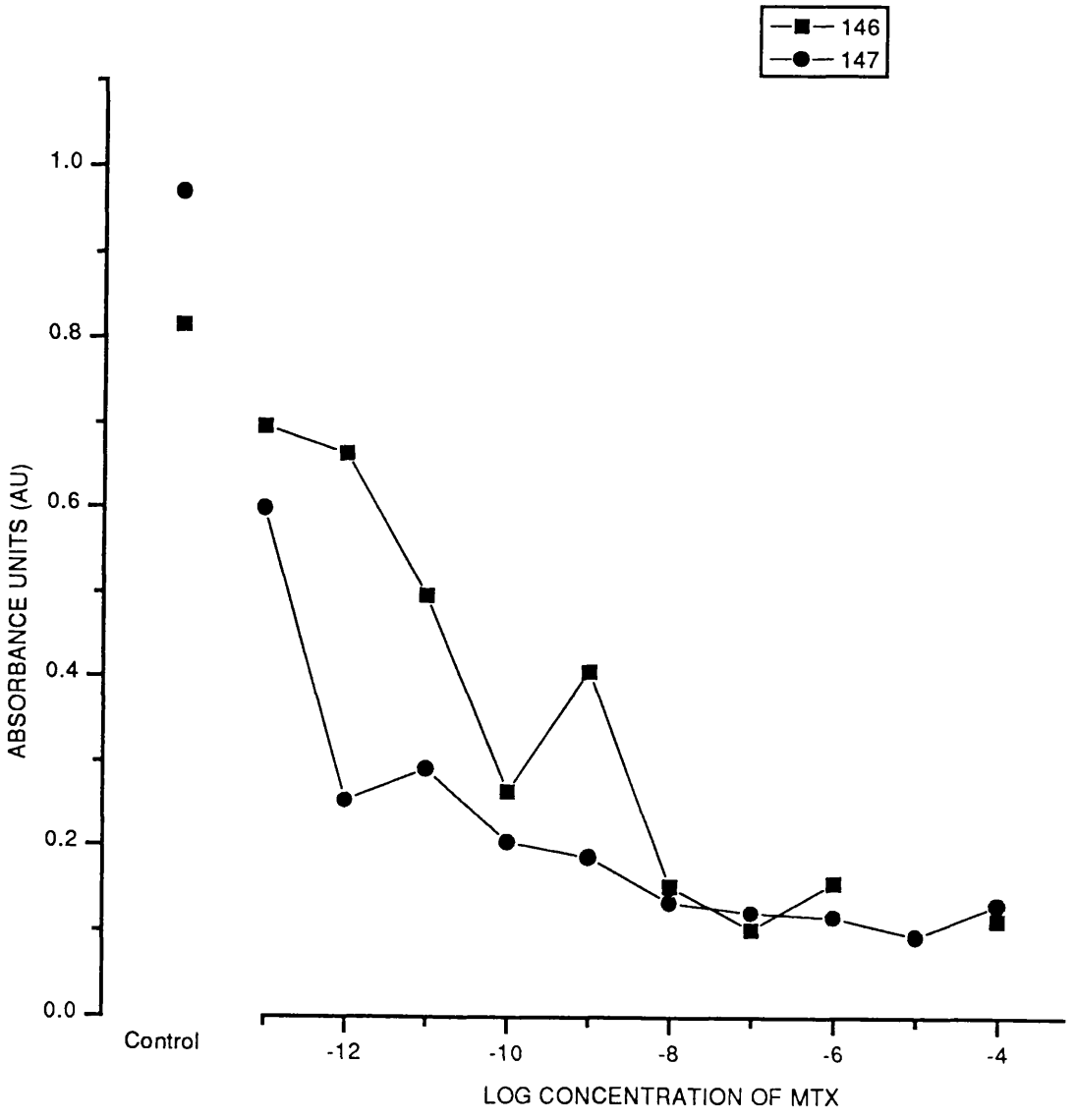

Figure 4.7. Net absorbance readings (540-690nm) obtained for transformed 293 cells with (146) and without (147) MC3 receptors. Each point is the mean of 8 wells. Error bars have been omitted for clarity.

Chapter 5.
N^{α}MTX-[Nle^4,D-Phe^7]α-MSH: Experimentation on Uptake and Growth Inhibitory Effects.

5.1. Introduction.

Methotrexate was chosen as the model drug in this study of site-specific drug delivery to melanoma cells. In order to increase the site specificity with which MTX exerted its inhibitory effects on melanoma cells, the molecule was chemically coupled to an analogue of the naturally occurring hormone, α–MSH namely: [Nle^4,D-Phe^7]α-MSH on an equimolar basis, forming the hormone-drug conjugate, N^{α}MTX-[Nle^4,D-Phe^7]α–MSH. The hypothesis was that if MTX was not taken up by its normal route i.e. the folic acid pathway but rather by a cell-specific receptor-mediated process (in this case utilising the α-MSH receptor) then the targeting of the drug to melanoma could be exploited and the side effects could be markedly reduced.

Binding experiments were performed with the radiolabelled conjugate N^{α}MTX-[^{125}I-Tyr^2,Nle^4,D-Phe^7]α-MSH in the presence of both the MC1 and the MC3 receptors. The results of these experiments allowed the estimate of the affinities of the ligand for the different receptors. Competition binding assays were done and gave Kd values for the unlabelled conjugate. The targeted molecule is the unlabelled rather than the radiolabelled N^{α}MTX-[Nle^4-,D-Phe^7]α-MSH and since radiolabelling affects the affinity of ligands for receptors, the affinity of the unlabelled moiety should be known.

Internalisation experiments were also performed with continuous exposure and Pulse-Chase labelling protocols in the presence and absence of NH_4Cl. These experiments traced the path of the N^{α}MTX-[^{125}I-Tyr^2,Nle^4,D-Phe^7]α-MSH

once it had bound to the receptor and helped to elucidate the intracellular fate of the ligand.

The inhibition of growth by N$^{\alpha}$MTX-[Nle^{4},D-Phe^{7}]α–MSH on a range of cell lines was investigated using the same assay as for MTX alone and hence the results of both (see Chapter 4 for MTX results) may be compared.

5.2. Degradation of N$^{\alpha}$MTX-[Nle^{4},D-Phe^{7}]α–MSH.

See chapter 2.12. for a detailed protocol.

To assess the degradation of N$^{\alpha}$MTX-[Nle^{4},D-Phe^{7}]α–MSH and hence to determine whether or not it is degraded into MTX and / or [Nle^{4},D-Phe^{7}]α-MSH, 3.05 x 10^{5} B16 cells were seeded per 25cm^{2} tissue culture flasks. 10ml of RPMI-FCS containing 5 x 10^{-5}M N$^{\alpha}$MTX-[Nle^{4},D-Phe^{7}]α–MSH was added. It should be noted that this concentration exceeds the $E.C._{50}$. The cells were gassed and placed in an incubator at 37°C. At various time intervals (24, 48 and 72 hours) a flask was removed and the medium decanted. The medium was then centrifuged and analysed by HPLC at 217 and 310nm. A control flask which contained no N$^{\alpha}$MTX-[Nle^{4},D-Phe^{7}]α–MSH was treated in a similar manner.

Figure 5.1 represents the HPLC trace of [Nle^{4},D-Phe^{7}]α-MSH (labelled NLDP) at 217nm and 310nm. [Nle^{4},D-Phe^{7}]α-MSH is known to be detected at 217nm (see purification procedure, Chapter 2.10.) and this trace demonstrated that the [Nle^{4},D-Phe^{7}]α-MSH is eluted at 48-52 minutes with detection at this wavelength whereas no absorption at 310nm was observed.

The elution profiles of the N$^{\alpha}$MTX-[Nle^{4},D-Phe^{7}]α-MSH (labelled MTX-NLDP) at 217nm and 310nm are shown in Figure 5.2.. Detection at 217nm shows that elution of the peptide takes place at 48-52 minutes as described

previously. Detection at 310nm shows the three peaks associated with the chromophore of MTX, which occurs at 50-52 minutes.

Figure 5.3. shows the effects of incubating the N$^{\alpha}$MTX-[Nle^{4},D-Phe^{7}]α-MSH with B16 cells in medium over a 72 hour period. It is clear that although there are more peaks associated with the profiles, these are probably due to any debris which may have accumulated over this time, but essentially the profile of the conjugate initially and after 72 hours remains similar.

Figure 5.4. gives the HPLC traces at 217nm of (i) the medium alone (RPMI), (ii) the [Nle^{4},D-Phe^{7}]α-MSH alone (NLDP), (iii) the N$^{\alpha}$MTX-[Nle^{4},D-Phe^{7}]α-MSH (MTX-NLDP) at a concentration of 5 x 10^{-5}M in medium and also (iv) N$^{\alpha}$MTX-[Nle^{4},D-Phe^{7}]α-MSH (10^{-5}M) in medium in the presence of B16 cells for 48 and (v) 72 hours. It should be noted that although they appear to elute at different times, in fact this is not the case, rather the chromatograms are automatically displaced by the printer in order to prevent any overlapping which subsequently allows a clearer visualisation of each sample individually. The RPMI produced no peaks which was to be expected, the [Nle^{4},D-Phe^{7}]α-MSH alone produced a single narrow peak at 48-52 minutes. The elution profiles for the sample N$^{\alpha}$MTX-[Nle^{4},D-Phe^{7}]α-MSH and those injected on days 2 and 3 were very similar and show no major new peaks on day 3 which indicates that the majority of the sample has remained intact.

Finally Figure 5.5. shows the HPLC traces at 310nm, where it is expected that the chromophore of MTX is eluted. The [Nle^{4},D-Phe^{7}]α-MSH does not exhibit any peaks at this wavelength, whereas the N$^{\alpha}$MTX-[Nle^{4},D-Phe^{7}]α-MSH shows the expected three peaks which were shown previously in Figure 5.2. The profiles of the N$^{\alpha}$MTX-[Nle^{4},D-Phe^{7}]α-MSH on days 1, 2, and 3 exhibit similar peaks, at elution times of 48-52 minutes. The profile of MTX alone and also that exhibited by the samples on days 1, 2 and 3 for elution time 40-42

exhibit similar peaks which must be due to the MTX. From the results of these traces it was clear that the major peaks associated with the individual molecules and also the N$^{\alpha}$MTX-[Nle^{4},D-Phe^{7}]α-MSH initially, still remain virtually the same after 72 hours exposure to B16 cells and hence it may be deduced that substantial degradation of N$^{\alpha}$MTX-[Nle^{4},D-Phe^{7}]α-MSH had not taken place.

5.3. Binding studies with N$^{\alpha}$MTX-[^{125}I-Tyr^{2},Nle^{4},D-Phe^{7}]α-MSH .

5.3.1. Binding Isotherm.

A binding isotherm is a method of determining the affinity of a particular ligand for a particular receptor, in this case the ligand was N$^{\alpha}$MTX-[^{125}I-Tyr^{2},Nle^{4},D-Phe^{7}]α-MSH and the receptors under investigation were the melanocortin 1 (MC1) and the melanocortin 3 (MC3) receptors. The results were expressed as the dissociation constant (Kd). The greater the Kd, the lower the affinity of the ligand for the receptor i.e. the more likely the ligand and receptor will remain dissociated. It can be described by the following equation:

$$[L] + [R] \underset{Kd}{\overset{Ka}{<==>}} [LR]$$

where:

[L] = Concentration of the ligand

[R] = Concentration of receptor

[LR] = Concentration of ligand-receptor complex

Ka = affinity constant for the forward reaction

Kd = dissociation constant for the reverse reaction

note: (Affinity constant = 1 / Kd)

Clearly it is advantageous when targeting a hormone to a receptor that the affinity is high as this implies a stronger association between the two which is also assumed to lead to increased levels of internalisation of the ligand-receptor complex.

Previous work performed with the radiolabelled hormone analogue ^{125}I-[Nle^4,D-Phe^7]α-MSH yielded Kd values in the region of 0.5nM for the MC1 receptor, (Erskine-Grout, 1993) (see Figure 5.6) and 1.66nM for the MC3 receptor, (Sahm, 1994). The threefold reduction in the affinity with which the ^{125}I-[Nle^4,D-Phe^7]α-MSH bound to the MC3 receptor relative to the MC1 receptor showed some degree of selectivity of the ligand for the MC1 receptor.

Although most studies of α-MSH receptors on melanoma cells were based on model systems such as the B16 mouse melanoma, more recently human melanoma cell lines have been investigated. The MeWo human melanoma cell line (MC1) was examined in this study to determine the Kd value for ^{125}I-[Nle^4,D-Phe^7]α-MSH. Initial time course experiments showed that no further increase in binding was apparent after 8 hours (Figure 5.7.) and hence this was the incubation period used. Figure 5.8. shows the results of a typical binding isotherm, and a Kd value of 5.82 x 10^{-8}M was determined, (n=3). Thus the MeWo cell line possessed MC1 receptors with a tenfold lower affinity for the ^{125}I-[Nle^4,D-Phe^7]α-MSH ligand than the corresponding MC1 receptors on the B16 cell line. From this it can be deduced that although the same receptor was expressed in both cell lines, the affinity of both for ^{125}I-[Nle^4,D-Phe^7]α-MSH was quite different. This value was not surprising as it has been established by other workers, (Eberle *et al.*, 1993) that human melanoma do not bind with as high an affinity as murine cell lines. It is also true that MeWo human melanoma cells do not express as many receptors on their cell surface which, although having no effect on the binding affinity, still makes the

reproducibility of the experiments more difficult. The advantage of using established cell lines e.g. B16 mouse melanoma, was the ease with which they were cultured in large quantities and the reproducibility of their responses.

Isotherms with N^{α}MTX-[^{125}I-Tyr^2,Nle^4,D-Phe^7]α -MSH :

The effect of the N^{α}MTX-[^{125}I-Tyr^2,Nle^4,D-Phe^7]α-MSH conjugate on the MC1 receptor was determined in this study and gave a Kd value of 7.35nM. This value was fourteen times lower than the value yielded with the ^{125}I-[Nle^4,D-Phe^7]α-MSH for the same receptor. This showed that the coupling of the MTX to the N-terminus of the ligand may have been responsible for inducing conformational problems at the receptor site. Steric hindrance which may have resulted from the increase in size of the ligand may account for the reduction in binding affinity. The binding of N^{α}MTX-[^{125}I-Tyr^2,Nle^4,D-Phe^7]α -MSH was assessed in the 293 cell line transfected with the gene encoding the MC3 receptor and a Kd of 1.69nM was found. This value is lower than that for the MC1 receptor and therefore implied a slightly higher binding affinity of N^{α}MTX-[^{125}I-Tyr^2,Nle^4,D-Phe^7]α-MSH to the MC3 receptor. Interestingly the affinities of the ^{125}I-[Nle^4,D-Phe^7]α-MSH and N^{α}MTX-[^{125}I-Tyr^2,Nle^4,D-Phe^7]α-MSH for the MC3 receptor are almost equal. This would seem to indicate that the MC3 receptor is not as sensitive to substitution at the N-terminus of the ligand as the MC1 receptor. The results of these binding isotherms are given in Figures 5.9. and 5.10.

5.3.2. Competition Binding Assays.

Chapter 2.13.3. contains a detailed account of the methods employed.

The most important value to consider for drug targeting is the Kd value of the unlabelled moiety i.e. N^{α}MTX-[Nle^4,D-Phe^7]α-MSH because this what was hoped to be used in the future for the site specific delivery of MTX to

melanoma. It has been shown with the binding isotherms that the N$^{\alpha}$MTX-[^{125}I-Tyr^{2},Nle^{4},D-Phe^{7}]α-MSH did not selectively bind to the MC1 receptor and further that the MC1 receptor was more susceptible to conformational changes.

A competitive binding assay assesses the ability of a ligand to displace a radioactive ligand from the receptor site. It is necessary that the Kd of the radioactive ligand for the receptor is known in order that the affinity of the unlabelled ligand may be calculated using the equation given in section 2.13.3.1.

Previous work was done to establish the affinity of the MC1 receptor for N$^{\alpha}$MTX-[Nle^{4},D-Phe^{7}]α-MSH and a Kd value of 1.54nM was found, (Erskine-Grout, 1993).

In this study three replicate binding experiments were done on the transformed 293 cells (with MC3 receptor) which gave an average value for Kd of 1.06 x 10^{-7} for N$^{\alpha}$MTX-[Nle^{4},D-Phe^{7}]α–MSH. This was over a hundred fold lower affinity for the ligand with the MC3 receptor than for the MC1 receptor. This has clear advantages in drug targeting terms since it implies that the unlabelled conjugate i.e. the targeting moiety, will exhibit a hundred fold increase in affinity and hence selectivity towards receptors on melanocytes (MC1) in preference to receptors located in the brain (MC3) leading to a reduction of any CNS side-effects. Figure 5.11. shows the results of a competitive binding assay.

In table 5.1 below, a list of the ligands together with their respective affinities (expressed as dissociation constant) for either the MC1 or the MC3 receptor are given.

Table 5.1. Relative affinities of various ligands for the two melanocortin receptors (MC1 and MC3) under investigation.

LIGAND	MC1 receptor (B16 cells)	MC3 receptor
α-MSH	Kd : 2.06 x 10^{-8} M (+/-) 5.31 x 10^{-9} n=3 (Sahm,1994)	Kd: 2.07 x 10^{-6}M (+/-) 1.18 x 10^{-6} n=3 (Sahm, 1994)
[Nle^4,D-Phe^7]α-MSH	Kd: 2.02 x 10^{-9} M (+/-) 7.81 x 10^{-11} n=3 (Sahm,1994)	Kd: 2.15 x 10^{-8} M (+/-) 1.73 x 10^{-8} n=14 (Sahm, 1994)
^{125}-I-[Nle^4,D-Phe^7]α-MSH	Kd: 0.48 x 10^{-9} M (+/-) 0.076 x 10^{-9} n=5 (Erskine-Grout, 1993)	Kd: 1.66 x 10^{-9} M (+/-) 2.63 x 10^{-10} n=3 (Sahm, 1994)
N$^{\alpha}$MTX-[Nle^4,D-Phe^7]α-MSH	Kd: 1.54 x 10^{-9}M (+/-) 2.01 x 10^{-10} n=3 (Erskine-Grout,1993)	Kd: 1.06 x 10^{-7} M (+/-) 5.83 x 10^{-9} n=3 (This study)
N$^{\alpha}$MTX-[^{125}I-Tyr^2,Nle^4,D-Phe^7]α-MSH	Kd: 7.35 x 10^{-9}M (+/-) 2.48 x 10^{-9} n=3 (This study)	Kd: 1.69 x 10^{-9} M (+/-) 8.37 x 10^{-10} n=3 (This study)

5.4. Internalisation Studies with N$^{\alpha}$MTX-[^{125}I-Tyr^{2},Nle^{4},D-Phe^{7}]α-MSH .

Internalisation studies were undertaken to pursue the pathway of N$^{\alpha}$MTX-[^{125}I-Tyr^{2},Nle^{4},D-Phe^{7}]α-MSH after the initial binding affinities had been established. The first experiments involved continual exposure of B16 cells to 0.1nM N$^{\alpha}$MTX-[^{125}I-Tyr^{2},Nle^{4},D-Phe^{7}]α-MSH in the presence of NH_4Cl. The protocol (see Chapter 2.13.) was carried out at 37°C over a four hour period which was interrupted at regular intervals so that the dynamic process of internalisation could be examined at these time points. Citrate buffer (pH 2.5) was used to remove any radioactivity that was not associated internally, as this has been shown to be effective (Adams, 1993). The presence of NH_4Cl was expected to increase the pH of the endosomal and lysosomal compartments to close to 7, due to the partitioning of ammonia into these compartments. This has the effect of neutralising the function of the proton pump which causes active accumulation of hydrogen ions in normal endosomes and lysosomes. The immediate consequence is an inactivation of proteolytic enzymes (particularly the thiol proteases known collectively as cathepsins) which have optimum enzymatic activity at low pH. Another consequence may be perturbation of vesicular traffic and intracellular compartmentalisation resulting in modifications of the pathways of internalised materials, such as hormone-receptor complexes. The result is the prevention of lysosomal degradation of the ligand-receptor complex.

Pulse-Chase labelling experiments allowed the binding of the ligand to the receptor over 2 hours at 4°C. This resulted in the immediate internalisation of molecules when the temperature of the experiment was increased to 37°C. NH_4Cl was present for half of the Pulse-Chase experiments to allow the quantification of specifically internalised molecules over 4 hours. The

experiments performed in the absence of NH_4Cl presented a more realistic and dynamic profile as the receptor was recycled and the ligand degraded.

5.4.1. Continual exposure to N^{α}MTX-[^{125}I-Tyr^2,Nle^4,D-Phe^7]α–MSH at 37°C: *(In the presence of 20mM NH_4Cl)*

See chapter 2.13.4. for a more detailed method, briefly:

5 x 10^5 B16 cells per well were seeded and incubated at 37°C overnight. Upon removal, from the incubator, the cells were washed with SFM and reincubated for 15 minutes at 37°C in SFM containing 20mM NH_4Cl. After 15 minutes 0.1nM of N^{α}MTX-[^{125}I-Tyr^2,Nle^4,D-Phe^7]α-MSH in SFM was placed on the cells and they were incubated for various time intervals. Half of the cells were also incubated with excess (10^{-6}M) non-iodinated ligand to assess the non-specific binding. The cells were lysed with NaOH and assayed for radioactivity on the gammacounter. A parallel series of wells were washed with citrate buffer at pH 2.5 for 5 minutes prior to NaOH treatment. This acid treatment strips the radioactivity off the cell surface and hence allows the estimation of the level of specifically internalised radioactive ligand. It is assumed in the calculation of results of this experiment that all the radioactivity counted is due to the N^{α}MTX-[^{125}I-Tyr^2,Nle^4,D-Phe^7]α-MSH even though this does not take into consideration the possibility that the conjugate may be degraded extracellularly and hence the radioactivity may be due to ^{125}I-[Nle^4,D-Phe^7]α-MSH alone. It appeared that the specific binding was still increasing at four hours (see Figure 5.12.(a)) and to determine the change in progress of internalisation after four hours another experiment was performed.

The same protocol as above, was used, but with different time intervals from 2 to 48 hours. It appeared (see Figure 5.12.(b)) that no further internalisation occurred after four hours. The reasons for this have not been fully elucidated although it is thought that the problems with non-specific binding are increased

over time. It is also possible that the effects of NH_4Cl became deleterious to the cells after prolonged exposure, which could be reflected in the cessation of internalisation.

The results of three experiments performed to show the pattern of internalisation of N^{α}MTX-[^{125}I-Tyr^2,Nle^4,D-Phe^7]α-MSH over a four hour period clearly demonstrated that as time elapsed more internalisation occurred (Table 5.2. and Figures 5.13 and 5.14.). It should be stressed that the presence of NH_4Cl resulted in continuous endocytosis of the radioligand over a four hour period which suggested that under these conditions the receptor was able to cycle between the plasma membrane and the early endosome but that sequestration or degradation of the receptor was unable to occur. No experiments were performed in the absence of NH_4Cl because previous work (Adams, 1993) showed that there was a reduction in specifically bound ligand (^{125}I-[Nle^4,D-Phe^7]α-MSH) after 60 minutes thought to be due to down-regulation of the receptor. It was assumed that a similar profile would have been obtained for the N^{α}MTX-[^{125}I-Tyr^2,Nle^4,D-Phe^7]α-MSH in the absence of NH_4Cl. Chronic exposure to 0.1nM of N^{α}MTX-[^{125}I-Tyr^2,Nle^4,D-Phe^7]α-MSH in the presence of NH_4Cl caused a continuous accumulation of ligand. The rate of internalisation, as estimated from the slope of the graphs of the three experiments, gave an average value of 9.3 molecules per cell per minute. As this occurred at receptor occupancy of 1.34% this suggested an uptake of 42,000 molecules per cell per hour at 100% receptor occupancy. Three replicate experiments were performed and the average value for the number of molecules taken up by the cells over a four hour period as estimated by the mean of the three experiments is 1792.5. (Table 5.2). This result does not agree with the result estimated using the slope of the graph (i.e. 9.3 x 240= 2232 molecules) but it still representative. The results are at variance with each

other due to the interexperimental differences in receptor number expressed by the cells, which can vary between 5,000 and 25,000 (Sahm, 1994). The results of two representative experiments are given in Figures 5.13 and 5.14. Experiments on the rate of pinocytosis conducted by ^{125}I-PVP suggested that at 0.1nM dissolved ligand the early endosome would contain about 6 molecules and that approximately 2 molecules would be delivered to the lysosome over 60 minutes, (Richards, 1992). This compares to 448-558 molecules by receptor mediated endocytosis, depending on method of assessment, suggesting that targeted toxins could be as much as 279 times more toxic to target cells than cells which did not express the α-MSH receptor.

Table 5.2. Results of three replicate experiments (121,122 and 123) ascertaining the number of molecules of N$^{\alpha}$MTX-[^{125}I-Tyr^{2},Nle^{4},D-Phe^{7}]α-MSH taken up by each cell in a B16 cell line. Column 1 contains the different time intervals and the following three columns give the number of molecules per cell.

Time (min.)	121	122	123
15	56.6	30.6	30.3
30	232.8	20	83.7
60	826	108.6	223
90	1325.4	481	238.8
120	1553.8	516.6	340.4
180	2374	1131	531.2
240	3462	1351.2	564.2

5.4.2. Pulse Chase Internalisation of N^{α}MTX-[^{125}I-Tyr^2,Nle^4,D-Phe^7]α-MSH : *(In the absence of NH_4Cl)*

See Chapter 2.13.5. for protocol.

B16 cells were seeded and incubated in the same way as for the previously described internalisation experiments. Once the cells had been incubated overnight, they were washed with SFM and incubated for 2 hours at 4°C in SFM containing N^{α}MTX-[^{125}I-Tyr^2,Nle^4,D-Phe^7]α-MSH in the presence or absence of 10^{-6}M non-iodinated ligand. After 2 hours the cells were washed and incubated at 37°C for various times. The radioactivity associated with the cells was assayed in the same way as before. All these Pulse-Chase experiments were performed at 37°C as it has been established in our laboratories (Adams, 1993) that at 4°C there was no evidence of ligand internalisation (^{125}I-[Nle^4,D-Phe^7]α-MSH) which implied that internalisation observed at 37°C involved an endocytic process requiring metabolic energy.

In the absence of NH_4Cl, a typical experimental profile was as follows: Due to the initial mass of radioligand bound to the surface of the cell, there was a high level of total activity and a high level of specific activity. As the time progressed and the ligand became internalised and subsequently degraded and was then released in to the extracellular fluid. The acid wash value was initially low, indicating that the specifically bound radioligand was localised at the cell surface. The overall process accounts for the decrease in intracellular radioactivity. After four hours, there was little specific activity associated with the cells which suggested that the ligand which had been bound at zero time, had now been internalised, and the waste iodinated molecules discarded. Four replicate experiments were performed and the results of one experiment are shown in Figure 5.15.

5.4.3. Pulse Chase Internalisation of N$^{\alpha}$MTX-[^{125}I-Tyr^{2},Nle^{4},D-Phe^{7}]α-MSH : *(In the presence of NH_4Cl)*

A detailed account of the method is given in chapter 2.13.6.

The profile of this experiment differed from the experiment in the absence of NH_4Cl in many respects. Firstly due to the prevention of (i) receptor recycling and (ii) release of the degraded ligand to the surface of the cell there was no degradation of internalised ligand so the acid wash value representing mass internalised, increased over time. The total activity was high at first and then started to decrease as the receptor recycling was prevented. As time progressed the amount of total radioactivity associated with the cell became constant as no new internalisation occurred and no degradation and subsequent release from the cells was allowed to proceed. Beyond the four hour period, a situation arose whereby there was a plateau phase of total and specific activity.

Pulse-Chase experiments were carried out at approximately 0.67% receptor occupancy. This is exactly half the receptor occupancy for the continual exposure and was calculated on the basis that after 2 hours binding equilibration is not achieved and from time course experiments about 50% maximal binding is achieved after 2 hours. Under these conditions all bound ligand was internalised during the course of the experiment. In previous experiments, in our laboratories, (Adams, 1993) at approximately 10% receptor occupancy uptake, 500-1000 molecules of ^{125}I-[Nle^{4},D-Phe^{7}]α-MSH was observed per cell. In these studies it represented an uptake of between 20-500 molecules per cell after four hours. The results vary dramatically between 20 and 500 molecules internalised which was due to fluctuations in receptor number (5,000-25,000) between experiments. The results of two representative Pulse-Chase Internalisation experiments are shown in Figures 5.16. and 5.17.

Table 5.3. Results of four replicate experiments (126,129,131 and 140) in which the number of molecules of N$^{\alpha}$MTX-[^{125}I-Tyr^{2},Nle^{4},D-Phe^{7}]α-MSH taken up intracellularly are given.

Molecules of N$^{\alpha}$MTX-[^{125}ITyr^{2},Nle^{4},D-Phe^{7}]α-MSH taken up by each B16 cell (in the presence of NH_4Cl)

Time (min.)	126	129	131	140
15	542	115.2	59.2	234
30	736	185.6	41.6	252
60	530	183.8	32.6	153.2
90	516	161.2	26.4	258
150	336	100	23.6	163.8
240	460	144.8	17.2	163.8

The results show that there is an increase in specifically bound N$^{\alpha}$MTX-[^{125}I-Tyr^{2},Nle^{4},D-Phe^{7}]α-MSH between 15 and 30 minutes but this is followed by a decrease at 60 minutes and there is little evidence of any increase as time progresses to 150 minutes and then tails off.

Summary:

It has been shown that binding of N$^{\alpha}$MTX-[^{125}I-Tyr^{2},Nle^{4},D-Phe^{7}]α-MSH to the MC1 receptor occurred, (Kd=7.35nM). The subsequent internalisation process was examined and the results of continual exposure to 0.1nM ligand, in the presence of NH_4Cl, showed that internalisation of N$^{\alpha}$MTX-[^{125}I-Tyr^{2},Nle^{4},D-Phe^{7}]α-MSH did take place over a four hour period with an average of 1793 molecules taken up by each cell in this time.

Pulse-Chase internalisation in the absence and presence of NH_4Cl was also studied to gain further insight into the process of internalisation of the ligand-

receptor complex. In the presence of NH_4Cl, it was deduced that between 20 and 500 molecules were taken intracellularly per cell in four hours following occupation of 0.67% of receptors.

Binding of N$^{\alpha}$MTX-[^{125}I-Tyr^{2},Nle^{4},D-Phe^{7}]α-MSH to the MC3 receptor was also investigated in this study using transformed 293 cells. This cell line is derived from human embryonic kidney (HEK) cells but these cells have been transformed so that they stably express the gene encoding the MC3 receptor. Other 293 cells that were used contain the gene vector alone and these were used as control cells. Due to the fact that α-MSH also binds to melanocortin receptors in the brain (MC3, MC4 and MC5) it was necessary to elucidate with what affinity the N$^{\alpha}$MTX-[^{125}I-Tyr^{2},Nle^{4},D-Phe^{7}]α-MSH bound to the MC3 receptor, as this would have a significant impact on the usefulness of the conjugate. The results obtained indicated that the affinity of N$^{\alpha}$MTX-[^{125}I-Tyr^{2},Nle^{4},D-Phe^{7}]α-MSH for both the MC1 and the MC3 receptors are quite close 7.35nM and 1.69nM respectively and this may present a problem of central nervous system (CNS) side-effects, if reflected by the unlabelled conjugate. The affinities of the MC1 and MC3 receptors for the unlabelled conjugate was examined in competitive binding assays and Kd values of 1.54nM and 1.06 x 10^{-7}M respectively were found. These values were quite promising in terms of preferential drug targeting to the MC1 receptor. There is also a great disparity in the number of MC1 receptors expressed on the surface of B16 cells (5,000-25,000) which varies with passage, (Erskine-Grout, 1993) and the number of MC3 receptors expressed on the surface of transformed 293 cells, (150,000-10,000) which is passage dependent, (Sahm,1994). The consequences of this disparity were hoped to be examined both in terms of the binding affinity and also in the growth inhibitory experiments with the MTT assay.

5.5. Growth Inhibitory Effects of N^{α}MTX-[Nle^4,D-Phe^7]α–MSH as assessed by the MTT Assay:

See Chapter 2.14. for a detailed account of the methods used.

Concentrations of N^{α}MTX-[Nle^4,D-Phe^7]α–MSH ranging from 10^{-4} to 10^{-13}M were employed to determine the $E.C._{50}$ value. Once the approximate value had been determined, the range was narrowed to achieve a more accurate estimate.

All cells were seeded at a density of 4 x 10^3 cells/well in 96 microwell plates. The cells were exposed to N^{α}MTX-[Nle^4,D-Phe^7]α–MSH in medium, over an incubation period equivalent to three doubling times of the cell line under investigation. The MTT assay was then performed. Control cells were treated in exactly the same way but without the N^{α}MTX-[Nle^4,D-Phe^7]α-MSH.

This series of experiments assessed the growth inhibitory effects of the hormone analogue-drug conjugate (N^{α}MTX-[Nle^4,D-Phe^7]α-MSH) on B16 murine melanoma cells and MeWo human melanoma cells. SVK14 keratinocytes were used as control cells because they do not express melanocortin receptors on their surface. The growth inhibitory effects of N^{α}MTX-[Nle^4,D-Phe^7]α-MSH on 293 cells transformed with the gene encoding the MC3 receptor was investigated to determine whether the higher number of receptors expressed influenced the cytotoxicity of N^{α}MTX-[Nle^4,D-Phe^7]α–MSH. 293 cells which were transfected with the pcDNA/neo vector were used as control cells for the transformed 293 cells, to check if the process of transfection with a vector in any way increased the cell susceptibility to the conjugate.

5.5.1. B16 murine melanoma cell line:

The results of the growth inhibition assays with B16 cells are given in Figures 5.18. (a) and (b). The mean absorbances of the experiments are listed in Table 5.4., the coefficient of variation expressed as a percentage (%) (i.e. ((S.D. / mean) x 100) was 20% for all of the experiments and demonstrated that there was a high degree of reproducibility between experiments.

B16 murine melanoma cell line:

Table 5.4. This table represents the mean net absorbance values calculated by subtracting the reference absorbance readings at 690nm from the test absorbance readings at 540nm. The columns labelled 93, 120, 156 and 159 contain the results of four replicate experiments. Each value is the mean of 8 replicates with the exception of the control cells which involved 16 replicates. Column 1 contains the concentrations of N$^{\alpha}$MTX-[Nle^{4},D-Phe^{7}]α–MSH used.The E.C.$_{50}$ and standard deviation values were generated using the MINSQ non-linear regression program (weighting=1).

	NET MEAN ABSORBANCE			
N$^{\alpha}$MTX-[Nle^{4},D-Phe^{7}]α–MSH (M)	(93)	(120)	(156)	(159)
Control	1.598	1.299	1.317	0.955
1.1 x 10^{-13}	1.708	1.069	1.202	------
1.1 x 10^{-12}	1.670	0.974	1.119	------
1.1 x 10^{-11}	1.600	0.884	1.167	------
1.1 x 10^{-10}	1.516	0.895	1.226	------
1.1 x 10^{-9}	1.504	1.034	1.230	------
1.1 x 10^{-8}	1.709	1.181	1.499	0.766
5.5 x 10^{-8}	------	------	------	0.790
1.1 x 10^{-7}	1.642	1.007	1.427	0.860
5.5 x 10^{-7}	------	------	------	1.376
1.1 x 10^{-6}	1.574	1.112	0.657	1.463
5.5 x 10^{-6}	------	------	------	0.844
1.1 x 10^{-5}	0.266	1.148	0.211	0.483
2.2 x 10^{-5}	------	------	------	0.581
5.5 x 10^{-5}	------	------	------	0.380
1.1 x 10^{-4}	0.087	0.259	0.191	0.367
E.C.$_{50}$ (M)	2.5 x10^{-6}	4.4 x10^{-5}	9.0 x10^{-7}	1.2 x10^{-5}
S.D. (+/-)	8.5 x10^{-7}	8.8 x10^{-6}	3.9 x10^{-7}	1.5 x10^{-5}

5.5.2. MeWo human melanoma cell line:

Figure 5.19. shows the results of the growth inhibition assays with the MeWo human melanoma cell line.

Table 5.5. This table represents the mean net absorbance values calculated by subtracting the reference absorbance readings at 690nm from the test absorbance readings at 540nm. The columns labelled 76,95,96 and 98 contain the results of four replicate experiments. Each value is the mean of 8 replicates with the exception of the control cells which involved 16 replicates. Column 1 contains the concentrations of N^{α}MTX-[Nle^4,D-Phe^7]α–MSH used. The $E.C._{50}$ and standard deviation values were generated using the MINSQ non-linear regression program (weighting=1).

	NET MEAN ABSORBANCE			
N^{α}MTX[Nle^4 D-Phe^7]α–MSH (M)	**(76)**	**(95)**	**(96)**	**(98)**
Control	**1.068**	**1.807**	**1.332**	**1.447**
1.1×10^{-13}	**1.317**	**1.106**	**------**	**------**
1.1×10^{-12}	**1.699**	**0.894**	**------**	**------**
1.1×10^{-11}	**1.274**	**1.071**	**------**	**------**
1.1×10^{-10}	**1.235**	**1.266**	**------**	**------**
1.1×10^{-9}	**0.709**	**1.160**	**0.778**	**1.114**
1.1×10^{-8}	**1.126**	**1.479**	**1.032**	**1.369**
5.5×10^{-8}		**------**	**1.358**	**1.325**
1.1×10^{-7}	**0.781**	**1.204**	**1.095**	**0.971**
5.5×10^{-7}		**------**	**0.552**	**1.446**
1.1×10^{-6}	**0.247**	**1.205**	**0.383**	**0.693**
5.5×10^{-6}		**------**	**0.261**	**0.319**
1.1×10^{-5}	**0.004**	**0.510**	**0.218**	**0.245**
5.5×10^{-5}		**------**	**0.083**	**0.119**
1.1×10^{-4}	**0.003**	**0.221**	**0.067**	**0.081**
$E.C._{50}$ (M)	**2.0×10^{-7}**	**7.2×10^{-6}**	**7.3×10^{-7}**	**1.8×10^{-6}**
S.D.(+/-)	**1.3×10^{-7}**	**4.5×10^{-6}**	**3.7×10^{-7}**	**7.8×10^{-7}**

5.5.3. SVK14 keratinocytes:

Figure 5.20. shows the results of growth inhibition assays with the keratinocytes, SVK14 in the presence of N^{α}MTX-[Nle^4,D-Phe^7]α–MSH.

Table 5.6. This table represents the mean net absorbance values calculated by subtracting the reference absorbance readings at 690nm from the test absorbance readings at 540nm. The columns labelled 88 and 94 contain the results of two replicate experiments. Each value is the mean of 8 replicates with the exception of the control cells which involved 16 replicates. Column 1 contains the concentrations of N^{α}MTX-[Nle^4,D-Phe^7]α–MSH used. The $E.C._{50}$ and standard deviation values were generated using the MINSQ non-linear regression program (weighting=1).

	NET MEAN ABSORBANCE	
N^{α}MTX-[Nle^4,DPhe^7]α–MSH (M)	**(88)**	**(94)**
Control	**1.069**	**0.992**
1.1×10^{-13}	**1.163**	**------**
1.1×10^{-12}	**1.065**	**------**
1.1×10^{-11}	**1.157**	**------**
1.1×10^{-10}	**0.969**	**------**
1.1×10^{-9}	**0.968**	**0.968**
1.1×10^{-8}	**1.047**	**0.946**
1.1×10^{-7}	**1.091**	**0.912**
1.1×10^{-6}	**1.223**	**0.925**
2.2×10^{-6}	**------**	**0.646**
5.5×10^{-6}	**------**	**0.107**
1.1×10^{-5}	**0.098**	**0.041**
2.2×10^{-5}	**------**	**0.039**
5.5×10^{-5}	**------**	**0.031**
1.1×10^{-4}	**0.032**	**0.037**
$E.C._{50}$	**2.1×10^{-6}M**	**1.2×10^{-6}M**
S.D.(+/-)	**1.1×10^{-6}**	**6.0×10^{-7}**

5.5.4. Effects of N^{α}MTX-[Nle^4,D-Phe^7]α–MSH on the transformed 293 cells:

The effects of N^{α}MTX-[Nle^4,D-Phe^7]α–MSH on the transformed 293 cells was investigated in experiments 146 and 147. Experiment 146 involved the transformed 293 cells which stably expressed the MC3 receptor. Experiment 147 involved the transfected 293 cells which had the vector alone (in the absence of any gene encoding information). The results of both experiments are given below in Table 5.7.

Figures 5.21. and 5.22. show the differences in the growth inhibitory effects of MTX versus N^{α}MTX-[Nle^4,D-Phe^7]α–MSH on the two different 293 cell lines i.e. in the presence and absence of cloned MC3 receptors respectively.

Transformed 293 cell lines:

Table 5.7. This table represents the mean net absorbance values calculated by subtracting the reference absorbance readings at 690nm from the test absorbance readings at 540nm. The columns labelled 146 and 147 contain the results of two separate experiments with the N$^{\alpha}$MTX-[Nle^{4},D-Phe^{7}]α–MSH conjugate. Each value is the mean of 8 replicates with the exception of the control cells which involved 16 replicates. Column 1 contains the concentrations of N$^{\alpha}$MTX-[Nle^{4},D-Phe^{7}]α–MSH used. The E.C.$_{50}$ and standard deviation values were generated using the MINSQ non-linear regression program (weighting=1).

	NET MEAN ABSORBANCE	
N$^{\alpha}$MTX-[Nle^{4},D-Phe^{7}]α–MSH (M)	**146 (Transfected with MC3 receptor)**	**147 (Vector alone)**
Control	**0.887**	**1.048**
1 x 10^{-13}	**0.760**	**0.650**
1 x 10^{-12}	**0.550**	**0.489**
1 x 10^{-11}	**1.085**	**0.948**
1 x 10^{-10}	**0.699**	**0.701**
1 x 10^{-9}	**0.880**	**0.728**
1 x 10^{-8}	**1.209**	**0.957**
1 x 10^{-7}	**1.104**	**1.284**
1 x 10^{-6}	**1.237**	**0.544**
1 x 10^{-5}	**0.438**	**0.140**
1 x 10^{-4}	**0.176**	**0.147**
E.C.$_{50}$	**1.1 x 10^{-5} M**	**1.7 x 10^{-6} M**
S. D.(+/-)	**1.4 x 10^{-5}**	**2.1 x 10^{-6}**

It can be seen from the above table and also in Figures 5.21 and 5.22. that MTX is effective at killing 293 transformed cell lines at a much lower inhibition (<10^{-11}M MTX) concentration than N$^{\alpha}$MTX-[Nle^{4},D-Phe^{7}]α–MSH.

Table 5.8. This table shows the $E.C._{50}$ values representing the growth inhibitory effects of MTX and N$^{\alpha}$MTX-[Nle^4,D-Phe^7]α-MSH on B16, MeWo, 293 (transformed) and SVK14 cell lines.

	$E.C._{50}$ values	
	MTX	**N$^{\alpha}$MTX-[Nle^4,D-Phe^7]α-MSH**
MC1 receptors:		
B16 cell line	**1.67×10^{-8}M**	**1.47×10^{-5}M**
MeWo cell line	**1.31×10^{-9}M**	**2.48×10^{-6}M**
MC3 receptors:		
293 (transformed) cell line	**3.03×10^{-11}M**	**1.07×10^{-5}M**
Control cell lines:		
(No MSH receptors)		
SVK14 cell line	**$< 10^{-13}$M**	**1.68×10^{-6}M**
293(transformed: vector alone)	**2.84×10^{-13}M**	**1.66×10^{-6}M**

Only cells with active mitochondria are able to convert MTT to MTT formazan which can be solubilised by DMSO giving a dark purple solution. The MTT growth inhibition assay measures cell viability in direct relation to the absorbance of MTT Formazan. B16 cells were examined and results gave an average $E.C._{50}$ value 1.47×10^{-5}M N$^{\alpha}$MTX-[Nle^4,D-Phe^7]α-MSH. The control values were quite high (>1.0AU) for most of the experiments and the absorbances remained at this level, if not greater, until a concentration of N$^{\alpha}$MTX-[Nle^4,D-Phe^7]α-MSH higher than 1.1×10^{-6}M. At concentrations

greater than 10^{-6}M, a decrease in absorbance, and cell viability, was obvious in all experiments with this cell line. The decrease was quite dramatic e.g. experiment "93" where absorbance of 1.574 AU was found for cells exposed to 10^{-6}M N$^{\alpha}$MTX-[Nle^{4},D-Phe^{7}]α-MSH and absorbance of 0.266 AU, i.e. a five fold decrease in cell viability, for 10^{-5}M N$^{\alpha}$MTX-[Nle^{4},D-Phe^{7}]α-MSH. Although the $E.C._{50}$ values obtained were over a wide range (1.152×10^{-5}M--9.015×10^{-7}M), the variation co-efficient was never higher than 20%. B16 cells have such a large variability in number of receptors expressed per cell (5,000-25,000) and this may have consequential effects on the uptake of the conjugate via receptor mediated endocytosis.

The effects of N$^{\alpha}$MTX-[Nle^{4},D-Phe^{7}]α-MSH on the MeWo cell line showed that these cells were more sensitive to the conjugate than the B16 cells. The average $E.C._{50}$ value was 2.48×10^{-6}M which was a greater than tenfold difference in susceptibility *vis à vis* the $E.C._{50}$ of 1.47×10^{-5}M for B16 cells. This may be explained if the binding affinity of the unlabelled conjugate for the MC1 receptors on MeWo cells was higher than the binding affinity of the MC1 receptors on B16 cells (1.54nM) but this value has yet to be determined. However this assumes that the inhibition of the cells was due to the receptor mediated uptake of the conjugate. If the N$^{\alpha}$MTX-[Nle^{4},D-Phe^{7}]α-MSH was degraded extracellularly then the MTX would be taken intracellularly via the folic acid pathway which would be independent of any binding data. However, this is not likely due to degradation profile.

The results of Chapter 4, where the effects of MTX alone were examined show that B16 cells had an $E.C._{50}$ value of 1.67×10^{-8}M and MeWo cells had an $E.C._{50}$ value of 1.31×10^{-9}M MTX. This showed a tenfold difference in their relative sensitivities to the inhibitor. In this respect the responses of B16 and MeWo cells to inhibiting agents are parallel, i.e. a thousand fold increase in

concentration of N$^{\alpha}$MTX-[Nle^{4},D-Phe^{7}]α-MSH relative to MTX concentration is necessary to cause the same reduction in growth.

The SVK14 cells possess no melanocortin receptors and hence act as control cells to examine whether their susceptibility to the conjugate relative to (i) effects of MTX on SVK14 cells and (ii) effects of the N$^{\alpha}$MTX-[Nle^{4},D-Phe^{7}]α-MSH on cells with MSH receptors. Table 5.8. shows that the SVK14 cells were highly sensitive to the cytotoxic effects mediated by MTX. Although a definite E.C.$_{50}$ value was impossible to determine, it was clear from the distribution of data that extracellular concentrations of >10^{-13}M were effective at killing the cells. The effects of N$^{\alpha}$MTX-[Nle^{4},D-Phe^{7}]α-MSH were not as dramatic and gave an average E.C.$_{50}$ value of 1.68 x 10^{-6}M. This concentration was lower than that required to effect the same level of inhibition in either the B16 or the MeWo cell lines. This would not be expected if MSH receptors were playing an integral role in the mediation of cytotoxic effects. On the contrary, it would be expected that the greater the number of MSH receptors expressed, the lower the extracellular concentration of N$^{\alpha}$MTX-[Nle^{4},D-Phe^{7}]α-MSH necessary to reduce growth. This did not bode well for the theory of specific targeting of N$^{\alpha}$MTX-[Nle^{4},D-Phe^{7}]α-MSH however when the overall effects of MTX and the conjugate were assessed, a more optimistic picture emerged: There was a thousand fold difference in the levels of N$^{\alpha}$MTX-[Nle^{4},D-Phe^{7}]α-MSH and MTX necessary to have the same inhibitory effects on B16 and MeWo cell lines, but this difference is augmented to seven orders of magnitude for SVK14 cells. This implied that the conjugation of MTX to [Nle^{4},D-Phe^{7}]α-MSH had decreased the sensitivity of SVK14 cells by seven orders of magnitude and this argued for selective route taken by the N$^{\alpha}$MTX-[Nle^{4},D-Phe^{7}]α-MSH.

Effects of the N^{α}MTX-[Nle^4,D-Phe^7]α-MSH on transformed 293 cells with and without MC3 receptors was then examined. As mentioned previously, MC3 receptors are located in the placenta, gut and most significantly, from a drug targeting viewpoint, the brain. The results of a preliminary experiment were reported, and showed an $E.C._{50}$ value of 1.07 x 10^{-5}M for 293 cells with MC3 receptors and 1.66 x 10^{-6}M, for 293 cells, without. This demonstrated a similar profile to that of the SVK14 cells but the errors associated with data from these 293 cells were quite high (variation co-efficient: 30%) and so further studies should be undertaken.

5.6. Control experiments in the presence of [Nle^4,D-Phe^7]α-MSH:

A control experiment was performed with [Nle^4,D-Phe^7]-α-MSH (10^{-4} to 10^{-13}M) which was incubated with the cells in the normal manner, this was done to establish its role in growth inhibition or indeed if such a role existed.The MTT assay was then performed. Control cells were treated in exactly the same way but the [Nle^4,D-Phe^7]-α-MSH was omitted.

The results of these experiments are shown in Figures 5.23 and 5.24 respectively. It was clear that [Nle^4,D-Phe^7]-α-MSH does not adversely affect the growth of cells until a concentration of 10^{-6}M or greater was used and at this point the cells experienced a decrease in viability which was transient. At the highest concentration of [Nle^4,D-Phe^7]-α-MSH (10^{-4}M) the level of absorbance and hence viability of the cells was similar, if not higher than, the control values.

5.7. Effects of lysomotropic agents on the growth inhibitory properties of N$^{\alpha}$MTX-[Nle^{4},D-Phe^{7}]α–MSH:

The effects of the ionophore, monensin and also the lysomotropic agent, chloroquine were examined to see whether any augmentation or reduction in activity of N$^{\alpha}$MTX-[Nle^{4},D-Phe^{7}]α–MSH was observed.

5.7.1. Monensin:

A growth inhibitory assay was set up with B16 cells and N$^{\alpha}$MTX-[Nle^{4},D-Phe^{7}]α–MSH according to the protocol in chapter 2.14. Monensin (10^{-5}M) was present at each concentration of N$^{\alpha}$MTX-[Nle^{4},D-Phe^{7}]α–MSH to and the results of three replicate experiments (160, 162 and 166) are given in Table 5.9. Figure 5.25. shows the results of one of these experiments. Monensin prevents receptor recycling to the surface of the cell and it would be expected that if N$^{\alpha}$MTX-[Nle^{4},D-Phe^{7}]α-MSH exerted effects by receptor mediated endocytosis then the E.C.$_{50}$ value for B16 cells in the presence of monensin, would be higher than for B16 cells with N$^{\alpha}$MTX-[Nle^{4},D-Phe^{7}]α-MSH alone. The average E.C.$_{50}$ value found was 1.56 x 10^{-5}M which does not differ significantly from the 1.47 x 10^{-5}M determined as the E.C.$_{50}$ for N$^{\alpha}$MTX-[Nle^{4},D-Phe^{7}]α-MSH alone. This was an indication that the N$^{\alpha}$MTX-[Nle^{4},D-Phe^{7}]α-MSH did not exert its effects via a surface membrane receptor that recycles.

B16 murine melanoma cell line:

Table 5.9. This table represents the mean net absorbance values calculated by subtracting the reference absorbance readings at 690nm from the test absorbance readings at 540nm. The columns labelled 160, 162 and 166 contain the results of three separate experiments with the N$^{\alpha}$MTX-[Nle^{4},D-Phe^{7}]α–MSH conjugate in the presence of 10^{-5}M monensin. Each value is the mean of 8 replicates with the exception of the control cells which involved 16 replicates. Column 1 contains the concentrations of N$^{\alpha}$MTX-[Nle^{4},D-Phe^{7}]α–MSH used. The E.C.$_{50}$ and standard deviation values were generated using the MINSQ non-linear regression program (weighting=1).

NET MEAN ABSORBANCE

N$^{\alpha}$MTX-[Nle^{4},D-Phe^{7}]α–MSH (M)	160	162	166
Control	1.433	1.026	1.242
1×10^{-8}	1.247	0.599	1.144
5×10^{-8}	1.374	0.854	1.315
1×10^{-7}	1.195	0.985	0.805
5×10^{-7}	1.092	0.873	0.636
1×10^{-6}	1.461	0.751	1.017
5×10^{-6}	1.689	0.704	0.543
1×10^{-5}	0.977	0.619	0.334
2×10^{-5}	0.796	0.593	0.213
5×10^{-5}	0.572	0.682	0.161
1×10^{-4}	0.373	-------	-------
E.C.$_{50}$ (M)	4.146×10^{-5}	4.079×10^{-6}	1.282×10^{-6}
S. D. (+/-)	3.660×10^{-5}	1.261×10^{-5}	1.086×10^{-6}

5.7.2. Chloroquine:

Figure 5.26. represents the results of an experiment in which B16 cells were treated with a range of concentrations of N^{α}MTX-[Nle^4,D-Phe^7]α–MSH in the presence of 10^{-4}M chloroquine. Previous experiments with chloroquine had demonstrated that it was quite a toxic agent at concentrations greater than 10^{-5}M when placed on the cells in the absence of any other agent e.g. MTX or N^{α}MTX-[Nle^4,D-Phe^7]α–MSH. Therefore the results of the experiment shown by Figure 5.26. should be viewed in the light of this statement. The dramatic inhibition of cell growth may not be attributed to the augmentation of cytotoxicity of N^{α}MTX-[Nle^4,D-Phe^7]α-MSH. Further experiments need to be performed using concentrations of chloroquine which were not lethal in their own right.

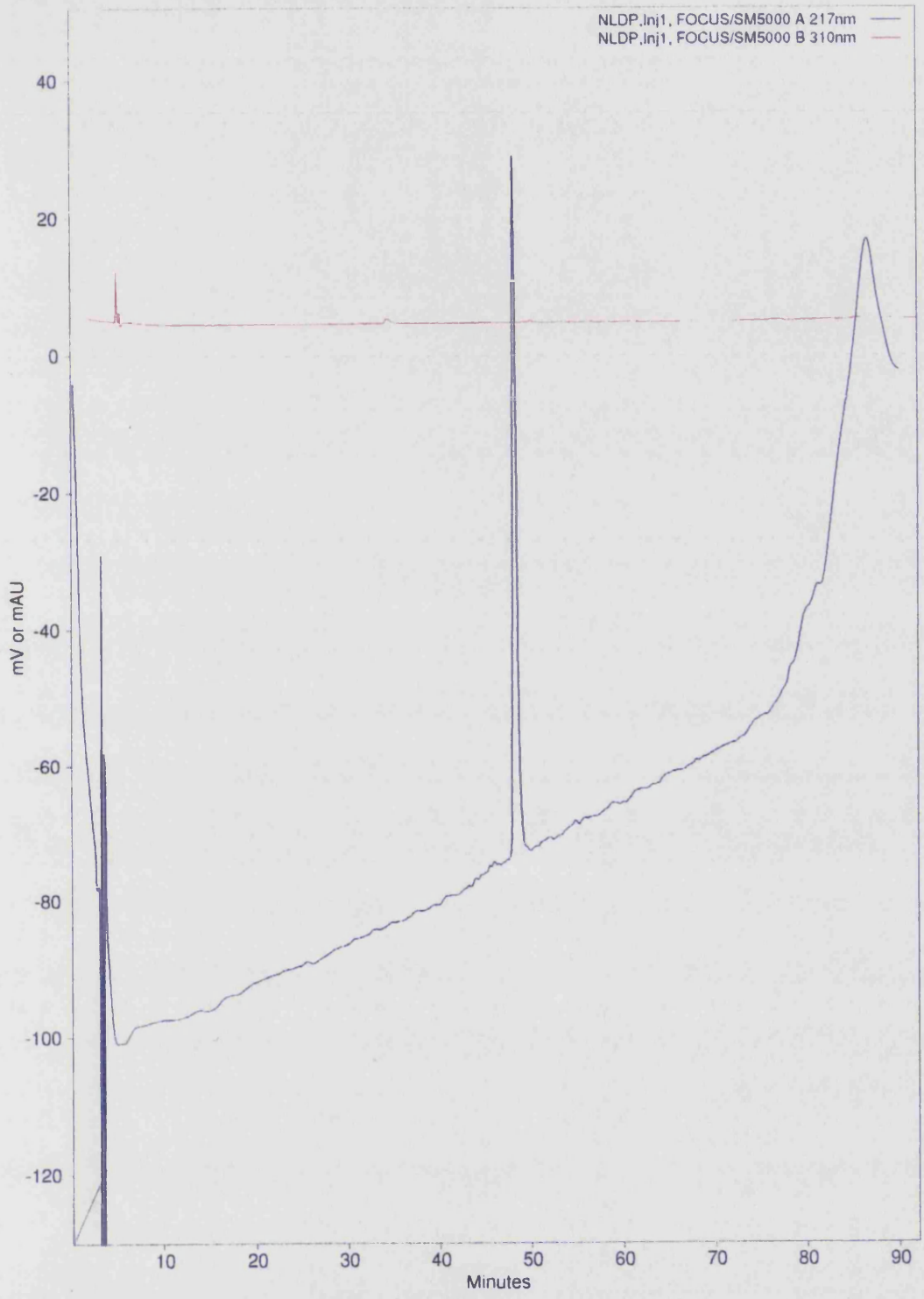

Figure 5.1. This figure represents the HPLC trace of [Nle^4,D-Phe^7]α-MSH labelled "NLDP" at 217nm and 310nm.

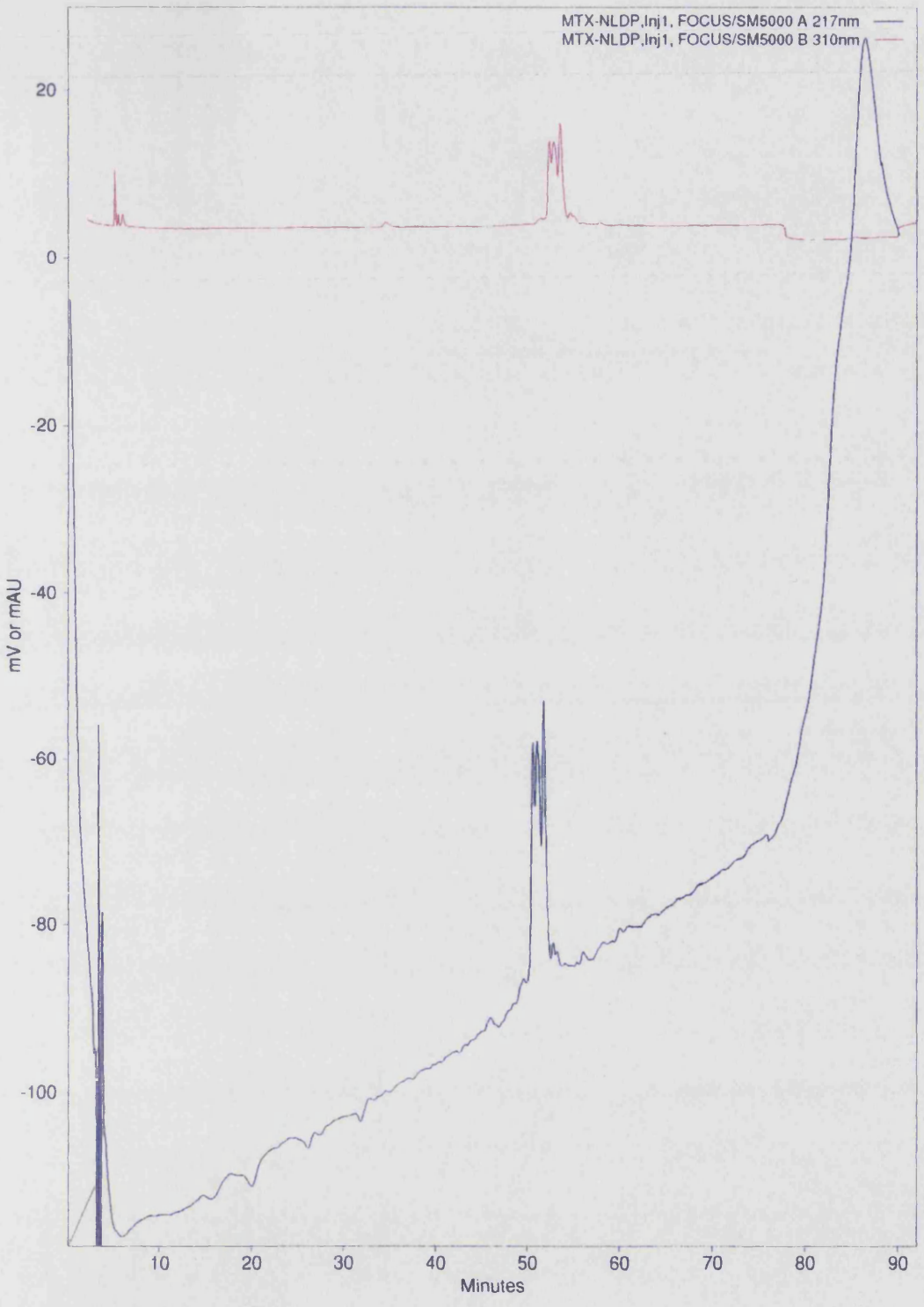

Figure 5.2. This figure shows the elution profile of N^{α}MTX-[Nle^4,D-Phe^7]α-MSH labelled "MTX-NLDP" at 217nm and 310nm.

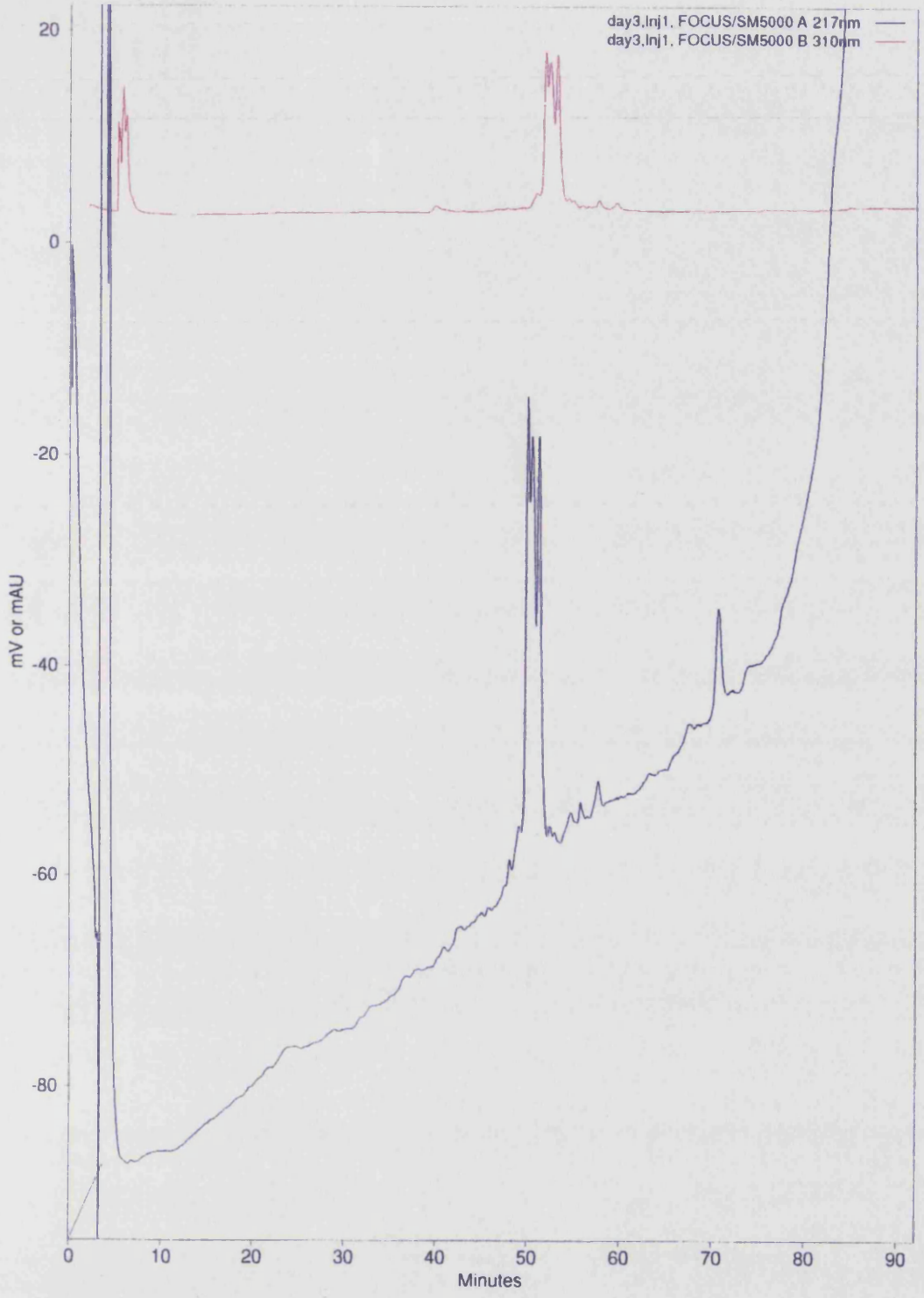

Figure 5.3. This represents the elution profile of N^{α}MTX-[Nle^{4},D-Phe^{7}]α-MSH after incubation with B16 cells at 37°C for 72 hours.

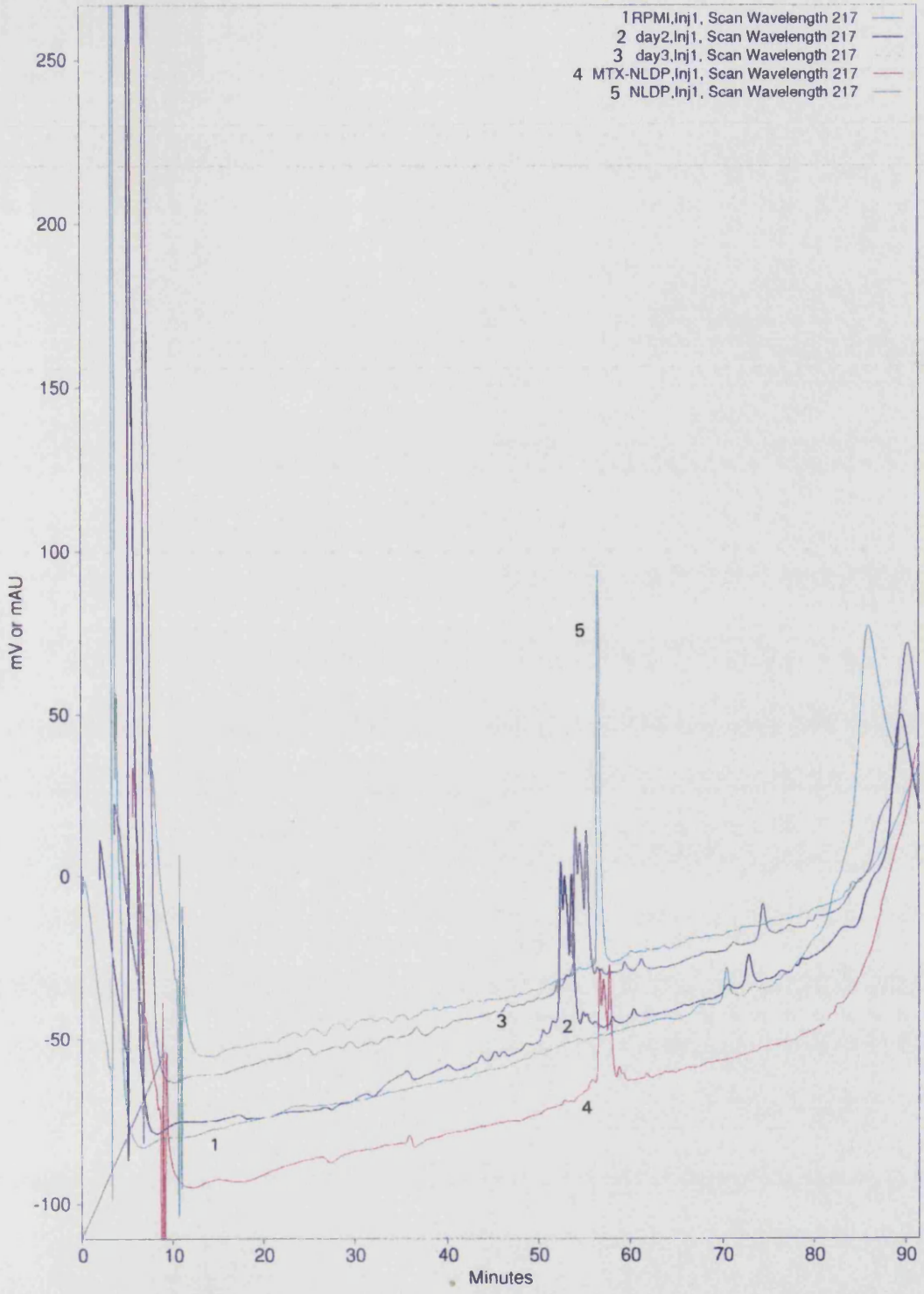

Figure 5.4. This shows the elution profile of the following samples at 217nm:
1: RPMI medium alone, 2: N^{α}MTX-[Nle^4,D-Phe^7]α-MSH after 48 hours with B16 cells, 3: N^{α}MTX-[Nle^4,D-Phe^7]α-MSH after 72 hours with B16 cells 4: N^{α}MTX-[Nle^4,D-Phe^7]α-MSH alone 5: [Nle^4,D-Phe^7]α-MSH alone. (See text for details).

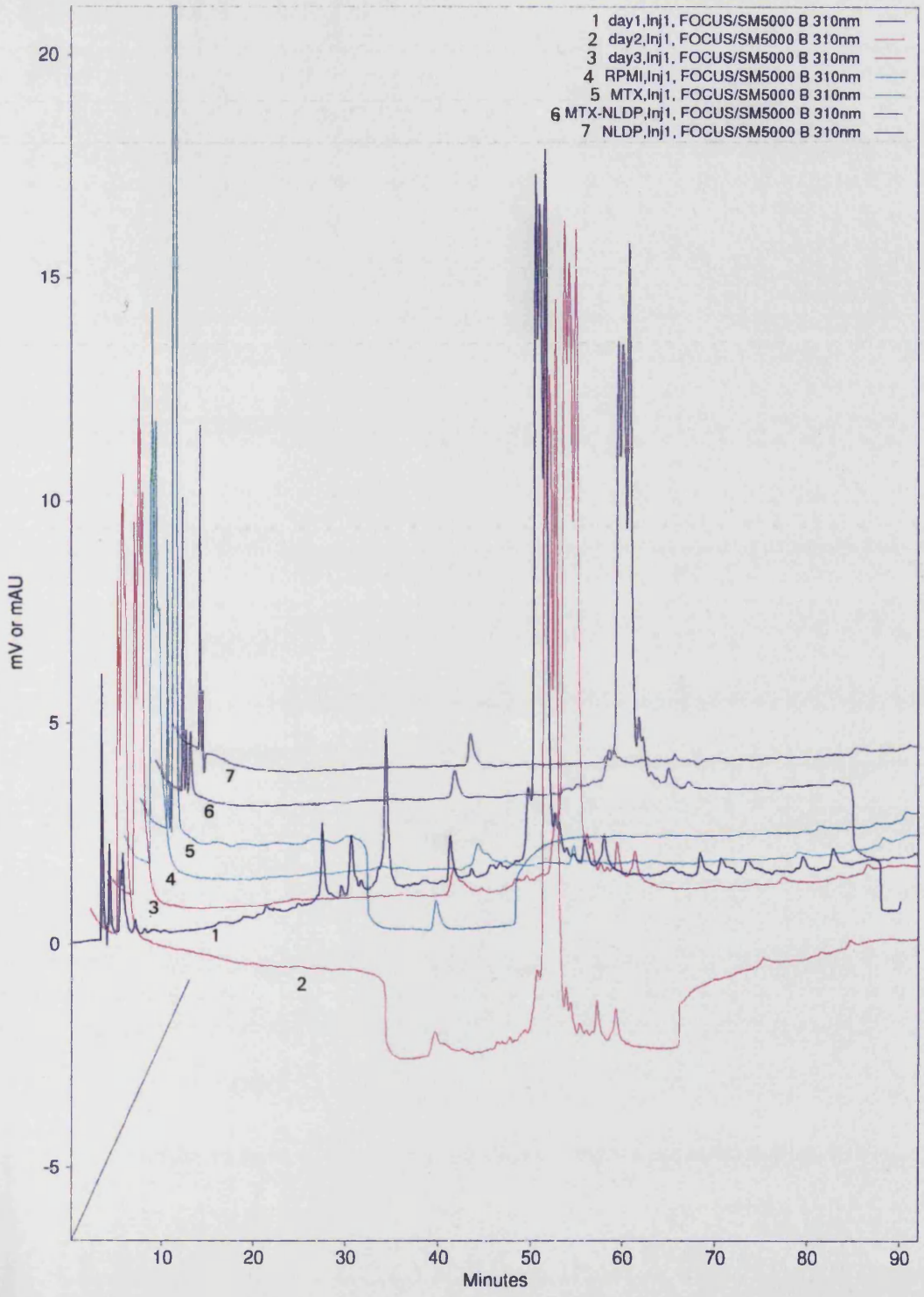

Figure 5.5. This figure represents the elution profile of the following samples at 310nm: 1: N^{α}MTX-[Nle^4,D-Phe^7]α-MSH after 24 hours with B16 cells, 2: N^{α}MTX-[Nle^4,D-Phe^7]α-MSH after 48 hours with B16 cells, 3: N^{α}MTX-[Nle^4,D-Phe^7]α-MSH after 72 hours with B16 cells, 4: RPMI medium alone, 5: MTX alone, 6: N^{α}MTX-[Nle^4,D-Phe^7]α-MSH alone and 7: [Nle^4,D-Phe^7] α-MSH alone. (See text for details).

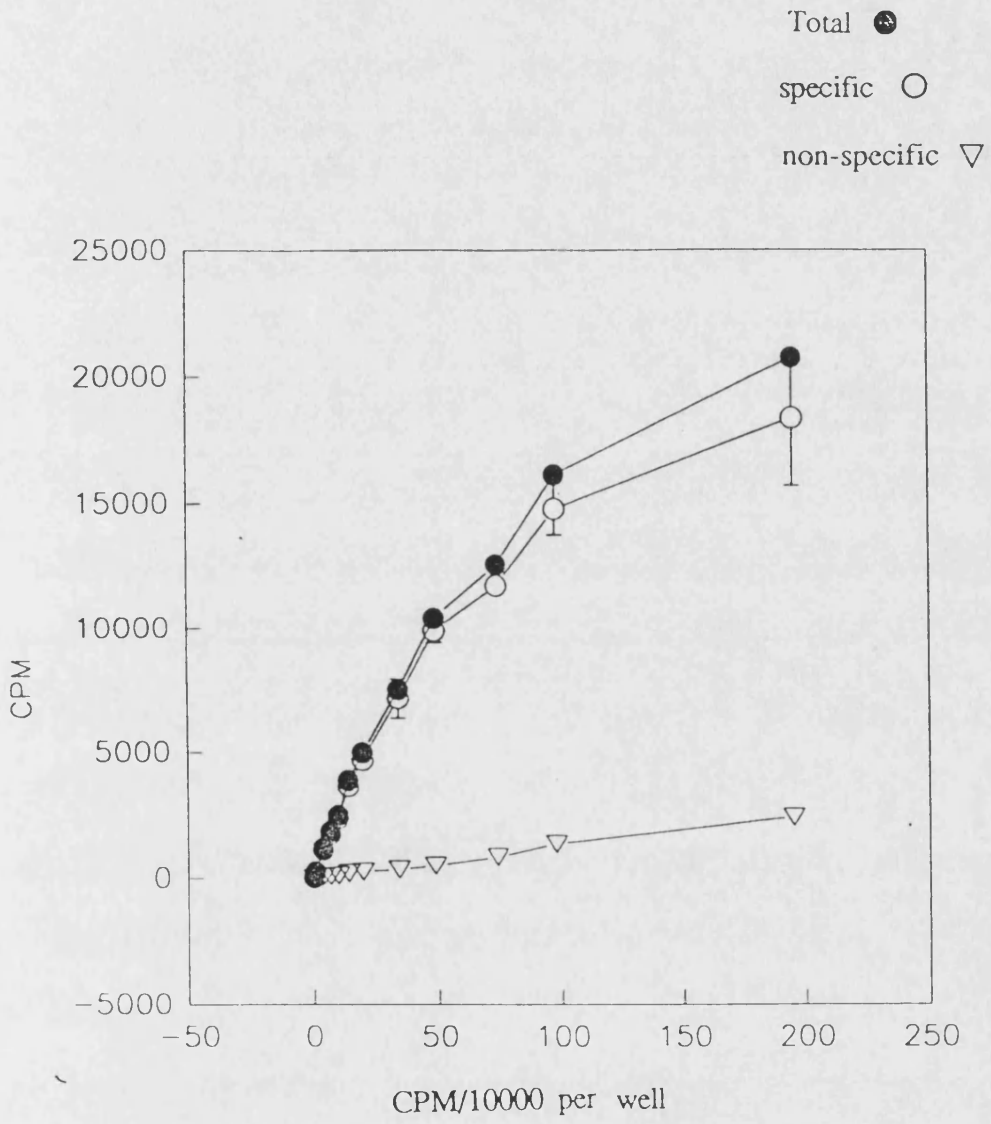

Figure 5.6. Binding isotherm with B16 cells incubated in the presence of various concentrations of ^{125}I-[Nle^4,D-Phe^7]α-MSH in the presence and absence of excess (10^{-6}M) non-iodinated [Nle^4,D-Phe^7]α-MSH. (Adapted from Erskine-Grout, 1993).

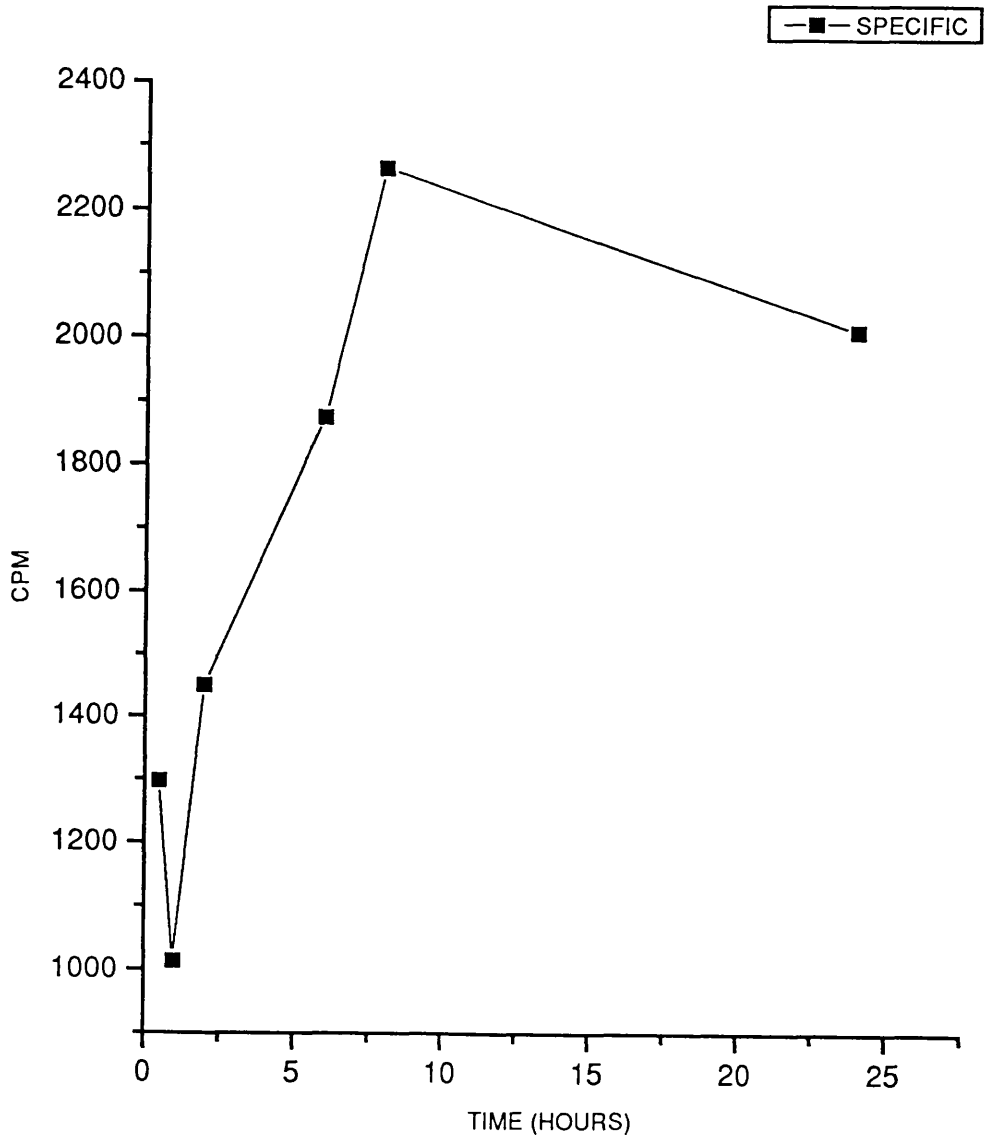

Figure 5.7. Time course experiment performed with the MeWo cell line and using 0.5nM ^{125}I- [Nle^4,D-Phe^7]α-MSH. Error bars have been omitted for clarity.

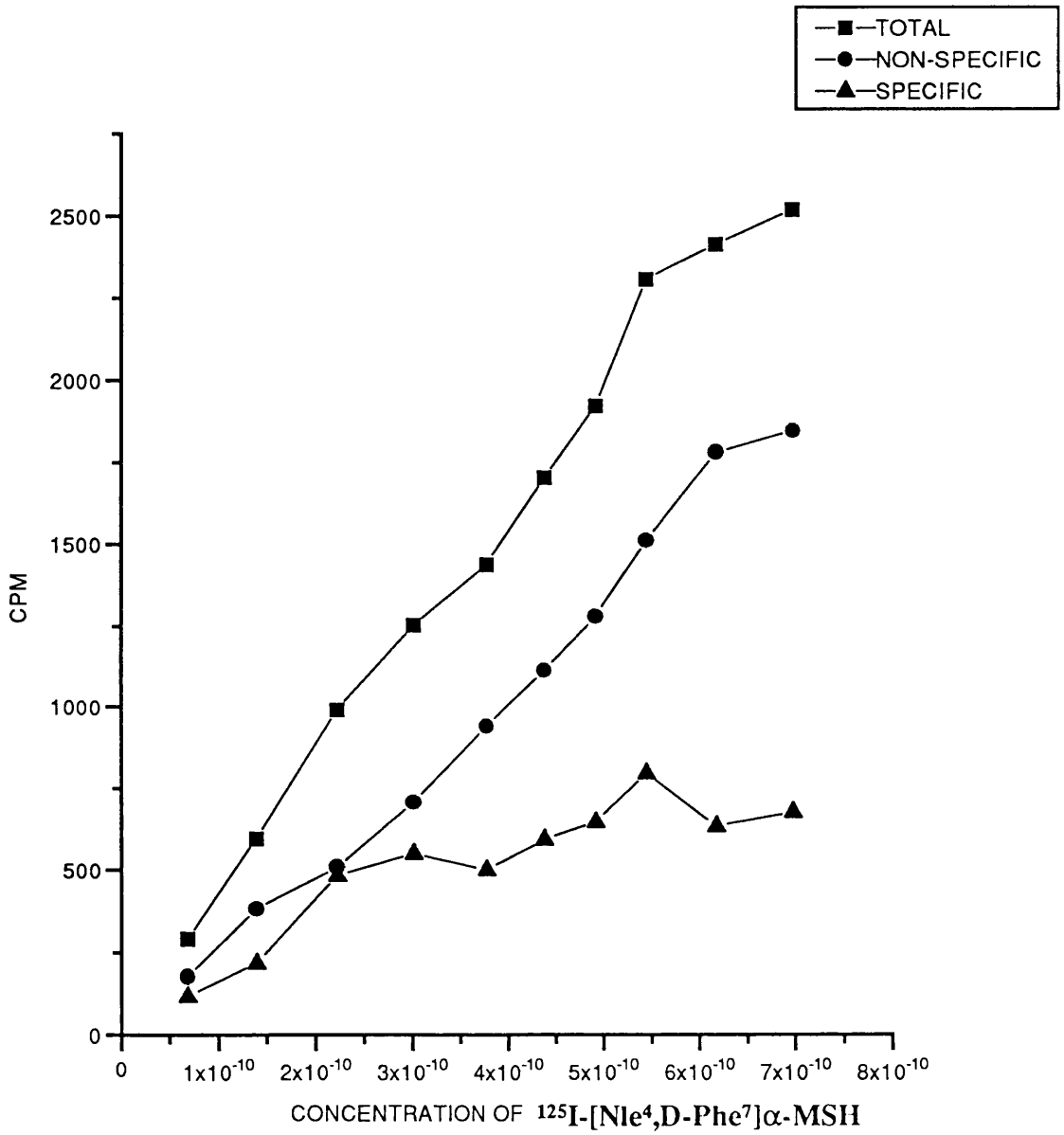

Figure 5.8. Binding isotherm with MeWo cells incubated in the presence of various concentrations of ^{125}I-[Nle^4,D-Phe^7]α-MSH in the presence and absence of excess (10^{-6}M) non-iodinated [Nle^4,D-Phe^7]α-MSH. Error bars have been omitted for clarity.

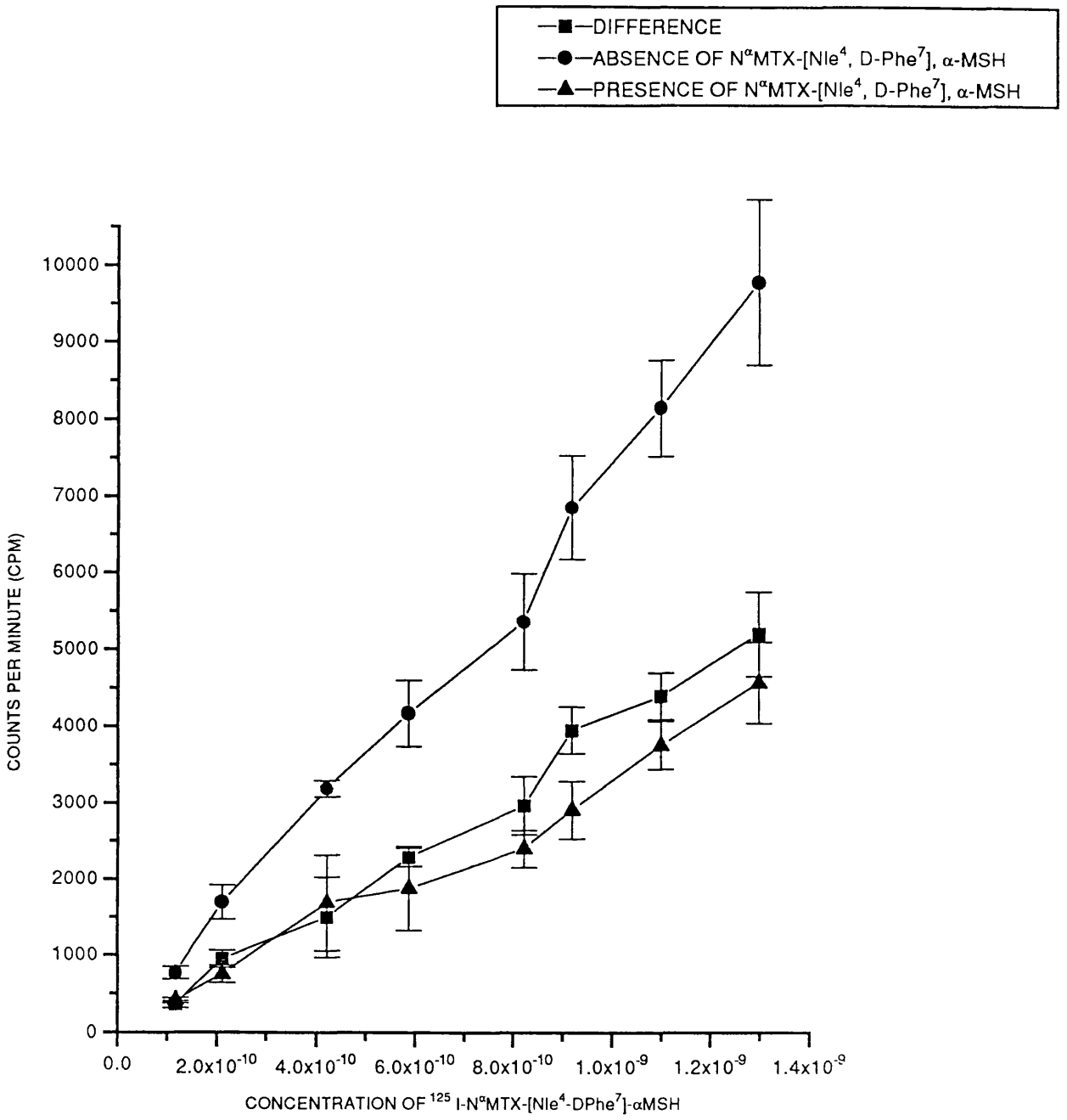

Figure 5.9. Binding isotherm with transformed 293 cells incubated in the presence of various concentrations of Nα MTX-[^{125}I-Tyr^{2},Nle^{4},D-Phe^{7}]α-MSH in the presence and absence of excess (10^{-6}M) non-iodinated Nα MTX-[Nle^{4},D-Phe^{7}]α-MSH.

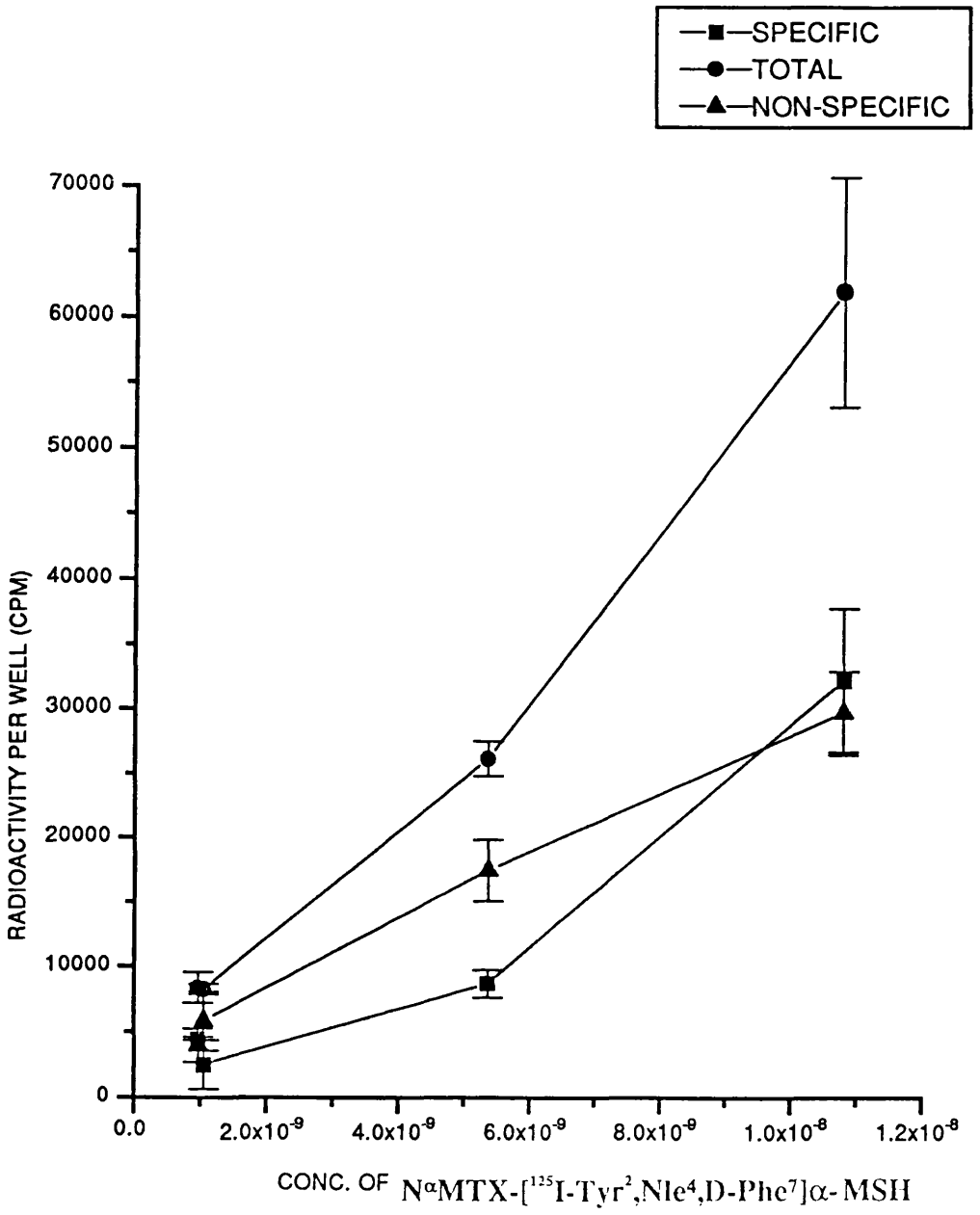

Figure 5.10. Binding isotherm with transformed 293 cells, expressing MC3 receptors incubated in the presence of various concentrations of N^{α}MTX-[^{125}I-Tyr^{2},Nle^{4},D-Phe^{7}]α-MSH in the presence and absence of excess (10^{-6}M) non-iodinated N^{α}MTX-[Nle^{4},D-Phe^{7}]α-MSH.

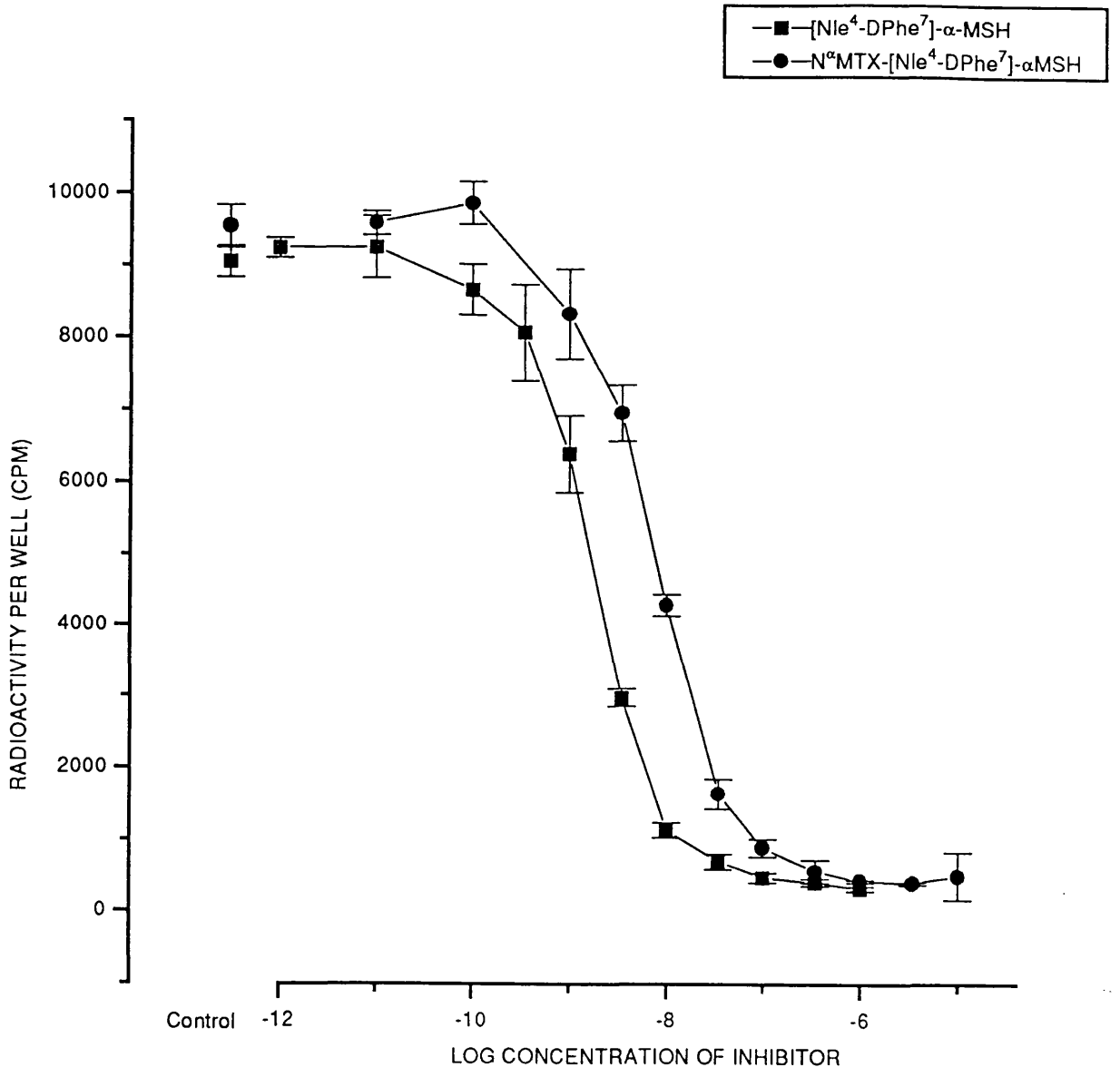

Figure 5.11. This figure shows the results of the competitive binding assay where 0.1nM ^{125}I- [Nle^4,D-Phe^7]α-MSH is incubated in the presence of varying concentrations of unlabelled [Nle^4,D-Phe^7]α-MSH and N$^\alpha$MTX-[Nle^4,D-Phe^7]α-MSH and was performed on transformed 293 cells expressing the MC3 receptors.

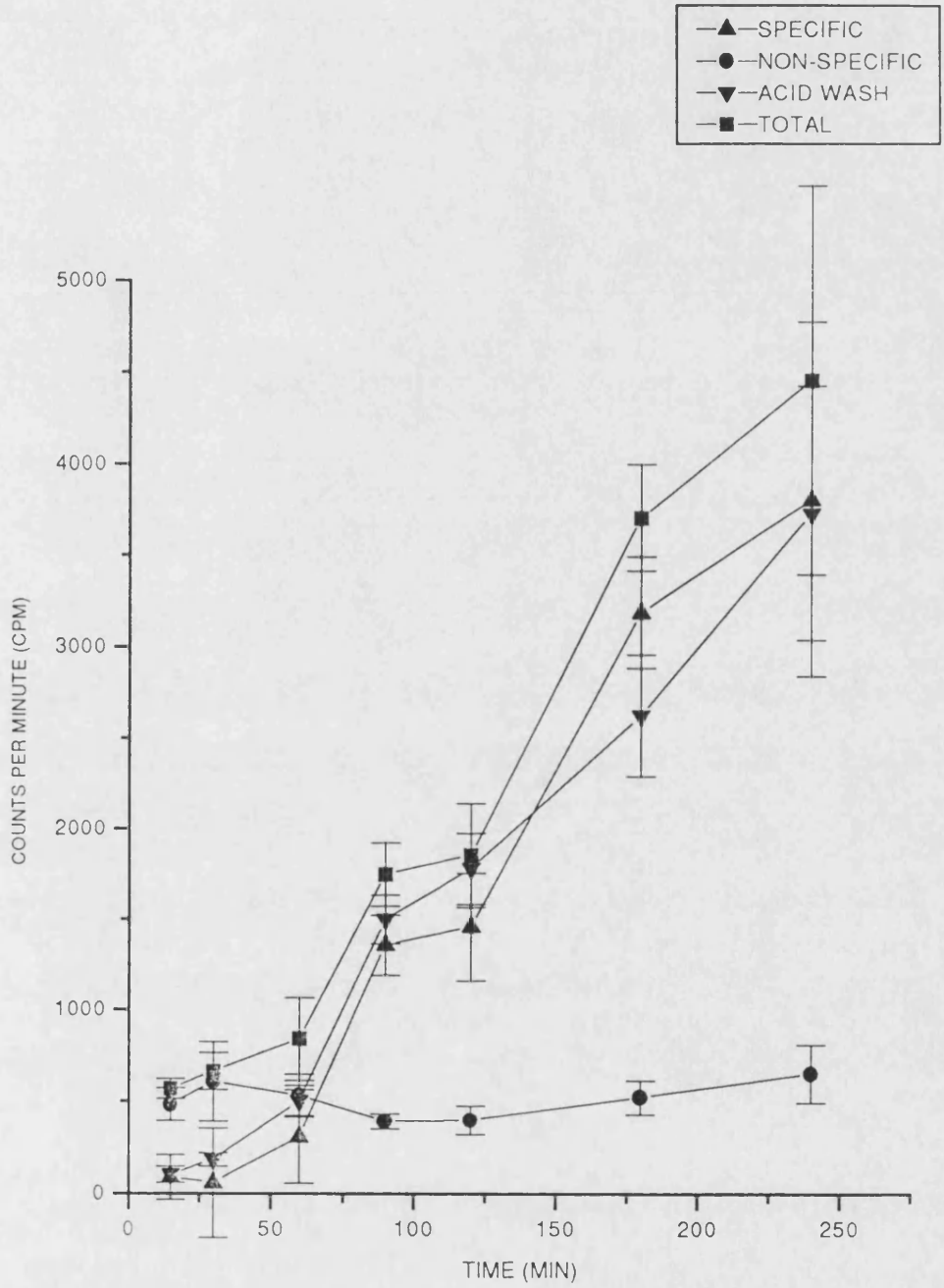

Figure 5.12.(a) Continual exposure internalisation of 0.1nM N$^{\alpha}$MTX-[^{125}I-Tyr^{2},Nle^{4},D-Phe^{7}]α-MSH with B16 cells in the presence of 20mM NH_4Cl. Experiment performed over 4 hours.

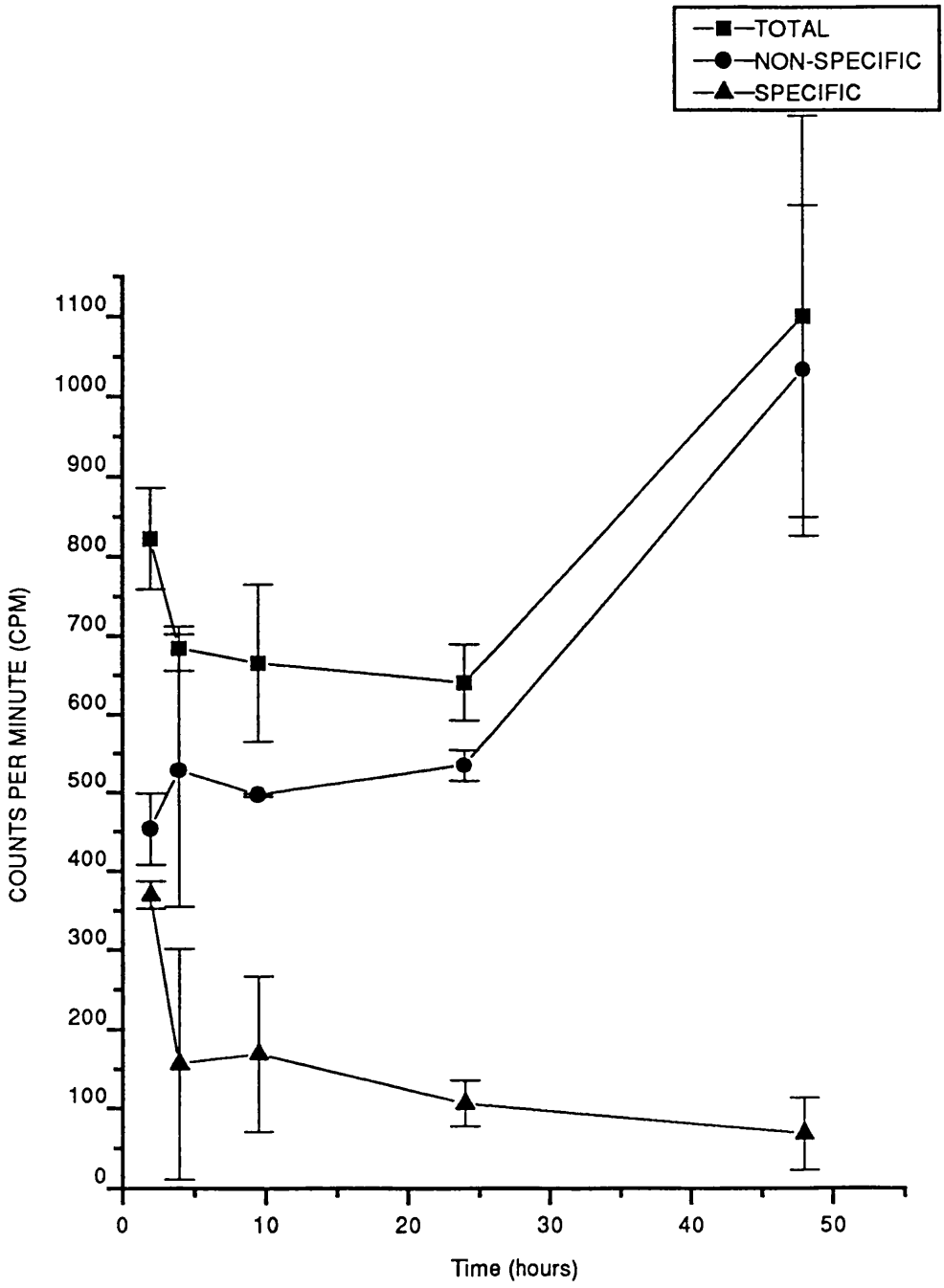

Figure 5.12.(b) Continual exposure internalisation of 0.1nM N$^{\alpha}$MTX-[^{125}I-Tyr^{2},Nle^{4},D-Phe^{7}]α-MSH with B16 cells in the presence of 20mM NH_4Cl. Experiment performed over 48 hours.

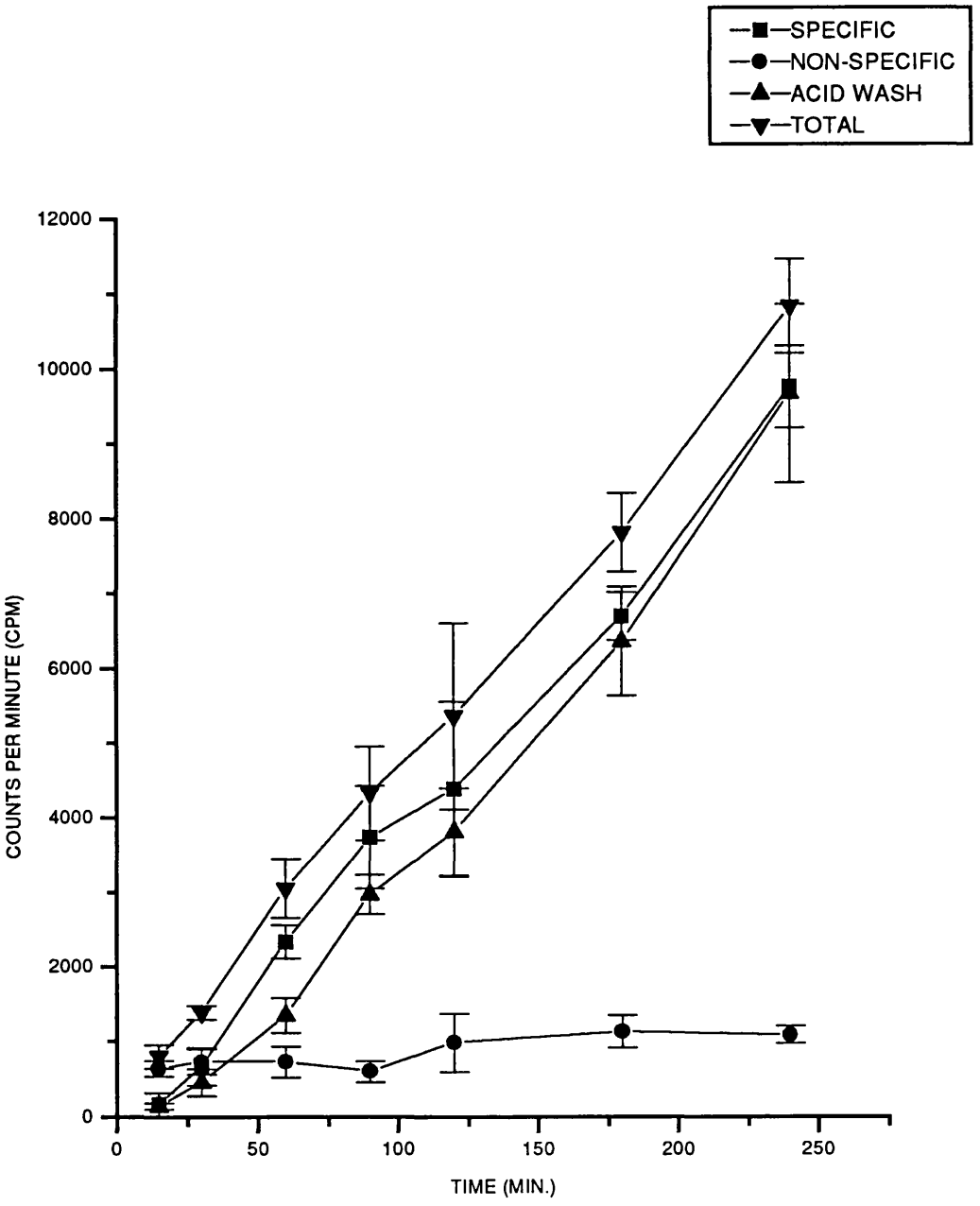

Figure 5.13. Continual exposure internalisation of 0.1nM N$^{\alpha}$MTX-[^{125}I-Tyr^{2},Nle^{4},D-Phe^{7}]α-MSH with B16 cells in the presence of 20mM NH_4Cl. Experiment performed over 4 hours.

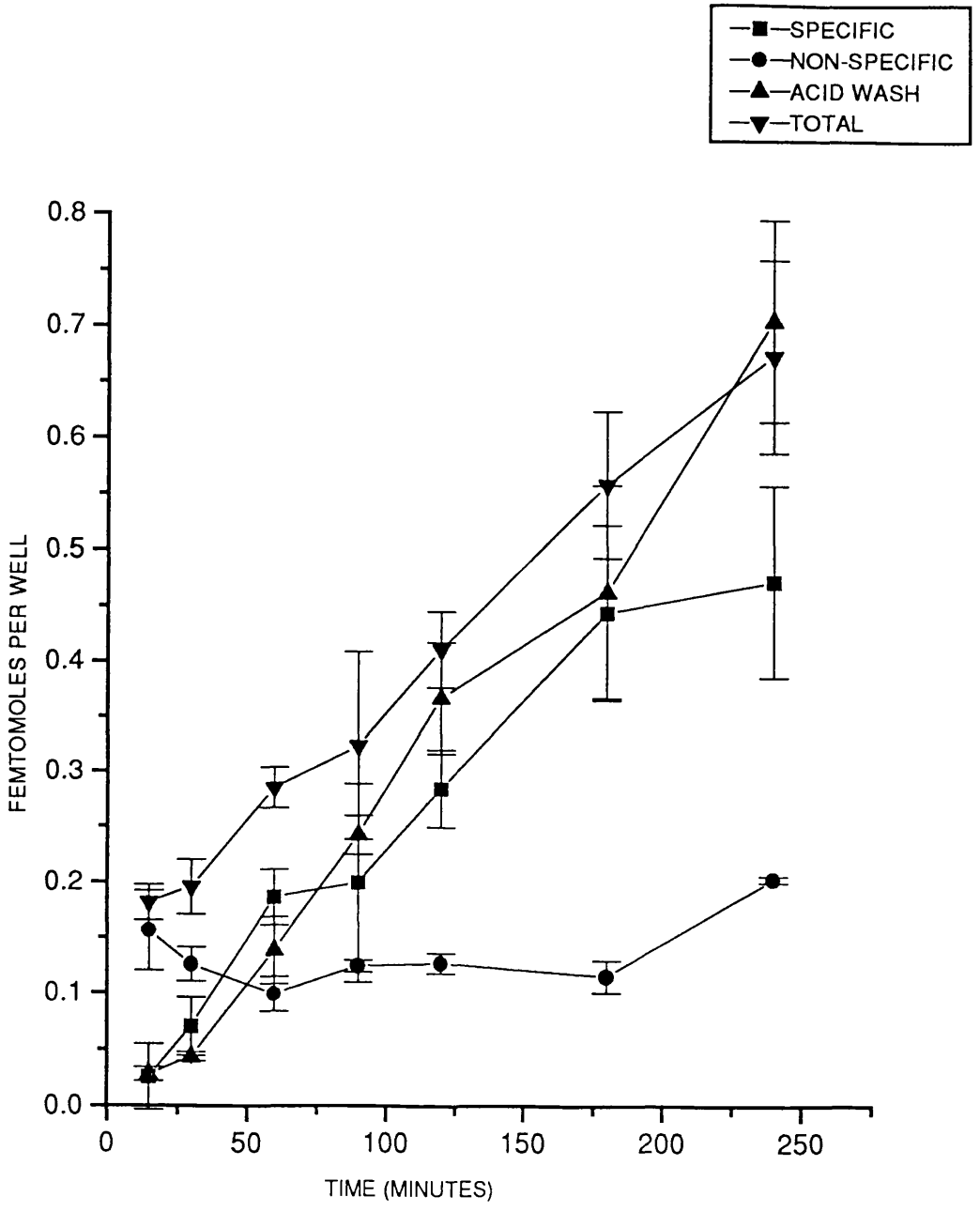

Figure 5.14. Continual exposure internalisation of 0.1nM N$^{\alpha}$MTX-[^{125}I-Tyr^{2},Nle^{4},D-Phe^{7}]α-MSH with B16 cells in the presence of 20mM NH_4Cl. Experiment performed over 4 hours.

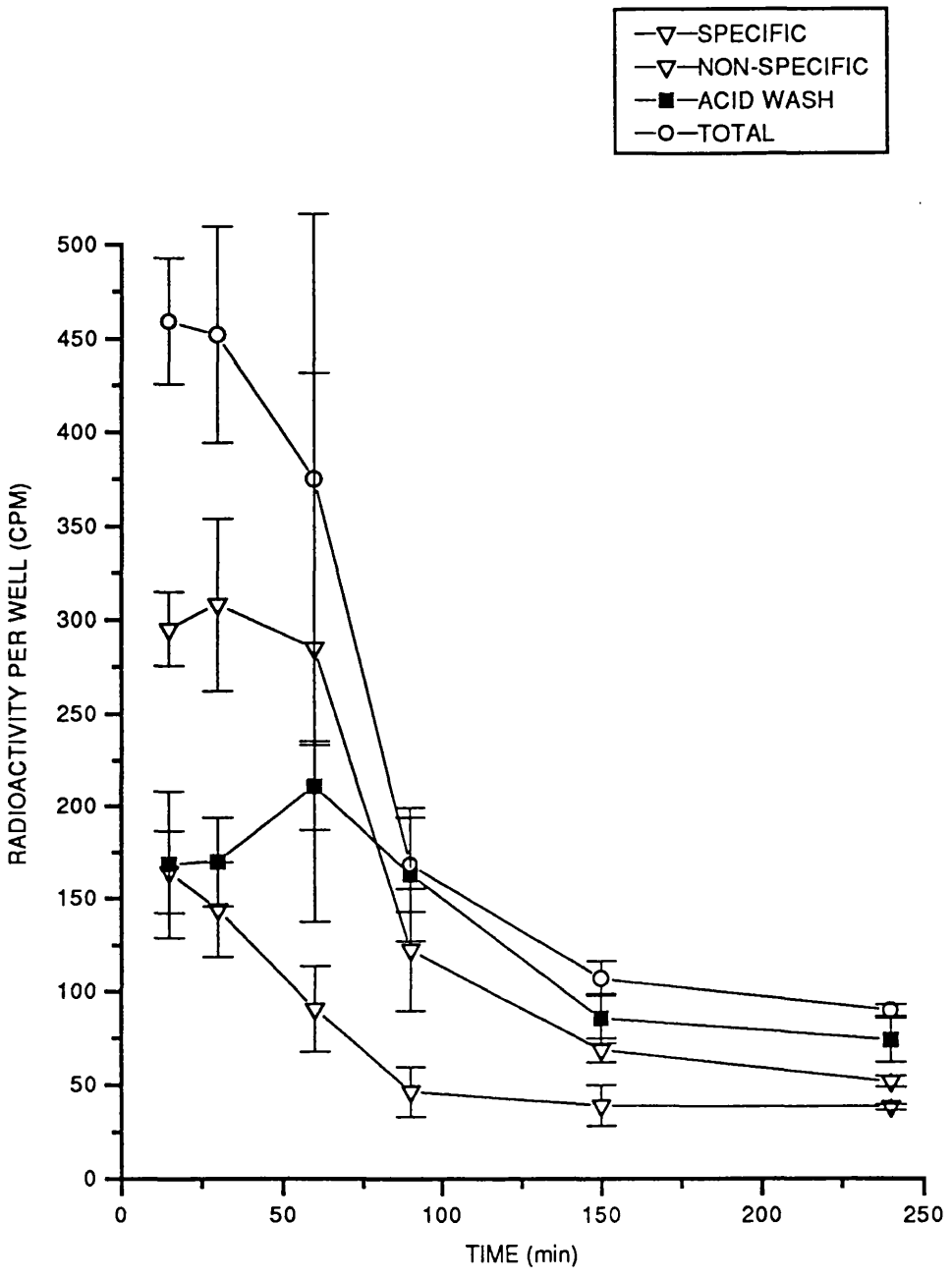

Figure 5.15. Pulse Chase internalisation of 0.1nM N$^{\alpha}$MTX-[^{125}I-Tyr^{2},Nle^{4},D-Phe^{7}]α-MSH with B16 cells in the absence of 20mM NH_4Cl. Experiment performed over 4 hours.

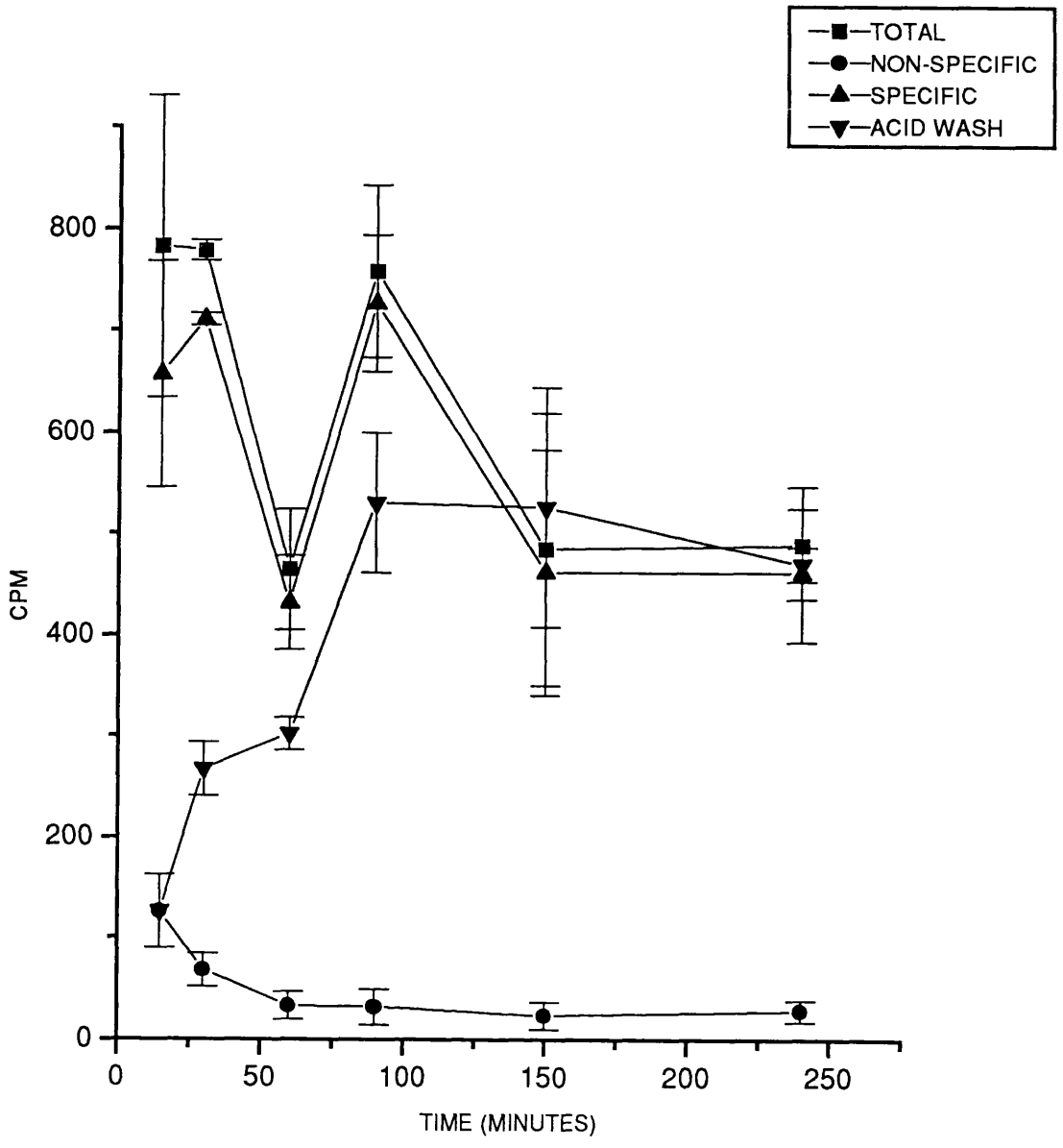

Figure 5.16. Pulse Chase internalisation of 0.1nM N$^{\alpha}$MTX-[^{125}I-Tyr^{2},Nle^{4},D-Phe^{7}]α-MSH with B16 cells in the presence of 20mM NH_4Cl. Experiment performed over 4 hours.

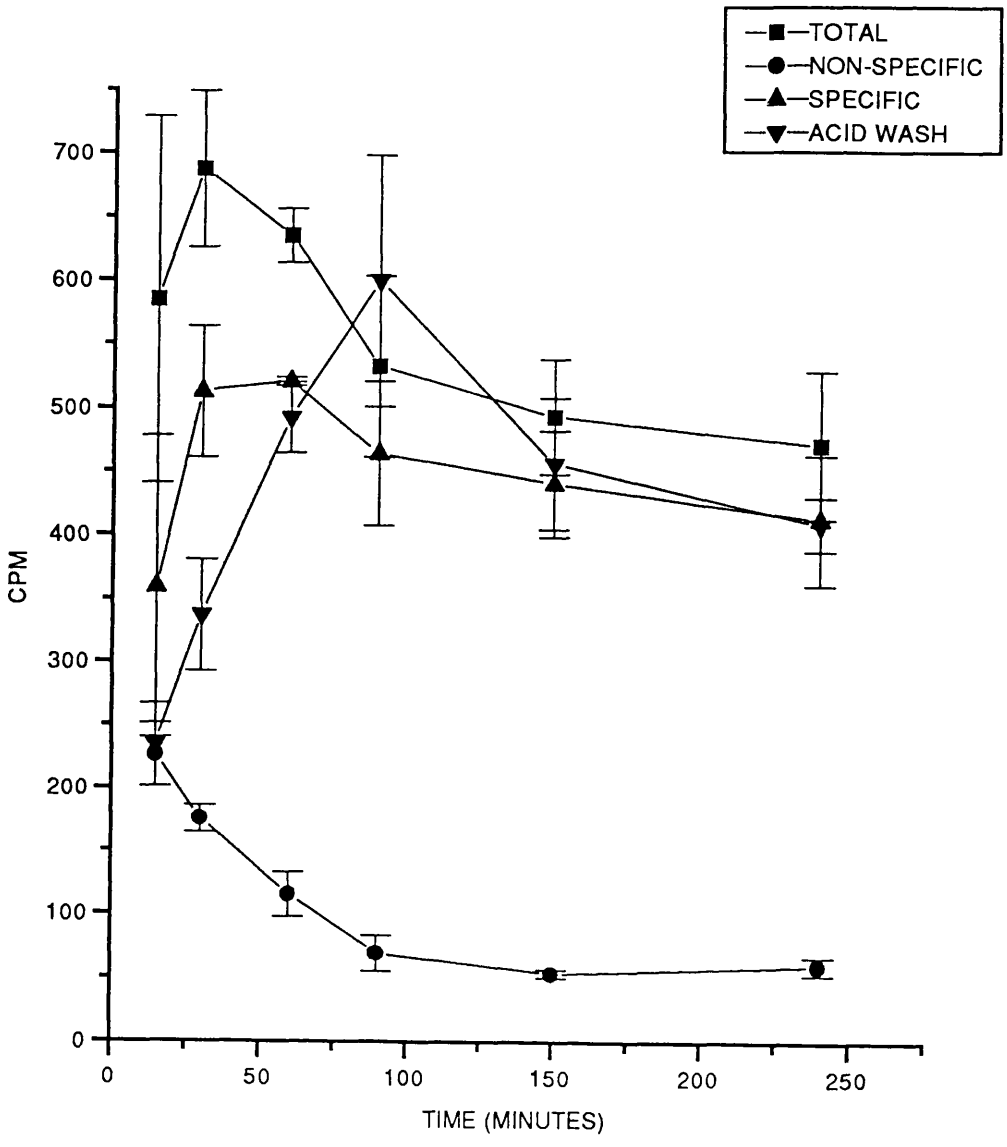

Figure 5.17. Pulse Chase internalisation of 0.1nM N$^{\alpha}$MTX-[^{125}I-Tyr^{2},Nle^{4},D-Phe^{7}]α-MSH with B16 cells in the presence of 20mM NH_4Cl. Experiment performed over 4 hours.

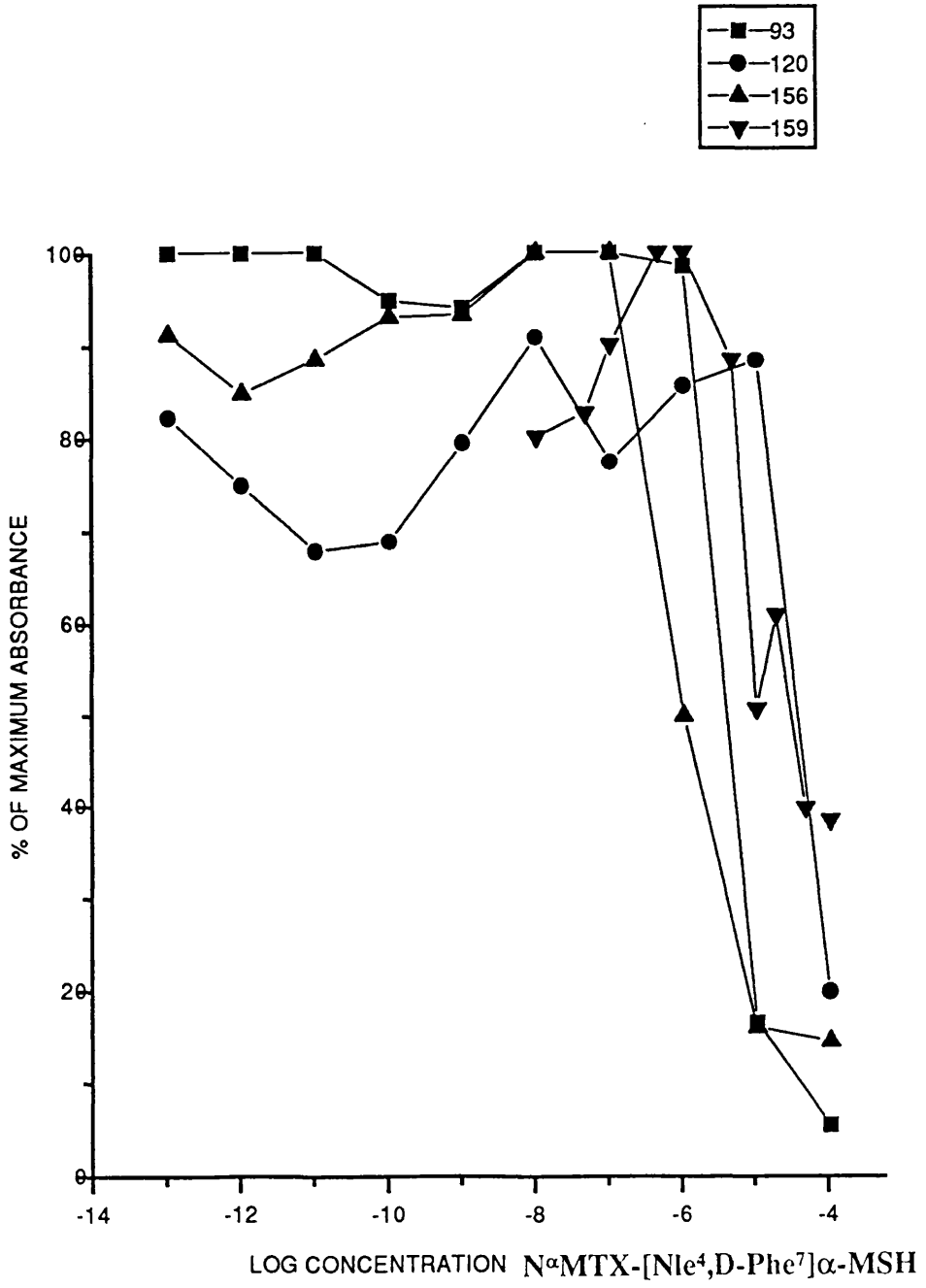

Figure 5.18.(a). Relative values obtained for absorbance of B16 cells exposed to NαMTX-[Nle^4,D-Phe^7]α-MSH . The results of 4 replicate experiments are shown. Each point is the mean of 8 wells. Error bars have been omitted for clarity.

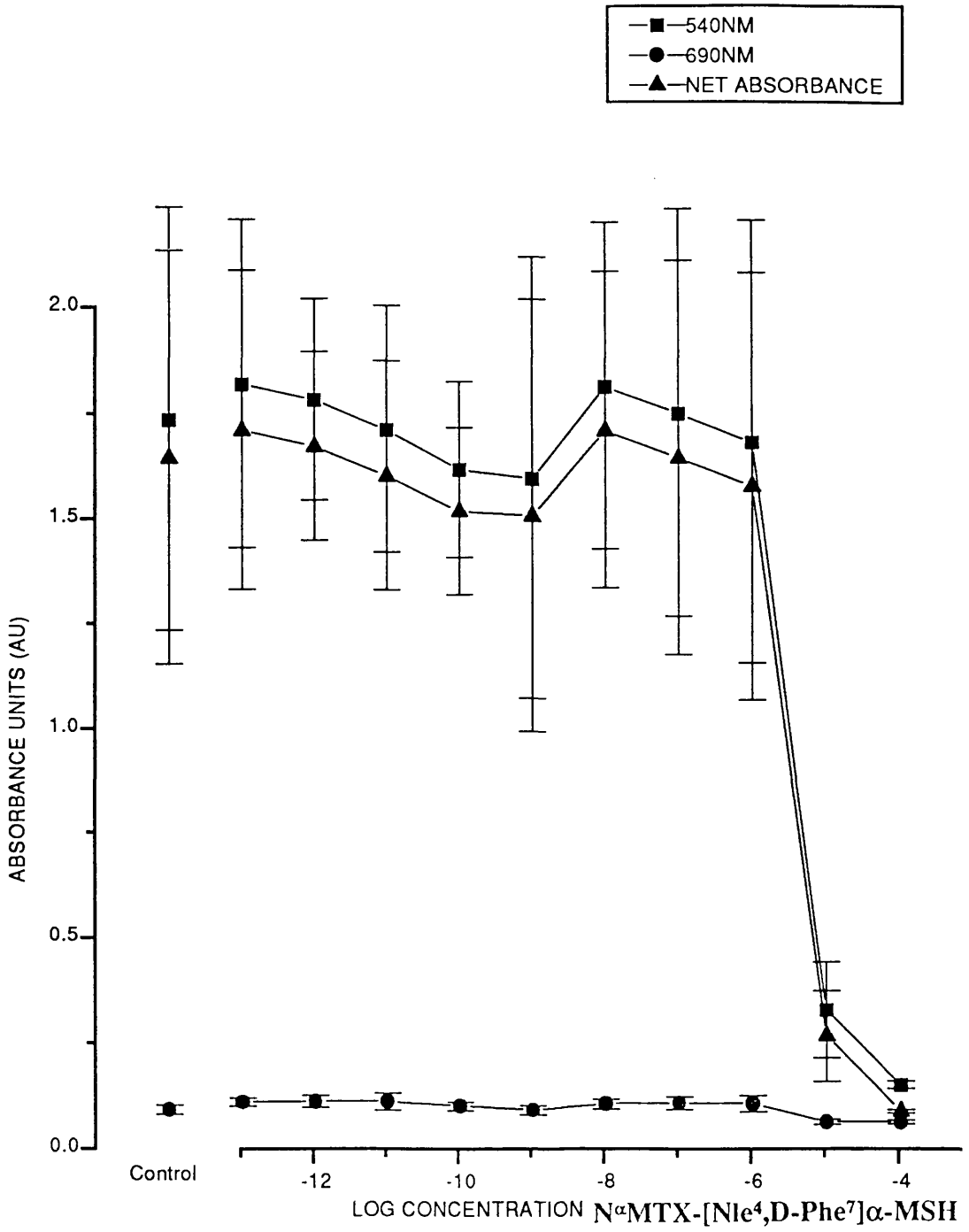

Figure 5.18.(b). Net absorbance readings (540-690nm) obtained with B16 cells incubated with N^{α}MTX-[Nle^4,D-Phe^7] . Each point is the mean of 8 replicates. Control values are the mean of 16 replicates. Standard deviation is shown by error bars.

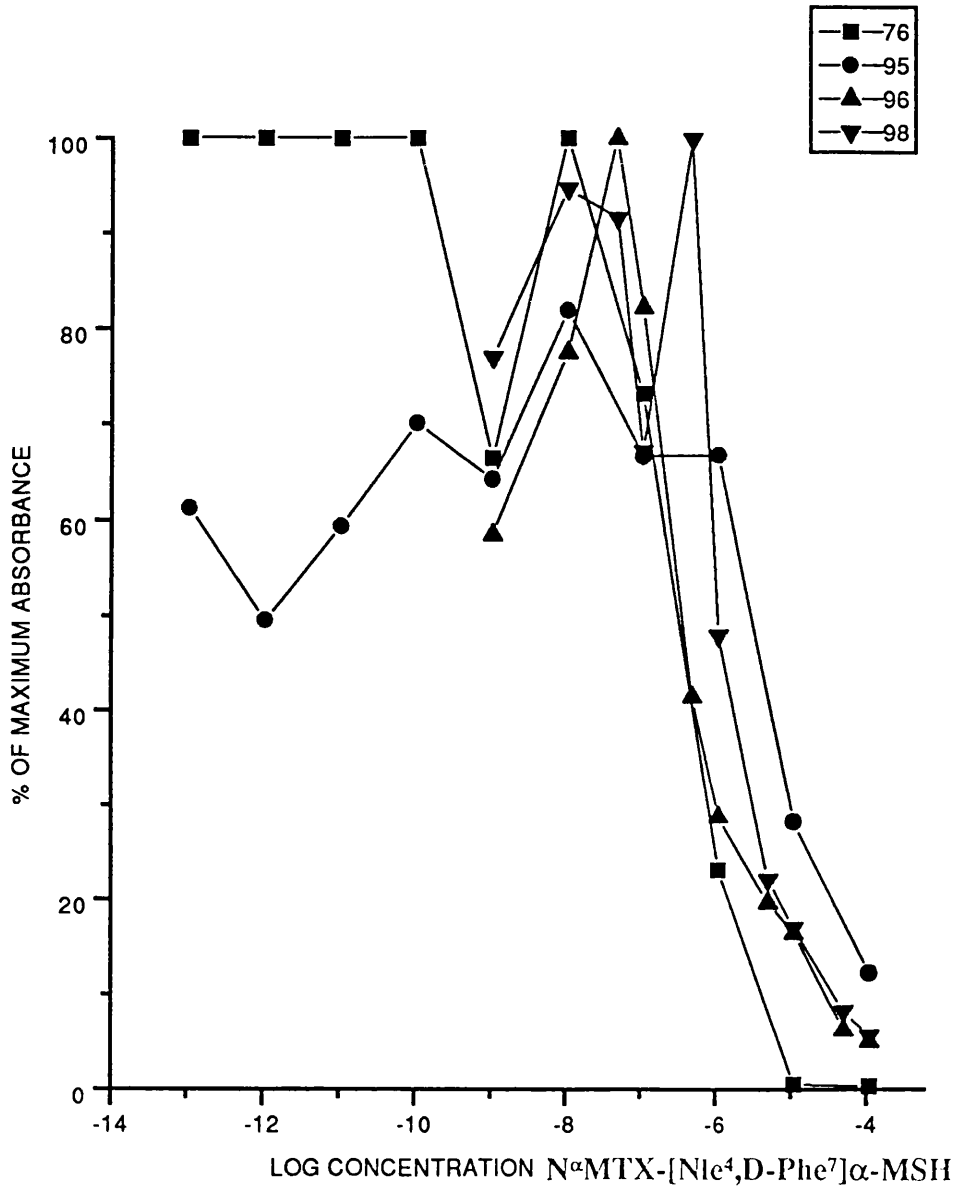

Figure 5.19.(a). Relative values obtained for absorbance of MeWo cells exposed to NαMTX-[Nle^4,D-Phe^7]α-MSH . The results of 4 replicate experiments are shown. Each point is the mean of 8 wells. Error bars have been omitted for clarity.

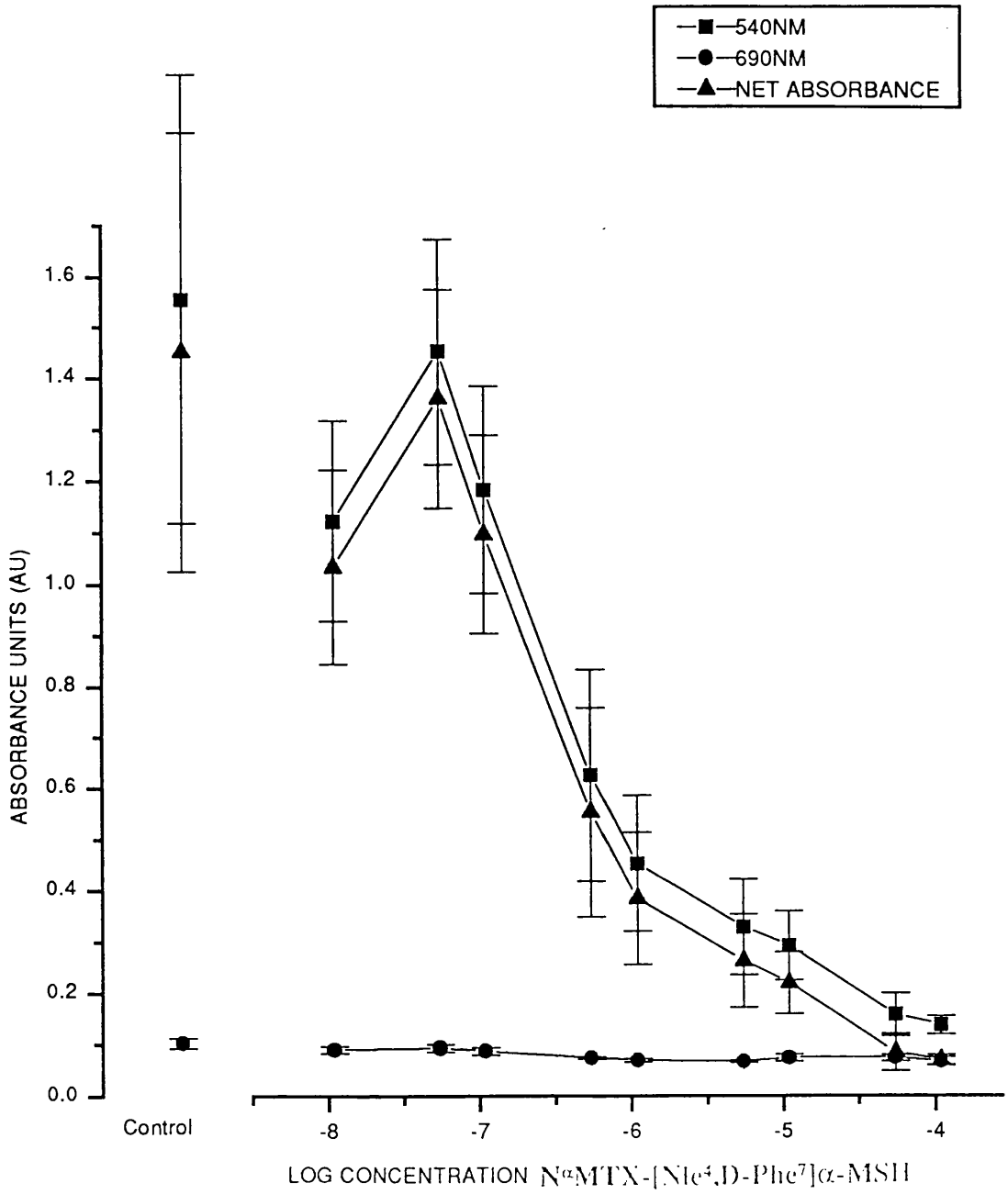

Figure 5.19.(b). Net absorbance readings (540-690nm) obtained with MeWo cells incubated with N^{α}MTX-[Nle^4,D-Phe^7] . Each point is the mean of 8 replicates. Control values are the mean of 16 replicates. Standard deviation is shown by error bars.

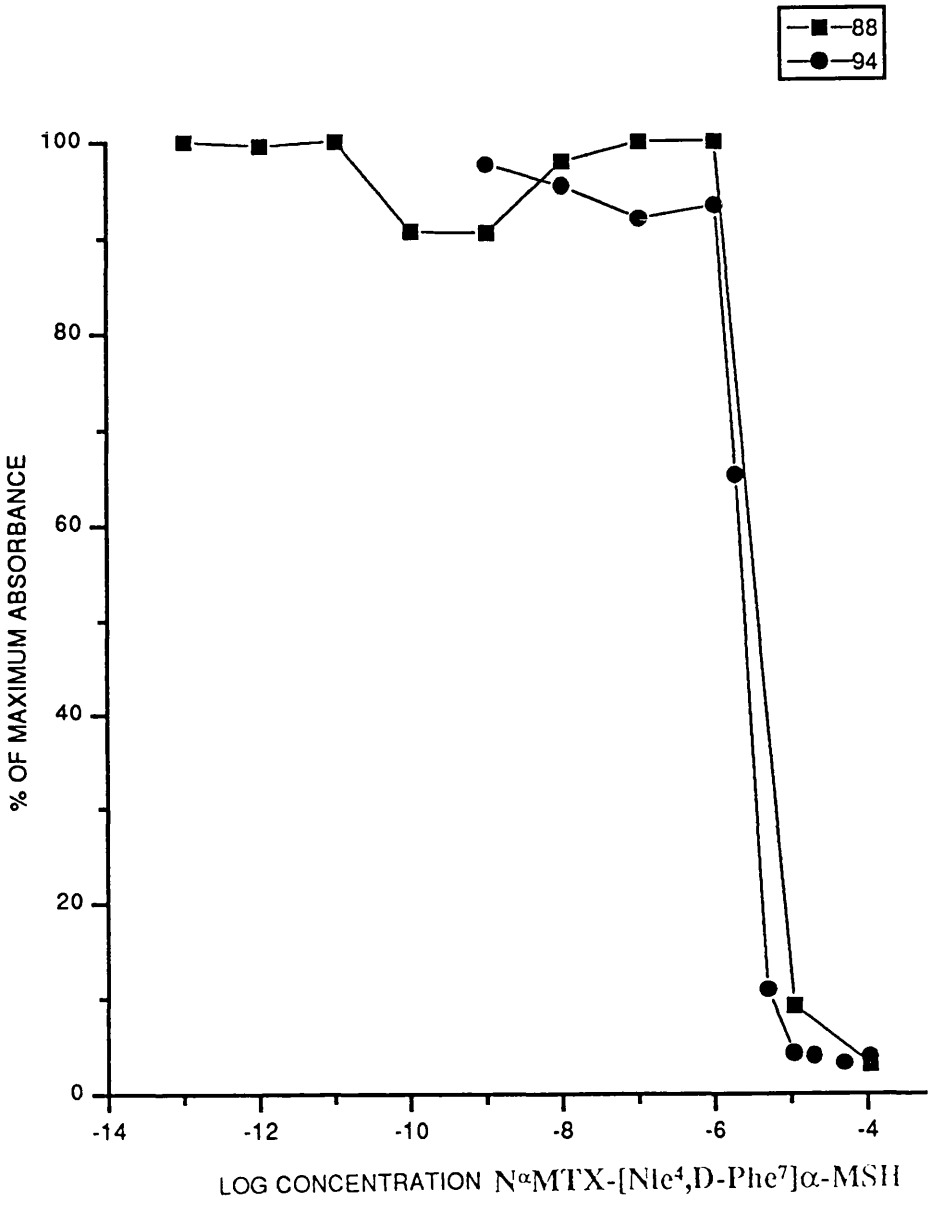

Figure 5.20. Net absorbance readings (540-690nm) obtained with SVK14 cells incubated with N$^{\alpha}$MTX-[Nle^{4},D-Phe^{7}]. Each point is the mean of 8 replicates. Control values are the mean of 16 replicates. Error bars have been omitted for clarity.

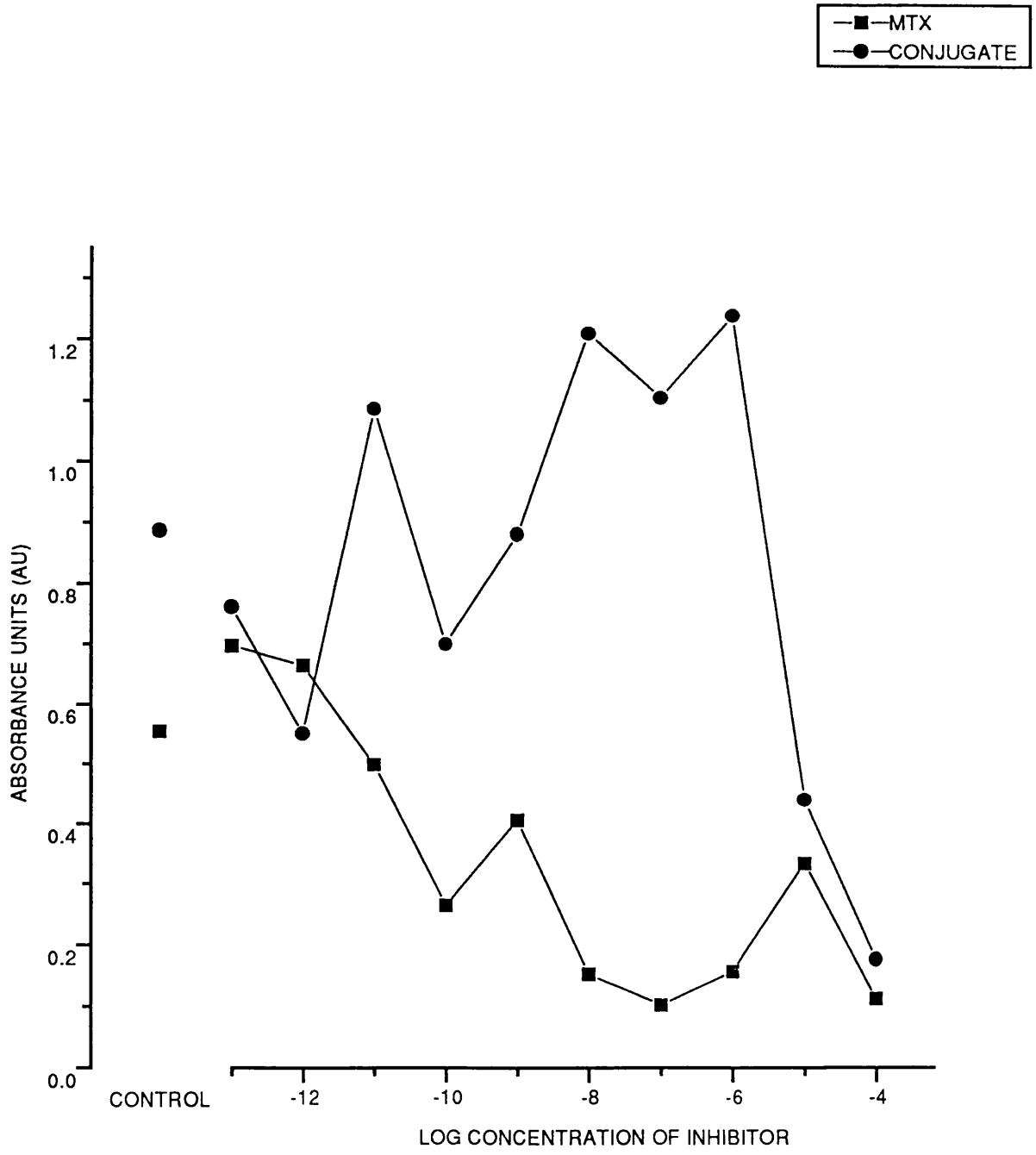

Figure 5.21. Net absorbance readings (540-690nm) obtained with transformed 293 cells (with MC3 receptors) incubated with N$^{\alpha}$MTX-[Nle^{4},D-Phe^{7}]. Each point is the mean of 8 replicates. Control values are the mean of 16 replicates. Error bars have been omitted for clarity.

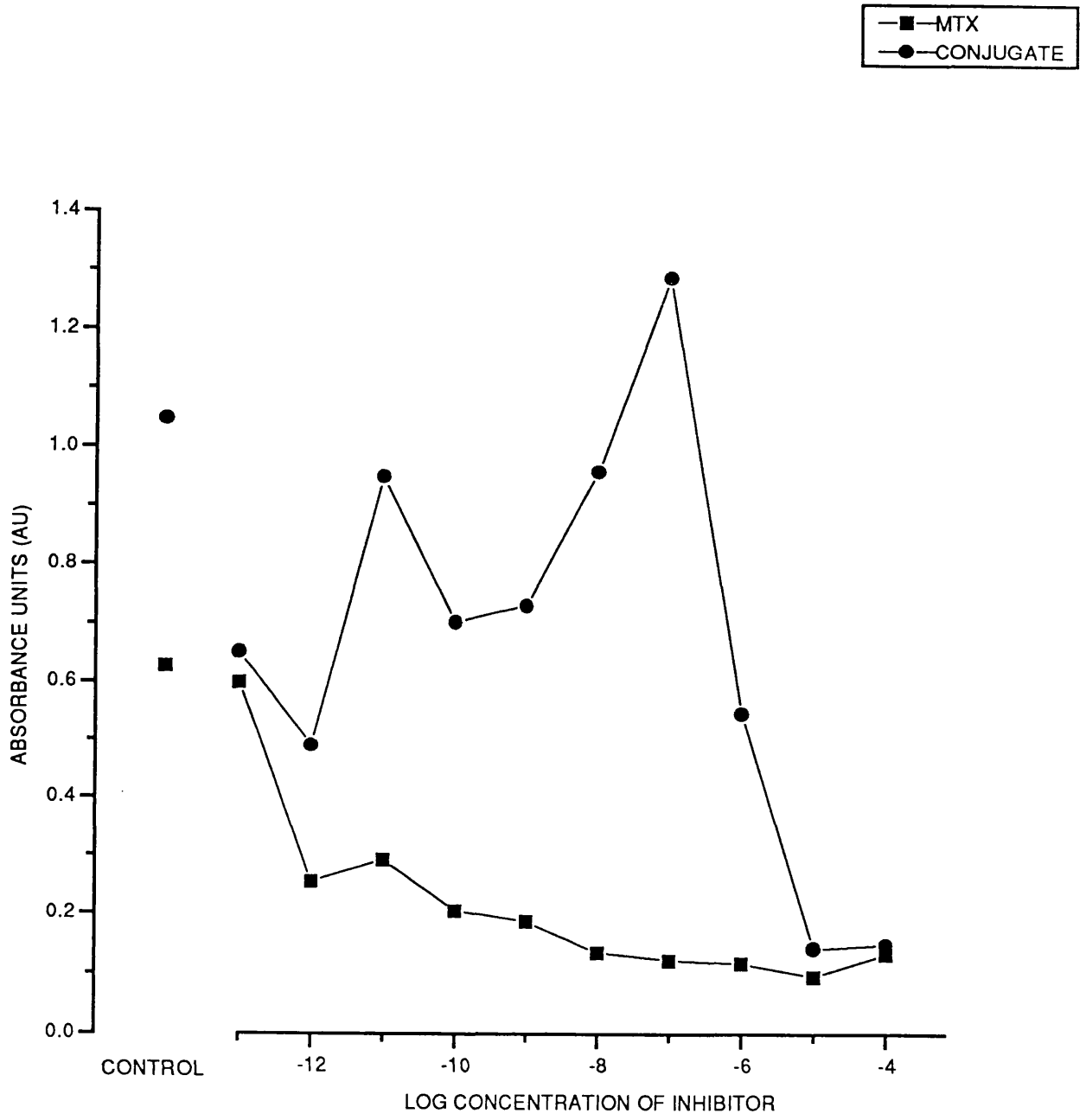

Figure 5.22. Net absorbance readings (540-690nm) obtained with transformed 293 cells (without MC3 receptors) incubated with N^{α}MTX-[Nle^4,D-Phe^7]. Each point is the mean of 8 replicates. Control values are the mean of 16 replicates. Error bars have been omitted for clarity.

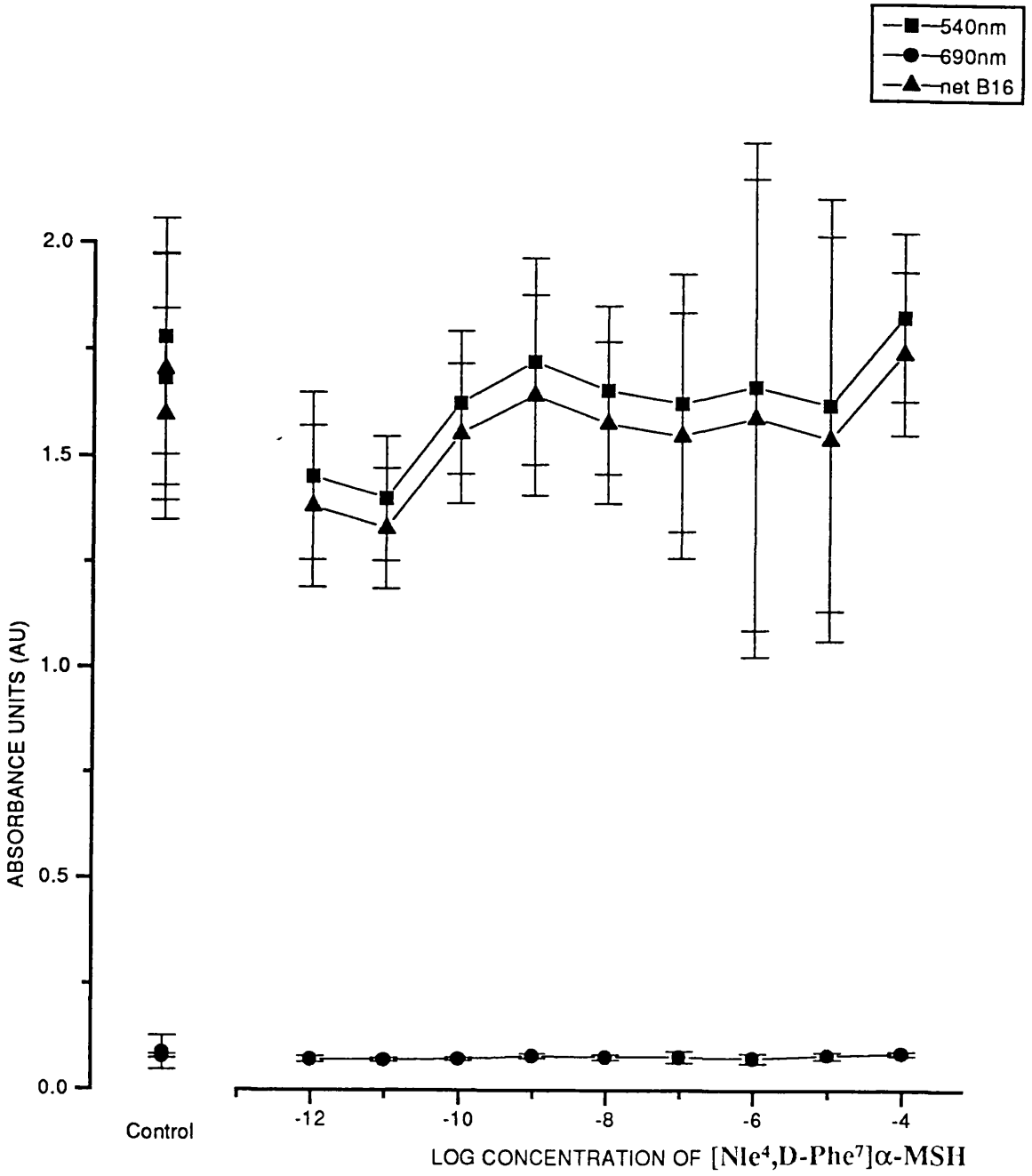

Figure 5.23. Absorbance readings obtained at test (540nm), reference (690nm) and net absorbance (540-690nm) readings for B16 cells exposed to [Nle^4,D-Phe^7]α-MSH. Each point is the mean of 8 wells. Control values are the mean of 16 wells. Standard deviation is shown by error bars.

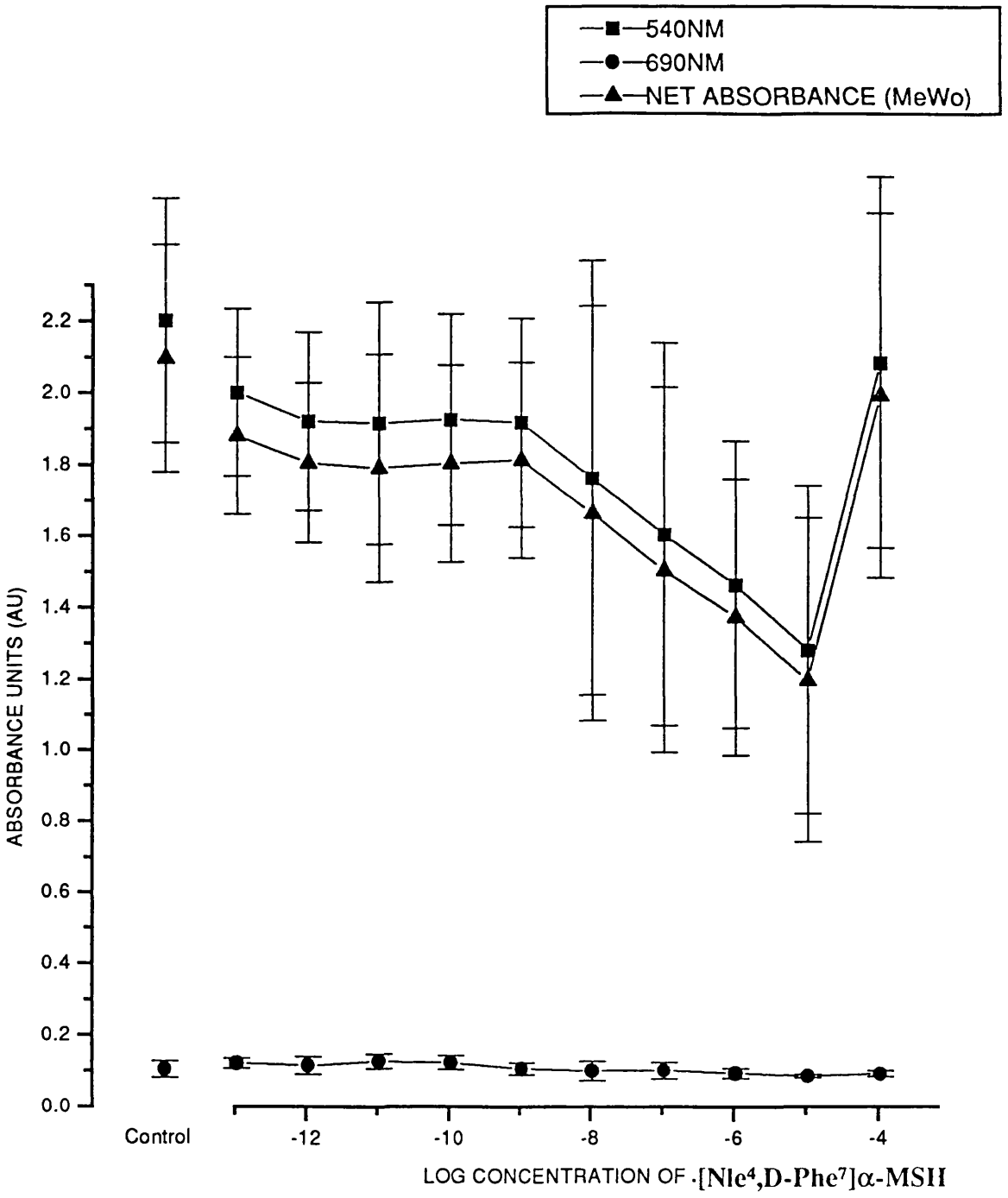

Figure 5.24. Absorbance readings obtained at test (540nm), reference (690nm) and net absorbance (540-690nm) readings for MeWo cells exposed to [Nle^4,D-Phe^7]α-MSH. Each point is the mean of 8 wells. Control values are the mean of 16 wells. Standard deviation is shown by error bars.

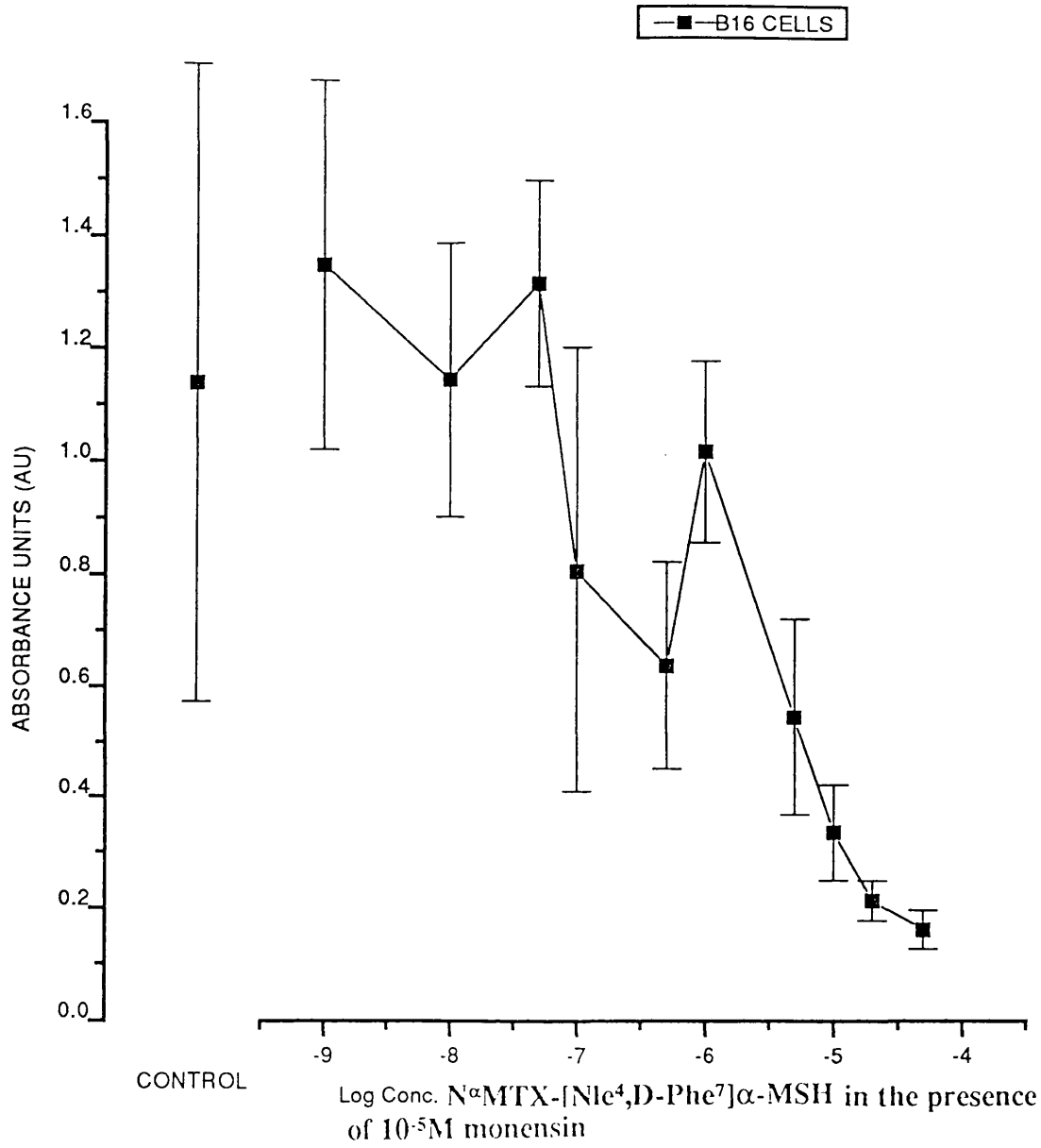

Figure 5.25. Absorbance readings obtained at test (540nm), reference (690nm) and net absorbance (540-690nm) readings for B16 cells exposed to [Nle^4,D-Phe^7]α-MSH in the presence of 10^{-5}M monensin. Each point is the mean of 8 wells. Control values are the mean of 16 wells. Standard deviation is shown by error bars.

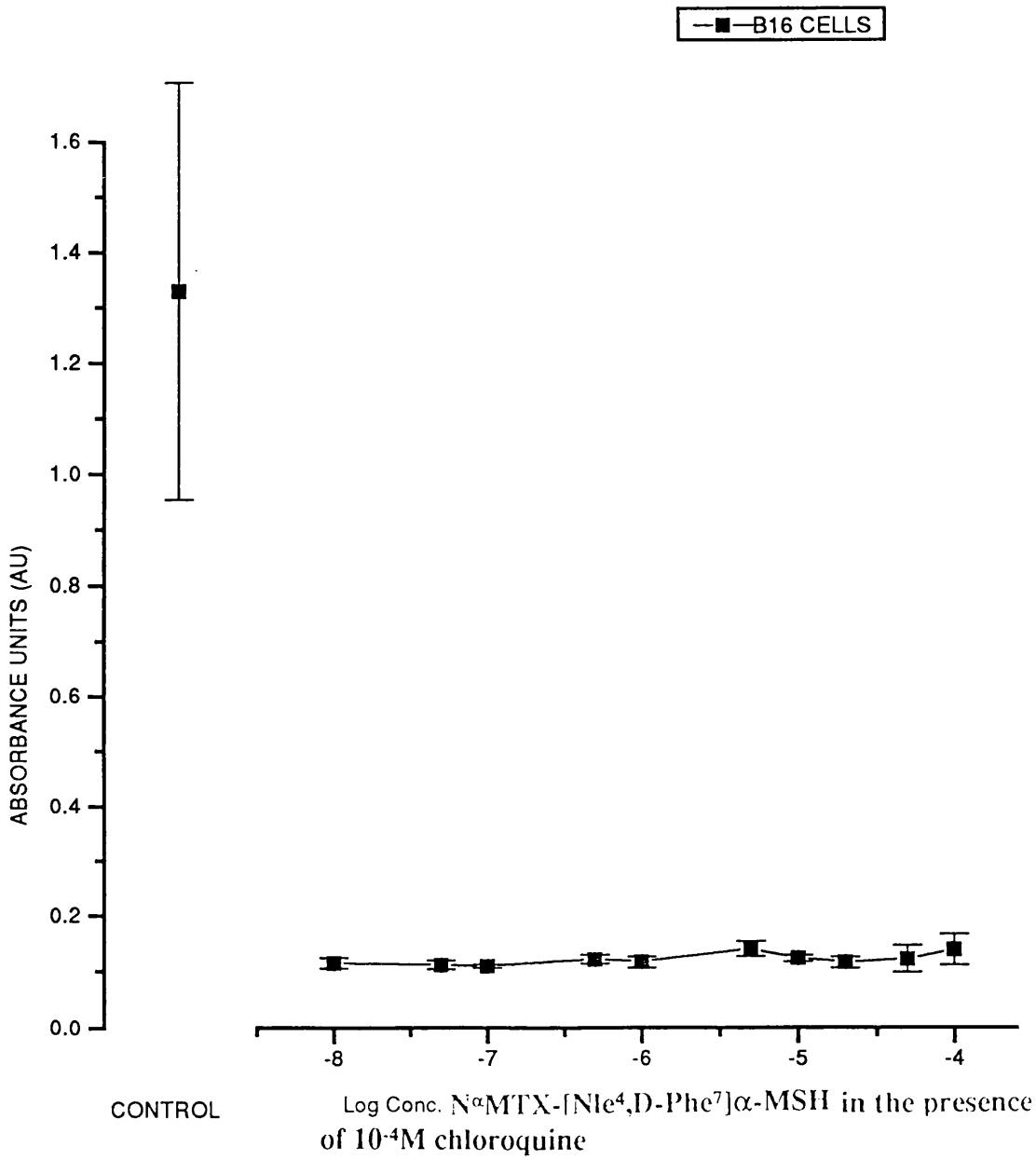

Figure 5.26. Absorbance readings obtained at test (540nm), reference (690nm) and net absorbance (540-690nm) readings for B16 cells exposed to [Nle^4,D-Phe^7]α-MSH in the presence of 10^{-4}M chloroquine. Each point is the mean of 8 wells. Control values are the mean of 16 wells. Standard deviation is shown by error bars.

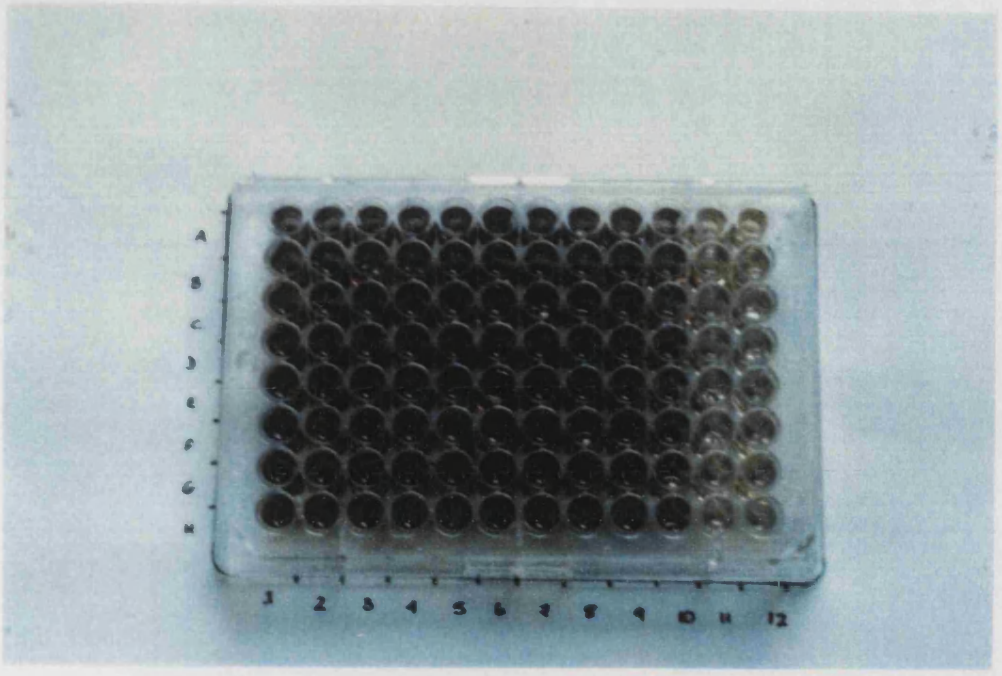

Figure 5.27. This photograph represents the growth inhibitory effects of N^{α}MTX-[Nle^4,D-Phe^7]α-MSH on B16 cells. Columns 1 and 6 represent the control cells while, columns 2-12 have increasing concentrations of the inhibitor from 10^{-13}M to 10^{-4}M. Each concentration has eight replicates labelled A-H.

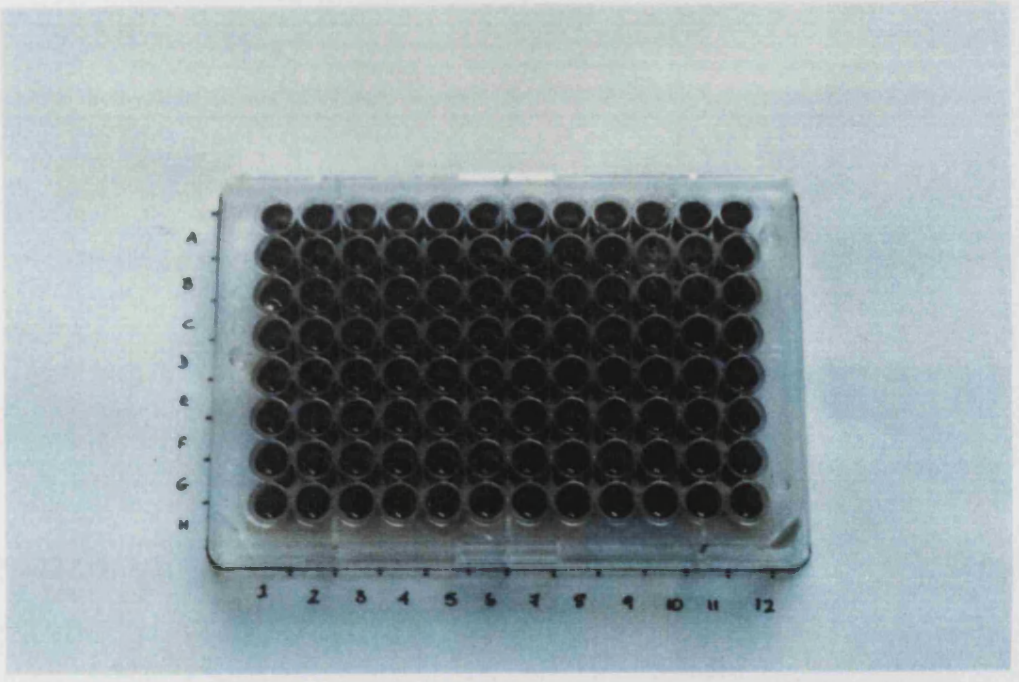

Figure 5.28. This photograph shows the effects of [Nle^4,D-Phe^7]α-MSH on B16 cells. Columns 1 and 6 represent the control cells while, columns 2-12 have increasing concentrations of [Nle^4,D-Phe^7]α-MSH from 10^{-13}M to 10^{-4}M. Each concentration has eight replicates labelled A-H.

CHAPTER 6.

Determination of the intracellular mass of methotrexate required to effect growth inhibition in B16 mouse melanoma.

6.1. INTRODUCTION

Since methotrexate was the model drug used in the investigations of drug targeting to melanoma cells, via the α-MSH receptors, it was logical to determine how much MTX was needed for growth inhibition to predict whether sufficient MTX would be delivered by receptor-mediated endocytosis. The immediate aim of this part of the work was to determine the number of molecules of methotrexate (MTX) required, intracellularly, to effect antimetabolic activity (i.e. growth inhibition). By determining the number of moles of MTX taken up by the cells in each well, and the number of viable cells present, it was then possible to estimate the corresponding number of MTX molecules taken up per cell as a function of MTX concentration.

The effect of varying concentrations of methotrexate on B16 murine melanoma cells was assessed by three methods in parallel; (i) viable cell counting using the Trypan Blue dye exclusion assay, (ii) cytostasis assay using the MTT (3-[4,5-Dimethylthiazol-2-yl]-2,5-diphenyltetrazolium bromide; Thiazoyl blue) metabolic assay (Mosmann, 1983) and finally (iii) determination of the cellular uptake of ^{3}H-MTX by scintillation counting. Methods are described in more detail in chapter 2.

6.2. RESULTS AND DISCUSSION:

TABLE 6.1: The table below shows the results of 3 sets of replicate experiments (135,136,137). The $E.C._{50}$ value was estimated in two ways; from the results of the MTT assay and also from the Trypan blue assay. When the $E.C._{50}$ value was estimated with the MTT assay it was evaluated as the concentration of MTX required to reduce the absorbance to half that of the control cells. The no. of cells per well refers to the Trypan blue assay and the no. of moles per cell refers to the ^{3}H-MTX uptake assay at the respective $E.C._{50}$ value. When the $E.C._{50}$ value is estimated from the Trypan blue viable count, it refers to the concentration of MTX necessary to reduce the number of cells per well to half that of the control cells. The no.of moles per cell refers to the ^{3}H-MTX uptake assay at the respective $E.C._{50}$ value. Each value is the mean of 8 replicate wells.

Experiment LJW135	MTT Assay		Trypan blue Assay
	Mean	St. Dev.	Mean
$E.C._{50}$ (M)	1.66×10^{-8}	+/- 4.80×10^{-9}	1.08×10^{-8}
moles per well	8.94×10^{-14}		5.23×10^{-14}
cells per well	4.54×10^{4}		6.15×10^{4}
moles per cell	1.97×10^{-18}		8.50×10^{-19}
molecules per cell	1.18×10^{6}		5.10×10^{5}
Experiment LJW136	MTT Assay		Trypan blue Assay
	Mean	St. Dev.	Mean
$E.C._{50}$ (M)	6.96×10^{-9}	+/- 7.81×10^{-9}	5.41×10^{-10}
moles per well	3.79×10^{-14}		3.03×10^{-15}
cells per well	4.56×10^{4}		7.1×10^{4}
moles per cell	8.31×10^{-19}		4.27×10^{-20}
molecules per cell	4.99×10^{5}		2.56×10^{4}
Experiment LJW137	MTT Assay		Trypan blue Assay
	Mean	St. Dev.	Mean
$E.C._{50}$ (M)	4.20×10^{-8}	+/- 1.83×10^{-8}	5×10^{-8}
moles per well	7.34×10^{-14}		8.84×10^{-14}
cells per well	2.29×10^{4}		2.17×10^{4}
moles per cell	3.21×10^{-18}		4.07×10^{-18}
molecules per cell	1.92×10^{6}		2.44×10^{6}

The $E.C._{50}$ value was defined as the concentration of methotrexate required in order to reduce the viability of the cells to half the viability relative to control cells. This was determined using the MTT assay and the Trypan blue assay. In each experiment there were two columns of control cells (equivalent to 16 replicates). These were at columns 1 and 6 of the microwell plate so as to compensate for any inconsistencies which may have arisen purely due to the cells positioning on the plate (i.e. edge effects). Figures 6.1. and 6.2. show the results of experiments LJW135,136 and 137.

Experiment LJW135 had control absorbance values in the region of 1.5 AU and this gradually decreased with increasing concentration of MTX until approximately 1 $x10^{-8}$M. Above this concentration there was a dramatic change in absorbance between 2 x 10^{-8}M and 5 x 10^{-8}M MTX. Using the MINSQ non-linear least square regression program (weighting = 2) estimate of the $E.C._{50}$ value was 1.66 x 10^{-8} M MTX. When the $E.C._{50}$ value was calculated using the number of viable cells, the result obtained was 1.08 x 10^{-8}M. Therefore in this experiment little disparity existed between both estimates, however because the number of moles and cells per well varied (depending upon the mode of calculation) the overall number of molecules per cell that was estimated varied between 1.18 x 10^6 (MTT) and 5.10 x 10^5 (Trypan blue).

The protocol observed in LJW135 was unchanged for the following two experiments. In LJW136, the untreated cells reached higher absorbance values (2.0-2.5) and these values were at the edge of the linear portion of the MTT formazan absorption spectrum (see Figure 3.1. and 3.2.). However as the concentration of MTX increased from 1 x 10^{-10}M to 1 x 10^{-9}M MTX, there was a dramatic change in the viability of the cells. The $E.C._{50}$ value calculated on the basis of absorbance gave 6.96 x 10^{-9}M and when the Trypan blue assay was used; 5.41 x 10^{-10}M. These results indicated that the B16 cells were more susceptible to the inhibitory effects of MTX because lower concentrations of

MTX were needed to effect cell kill. In this experiment it was necessary to have an average of 2.62 x 10^5 molecules of MTX internalised per cell as opposed to the 8.45 x 10^5 molecules per cell for LJW135.

LJW137 control absorbance values were within the linear range and the $E.C._{50}$ value calculated was 4.20 x 10^{-8}M. The interexperimental differences which arose between LJW135 and 137 were much smaller than the differences between either of these experiments versus LJW136 which would seem to imply that the former results were a more reasonable estimate of the cell reaction to MTX under identical conditions.

The direct relationship between the concentration of ^{3}H-MTX present within each well and the number of moles of ^{3}H-MTX taken up by the cells in each well is demonstrated by Figure 6.3. This level is initially very low but gradually a greater number of moles accumulated until a plateau was reached at approximately 1 x 10^{-7}M. At this point there was a level of between 3.03 x 10^{-15} and 8.94 x 10^{-14} moles in each well (depending on the experiment). This in itself does not allow estimation of cellular uptake until taken in conjuction with the results of the Trypan blue assays, which gives the number of viable cells at a given concentration of MTX, see Figure 6.4.

Table 6.2. This shows the result of another determination of the intracellular mass of MTX needed to inhibit the growth of B16 cells. The $E.C._{50}$ value is estimated in two ways; from the results of the MTT assay and the Trypan blue assay. When the $E.C._{50}$ value is estimated with the MTT assay it is given in terms of the concentration of MTX required to reduce the absorbance to half that of the control cells. The no. of cells per well refers to the Trypan blue assay and the no.of moles per cell refers to the ^{3}H-MTX uptake assay at the respective $E.C._{50}$ value. When the $E.C._{50}$ value is estimated from the Trypan blue viable count, it refers to the concentration of MTX necessary to reduce the number of cells per well to half that of the control cells.The no.of moles per cell refers to the ^{3}H-MTX uptake assay at the respective $E.C._{50}$ value. Each value is the mean of 8 replicate wells.

Experiment LJW138	MTT Assay		Trypan blue Assay
	Mean	St. Dev.	Mean
$E.C._{50}$ (M)	2.42×10^{-8}	+/- 9.47×10^{-9}	1×10^{-8}
moles per well	1.64×10^{-14}		9.19×10^{-15}
cells per well	3.78×10^{4}		7.40×10^{4}
moles per cell	4.34×10^{-19}		1.24×10^{-19}
molecules per cell	2.60×10^{5}		7.45×10^{4}

In experiment LJW138, the protocol was changed: Four separate rinsings with 200µl SFM were used instead of two as in the previous three experiments. This extra washing was done to reduce the non-specific binding of ^{3}H-MTX to the plates. Inevitably it also caused increased cell stress with subsequent detachment of some cells. These cell effects were most noticeable in the disparity of results yielded. The $E.C._{50}$ estimated from MTT assay results gave a value of 2.42×10^{-8}M MTX and the number of cells that were consequently viable at this concentration was given as 3.78×10^4 per well. Based on the initial number of cells present in the control well of 1.48×10^5, the $E.C._{50}$ occurred at a concentration of MTX which corresponded to 7.4×10^4 cells per well. Although the wells all received the same number of washings and hence one well cannot have been subjected to more stress than another, the following was worth consideration; according to the results of the MTT assay, the number of cells

per well present at a concentration of 2.42 x 10^{-8}M MTX was 3.78 x 10^4 cells per well and since the scale of viability and absorbance was a linear one then this implied that at a level of 7.4 x 10^4 cells per well the concentration of MTX present should have been in the region of 4.74 x 10^{-8}M.

The results of the Trypan blue assay have shown this level of cells corresponded to a value of 1 x 10^{-8}M MTX. The difference between the two could be explained by the method of estimation of the values which were taken directly off the graphs (and hence subject to error) but some of the disparity must be due to the increased number of washing steps which placed more stress an B16 cells already compromised by the presence of MTX. The subsequent effects on a molecular level were quite obvious as the values for the intracellular mass of MTX necessary to inhibit cell growth may have been underestimated.

There were many problems to overcome with regard to the maintenance of reproducibility of protocol in these experiments. The Trypan blue dye exclusion assay was not without complications. The main source of error associated with this method was the need to economise on time so that only a sample of cells were counted at any one time. One could only assume that this sample was representative of the whole population and also that enough samples were taken. The cells from four wells were pooled which gave two replicates per concentration gradient and four replicates for the control cells.

The principal difficulty associated with the tritiated MTX assay was the non-specific ^{3}H-MTX which was attached to the plastic wells. Table 6.3. shows the results a control experiment performed in order to determine how many washes, with SFM, were necessary to reduce the residual radioactivity, i.e. the non-specifically bound ^{3}H-MTX, to an acceptable level.

Table 6.3. This shows the "dpm" values obtained by incubating 1 x 10^{-6}M ^{3}H-MTX over 72 hours on a microwell plate versus the number of washing steps with 200µl SFM.

No. of washing steps with SFM	"dpm" values obtained
1	161135.7
2	36298.0
3	7127.7
4	2954.5
5	1032.0
6	366.1
7	381.0
8	256.1

As can be seen from the table, the washing regimen adopted which included five separate rinsings with SFM removed the majority of radioactivity that was non cell bound. Eight washing steps would have removed ten times more non-specific radioactivity and hence would have been preferable. However, each additional washing step caused cell stress which was manifested as cell detachment, therefore five washings steps was judged to be a sufficient number. Figure 6.5. demonstrates another experiment in which the microwell plate was treated with exactly the same concentrations of tritiated MTX in the absence of any B16 cells. It is clear from the graph that there was a quite a distinct difference in non-specific activity between the plates which were washed twice as opposed to five times and this was largely independent of the initial concentration, with the exception of 1 x 10^{-6}M, but this concentration was higher than the concentrations used in uptake experiments.

TABLE 6.4. The table below shows the results of 3 later experiments (151,152,154). The $E.C._{50}$ value is estimated in two ways; from the results of the MTT assay and the Trypan blue assay. When the $E.C._{50}$ value is estimated with the MTT assay it is given in terms of the concentration of MTX required to reduce the absorbance to half that of the control cells. The no. of cells per well refers to the Trypan blue assay and the no. of moles per cell refers to the ^{3}H-MTX uptake assay at the respective $E.C._{50}$ value. When the $E.C._{50}$ value is estimated from the Trypan blue viable count, it refers to the concentration of MTX necessary to reduce the number of cells per well to half that of the control cells. The no.of moles per cell refers to the ^{3}H-MTX uptake assay at the respective $E.C._{50}$ value. Each value is the mean of 8 replicates.

Experiment LJW151	MTT Assay		Trypan blue Assay
	Mean	St. Dev.	Mean
$E.C._{50}$ (M)	2.86×10^{-10}	$+/-9.66 \times 10^{-11}$	2.30×10^{-9}
moles per well	9.50×10^{-15}		2.14×10^{-14}
cells per well	3.14×10^{4}		6.75×10^{4}
moles per cell	3.03×10^{-19}		3.17×10^{-19}
molecules per cell	1.82×10^{5}		1.90×10^{5}
Experiment LJW152	MTT Assay		Trypan blue Assay
	Mean	St. Dev.	Mean
$E.C._{50}$ (M)	1.13×10^{-9}	$+/-5.36 \times 10^{-10}$	3.26×10^{-9}
moles per well	1.12×10^{-14}		5.51×10^{-15}
cells per well	6.06×10^{4}		6.25×10^{4}
moles per cell	1.85×10^{-19}		1.76×10^{-19}
molecules per cell	1.11×10^{5}		1.06×10^{5}
Experiment LJW154	MTT Assay		Trypan blue Assay
	Mean	St. Dev.	Mean
$E.C._{50}$ (M)	2.79×10^{-9}	$+/-8.61 \times 10^{-10}$	7.14×10^{-9}
moles per well	4.5×10^{-15}		6.25×10^{-15}
cells per well	7.63×10^{4}		5.09×10^{4}
moles per cell	5.90×10^{-20}		1.23×10^{-19}
molecules per cell	3.54×10^{4}		7.37×10^{4}

Having established the optimum number of washing steps to use, the protocol was altered. In experiments LJW151 and 152 all of the plates were rinsed five times with SFM. The $E.C._{50}$ values obtained in LJW151 varied between 2.86 x 10^{-10}M (MTT assay) and 2.3 x10^{-9}M (Trypan blue). The intraexperimental differences cannot be fully explained in terms of the increased rinsings because the MTT assay suggested that the cells became more sensitive to MTX. This was also the result of LJW152 where the $E.C._{50}$ values were lower and in the 10^{-9}M range. This had consequential effects on the number of moles per cell and also cells per well which gave the overall estimate as 10^5 molecules (approx.) which were needed intracellularly to inhibit the growth of B16 cells.

In LJW154 a modification of the method to assess the mass of ^{3}H-MTX taken up intracellularly was investigated making use of the "Millipore" multiscreen filtration plate. The contents of the wells containing the tritiated MTX and the cells were transferred to the filtration plate. With this technique the need to remove the cells from the well was obviated because after washing steps have been undertaken the wells themselves (made of "Durapore") were punched directly into the scintillation vials and the filter was then solubilised by use of 1M HCl and 1M NaOH in equal portions (100µl). Finally 2ml of "Optiphase" scintillation fluid was added to each scintillation vial. This method would have been preferred since no loss of cells occurred during washing. The MTT and the Trypan blue plates were rinsed twice with SFM as there was no need to ensure non-specific binding was minimised. The results (shown in table 6.4) indicated that despite the fact the rinsing steps were quite different depending on the aspect of the assay, the $E.C._{50}$ values were quite close. There was a decrease in the number of moles per well estimated and this lead to a calculation of molecules per cell in the 10^4 region. These were the lowest values obtained however this does not mean that it was an underestimation of the intracellular mass necessary to inhibit the cells but rather that due to the difference in protocol, a difference in the estimated value was to be expected.

One of the problems with this method was that in order to compare the three parallel experiments, it would have been necessary to use the filtration plates for the MTT assay and this was attempted in LJW155. It proved to be impossible due to the problems encountered at the plate reading stage where the multiscreen filtration plate did not yield results that were comparable to other MTT assays. The manufacturers recommendations suggested that MTT assays should be possible, but this was not supported by the present study.

6.3. Summary.

As previously shown in Figures 6.3. and 6.4. the number of moles of ^{3}H-MTX per well and the number of viable cells present at this concentration respectively can be estimated. It was then possible to work out the number of moles of MTX associated with each cell, an example of which is given in Figure 6.6. By multiplying the number of moles per cell by Avogadros number (6×10^{23}), the number of molecules of MTX per cell was calculated. Given the problems associated with the assay procedures, a mean value for the $E.C._{50}$ was used based on the results of the MTT and Trypan blue assays. Therefore a conclusion can be drawn that by employing an extracellular concentration of MTX in the region of 1.34×10^{-8}M and 1.2×10^{-8}M MTX an average of 5.98×10^{5} (+/- 6.99×10^{5}) and 4.89×10^{5} (+/- 8.76×10^{5}) molecules of MTX were taken up by each cell for the MTT and the Trypan blue estimation methods respectively i.e. each cell needs, in the region of, half a million molecules of MTX in order to be effectively inhibited. A detailed discussion on the plausibility of achieving this level has been presented in Chapter 7.

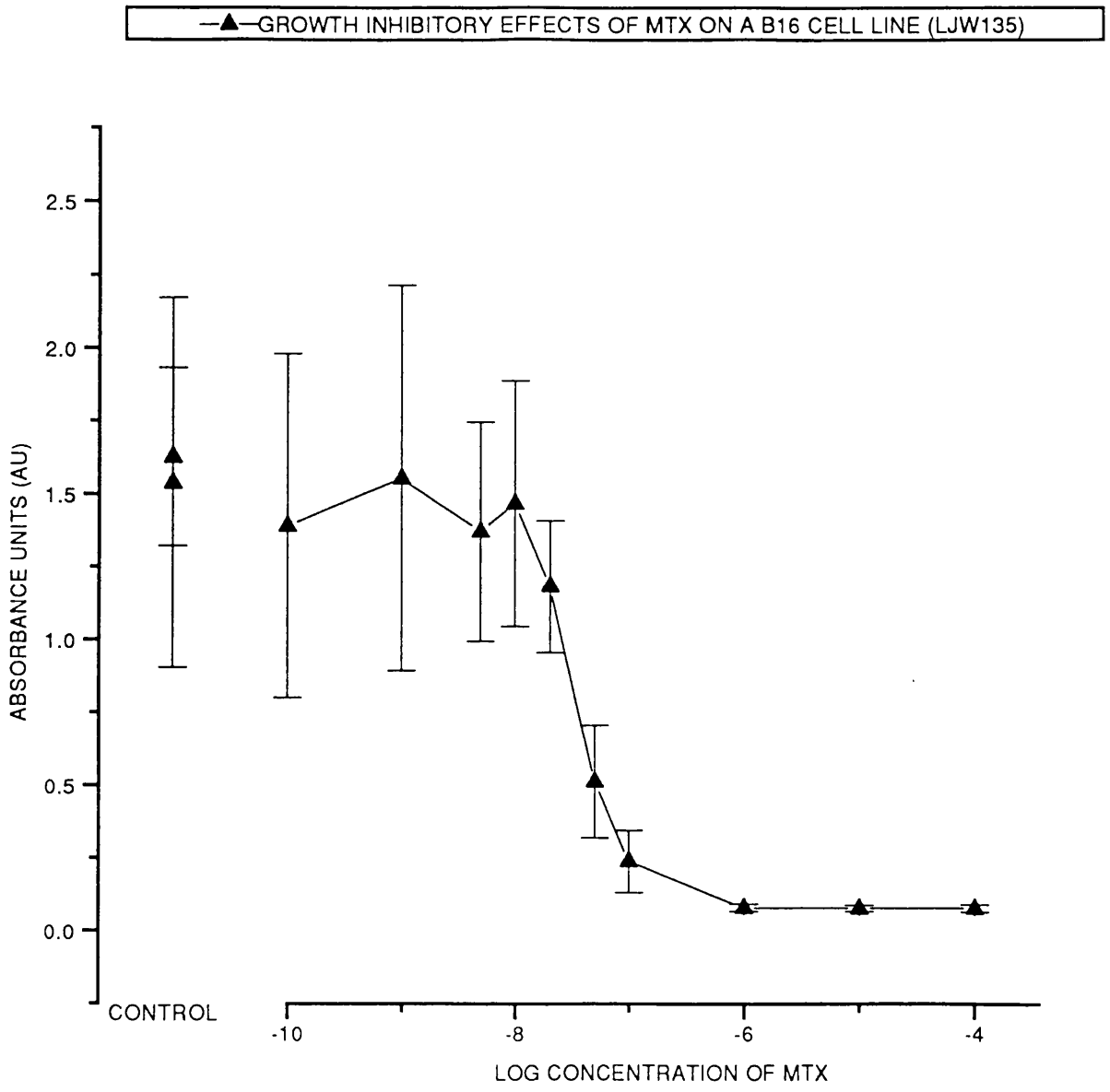

Figure 6.1: Net absorbance (540-690nm) of MTT formazan produced by B16 cells after treatment with varying concentrations of MTX over 72 hour period. Each point is the mean of 8 wells. Standard deviation is shown by error bars. Figure 6.2. shows the relative toxicities with three replicate experiments.

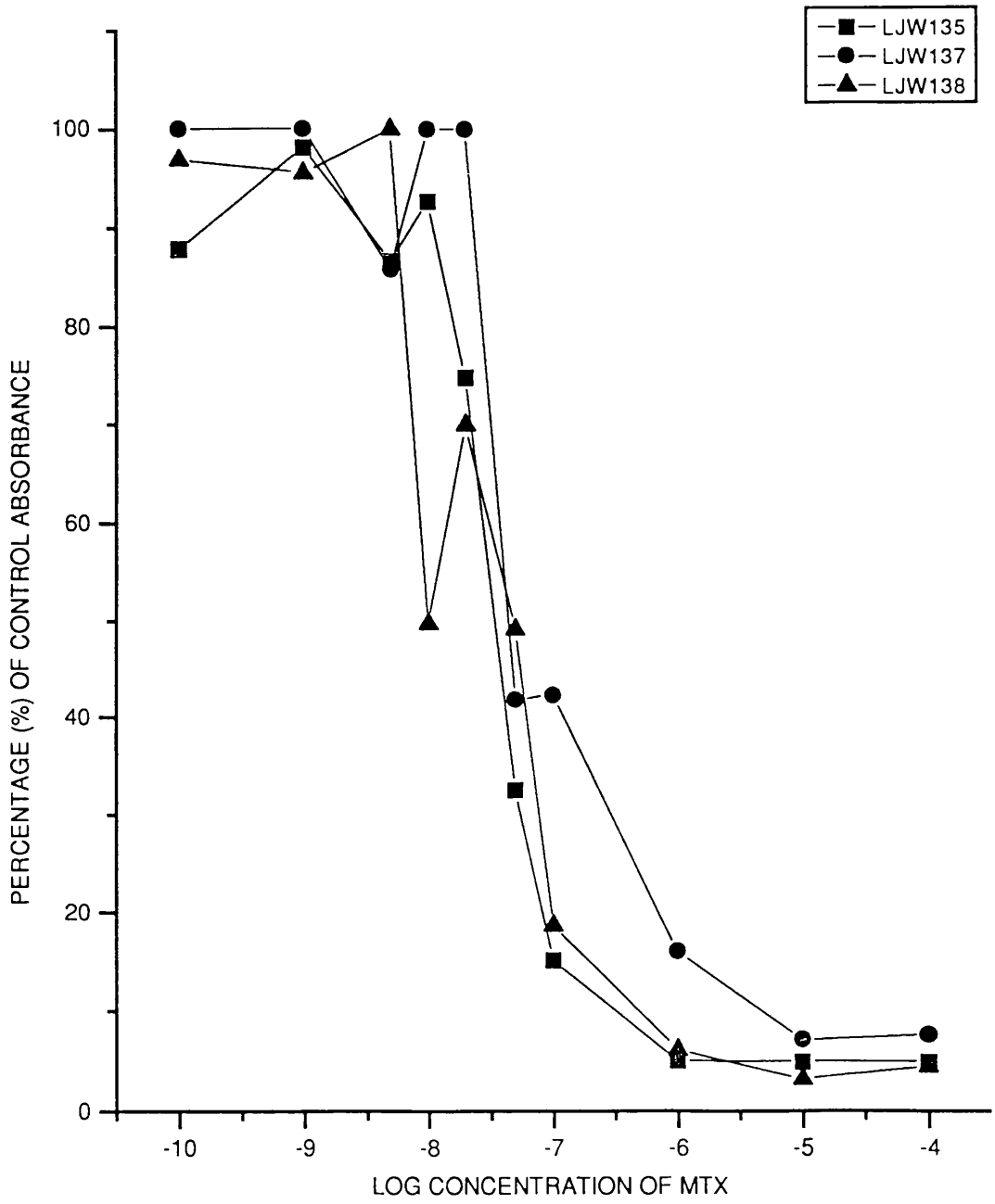

Figure 6.2: Percentage of control (i.e. maximum) absorbance (540-690nm) of MTT formazan produced by B16 cells in three replicate experiments after treatment with MTX. Each point is the mean of 8 wells. Error bars have been omitted for clarity.

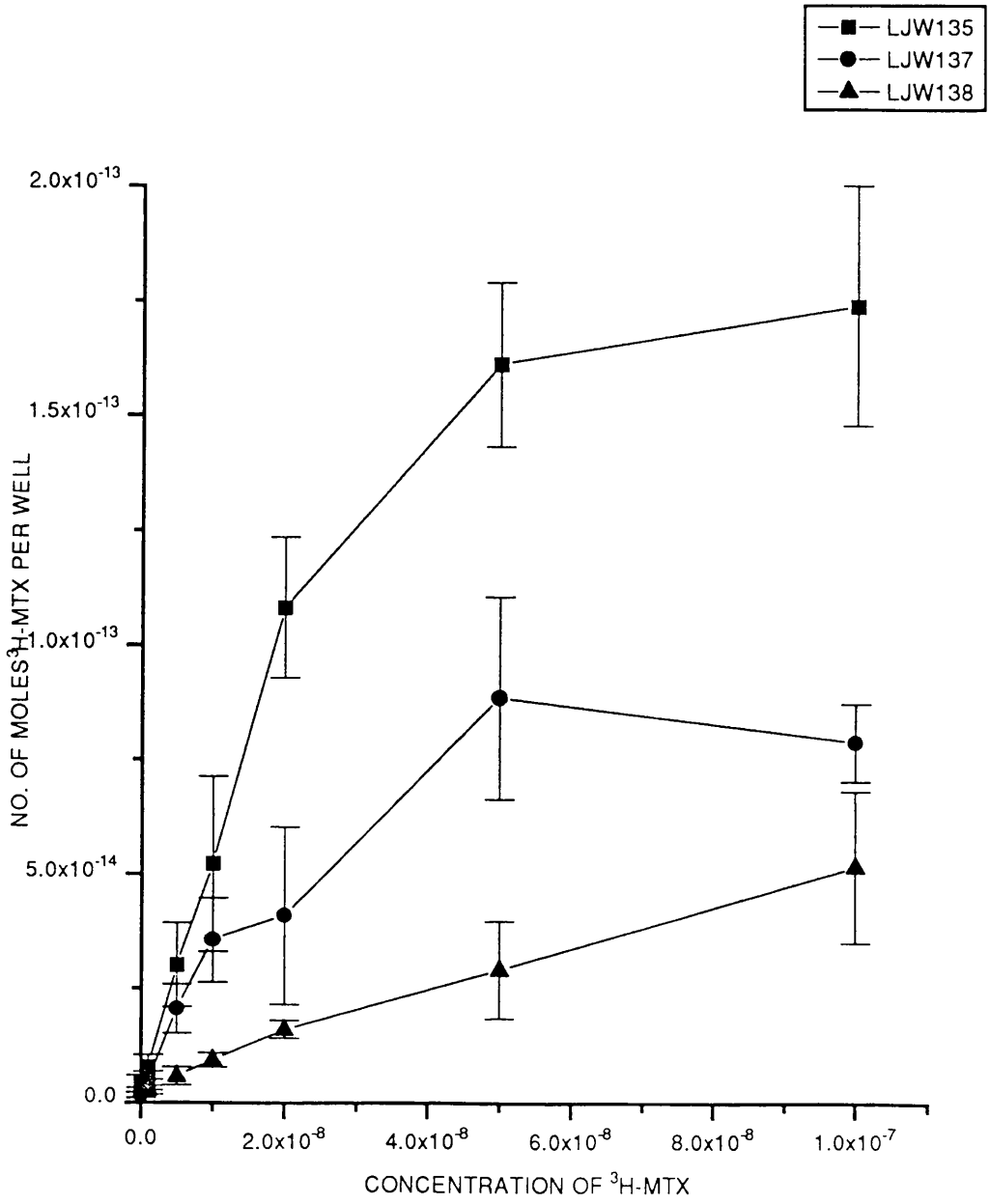

Figure 6.3: Number of moles of ^{3}H MTX remaining per well after 72 hours and washing steps have been completed versus the initial molar concentration of ^{3}H-MTX in the well. The results are for 3 replicate experiments. Each point is the mean of 8 wells.

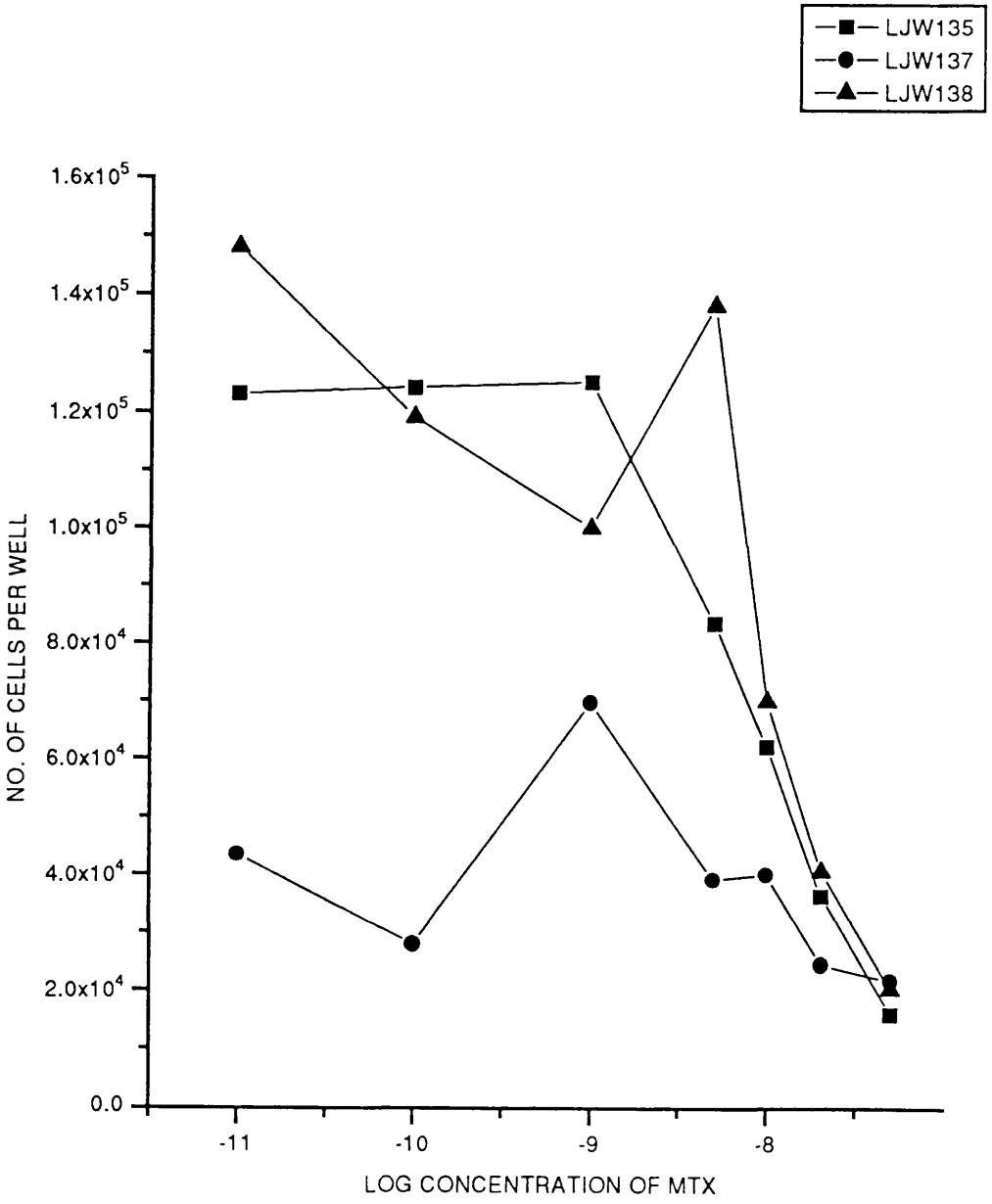

Figure 6.4: Relationship between the number of cells per microwell as assessed by the Trypan blue assay versus the concentration of MTX per well for 3 replicate experiments. Each point is the mean of 8 wells.

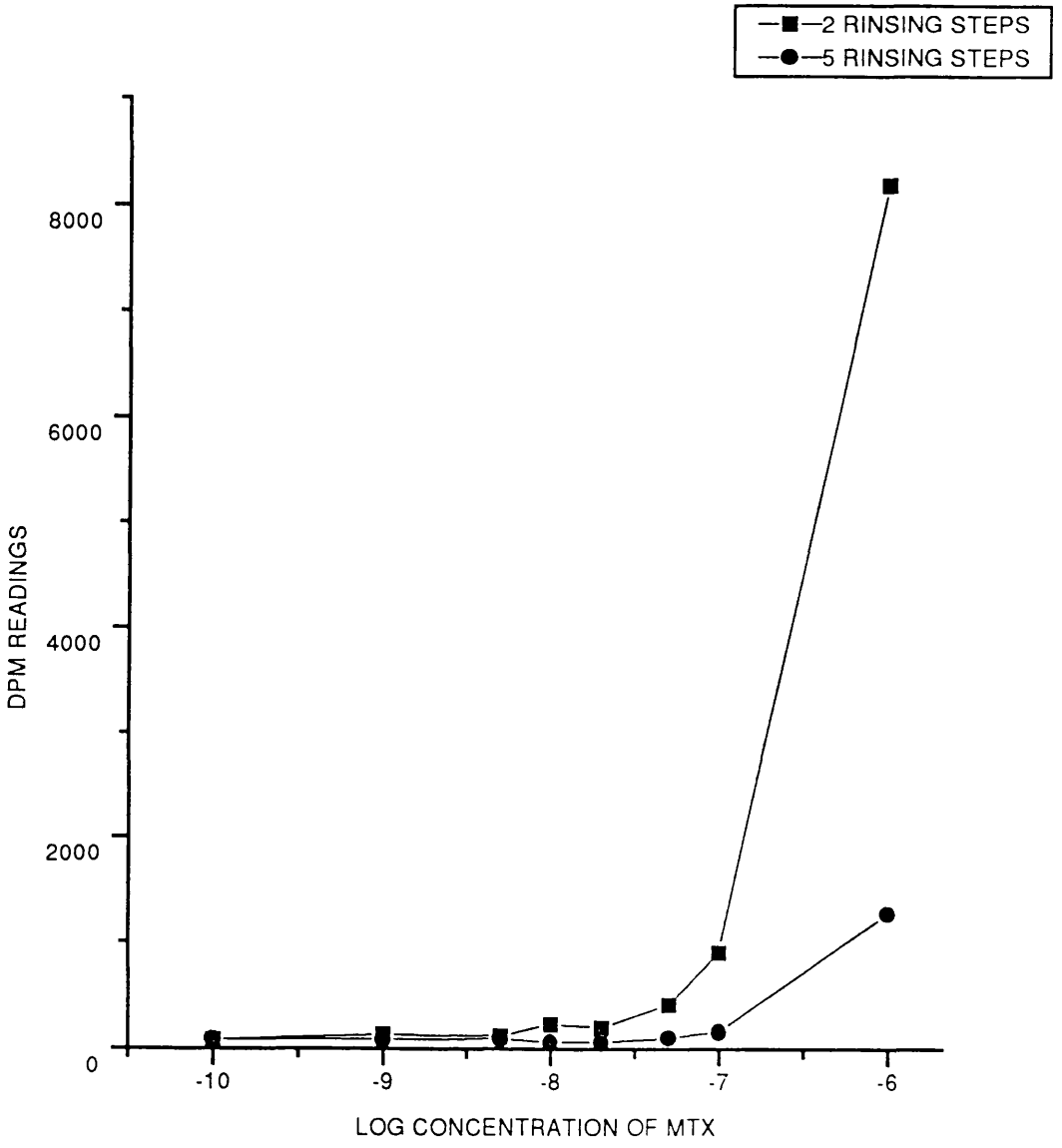

Figure 6.5: Control experiment showing the "dpm" values obtained for 1 x 10^{-6}M ^{3}H-MTX on microwell plate versus number of washings steps with 200µl SFM.

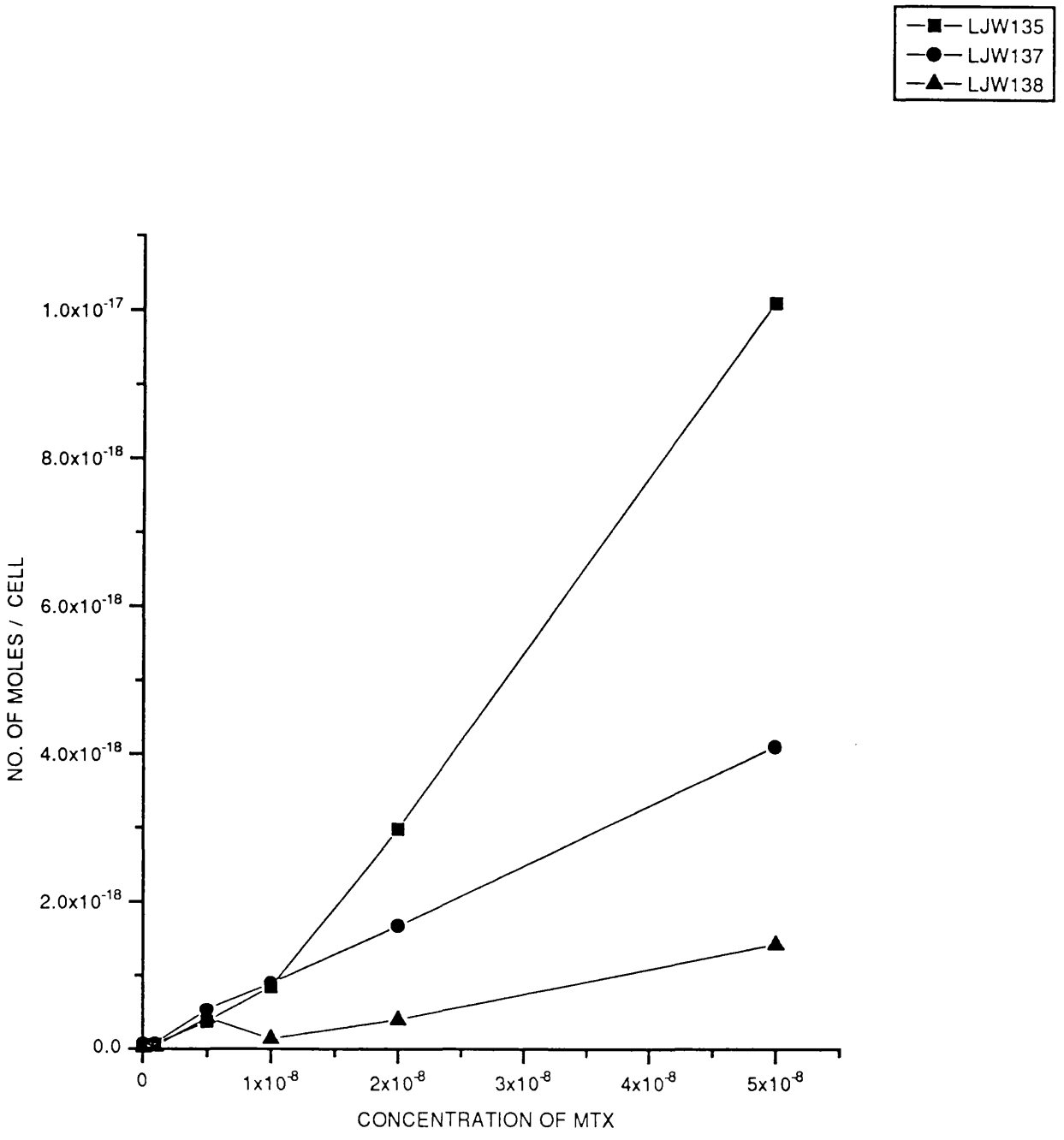

Figure 6.6: This illustrates the number of moles of methotrexate taken up per cell as a function of extracellular MTX (M) per well for 3 replicate experiments.

Chapter 7.

Discussion.

The aim of this study was to verify whether the hormone-drug conjugate, N$^{\alpha}$MTX-[Nle^{4},D-Phe^{7}]α-MSH, would successfully achieve site specific toxicity against melanoma cells in culture. The experiments described in Chapters 3, 4, 5, and 6 were undertaken in order to gain a greater insight in to the various aspects of the study including: the growth inhibition assay procedure used (Chapter 3), the growth inhibitory effects of the free drug, MTX, (Chapter 4), the uptake, internalisation and growth inhibitory effects of N$^{\alpha}$MTX-[Nle^{4},D-Phe^{7}]α-MSH (Chapter 5), and the intracellular mass of MTX necessary to cause growth inhibition (Chapter 6). All of the results obtained in this work were then compared with related results obtained previously by others, Adams, (1993), Erskine-Grout, (1993) and Sahm, (1994). The cumulative results could then be assessed in their correct context and sensible conclusions could be drawn in the light of all the findings, as to the feasibility of using N$^{\alpha}$MTX-[Nle^{4},D-Phe^{7}]α-MSH in site specific drug delivery.

The MTT assay provided a low cost, rapid and accurate method (Mosmann, 1983) by which the growth inhibitory characteristics of MTX and N$^{\alpha}$MTX-[Nle^{4},D-Phe^{7}]α-MSH could be examined. The conditions of the assay were optimised for each cell line used e.g. B16 murine melanoma, MeWo human melanoma, SVK14 keratinocytes and the transformed 293 cells. Individual aspects of the protocol were examined e.g. the limits of linearity, seeding density, optimal incubation time and solvents. Using the Beer-Lambert laws, the limits of linearity of the assay were determined. Absorbance readings up to

1.0 AU were in accordance with the laws whilst readings between 1.0-2.0 AU were still close to linear.

The seeding density was optimised at a level of 4 x 10^3 cells per microwell. This allowed for sufficient growth and ensured that throughout the experiment the cells could proliferate with adequate space and nutrients. In addition, the seeding density was low enough to preclude the refeeding of cells during the experiment, as this would have increased the potential for contamination.

A three hour incubation time was judged sufficient to allow conversion of the MTT to MTT formazan. DMSO was used as the solvent of choice because despite the deleterious effects on laboratory equipment and the possible risks to the operator, it was very efficient at rapid and complete solubilisation of the formazan crystals.

The majority of work carried out in this study has been performed on the B16 murine melanoma cell line. In the MTT assessment of the growth inhibitory effects of MTX on B16 cells, a range of concentrations from 10^{-2} down to 10^{-11}M MTX were employed. The results of five separate experiments were analysed by the MINSQ non-linear regression programme producing a mean $E.C._{50}$ value of 1.67 x 10^{-8}M MTX. This implied that an extracellular concentration of 1.67 x 10^{-8}M or greater must be achieved in order to reduce the viability of the cells to 50% relative to the control cells. The result was in close agreement with similar experiments described in Chapter 6, in which it was estimated that between 1.34 x 10^{-8}M and 1.2 x 10^{-8}M MTX were needed for a similar reduction in viability of B16 cells using the MTT and Trypan blue methods of assessment, respectively.

It is also shown in Chapter 6 that it is necessary to have an intracellular mass of 5.44 x 10^5 molecules of MTX in order to achieve growth inhibition of half the cells present. It is quite possible to achieve this level of intracellular MTX

due to the folic acid transport pathway by which MTX is taken up intracellularly. However, the drawback of this approach lies in the localisation of this folic acid pathway i.e. it is a pathway not confined to specialised cells but rather found in all cells. This has more serious implications when related to an *in vivo* situation whereby the cells of the whole body will be placed under the same threat of the cytotoxic potential of MTX irrespective of whether or not these cells are cancerous. The more rapidly dividing the cell e.g. bone marrow, the more serious the consequences since MTX became lethal if exposed to cells in the S-phase during logarithmic growth. A whole host of side-effects ranging from nausea and vomiting to impaired renal function may then ensue.

The use of the hormone conjugate was postulated in order to reduce these side-effects by localising the actions of MTX to those cells where MSH receptors were present e.g. cells of the melanocyte lineage. It was also necessary to target the MTX to the MC1 receptor specifically as the other four receptors (MC2-MC5) are found in areas other than the melanocytes e.g. brain, placenta, gut. However it is very difficult to achieve this level of specificity especially in light of the likely conformational similarities exhibited by all five of the MSH receptors identified to date, (Mountjoy *et al.*, 1992, Chhajlani and Wikberg, 1992, Gantz *et al.*, 1993a and 1993b, Chhajlani *et al.*, 1993). Thus the next step taken was to assess the binding affinity of N^{α}MTX-[Nle^4,D-Phe^7]α-MSH and N^{α}MTX-[^{125}I-Tyr^2,Nle^4,D-Phe^7]α-MSH in the presence of both MC1 (B16 and MeWo cells) and MC3 (transformed 293 cells) receptors to establish whether or not a greater sensitivity was achieved by N^{α}MTX-[Nle^4,D-Phe^7]α-MSH for the MC1 rather than the MC3.

The labelled conjugate (N^{α}MTX-[^{125}I-Tyr^2,Nle^4,D-Phe^7]α-MSH) resulted in a binding affinity of 7.35nM for the MC1 receptor as opposed to 1.69nM for the

MC3 receptor implying a greater affinity of the N$^{\alpha}$MTX-[^{125}I-Tyr^{2},Nle^{4},D-Phe^{7}]α-MSH for the MC3 receptor. This result suggested that the radiolabelled conjugate does not exhibit selective affinity for the MC1 receptor but in fact binds with stronger affinity to the MC3 receptor. This result was discouraging from a targeting viewpoint as it would have been preferable to have the conjugate exhibiting greater affinity for the MC1 receptors, which are located specifically on melanocytes. MC3 receptors are located in the placenta, gut, but more importantly, from the point of view of side-effects, the brain which could result in toxic CNS effects.

Internalisation data with continual exposure of B16 cells to 0.1nM of N$^{\alpha}$MTX-[^{125}I-Tyr^{2},Nle^{4},D-Phe^{7}]α-MSH in the presence of NH_4Cl suggested that B16 cells were capable, at this extracellular concentration, of internalising 1793 molecules of ^{125}I-N$^{\alpha}$MTX- [Nle^{4},D-Phe^{7}]α-MSH over a 4 hour period. This figure was calculated on the basis of radioactive counts using the data generated over three separate experiments. The variance in the number of molecules internalised ranged from 565 to 3,500 and was probably a reflection of the variable number of receptors expressed on the surface of B16 cells with changing conditions or passage. It is clear that the higher the number of receptors on the cell surface, the greater the number of molecules internalised and with a receptor number oscillating between 5,000-25,000 for B16 cells (Sahm, 1994), this degree of interexperimental disparity is understandable. It follows that if 1793 molecules are internalised over a four hour period that 448 molecules of N$^{\alpha}$MTX-[^{125}I-Tyr^{2},Nle^{4},D-Phe^{7}]α-MSH are taken up per hour by receptor mediated endocytosis.

By using the slopes of the graphs of the specifically bound ligand in these experiments, it was possible to assess the mass of internalised N$^{\alpha}$MTX-[^{125}I-Tyr^{2},Nle^{4},D-Phe^{7}]α-MSH by a second method. An average value of 9.3

molecules per cell per minute were internalised. However, the receptor occupancy at this point must be considered, a value of 1.34% has been estimated based on the affinity of the ligand for the receptor. This would amplify the result from 9.3 molecules per cell per minute at 1.34% receptor occupancy, to 42,000 molecules internalised per cell per hour at maximum receptor occupancy. Obviously although it would be theoretically possible to achieve this, it would require a huge increase in the concentration of extracellular ligand and such a level is neither desired nor realistic for drug targeting studies. The aim is to introduce the minimum efficient level of active substance sufficient to cause growth inhibition of the cancerous cells whilst limiting the harmful effects to healthy cells. In the Pulse-Chase internalisation experiments carried out at 0.1nM, only 20-500 molecules N^{α}MTX-[^{125}I-Tyr^{2},Nle^{4},D-Phe^{7}]α-MSH were taken up specifically as opposed to 500-1000 molecules of ^{125}I- [Nle^{4},D-Phe^{7}]α-MSH (Adams, 1993). However although Pulse-Chase labelling studies were performed at approximately 10% receptor occupancy for ^{125}I- [Nle^{4},D-Phe^{7}]α-MSH, this was substantially reduced to 0.67% for N^{α}MTX-[^{125}I-Tyr^{2},Nle^{4},D-Phe^{7}]α-MSH. This explains the decrease in internalisation of N^{α}MTX-[^{125}I-Tyr^{2},Nle^{4},D-Phe^{7}]α-MSH, relative to ^{125}I-[Nle^{4},D-Phe^{7}]α-MSH. Another possibility for the reduced number of molecules of N^{α}MTX-[^{125}I-Tyr^{2},Nle^{4},D-Phe^{7}]α-MSH internalised may be the conjugation of MTX to [Nle^{4},D-Phe^{7}]α-MSH which resulted in a reduction in the uptake of the latter, which may have been due to the increased size of N^{α}MTX-[Nle^{4},D-Phe^{7}]α-MSH (FW:2040) as opposed to [Nle^{4},D-Phe^{7}]α-MSH (FW:1648) possibly inducing conformational changes and difficulties at the receptor site.

Data obtained from the growth inhibitory effects of N^{α}MTX-[Nle^{4},D-Phe^{7}]α-MSH on the B16 cells suggested that an extracellular concentration of 1.47 x

10^{-5}M was necessary to reduce the viability of the cells to 50% relative to control cells. This is a thousand fold greater concentration than the level required for the MTX alone and implied that instead of the conjugate decreasing the amount of drug needed quite the reverse had occurred. A further implication of this was that the pathway taken by N^{α}MTX-[Nle^4,D-Phe^7]α-MSH was a 1000 fold less effective at delivering MTX to the intracellular compartments and therefore a greater concentration of the conjugate was necessary to achieve the same decrease in cell viability.

Varga *et al.*, (1977) used a melanotropin-daunomycin conjugate to show receptor mediated cytotoxicity in cultured murine melanoma cells. On a molar basis, their conjugate was 3 times more toxic to melanoma cells than free daunomycin. This contrasts dramatically with the results obtained in the growth inhibition assays with N^{α}MTX-[Nle^4,D-Phe^7]α-MSH using cultured murine melanoma cells, where a 10^3 increase in conjugate concentration is required to effect the same level of inhibition as free MTX.

MeWo human melanoma cells were also treated by MTX and N^{α}MTX-[Nle^4,D-Phe^7]α-MSH. The results indicated that an extracellular concentration of 1.31 x 10^{-9}M MTX reduced the viability of the MeWo cells to 50% of the viability of control cells. This concentration was tenfold lower than that necessary to inhibit the B16 cells and implied that MeWo cells were more susceptible to the effects of MTX. It was therefore expected that the conjugate would exhibit a similar profile namely: a tenfold lower concentration necessary to show the same decrease relative to the effects of N^{α}MTX-[Nle^4,D-Phe^7]α-MSH to B16 cells. The results gave an $E.C._{50}$ value of 2.48 x 10^{-6}M, which although lower than the B16 cells required, was still a very high concentration of N^{α}MTX-[Nle^4,D-Phe^7]α-MSH and the difference with respect to free MTX was also a thousand fold.

The results of neither the B16 nor the MeWo cells indicated a greater efficacy of the conjugate over MTX as demonstrated by the results above.

SVK14 keratinocytes were used as a control specifically due to the fact that they possess few, if any, MSH receptors on their surface. Therefore if the effects of the conjugate were mediated exclusively through these receptors it would be logical to assume that a very high level of N^{α}MTX-[Nle^4,D-Phe^7]α-MSH must be present before any effect is seen. This concentration should be in excess of the levels previously required by B16 and MeWo cells or else selectivity for MSH receptors cannot be said to be shown. This was similar to the use of 3T3 fibroblasts by Varga and co-workers (1977) in the testing of selectivity exhibited by their melanotropin-daunomycin conjugate. They found that whereas daunomycin was toxic to the 3T3 cells, the conjugate was not showing the selectivity of this inhibitor for cells which possessed the relevant (MSH) receptor.

The $E.C._{50}$ value achieved for the SVK14 keratinocytes in the presence of MTX could not be accurately estimated by the MINSQ programme. This was because there were only two levels of viability obvious from the results namely the growth levels of the control cells and the lack of growth by all of the treated cells. Therefore in the first experiment (88), all that can be deduced was that a level of MTX equivalent to 10^{-11}M was too high and effectively killed the cells. For the next experiment (94) a level of 10^{-13}M was still too high and exerted lethal effects on all the cells.

Although this did not yield an $E.C._{50}$ value for the MTX with SVK14 cells, it did give an estimate of the sensitivity of these keratinocytes to the antimetabolite. In the presence of N^{α}MTX-[Nle^4,D-Phe^7]α-MSH an $E.C._{50}$ value of 1.68×10^{-6}M (n=2) was found. This contrasted dramatically to the effects of free MTX and showed that these keratinocytes are at least seven

orders of magnitude more susceptible to MTX than to N^{α}MTX-[Nle^4,D-Phe^7]α -MSH. This result was what would be expected because in the exposure of SVK14 cells to MTX, the MTX would be taken up via the folic acid pathway which is present in SVK14 cells. However, because of the lack of MSH receptor sites on the surface of the keratinocytes, the N^{α}MTX-[Nle^4,D-Phe^7]α-MSH does not have a proper pathway of entry and hence would not be taken up into the cell actively but rather any uptake process would be both passive and non-specific e.g. pinocytosis. This would require a high extracellular concentration of N^{α}MTX-[Nle^4,D-Phe^7]α-MSH so that sufficient N^{α}MTX-[Nle^4,D-Phe^7]α-MSH is taken into the cell and subsequently degraded allowing the release of MTX which is then free to exert its effects. The other means by which the conjugate may have exerted its toxic effects include degradation of the hormone-drug conjugate extracellularly and subsequent internalisation of the MTX molecules. It is clear that these modes of entry of MTX would seem to exist only in the presence of very high concentrations of N^{α}MTX-[Nle^4,D-Phe^7]α-MSH ($>10^{-6}$M). However, it has been shown that B16 and MeWo cells need an equal if not greater level of N^{α}MTX-[Nle^4,D-Phe^7]α-MSH before the latter exerts any significant growth inhibitory effects. Hence although internalisation data would seem to suggest that ^{125}I-N^{α}MTX-[Nle^4,D-Phe^7]α-MSH was specifically taken up into melanoma cells, this may not be true. This finding was based on the assumption that the radioactivity associated intracellularly was ^{125}I-N^{α}MTX- [Nle^4,D-Phe^7]α-MSH whereas it may be that the MTX was cleaved so that only ^{125}I- [Nle^4,D-Phe^7]α-MSH was internalised with the MTX portion dissociated. An attempt to rule out this possibility was carried out by demonstrating, using HPLC, that over the period of culture the MTX configuration was stable. A further argument in favour of selective uptake by melanoma cells can be made: If the toxicity was due to free

MTX released into the medium and then taken up by the active transport system one would have expected that the conjugate would have been more toxic to SVK14 cells which were very highly sensitive to free MTX. In fact with SVK14 cells there was at least a 10^7 fold difference in the toxicity of free MTX and conjugate, whereas the comparative figure for melanomas was 10^3.

The growth inhibitory capacity of the N$^{\alpha}$MTX-[Nle^4,D-Phe^7]α-MSH on the 293 (transformed) cell lines was also examined. The 293 cells containing the MC3 receptors yielded and $E.C._{50}$ value of 3.03×10^{-11}M for MTX. This showed that these 293 cells were more sensitive to the effects of MTX than the B16 or MeWo cells. It would be expected that since these cells possess such large numbers of MC3 melanocortin receptors on their surfaces that their ability to internalise the N$^{\alpha}$MTX-[Nle^4,D-Phe^7]α-MSH would be greater than for example: SVK14 cells which do not possess any of the MSH receptors. However this assumes that the major route of internalisation of N$^{\alpha}$MTX-[Nle^4,D-Phe^7]α-MSH is via receptor mediated endocytosis, something which is not supported by recent experiments. The $E.C._{50}$ value for the 293 cells with MC3 receptors treated with N$^{\alpha}$MTX-[Nle^4,D-Phe^7]α-MSH was 1.07×10^{-5}M which was higher than the $E.C._{50}$ obtained with SVK14 cells.

293 cells which possess the vector alone in the absence of any receptors were even more sensitive to MTX treatment ($E.C._{50}= 2.84 \times 10^{-13}$M) and yet they required an order of magnitude less of the N$^{\alpha}$MTX-[Nle^4,D-Phe^7]α-MSH to achieve the same degree of inhibition as the 293 cells with MC3 receptors ($E.C._{50}= 1.66 \times 10^{-6}$M). This may imply that the process of transfection of the vector alone had heightened the sensitivity of the 293 cells, since the cells with both the vector and the gene encoding information were more resistant to the effects of MTX and N$^{\alpha}$MTX-[Nle^4,D-Phe^7]α-MSH, however the inhibitory effects of untreated 293 (HEK) would also have to be examined to substantiate

this theory. Even though the results of the 293 cells were only preliminary and further replicates should be done to confirm the above conclusions, the experiments labelled 146 and 147 are still valid as giving representative results. The results obtained with transformed 293 cells could be explained if the rate of receptor-mediated endocytosis was slow, or if the release and degradation of the conjugate was impaired. More work needs to be done to explore these effects.

Control experiments in the presence of [Nle^4,D-Phe^7]α-MSH alone with B16 and MeWo cells were performed to establish whether the [Nle^4,D-Phe^7]α-MSH exerted any growth inhibitory effects. It has been shown (Figures 5.25 and 5.26) that any decrease in viability was transient and at the highest concentration of [Nle^4,D-Phe^7]α-MSH (10^{-4}M) there was no reduction in absorbance and hence no reduction in cell viability. This implied that the [Nle^4,D-Phe^7]α-MSH portion of the N$^\alpha$MTX-[Nle^4,D-Phe^7]α-MSH was not inherently toxic and therefore any inhibitory effects mediated by the latter were due solely to the MTX portion.

The effects of monensin on the inhibitory actions of N$^\alpha$MTX-[Nle^4,D-Phe^7]α-MSH were examined by incubating the B16 cells with a range of concentrations of N$^\alpha$MTX-[Nle^4,D-Phe^7]α-MSH in the presence of a fixed (10^{-5}M) concentration of monensin. The theory behind this was that monensin is an ionophore which prevents receptor recycling in its role as a lysomotropic agent. Therefore if the N$^\alpha$MTX-[Nle^4,D-Phe^7]α-MSH was internalised specifically via MSH receptor mediated endocytosis then treatment with monensin would decrease the number of available receptors, over time, and the overall result would be an increase in the $E.C._{50}$ value relative to the $E.C._{50}$ value of B16 cells untreated by monensin. These experiments yielded a mean $E.C._{50}$ value of 1.56 x 10^{-5}M (n=3) which compared to 1.47 x 10^{-5}M for

untreated B16 cells. Therefore any effects on receptor recycling within the cells were not manifested by a parallel increase in concentration of N$^{\alpha}$MTX-[Nle^{4},D-Phe^{7}]α-MSH necessary to inhibit growth and so one of two conclusions may be drawn: (i) the receptor recycling of the MSH receptors was not significantly reduced by the 10^{-5}M monensin or, (ii) there was a significant reduction in receptor recycling but this did not interfere with the actions of the N$^{\alpha}$MTX-[Nle^{4},D-Phe^{7}]α-MSH as receptor mediated endocytosis was not the major route of entry for N$^{\alpha}$MTX-[Nle^{4},D-Phe^{7}]α-MSH.

Finally the cells were treated with 10^{-4}M chloroquine which caused cell death in the absence of any other agent and hence no conclusions could be drawn as to the efficacy of chloroquine in reduction in receptor recycling and if this affected the N$^{\alpha}$MTX-[Nle^{4},D-Phe^{7}]α-MSH.

The lack of efficacy shown by N$^{\alpha}$MTX-[Nle^{4},D-Phe^{7}]-α-MSH in growth inhibition of cells relative to MTX was disappointing in so far as a selective effect on melanoma cells could not be demonstrated and this contrasted with the previous success of others in the field.

Morandini *et al.* (1994) used four peptide-melphalan conjugates: Pep1 and Pep2 (central fragments) which contained the 4-10 sequence known to be the main α-MSH binding site and Pep3 and Pep4 which comprised two C terminal fragments. They were all tested against melanoma, carcinoma and fibroblasts. When comparisons were made on the basis of the $E.C._{50}$ values, a clear selective cytotoxic effect on melanoma cells could be observed even though all four were less active than melphalan alone. The results obtained by this group and by Varga *et al.* (1977) using daunomycin conjugates of β-MSH are all the more surprising when the binding affinity of the conjugates is considered. Data from the Bath group shows that coupling of drugs to the N-terminus of α-MSH is acceptable without extensive loss of affinity. Other sites of coupling would

be expected to have a considerable effect on binding. Varga *et al.* (1977) did not determine receptor binding but this conjugate would be expected to have low affinity for MC1 receptors.

Bard *et al.* (1986, 1990) showed how α-MSH derivatives could aid imaging of melanoma: Conjugation of MSH to diethylenetriaminepenta-acetic acid (DTPA) was done initially in order to investigate the ability of MSH-DPTA to target ^{111}In to Cloudman melanoma cells and tumours. The results obtained showed that MSH-DTPA-^{111}In was selectively retained by tumour tissue.

This was then enhanced by the synthesis of *bis*-MSH-DTPA by Bard *et al.* (1990) in which two molecules of the hormone were cross-linked by DPTA. When DBA/2 mice were injected with the *bis*-MSH-DPTA-^{111}In, the radioactivity was rapidly associated with the melanoma tissue. The radioactivity in tumour tissue was significantly higher ($P<0.001$) than in the spleen, lung, brain, eye or the skin. A conclusion that *bis*-MSH-DTPA may offer an alternative to antibody targeting in the imaging of malignant melanoma , was reached by the authors. This would be a great advantage to aid imaging of melanoma since the reliable detection of metastases presents a major clinical problem in the management of malignant melanoma.

The conjugation of α-MSH to diphtheria toxin forming a fusion protein: DAB_{389}-MSH by Murphy *et al.* (1986) was developed into a system for use with MC receptors in human melanoma metastases by Tatro *et al.* (1992). Due to the results of competitive binding of DAB_{389}-MSH in the presence of ^{125}I-[Nle^4,D-Phe^7]α-MSH on biopsy specimens of human and mouse melanoma metastases, it was concluded that DAB_{389}-MSH could displace the ^{125}I-[Nle^4,D-Phe^7]α-MSH from its receptor site. Other probes tested were [Nle^4,D-Phe^7]α-MSH and α-MSH and they were ranked in decreasing order of binding affinities as follows: [Nle^4,D-Phe^7]α-MSH, 1.80nM, α-MSH, 2.43nM and

DAB_{389}-MSH, 11.9nM. These values were very close and since melanotropin receptors are detectable in melanoma metastases of about 80% of human patients (Tatro *et al.*, 1990) it has been postulated (Tatro *et al.*, 1992) that malignant melanoma cells of many patients may be susceptible to the targeted cytotoxin DAB_{389}-MSH.

Future work in our laboratories will involve the use of the diphtheria toxin fusion protein conjugated to α-MSH in our system, where it is hoped to act as a positive control showing that selectivity does occur but that MTX may not be the optimal choice for demonstrating this. Although MTX is a toxic molecule, it is also possible that fewer diphtheria toxin molecules would be needed to effect cell kill and hence this may be a more efficient site specific delivery system.

In vitro work is an important first step on the road to more efficacious therapy and even though it may not necessarily reflect success *in vivo* (Suli-Vargha *et al.*, 1990), it is still a valuable indicator.

REFERENCES:

Adams, G. Internalisation of α-MSH analogues to B16 murine melanoma cells via the α-MSH receptor. Ph.D. thesis. University of Bath. (1993).

Albert, A. Selective toxicity: The physico-chemical basis of therapy. 5th edition. Chapman and Hall. London. (1973).

Alley, M. C., Scudiero, D. A., Monks, A., Hursey, M. L., Czerwinski, M. J., Fine, D. L., Abbott, B. J., Mayo, J. G., Shoemaker, R. H., and Boyd, M. R. Feasibility of drug screening with panels of human tumour cell lines using a microculture tetrazolium assay. *Cancer Res.* **48**: 589-601 (1988).

Arnould, R., Dubois, J., Abikhalil, F., Libert, A., Ghanem, G., Atassi, G., Hanocq, M. and Lejeune, F.J. Comparison of two cytotoxicity assays - tetrazolium derivative reduction (MTT) and tritiated thymidine uptake on three malignant mouse cell lines using chemotherapeutic agents and investigational drugs. *Anticancer Res.* **10**: 145-154. (1990).

Assaraf, Y.G. and Schimke, R.T. Identification of methotrexate transport deficiency in mammalian cells using fluoresceinated methotrexate and flow cytometry. *Proc. Natl. Acad. Sci. USA* **84**: 7154-7158. (1987).

Atherton, E. and Sheppard, R.C. Solid-phase peptide synthesis - A practical approach. IRL Press. (1989).

Baggott, J.E. Inhibition of purified avian liver aminoimidazolecarboxamide ribotide transformylase by polyglutamates of methotrexate and oxidized folates. *Fed. Proc.* **42:** 667. (Abstract). (1983).

Balis, F.M., Holcenberg, J.S. and Bleyer, W.A. Clinical pharmacokinetics of commonly used anticancer drugs. *Clinical Pharmacokinetics.* **8**: 202-232. (1983).

Bard, D.R., Knight, C. G. and Page-Thomas, D.P. Targetting of a radionuclide to Cloudman melanoma cells in vitro and in vivo. *Biochem. Soc. Trans.* **14:** 614-615. (1986).

Bard, D.R., Knight, C. G. and Page-Thomas, D.P. A chelating derivative of α-melanocyte stimulating hormone as a potential imaging agent for malignant melanoma. *Br. J. Cancer.* **62:** 919-922. (1990).

Basu, S.K. Receptor-mediated endocytosis: An overview of a dynamic process. *J. Biosci.* **6:** 535-542. (1984).

Basu, S.K. Receptor-mediated endocytosis of macromolecular conjugates in selective drug delivery. *Biochem. Pharmacol.* **40**: 1941-1946. (1990).

Bernard, S., Etienne, M.C., Fischel, J.L., Formento, P. and Milano, G. Critical factors for the reversal of methotrexate cytotoxicity by folinic acid. *Br. J. Cancer.* **63**: 303-307. (1991).

Bertino, J.R. Folate Antagonists. In: Sartorelli, A.C.,(ed.): Antineoplastic and immunosuppressive agents II. New York. Springer. 468-483. (1975).

Bleyer, W.A. Therapeutic drug monitoring of methotrexate and other antineoplastic drugs; in Interpretations in Therapeutic Drug Monitoring, Baer and Dito (Eds.) American Society of Clinical Pathology, (1981).

Bremnes, R.M., Slordal, L., Wist, E. and Aarbakke, J. Formation and elimination of 7-hydroxymethotrexate in the rat *in vivo* after methotrexate administration. *Cancer Res.* **49**: 2460-2464. (1989).

Buttke, T.M., McCubrey, J.A. and Owen, T.C. Use of an aqueous soluble tetrazolium /formazan assay to measure viability and proliferation of lymphokine-dependent cell lines. *J. Immunol. Methods.* **157**: 233-240. (1993).

Cannon, J.G., Tatro, J.B., Reichlin, S. and Dinarello, C.A. Alpha melanocyte stimulating hormone inhibits immunostimulatory and inflammatory actions of interleukin 1. *J. Immunol.* **137:** 2232-2236. (1986).

Carmichael, J., DeGraff, W.G., Gazdar, A.F., Minna, J.D. and Mitchell, J.B. Evaluation of a tetrazolium-based semiautomated colorimetric assay: assessment of chemosensitivity testing. *Cancer Res.* **47:** 936-942. (1987).

Carmichael, J., DeGraff, W.G., Gazdar, A.G., Minna, J.D. and Mitchell J.B. Evaluation of a tetrazolium-based semiautomated colorimetric assay: asssessment of radiosensitivity. *Cancer Res.* **47**: 943-946. (1987).

Carmichael, J., Mitchell, J.B., De Graff, W.G., Gamson, J., Gazdar, A.F., Johnson, B.E., Glatstein, E. and Minna, J.D. Chemosensitivity testing of human lung cancer cell lines using the MTT assay. *Br. J. Cancer.* **57:** 540-547, (1988).

Carter, S.K. Cyclophosphamide in solid-tumours. *Cancer Treatment Rev.* **2:** 295-322. (1975).

Castrucci, A.M. deL., Hadley, M.E., Sawyer, T.K. and Hruby, V.J. Enzymological studies of melanotropins. *Comp. Biochem. Physiol.* **78B:** 519-524. (1984).

Chabner, B.A. Methotrexate. *in:* Pharmacologic Principles of Cancer Treatment. (B.A. Chabner, ed.) W.B. Saunders. Philadelphia 229-255. (1982).

Chabner, B.A. and Young, R.C. Threshold methotrexate concentration for *in vivo* inhibition of DNA synthesis in normal and tumorous target tissues. *J.Clin. Invest.* **52:** 1804-1811. (1973).

Chhajlani, V., Muneniece, R. and Wikberg, J.E.S. Molecular cloning of a novel human melanocortin receptor. *Biochem and Biophys. Res. Commun.* **195:** 866-873. (1993).

Chhajlani, V. and Wikberg, J.E.S. Molecular cloning and expression of the human melanocyte stimulating hormone receptor cDNA. *FEBS. Lett.* **309:** 417-420. (1992).

Chu., B.C.F., Fan, C.C. and Howell, S.B. Activity of free and carrier-bound methotrexate against transport-deficient and high dihydrofolate dehydrogenase-containing methotrexate-resistant L1210 cells. *J. Natl. Cancer. Inst.* **66:** 121-124. (1981).

Chu, M-Y. Incorporation of arabinosyl cytosine into 2-7S ribonucleic acid and cell death. *Biochem. Pharmacol.* **20:** 2057-2063. (1971).

Clark, D., Thody, A.J., Shuster, S. and Bowers, H. Immunoreative α-MSH in human plasma in pregnancy. *Nature.* **273:** 163-164. (1978).

Clark, W.G., Holdeman, M. and Lipton, J.M. Analysis of the antopyretic action of alpha-melanocytes-stimulating hormone in rabbits. *J. Physiol.* **359:** 459-465. (1985).

Cobb, J.P. Effects of in vitro X irradiation on pigmented and pale slices of Cloudman S91 mouse melanoma as measured by subsequent proliferation in vivo. *J.Natl. Cancer Inst.* **17:** No.5. 657-666. (1956).

Condit, P.T. Chemotherapy of neoplastic disease with folate antagonists. *Ann N .Y. Acad. Sci.* **186:** 475-485. (1971).

Cory, A.H., Owen, T.C., Barltrop, J.A. and Cory, J.G. Use of an aqueous soluble tetrazolium/formazan assay for cell growth assays in culture. *Cancer Commun.* **3:** 207-212. (1991).

Cowan, K. H. and Jolivet, J. A novel mechanism of resistance to methotrexate (MTX) in human breast cancer cells: Lack of polyglutamate formation. Abstract. *Clinical Research.* **31:** 508A. (1983).

Creasey, W.A. Vinca alkaloids; in Cancer Chemotherapy III (Brodsky et al., (Eds.)) 49-58. Grune and Stratton, New York, (1978).

Crine, P., Gossard, F., Seidah, N.G., Blanchette, L., Lis, M. and Chretien, M. Concomitant synthesis of β-endorphin and α-melanotropin from two forms of pro-opiomelanocortin in the rat pars intermedia. *Proc. Natl. Acad. Sci. USA.* **76:** 5085-5089. (1979).

Curt, G.A., Jolivet, J., Carney, D.N., Bailey, B.D., Drake, J.C., Clendeninn, N.J. and Chabner, B.A. Determinants of the sensitivity of human small-cell lung cancer cell lines to methotrexate. *J. Clin. Invest.* **76**: 1323-1329. (1985)

DeDuve, C., De Barsy, T., Poole, B., Trout, A., Tulkens, P. and VanHoof, F. Lysosomotropic agents. *Biochemical Pharmacology.* **23:** 2495-2531. (1974).

DeWied, D. and Jolles, J. Neuropeptides derived from pro-opiocortin, behavioural, physiological and neurochemical effects. *Physiol. Rev.* **62:** 976-1059. (1982).

Denizot, F. Lang, R. Rapid colorimetric assay for cell growth and survival, (modifications to the tetrazolium dye procedure giving improved sensitivity and reliability). *J. Immunol. Methods.* **89**: 271-277. (1986).

Eberle, A.N. The melanotropins- chemistry, physiology and mechanisms of action. Karger, Basel. (1988).

Eberle, A.N., Siegrist, W., Bagutti, C., Chluba-de Tapia, J., Solca, F., Wikberg, J.E.S. and Chhajlani, V. Receptors for melanocyte-stimulating hormone on melanoma cells. *Ann. N. Y. Acad. Sci.* **680:** 320-341. (1993).

Embleton, M.J., Gunn, B., Byers, V.S. and Baldwin, R.W. Antitumour reactions of monoclonal antibody against a human osteogeic sarcoma cell line. *Br. J. Cancer.* **43:** 582-587. (1981).

Endo, N., Kato, Y., Takeda, Y., Saito, M., Umemoto, N., Kishida, K. and Hara, T. *In vitro* cytotoxicity of a human serum albumin-mediated conjugate of methotrexate with anti-MM46 monoclonal antibody. *Cancer Res.* **47:** 1076-1080. (1987).

Endo, N., Takeda, Y., Umemoto, N., Kishida, K., Watanabe, K., Saito, M., Kato, Y. and Hara, T. Nature of linkage and mode of action of methotrexate conjugated with antitumour antibodies: implications for future preparations of conjugates. *Cancer Res.* **48:** 3330-3335. (1988).

Erskine-Grout, M.B. Interaction of alpha-melanocyte stimulating hormone with its receptor. Ph.D. thesis. University of Bath. (1993).

Etievant, C., Kruczynski, A., Pauwels, O. and Kiss, R. The combination of the tetrazolium derivative reduction (MTT) and digital cell image analysis to monitor in vitro the cytotoxicity of anti-neoplastic drugs. *Anticancer Res.* **11**: 305-312. (1991).

Fahrig, L., Brasch, H. and Iven, H. Pharmacokinetics of methotrexate (MTX) and 7-hydroxymethotrexate (7-OH-MTX) in rats and evidence for the metabolism of MTX to 7-OH-MTX. *Cancer Chemother. Pharmacol.* **23**: 156-160. (1989).

Finlay, G.J., Baguley, B.C. and Wilson, W.R. A semiautomated microculture method for investigating growth inhibitory effects of cytotoxic compounds on exponentially growing carcinoma cells. *Anal. Biochem.* **139**: 272-277. (1984).

Fitzpatrick, J.J. Drug release from methotrexate polymer conjugates. Ph.D. thesis. University of Nottingham. (1994).

Friend, D.S. and Farquhar, M.G. Functions of coated vesicles during protein absorption in the rat vas deferens. *J. Cell. Biol.* **35:** 357-376. (1967).

Frei, E., Blum, R.H. and Pitman, S.W. High dose methotrexate with leucovorin rescue: rationale and spectrum of antitumour activity. *Am. J. Med.* **68:** 370-376. (1980).

Fujii, R. and Oshima, N. Control of chromatophore movements in teleost fishes. *Zool. Sci.* **3:** 13-47. (1986).

Furst, D.E. and Kremer, J.M. Methotrexate in rheumatoid arthritis. *Arthritis Rheum.* **31:**305-314. (1988).

Gale, R.P. Advances in the treatment of acute myelogeous leukemia. *New England J. Med.* **300:** 1189-1199. (1979).

Gallant, G., Salvador, R. and Dulude, H. *In Vitro* cytotoxicity and differential cellular sensitivity of new N-methyl and N-propargyl urea and nitrosurea derivatives of diamino acids against sixty human NCI tumor cell lines. *Anticancer Res.* **13**: 133-140. (1993).

Gantz, I., Konda, Y., Tashiro, T., Shimoto, Y., Miwa, H., Munzert, G., Watson, S.J., Del Valle, J. and Yamada, T. Molecular cloning of a novel melanocortin receptor. *J. Biol. Chem.* **268:** No.11. 8246-8250. (1993a).

Gantz, I., Miwa, H., Konda, Y., Shimoto, Y., Tashiro, T., Watson, S.J., Del Valle, J. and Yamada, T. Molecular cloning, expression, and gene localisation of a fourth melanocortin receptor. *J. Biol. Chem.* **268:** 15174-15179. (1993b).

Garn, H., Krause, H., Enzmann, V. and Drossler, K. An improved MTT assay using the electron-coupling agent menadione. *J. Immunol. Methods.* **168**: 253-256. (1994).

Garnett, M.C., Embleton, M.J., Jacobs, E. and Baldwin, R.W. Preparation and properties of a drug-carrier antibody conjugate showing selective antibody-directed cytotoxicity in vitro. *Int. J. Cancer.* **31:** 661-670. (1983).

Garnett, M.C., Embleton, M.J., Jacobs, E. and Baldwin, R.W. Studies on the mechanism of action of an antibody-targetted drug-carrier conjugate. *Anti-Cancer Drug Design.* **1:** 3-12. (1985).

Gaumont, Y., Kisliuk, R.L., Parsons, J.C. and Greco, W.R. Quantitation of folic acid enhancement of antifolate synergism. *Cancer Res.* **52**: 2228-2235. (1992).

Geiger, R., Gerhards, H.J., Wiemer, G. and Hock, F.J. Studies with peptides related to the sequence 4-9 of ACTH. In: Theodoropoulos D. (Ed.) Peptides 489-492. de Gruyter, Berlin, (1986).

Ghose, T. and Blair, A.H. Antibody-linked cytotoxic agents in the treatment of cancer: current status and future prospects. *J. Natl. Cancer Inst.* **61:** 657-676. (1978).

Goldman, I.D., Lichtenstein, N.S. and Oliverio, V.T. Carrier-mediated transport of the folic acid analogue, methotrexate in the L1210 leukaemia cell. *J. Biol. Chem.* **243:** 5007-5017. (1968).

Goldstein, J.L., Anderson, R.G.W. and Brown, M.S. Coated pits, coated vesicles, and receptor-mediated endocytosis. *Nature.* **279:** 679-685. (1979).

Gottlieb, J.A. and Serpick, A.A. Prolonged intravenous methotrexate therapy in the treatment of acute leukaemia and solid tumours. *Cancer Res.* **30:** 2132-2138. (1970).

Haber, M., Madafiglio, J. and Norris, M.D. Methotrexate cytotoxicity determination using the MTT assay following enzymatic depletion of thymidine and hypoxanthine. *J. Cancer Res. Clin. Oncol.* **119:** 315-317. (1993).

Hadley, M.E., Wood, S.H., Lemus-Wilson, A.M., Dawson, B.V., Levine, N., Dorr, R.T. and Hruby, V.J. Current Concepts: The melanotropic peptides. VII Topical application of a melanotropic peptide induces systemic follicular melanogenesis. *Life Sci.* **40:** 1889-1895. (1987).

Halpern, S.E., Hagan, P.L., Garver, P.R., Koziol, J.A., Chen, A.W.N., Frincke, J.M., Bartholomew, R.W., David, G.S. and Adams, T.H. Stability, characterization and kinetics of ^{111}In labelled monoclonal antitumor antibodies in normal animals and nude mouse tumour models. *Cancer. Res.* **43:** 5307-5355. (1983)

Hansen, J., Kreilgard, B., Nielsen, O. and Veje J. Kinetics of degradation of methotrexate in aqueous solution. *Int. J. Pharmaceutics.* **16**: 141-152. (1983).

Hansen, M.B., Nielsen, S.E. and Berg, K. Re-examination and further development of a precise and rapid dye method for measuring cell growth / cell kill. *J. Immunol. Methods.* **119**: 203-210. (1989).

Hart, P.D. and Young, M.R. Ammonium chloride, an inhibitor of phagosome-lysosome fusion in macrophages, concurrently induces phagosome-endosome fusion and opens a novel pathway: studies of a pathogenic mycobacterium and nonpathogenic yeast. *J. Exp. Med.* **174:** 881-889 (1991).

Hill, B.T., Bailey, B.D., Courtland White, J. and Goldman, I.D. Characteristics of transport of 4-amino antifolates and folate compounds by two lines of L5178Y lymphoblasts, one with impaired transport of methotrexate. *Cancer Res.* **39:** 2440-2446. (1979).

Hryniuk W.M. and Bertino, J.R. The treatment of leukaemia with large doses of MTX and folinic acid: clinical-biochemical correlates. *J. Clin. Invest.* **48:** 2140-2155. (1969).

Hryniuk, W.M., Fischer, G.A. and Bertino, J.R. S-phase cells of rapidly growing and resting populations differences in response to methotrexate. *Mol. Pharmacol.* **5**: 557-564. (1969).

Hudecz, F., Clegg, J.A., Kajtar, J., Embleton, M.J. Pimm, M.V., Szekerke, M. and Baldwin, R.W. Influence of carrier on biodistribution and *in vitro* cytotoxicity of methotrexate-branched polypeptide conjugates. *Bioconjugate Chem.* **4:** 25-33. (1993).

Hudecz, F., Clegg, J.A., Kajtar, J., Embleton, M.V., Szekerke, M. and Baldwin, R.W. Synthesis , conformation, biodistribution and *in vitro* cytotoxicity of daunomycin branched polypeptide conjugates. *Bioconjugate Chem.* **3:** 49-57. (1992).

Huennekens, F.M. and Henderson, G.B. Transport of folate compounds into mammalian and bacterial cells. *Proceedings of the 5th international symposium on the chemistry and biology of pteridines.* 179-196. (1975).

Husoy, T., Syversen, T. and Jenssen, J. Comparisons of four *in vitro* cytotoxicity tests: The MTT assay, NR assay, uridine incorporation and protein measurements. *Toxicology in vitro.* **7:** 149-154. (1993).

Jabbar, S.A.B., Twentyman, P.R. and Watson, J.V. The MTT assay underestimates the growth inhibitory effects of interferons. *Br. J. Cancer.* **60**: 523-528. (1989).

Jeney, A., Kopper, L., Nagy, P., Lapis, K., Suli-Vargha, H. and Medzihradszky, K. Anti-tumour action of *N*-(2-chloroethyl)-*N*-nitrosocarbamoyl derivatives of biologically active polypeptide hormone fragments. *Cancer Chemother. Pharmacol. 16:* 129-132. (1986).

Jiao, H. Y., Soejima, Y., Ohe, Y. and Saijo, N. A new MTT assay for examining the cytotoxicity of activated macrophages towards the non-adherent P388 leukaemia cell line. *J. Immunol. Methods.* **153:** 265-266. (1992).

Jolivet, J., Cowan, K.H., Curt, G.A., Clendeninn, N.J. and Chabner, B.A. The pharmacology and clinical use of methotrexate. *New England J. Med.* **309:** 1094-1104. (1983).

Juraskova, V. The cytotoxic effect of methotrexate as evaluated by colony forming activity of hemopoietic and tumor cells. *Neoplasma.* **35**: 583-589. (1988).

Kalra, R., Jones, A.-M., Kirk, J., Adams, G.E. and Stratford, I.J. The effect of hypoxia on acquired drug resistance and response to epidermal growth factor in Chinese hamster lung fibroblasts and human breast cancer cells *in vitro*. *Int. J. Cancer.* **54:** 650-655. (1993).

Kamen, B.A. and Capdevila, A. Receptor-mediated folate accumulation is regulated by the cellular folate content. *Proc. Natl. Acad. Sci. USA.* **83:** 5983-5987. (1986).

Kamen, B.A., Wang, M-T., Streckfuss, A.J., Peryea, X. and Anderson, R.G.W. Delivery of folates to the cytoplasm of MA104 cells is mediated by a surface membrane receptor that recycles. *J. Biol. Chem.* **263**: 13602-13609. (1988).

Kamen, B.A., Whyte-Bauer, W. and Bertino, J.R. A mechanism of resistance to methotrexate. *Biochem. Pharmacol.* **32**: 1837-1841. (1983).

Kawashima, I., Kotani, M., Ozawa, H., Suzuki, M. and Tai, T. Generation of monoclonal antibodies specific for ganglioside lactones: evidence of the expression of lactone on human melanoma cells. *Int. J. Cancer.* **58:** 263-268. (1994)

Lankelma, J., van der Kleijn, E. and Termond, F.S. Assay of methotrexate and 7-hydoxymethotrexate by high pressure liquid chromatography and its application to clinical pharmacokinetics, in *Clinical Pharmacology of Anti-Neoplastic Drugs*. ed. Pinedo, H.M. Elsevier / North-Holland Biomedical Press. (1978).

Lee, T.H., Lee, M.S. and Lu, M.Y. Effects of α-MSH on melanogenesis and tyrosinase of B16 melanoma. *Endocrinology.* **91:**1180-1188. (1972).

Levine, N., Lemus-Wilson, A., Wood, S.H., Abdel Malek, Z.A., Al-Obeidi, F., Hruby, V.J. and Hadley, M.E. Stimulation of follicular melanogenesis in the mouse by topical and injected melanotropins. *J. Invest. Dermatol.* **89:** 269-273. (1987).

Li, W. W. and Bertino, J.R. Inability of leucovorin to rescue a naturally methotrexate-resistant human soft tissue sarcoma cell line from trimetrexate cytotoxicity. *Cancer Res.* **52**: 6866-6870. (1992).

Liu, M.A., Nussbaum, S.R. and Eisen, H.N. Hormone conjugated with antibody to CD3 mediates cytotoxic T cell lysis of human melanoma cells. *Science.* **239:** 395-398. (1988).

MacKie, R. (Ed.) Malignant melanoma. Pigment Cell 6. Karger, Basel. (1983).

Mains, R.E. and Eipper, B.A. Synthesis and secreation of corticotropins, melanotropins and endorphins by rat intermediate pituitary cells. *J. Biol. Chem.* **254:** 78885-7894. (1979).

Mains, R.E., Eipper, B.A. and Ling, N. Common precursor to corticotropins and endorphins. *Proc. Natl. Acad. Sci. USA.* **74:** 3014-3018. (1977).

Mishima, Y. Neutron capture treatment of malignant melanoma using ^{10}B-chlorpromazine compound. *Pigment Cell.* **1:** 215-221. (Karger, Basel. 1973).

Moran, R.G., Mulkins, M. and Heidelberger, C. Role of thymidylate synthetase activity in development of MTX cytotoxicity. *Proc. Natl. Acad. Sci.* **76:** 5924-5928. (1979).

Morandini, R., Suli-Vargha, H., Libert, A., Loir, B., Botyanszki, J., Medzihradszky, K. and Ghanem, G. Receptor-mediated cytotoxicity of α-MSH fragments containing melphalan in a human melanoma cell line. *Int. J. Cancer.* **56:** 129-133. (1994).

Morison, W.L., Momtaz, K., Parrish, J.A. and Fitzpatrick, T.B. Combined methotrexate-PUVA therapy in the treatment of psioriasis. *J. Am. Acad. Dermatol.* **6:** 46-51. (1982).

Mosmann, T. Rapid colorimetric assay for cellular growth and survival: application of proliferation and cytotoxicity assays. *J. Immunol. Methods.* **65**: 55-63. (1983).

Mountjoy, K.G., Robbins, L.S., Mortrud, M.T. and Cone, R.D. The cloning of a family of genes that encode the melanocortin receptors. *Science.* **257:**1248-1251. (1992).

Murphy, J.R., Bishai, W., Borowski, M., Miyanohara, A., Boyd, J. and Nagle, S. Genetic construction, expression and melanoma-selective cytotoxicity of a diphtheria toxin-related α-melanocyte-stimulating hormone fusion protein. *Proc. Natl. Acad. Sci. USA.* **83**: 8258-8262. (1986).

Myers, C.E., Diasio, R., Eliot, H.M. and Chabner, B.A. Pharmacokinetics of the fluoropyrimidines: Imperatives for their clinical use. *Cancer Treatment Reviews.* **3:** 175-183. (1976).

Oka, M., Maeda, S., Koga, N., Kato, K. and Saito, T. A modified colorimetric MTT assay for primary cultured hepatocytes: Application to proliferation and cytotoxicity assays. *Biosci. Biotech. Biochem.* **56:** 1472-1473. (1992)

Pimm, M.V., Robins, R.A., Embleton, M.J., Jacobs, E., Markham, A.J., Charleston, A. and Baldwin, R.W. A bispecific monoclonal antibody against methotrexate and a human tumour associated antigen augments cytotoxicity of methotrexate-carrier conjugate. *Br. J. Cancer.* **61**: 508-513. (1990).

Poznansky, M.J. and Juliano, R.L. Biological approaches to the controlled delivery of drugs: A critical review. *Pharmacol. Rev.* **6:** 227-336. (1984).

Rice, G.C., Ling, V. and Schimke, R.T. Frequencies of independent and simultaneous selection of Chinese hamster cells for methotrexate and doxorubicin (adriamycin) resistance. *Proc. Natl. Acad. Sci. USA.* **84:** 9261-9264. (1987).

Richards, A.C. Targeting of methotrexate to melanoma by way of melanocyte stimulating hormone. Ph.D. thesis. University of Bath. (1992).

Roehm, N.W., Rodgers, G.H., Hatfield, S.M. and Glasebrook, A.L. An improved colorimetric assay for cell proliferation and viability utilizing the tetrazolium salt XTT. *J. Immunol. Methods.* **142**: 257-265. (1991).

Romanini, A., Sobrero, A.F., Chou, T-C., Sherwood, R.F. and Bertino, J.R. Enhancement of trimetrexate cytotoxicity *in vitro* and *in vivo* by carboxypeptidase G_2. *Cancer Res.* **49:** 6019-6023. (1989).

Roth, T.F. and Porter, K. R. Yolk protein uptake in the oocyte of the mosquito *Aedes Aegypto. L. J. Cell. Biol.* **20:** 313-332. (1964).

Sahm, U.G. Interaction of naturally occurring and synthetic MSH peptides with peripheral and CNS melanocortin receptors. Ph.D. thesis. University of Bath. (1994).

Sakata, K., Kwok, T.T., Murphy, B.J., Laderoute, K.R., Gordon, G.R. and Sutherland, R.M. Hypoxia-induced drug resistance: comparison to P-glycoprotein-associated drug resistance. *Br. J. Cancer.* **64:** 809-814. (1991).

Sandberg, H.E. Proceedings of the International Workshop on Technology for Protein Separation and Improvement of Blood Plasma Fractionations. U.S. Dept. Health, Education, Welfare, Publ. no. (NIH) 78-1422, U.S.A. (1977).

Sanna, K. and Rofstad, E.K. Hypoxia-induced resistance to doxorubicin and methotrexate in human melanoma cell lines in vitro. *Int. J. Cancer.* **58:** 258-262. (1994).

Sawyer, T.K., Sanfilippo, P.J., Hruby, V.J., Engel, M.H., Heward, C.B., Burnett, J.B. and Hadley, M.E. 4-Norleucine, 7-D-phenylalanine-α-melanocyte-stimulating hormone. A highly potent α-melanotropin with ultralong biological activity. *Proc. Natl. Acad. Sci. USA.* **77:** 5754-5758. (1980).

Sladowski, D., Steer, S.J., Clothier, R.H. and Balls, M. An improved MTT assay. *J. Immunol. Methods.* **157**: 203-207. (1993).

Stratford, I.J. and Stephens, M.A. The differential hypoxic cytotoxicity of bioreductive agents determined in vitro by the MTT assay. *Int. J. Radiat. Oncol. Biol. Phys.* **16**: 973-976. (1988).

Süli-Vargha, H., Csukas, I., Botyanski, J., Jeney, A., Kopper, L. and Lapis, K. Anti-tumour action and mutagenicity of melphalan containing α-MSH fragments. *J Cancer. Res. Clin. Oncol.* **116:** 939. (1990).

Szeto, D.W., Cheng, Y-C., Rosowsky, A., Yu, C-S., Modest, E.J., Piper, J.R., Temple Jr. C., Elliott, R.D., Rose, J.D. and Montgomery, J.A. Human thymidylate sythetase-III: Effects of methotrexate and folate analogs. *Biochem. Pharmacol.* **28:** 2633-2637. (1979).

Tatro, J.B., Entwistle, M.L., Lester, B.R. and Reichlin, S. Melanotropin receptors of murine melanoma characterised in cultured cells and demonstrated in experimental tumours. *Cancer Res.* **50:** 1237-1242. (1990).

Tatro, J. B., Wen, Z., Entwistle, M.L., Atkins, M.B., Smith, T.J., Reichlin, S. and Murphy, J.R. Interaction of an α-melanocyte-stimulating hormone-diphtheria toxin fusion protein with melanotropin receptors in human melanoma metastases. *Cancer Res.* **53**: 2545-2548. (1992).

Teicher, B.A., Lazo, J.S. and Sartorelli, A.C. Classification of antineoplastic agents by their selective toxicities toward oxygenated and hypoxic tumor cells. *Cancer Res.* **41**: 73-81. (1981).

Thillet, J., Absil, J., Stone, S.R. and Pictet, R. Site-directed mutagenesis of mouse dihydrofolate reductase. *J. Biol. Chem.* **263**: 12500-12508. (1988).

Tomlinson, E. Theory and practice of site-specific drug delivery. *Advanced Drug Delivery Reviews.* **1:** 87-198. (1987).

Twentyman, P.R. and Luscombe, M. A study of some variables in a tetrazolium dye (MTT) based assay for cell growth and chemosensitivity. *Br. J. Cancer.* **56**: 279-285, (1987).

Underhill, T. M. and Flintoff, W.F. Mutant chinese hamster ovary cells with defective methotrexate uptake are distinguishable by reversion analysis. *Somatic Cell and Molecular Genetics.* **15**: 49-59. (1989).

van der Kleijn, E., Lippens, R. and Oosterbaan, M. Clinical pharmacokinetics in the therapeutic management of cancer patients with methotrexate and adriamycin. (1984)